POLYTECHNIQUE MONTRÉAL

affiliée à l'Université de Montréal

Mécanismes d'enlèvement et la stabilité des solides du DNC-As dans les biofiltres passifs en climat froid

HSAN YOUSSEF MEHDAOUI

Département de génies civil, géologique et des mines

Thèse présentée en vue de l'obtention du diplôme de *Philosophiæ Doctor*

Génie minéral

Avril 2025

POLYTECHNIQUE MONTRÉAL

affiliée à l'Université de Montréal

Cette thèse intitulée :

Mécanismes d'enlèvement et la stabilité des solides du DNC-As dans les biofiltres passifs en climat froid

Présenté par **Hsan Youssef MEHDAOUI**

en vue de l'obtention du diplôme de *Philosophiæ Doctor*

a été dûment acceptée pour une thèse par le jury d'examen constitué de :

Mehrez Hermassi, président
Carmen Mihaela Neculita, membre et directrice de recherche
Marouen Jouini, membre et codirecteur de recherche
Mostafa Benzaazoua, membre et codirecteur de recherche
Thomas Pabst, membre et codirecteur de recherche
Dominique Richard, membre interne
Sydney Omelon, membre externe

DÉDICACE

À mes parents,

A ma conjointe,

À mon frère et mes sœurs,

À mes beaux-frères et mes belles-sœurs,

À mes beaux-parents,

À toute ma famille et ami(e)s,

À tous ceux que je ne nomme pas, mais qui se reconnaîtront,

Et dis : « Ô mon Seigneur, accroît mes connaissances ! »

REMERCIEMENTS

Je rends tout d'abord grâce à Dieu pour la santé et la force qui m'ont accompagné tout au long de ce parcours et permis d'achever la rédaction de cette thèse.

Je tiens à exprimer ma profonde gratitude à ma directrice de recherche, Professeure Carmen Mihaela Neculita, dont le soutien constant, la patience et les conseils éclairés ont été essentiels à la réussite de ce travail. Par son encadrement bienveillant et son immense savoir, elle m'a guidé dans chaque étape de la recherche. Son exemplarité, tant sur le plan scientifique qu'humain, a nourri ma motivation et m'a permis de donner le meilleur de moi-même.

Je remercie également mes codirecteurs, Professeurs Mostafa Benzaazoua, Thomas Pabst et Marouen Jouini, pour leur disponibilité, leurs remarques constructives et leur accompagnement précieux, en particulier lors de la finalisation de mes articles. Leurs recommandations pertinentes et leur soutien indéfectible ont contribué à enrichir ce travail et à mener à bien ce projet de recherche. Je leur suis profondément reconnaissant pour leurs encouragements et la confiance qu'ils m'ont accordée tout au long de ce parcours.

Je tiens également à remercier le personnel universitaire qui m’ont bien renseigné sur les différents aspects administratifs. Je remercie aussi l’ensemble des membres de l’équipe du laboratoire de l’Unité de recherche et de service en technologie minérale (URSTM) pour leur soutien et leur contribution, directe ou indirecte, à la réalisation de ce projet. J’exprime une gratitude particulière à Sylvette Awoh et Étienne Bélanger pour leur aide précieuse.

Je suis également reconnaissant aux membres du jury d’avoir accepté d’évaluer ce travail de recherche : le président de jury Mehrez Hermassi, l’évaluateur externe Sidney Omelon et l’évaluateur interne Dominique Richard. Je tiens à remercier également tous mes enseignants, dont les enseignements et conseils m’ont accompagné tout au long de mon parcours universitaire.

Je tiens à exprimer toute ma reconnaissance aux personnes avec qui j'ai eu la chance de collaborer dans le cadre de leurs projets, et en particulier à Muhamado, Sophie, Séraphine, Diae, Hoda, Audrey et Tayssir. Même si notre temps de travail ensemble a été relativement court, j'ai sincèrement apprécié chaque échange et chaque moment partagé avec vous. Votre implication et votre énergie ont rendu cette collaboration particulièrement enrichissante.

Je tiens à remercier chaleureusement le CRSNG ainsi que l'ensemble des partenaires de l'IRME UQAT-Polytechnique pour leur précieux soutien tout au long de mon projet de thèse. J'exprime une reconnaissance particulière à la mine Dhilmar-Éléonore et au Ministère des Ressources Naturelles et des Forêts pour leur collaboration active, l'accès à leurs installations, le partage d'informations et l'autorisation de réaliser les échantillonnages nécessaires à mes travaux. Leur appui a grandement contribué à l'avancement de cette recherche.

À mes piliers de vie, mes parents Youssef et Jalila, dont l'amour infaillible et les précieux conseils m'accompagnent dans tout ce que j'entreprends : je vous dois tout. Votre soutien, vos sacrifices et votre confiance ont été mes plus grandes forces. Je vous dédie ce travail avec une profonde gratitude.

À Hasna, ma conjointe et mon amour, merci du fond du cœur pour ta présence constante, tes encouragements et ton amour inconditionnel qui m'ont porté dans les moments de doute. Ce chemin n'aurait pas été le même sans toi à mes côtés.

Je tiens également à exprimer toute ma reconnaissance à mon frère Tarek, à mes sœurs Amira, Asma, Ikram et Ichrak, ainsi qu'à l'ensemble de ma famille. Votre soutien spirituel, vos paroles réconfortantes et votre présence, malgré la distance et le décalage horaire, m'ont donné la force d'avancer. Merci d'avoir toujours été là, même de loin, avec vos encouragements et votre amour.

Je tiens également à exprimer toute ma reconnaissance à ceux que je considère bien plus que des amis : Marouen, Abdessalem, Youssef Toubri, Hassen, Xavier, Sofien, Ricot, Mohamed Meite, Safa, Sabrine, Yosra et Ansar. Votre présence a été une véritable bénédiction dans ma vie. Merci pour les moments précieux partagés et pour la joie que vous avez apportée tout au long de ces années. Je suis profondément reconnaissant de vous avoir à mes côtés.

Je tiens à exprimer ma profonde gratitude à toutes les personnes avec qui j'ai eu l'honneur de collaborer, d'échanger et de travailler dans le cadre de mon engagement au sein de l'Association générale étudiante de l'UQAT (AGEUQAT). Ces expériences enrichissantes ont été marquées par de belles rencontres humaines et professionnelles qui ont profondément contribué à mon épanouissement.

Je remercie tout particulièrement Monsieur le recteur Vincent Rousson, Madame la vice-rectrice Manon Champagne, Monsieur Bryan Trudel, doyen aux études, ainsi que Madame Yvette

Fournier, ancienne attachée à l'exécutif de l'AGEUQAT, pour leur disponibilité, leur écoute et leur précieux soutien tout au long de mon parcours associatif.

Je souhaite également adresser mes remerciements sincères à mes collègues de l'exécutif avec qui j'ai partagé de nombreux défis et succès : Mamadou, Daphnée, Sara, Mariem, Zeineb, Yosra, Ricot et Ghita. Votre engagement et votre camaraderie ont fait de cette aventure une expérience inoubliable.

Je n'oublie pas non plus les collaborateurs du CERME avec qui j'ai eu le plaisir de mener plusieurs projets au cours de mes deux mandats : Abdoulaye, Ricot, Mohamed Meïté, Vincent, Élaura, Wejdene, Mohamed Cissé, Chérif et Karine. Merci à vous tous pour votre dévouement, votre esprit d'équipe et les riches échanges qui ont marqué ces années de collaboration.

Je voudrais remercier également 'mes amis pour la vie' : Hassen, Ahmed, Mohamed Jemli, Bilel Ben Hamed, Taher, Riadh, Oussema Aloui, Majdi, Rayda et Ilhem.

Je souhaite remercier mes amis que j'ai rencontré ici, au Canada : Vincent, Youssef Guesmi, Khouloud, Mariem, Éléonore, Ikram, Eya, Yassine, Chahid, Abdelehi, Bilel Bouaziz, Bilel Chtiba, Amal, Seif, Ismail, Lahcen, Abdelbasset, Fedi et Oussema Nasr. Je m'excuse auprès des personnes que je n'ai pas citées, mais soyez sûrs que vous êtes toujours dans mon esprit.

Merci pour vos encouragements continus! Je resterai reconnaissant à vie !

RÉSUMÉ

Le drainage neutre contaminé (DNC) est une problématique environnementale récente, moins étudiée que le drainage minier acide (DMA), toutefois susceptible de causer des impacts considérables sur les milieux naturels. Le DNC est caractérisé par des concentrations faibles à modérées en contaminants dissous, tout en gardant un pH proche de la neutralité (6,5–9). Le traitement du DNC est complexe, pour certains contaminants en particulier (ex. As) et surtout sur les sites miniers fermés et abandonnés. Les résidus associés aux anciennes mines d'or et d'argent sont souvent enrichis en As entrainant la formation du DNC-As. La remobilisation de l'As en provenance des résidus est un risque potentiel qui demeure peu documenté dû au manque de connaissance sur la stabilité à long terme de l'As capturé au sein de ces résidus. Par conséquent, des solutions de traitement efficaces sont nécessaires pour gérer le DNC-As et limiter son impact sur les écosystèmes environnants. Les systèmes de traitement passifs, reconnues comme des technologies développées pour résoudre la problématique du DMA sur les sites miniers restaurés et abandonnés, ont montré une efficacité satisfaisante pour le traitement du DNC. Les biofiltres passifs, en particulier, ont prouvé leur efficacité pour traiter un DNC-As à l'échelle pilote et sur le terrain. Néanmoins, les biofiltres passifs génèrent des quantités considérables de résidus de post-traitement avec une stabilité chimique et environnementale variable. Pour mieux anticiper leur devenir en fin de cycle de vie et après excavation, une caractérisation au cas par cas de ces résidus de post-traitement est nécessaire afin de mieux comprendre leur comportement, sélectionner les voies de gestion adéquates et limiter le potentiel de lixiviation des contaminants.

Dans ce contexte, les principaux objectifs de la thèse étaient comme suit : (1) évaluer et quantifier les mécanismes et les processus responsables de l'immobilisation de l'As dans les biofiltres passifs étudiés et identifier les principaux facteurs influençant cette immobilisation; (2) identifier les phases minérales porteuses d'As et étudier la stabilité des résidus de post-traitement passif contaminés en As; (3) évaluer l'influence de l'échelle du biofiltre sur la nature des phases minérales et les mécanismes d'enlèvement prépondérant de l'As. L'approche méthodologique consistait, dans un premier temps, à échantillonner les résidus de post-traitement du biofiltre passif de terrain Wood-Cadillac avant de réaliser des caractérisations physicochimiques et minéralogiques. Ensuite, des essais de lixiviations statiques ont été réalisés pour évaluer la mobilité potentielle des contaminants, en particulier de l'As, et statuer sur la stabilité des résidus de post-traitement. La deuxième étape consistait à échantillonner les résidus de post-traitement d'un biofiltre de

laboratoire ainsi que deux biofiltres pilotes de terrain traitant le DNC-As. L'ensemble des échantillons a été soumis à des caractérisations physicochimiques, minéralogiques et environnementales pour déterminer les mécanismes de l'enlèvement de l'As et statuer sur la stabilité chimique des résidus.

L'analyse de la revue de littérature a révélé que, bien que plusieurs travaux de recherches portent sur le traitement passif du drainage minier acide (DMA) et la stabilité de ses résidus de post-traitement, peu d'études se sont spécifiquement intéressées au DNC. De plus, bien que quelques études aient porté sur le traitement du DNC-As, le potentiel de mobilité de l'As dans les résidus de post-traitement et l'effet d'échelle restent peu documentés. Il a été conclu que la stabilité des résidus de post-traitement est influencée entre autres par le type d'eau à traiter, la technologie de traitement et la charge des contaminants. Ainsi, il est nécessaire de transférer les connaissances actuelles sur les différentes méthodes de traitement du DMA et la stabilité des résidus de post-traitement vers le traitement passif du DNC, et plus particulièrement du DNC-As. Une combinaison des caractérisations physico-chimiques et minéralogiques combinées à des tests de lixiviation pourrait permettre de mieux prédire le comportement environnemental des résidus issus du traitement passif du DNC.

Dans ce contexte, la première étape consistait à échantillonner les résidus de post-traitement issus d'un biofiltre de terrain sur le site minier réclamé Wood-Cadillac, traitant un DNC-As efficacement depuis 1999. Une trentaine d'échantillons ont été collectés, à différentes profondeurs (0–30 cm, 30–60 cm, et 60–90 cm), et répartis sur cinq placettes distinctes couvrant les deux entrées et la sortie du biofiltre. Des caractérisations physico-chimiques et minéralogiques ont été réalisées afin d'élucider les mécanismes de rétention de l'As au sein du biofiltre. La mobilité potentielle des métaux a été évaluée à l'aide de tests de lixiviation statiques, notamment le TCLP (Toxicity Characteristic Leaching Procedure), le SPLP (Synthetic Precipitation Leaching Procedure) et le FLT_m (Field Leach Test modified). Les résultats ont montré que les résidus étaient caractérisés par des concentrations élevées en métaux, atteignant jusqu'à 2,3 g/kg d'As, 41,1 g/kg de Fe et 19,5 g/kg d'Al, principalement accumulés dans les couches supérieures du biofiltre. Les métaux sont précipités sous forme d'oxyhydroxydes dans les couches supérieures et intermédiaires, tandis que des sulfures secondaires se sont formés au fond du biofiltre. L'enlèvement de l'As s'est produit majoritairement par adsorption sur les oxyhydroxydes de Fe et d'Al dans les couches supérieures. En revanche, les conditions réductrices présentes au fond du biofiltre ont favorisé la précipitation

de sulfures d'arsenic amorphes (FeAsS et AsS). Les résultats des tests TCLP et SPLP ont révélé que les concentrations d'As lixiviées par les résidus étaient conformes aux directives de l'USEPA, permettant de classer ces résidus comme non dangereux et indiquant un faible risque de contamination des eaux souterraines. Toutefois, 66 % des concentrations d'As mesurées dans les tests TCLP et 20 % dans les tests SPLP ont dépassé la limite réglementaire de la directive D019 (0,1 mg/L) pour l'As dans les effluents miniers. De plus, les résultats du FLT_m ont mis en évidence un potentiel de lixiviation élevé pour l'As, dépassant 1 mg/L. Par conséquent, il est recommandé d'éviter le broyage et le séchage de ces résidus avant leur disposition finale afin de limiter une potentielle mobilisation de l'As.

Dans la deuxième étape de ce projet de thèse, une caractérisation similaire à celle réalisée dans la première étape a été effectuée pour des échantillons de post-traitement provenant d'un biofiltre de laboratoire et deux biofiltres pilotes de terrain. Un intérêt particulier a été porté à l'influence de l'effet d'échelle entre les différents biofiltres sur les mécanismes d'enlèvement et la stabilité des résidus. Ainsi, vingt échantillons ont été prélevés sur les trois biofiltres, en ciblant quatre couches distinctes (I-1, A, B et I-2). Les mécanismes d'enlèvement de l'As ainsi que les phases porteuses d'As ont été analysés à travers des caractérisations physico-chimiques et minéralogiques. La stabilité des résidus post-traitement a été évaluée au moyen de tests de lixiviation statiques (TCLP, SPLP et FLT). Les résultats ont montré que les résidus contenaient des concentrations élevées en contaminants, notamment en As (de 1,2–3,5 g/kg pour les biofiltres pilotes et de 2–3,6 g/kg pour le biofiltre en laboratoire), en Fe (de 42,9–86,3 g/kg pour les biofiltres pilotes et de 58,4–66,9 g/kg pour le biofiltre de laboratoire), en Al (de 5,7–7,9 g/kg pour les biofiltres pilotes et de 4,9–6,1 g/kg pour le biofiltre de laboratoire) et en S (de 5,7–7,9 g/kg pour les biofiltres pilotes et de 1,7–2,4 g/kg pour le biofiltre de laboratoire), confirmant ainsi l'efficacité du procédé de traitement. Les phases dominantes dans les trois biofiltres étaient constituées d'oxyhydroxydes métalliques et de silicates. Les biofiltres pilote ont révélé la présence d'oxyhydroxydes d'aluminium, d'arsénopyrite (FeAsS), de sulfates ainsi que de traces de sulfures métalliques. Dans le biofiltre de laboratoire, la rétention de l'As s'est principalement produite par adsorption sur les oxyhydroxydes de Fe(III). En revanche, à l'échelle terrain, l'immobilisation de l'As a impliqué une précipitation sous forme de FeAsS et une coprécipitation avec les oxyhydroxydes de Fe(III) et Al, tandis que les mécanismes de sorption étaient dominants dans les couches supérieures. L'ensemble des résultats des tests de lixiviation statiques (TCLP, SPLP et FLT) a respecté les normes de l'USEPA, permettant de classer les résidus

comme non dangereux, avec une possibilité de co-disposition avec les déchets municipaux. Les résultats du TCLP n'ont pas dépassé les recommandations de table T1-AII de la D019, classifiant les résidus à faible risque.

Le présent travail a permis d'approfondir les connaissances sur les mécanismes d'enlèvement de l'As dans les biofiltres passifs utilisés pour traiter le DNC-As, ainsi que d'étudier la mobilité potentielle de l'As à partir des résidus de post-traitement afin de statuer sur leur stabilité chimique. Les résultats obtenus ont également montré l'efficacité des biofiltres passifs pour le traitement du DNC-As. De plus, les méthodes mises en place dans le cadre de cette étude présentent un potentiel d'application pour l'analyse d'autres résidus post-traitement, permettant ainsi une meilleure évaluation de leur comportement à long terme en vue d'une gestion environnementale plus efficace.

Mots clés : drainage neutre contaminé, biofiltre passif, enlèvement d'arsenic, essais de lixiviation, stabilité des résidus post-traitement

ABSTRACT

Contaminated neutral mine drainage (CND) represent an emerging environmental issue that has received less attention compared to acid mine drainage (AMD), yet it can have significant impacts on natural ecosystems. CND is characterized by low to moderate concentrations of dissolved contaminants while maintaining a pseudo-neutral pH (6.5–9). CND treatment remains challenging for certain contaminants (e.g., As) particularly at closed and abandoned mining sites. Tailings from old gold and silver mines are often rich in arsenic (As) leading to the formation of As-CND. The remobilization of As from tailings is a potential risk that remains poorly understood due to a lack of knowledge about the long-term stability of As trapped in tailings. Therefore, efficient treatment solutions are essential to manage As-CND and mitigate its impact on surrounding ecosystems. Passive treatment systems, widely recognized as efficient technologies for addressing AMD on closed and abandoned mining sites, have shown promising results in CND treatment. Among these, passive biofilters have demonstrated their efficiency in treating As-CND at both pilot and field scales. However, passive biofilters generate significant quantities of post-treatment residues with variable chemical and environmental stability. At their end-of-life cycle, to better anticipate their fate after excavation, a case-by-case characterization of these residues is necessary to better understand their behavior, select appropriate management strategies and minimize potential risks of contaminant leaching.

In this context, the main objectives of the thesis were the following: (1) evaluate and characterize the mechanisms governing As immobilization within the studied passive biofilters while identifying the most dominant processes; (2) Identify the As-bearing mineral phases and assess the stability of As-contaminated post-treatment residues; (3) Assess the influence of the biofilter scale on the nature of mineral phases and the predominant As removal mechanisms. The methodological approach initially involved sampling the post-treatment residues from the Wood-Cadillac field passive biofilter before conducting physicochemical and mineralogical characterizations. Subsequently, static leaching tests were performed to assess the potential mobility of contaminants, particularly As, and to determine the stability of the post-treatment residues. The second step involved sampling the post-treatment residues from a laboratory biofilter as well as two field pilot-scale biofilters treating As-CND. All samples were subjected to physicochemical, mineralogical, and environmental characterizations to determine the mechanisms of As removal and access the chemical stability of the residues.

The literature review revealed that, although substantial research has been conducted on passive treatment of acid mine drainage (AMD) and the stability of its post-treatment residues, studies specifically addressing contaminated neutral mine drainage (CND) remain limited. Moreover, although some studies have focused on the treatment of As-CND, the potential mobility of As in post-treatment residues and the scale effect remain poorly documented. It was concluded that the stability of post-treatment residues is influenced, in most cases, by the type of water to be treated, the treatment technology, and the contaminant load. Thus, it is necessary to transfer current knowledge on various DMA treatment methods and the stability of post-treatment residues to the passive treatment of CND, particularly As-CND. A combination of physico-chemical and mineralogical characterizations, along with leaching tests, could improve the prediction of the environmental behavior of residues from the passive treatment of CND.

In this study, the first phase involved sampling post-treatment residues from a field-scale passive biofilter at the reclaimed Wood-Cadillac mine site, which has been effectively treating As-CND since 1999. Thirty samples were collected from different depths (0–30 cm, 30–60 cm, and 60–90 cm) at five distinct locations within the biofilter, including the two inlets and the outlet. Physicochemical and mineralogical characterizations were conducted to elucidate the removal mechanisms of As within the biofilter. The potential mobility of metals was assessed through static leaching tests, including the Toxicity Characteristic Leaching Procedure (TCLP), the Synthetic Precipitation Leaching Procedure (SPLP), and the modified Field Leach Test (FLT_m). The results showed that the residues contained elevated metal concentrations, reaching up to 2.3 g/kg of As, 41.1 g/kg of Fe, and 19.5 g/kg of Al, primarily concentrated in the upper layers of the biofilter. Metals precipitated as oxyhydroxides in the upper and intermediate layers, while secondary sulfides were formed at the bottom of the biofilter. Removal of As occurred mainly via adsorption onto Fe and Al oxyhydroxides in the upper layers. In contrast, reducing conditions in the bottom layers favored the formation of amorphous As sulfide-bearing minerals, such as FeAsS and AsS. Leaching tests (TCLP and SPLP) showed that As concentrations released from the residues met USEPA guidelines, classifying them as non-hazardous with low risk for groundwater contamination. However, 66% of As concentrations in the TCLP tests and 20% in the SPLP tests exceeded the threshold set by the D019 guidelines (0.1 mg/L). Additionally, FLT_m results indicated a high As leaching potential, exceeding 1 mg/L. It is therefore recommended to avoid grinding and drying the post-treatment residues prior to final disposal to limit potential As mobilization.

The second phase of this thesis project involved similar characterization of post-treatment residues from a laboratory biofilter and two pilot-scale field biofilters. In this phase, particular attention was given to the influence of scale effects on As removal mechanisms and residues stability. Thus, twenty samples were collected from the three biofilters, targeting four distinct layers targeting the bottom, middle and upper sections (I-1, A, B, and I-2). As removal mechanisms and As-bearing phases were analyzed through physicochemical and mineralogical characterizations, while the stability of the post-treatment residues was assessed using static leaching tests (TCLP, SPLP, and FLT). The results showed that the post-treatment residues contained high contaminant concentrations, notably As (ranging from 1.2–3.5 g/kg in field pilot biofilters and 2–3.6 g/kg in the laboratory biofilter), Fe (42.9–86.3 g/kg in pilots and 58.4–66.9 g/kg in the laboratory), Al (5.7–7.9 g/kg in pilots and 4.9–6.1 g/kg in the laboratory), and S (5.7–7.9 g/kg in pilots and 1.7–2.4 g/kg in the laboratory), confirming the effectiveness of the treatment process. The dominant phases in all three biofilters were composed of metal oxyhydroxides and silicates. Additionally, the pilot-scale biofilters revealed the presence of Al oxyhydroxides, arsenopyrite (FeAsS), sulfates, and traces of metallic sulfides. In the laboratory biofilter, As retention occurred mainly through adsorption onto Fe(III) oxyhydroxides, whereas, at the field scale, As removal involved precipitation as FeAsS, coprecipitation with Fe(III) and Al oxyhydroxides, and adsorption in the upper layers. Static leaching tests (TCLP, SPLP, and FLT) confirmed that most of the residues complied with USEPA regulations, classifying them as non-hazardous and suitable for co-disposal with municipal waste. Additionally, the TCLP results did not exceed the recommendations of Table T1-AII of D019, classifying the residues as low-risk.

This work has advanced knowledge on As removal mechanisms in passive biofilters used to treat As-CND, as well as examined the potential mobility of As from post-treatment residues to assess their chemical stability. The findings demonstrated the effectiveness of passive biofilters for As-CND treatment. In addition, the methods developed in this research hold promise for application in the analysis of other post-treatment residues, allowing for more accurate long-term predictions of their behavior and more effective environmental management strategies.

Keywords: contaminated neutral mine drainage, passive biofilter, arsenic removal, leaching tests, post-treatment residues stability

TABLE DES MATIÈRES

LISTE DES TABLEAUX

LISTE DES FIGURES

LISTE DES SIGLES ET ABRÉVIATIONS

ABA	Acid Base Accounting
AMD/DMA	Acid Mine Drainage/Drainage minier acide
ALDs	Anoxic Limestone Drains
AlkD	Alkaline Mine Drainage
As-CND/DNC-As	As-rich Contaminated Neutral Drainage/Drainage neutre contaminé en As
BCR	European Community Bureau of References
CND/DNC	Contaminated Neutral Drainage/Drainage neutre contaminé
C-S-H	Calcium Silicate Hydrates
CWs	Constructed Wetlands
DAS	Dispersed Alkaline Substrate
D019	Directive 019 sur l'industrie minière, Québec, Canada
EDX = EDS	Energy-Dispersive (X-ray) Spectroscopy
EPMA	Electron Probe Microanalyzer
EXAFS	X-ray Adsorption Fine Structure
FLT	Field Leaching Test
FLT_m	Modified Field Leaching Test
HRT/TRH	Hydraulic residence time/Temps de résidence hydraulique
LCA	Life Cycle Analysis
MD	Mine Drainage
MD-S	Mine Drainage Sludge
N-SEP	Non-Sequential Extraction Procedure
OC	Organic Carbon/Carbone organique
OM/MO	Organic Matter/Matière organique

OLCs	Oxic Limestone Channels
OLDs	Oxic Limestone Drains
PBRs/RPB	Passive Biochemical Reactors/Réacteur passif biochimique
PTSs	Passive Treatment Systems
REEs	Rare Earth Elements
REMMD	Règlement sur les effluents des mines de métaux et des mines de diamants
µXRF	Micro X-ray Fluorescence
SEM	Scanning Electron Microscopy
SEP	Sequential Extraction Procedure
S/L	Solid/Liquid
SPLP	Synthetic Precipitation Leaching Procedure
SRB	Sulfate-Reducing Bacteria
S/S	Stabilization/Solidification
$S_{sulfates}$	Sulfates Concentration
TCLP	Toxicity Characteristic Leaching Procedure
TC/CT	Total Carbon/Carbone total
TEM	Transmission Electron Microscopy
TN/NT	Total Nitrogen/Azote total
TOF-SIMS	Time-of-Flight Secondary Ion Mass Spectrometry
TS/ST	Total Sulfur/Soufre total
USEPA	United States Environmental Protection Agency/Agence de protection de l'environnement des États-Unis
XANES	X-ay Adsorption Near-Edge Structure
XAS	X-ray Adsorption Spectroscopy

XPS	X-ray Photoelectron Spectroscopy/Spectroscopie photoélectronique aux rayons X
XRD	X-ray Diffraction
XRF	X-ray Fluorescence
WA	Wood Ash

AVANT-PROPOS

Les travaux de recherche réalisés dans le cadre de cette thèse ont permis d'acquérir des connaissances qui ont été valorisées à travers plusieurs contributions scientifiques. Ces travaux ont donné lieu à des publications dans des revues spécialisées et à des présentations lors de conférences nationales et internationales, ainsi que dans des symposiums scientifiques, avec comités de lecture.

Cette thèse est structurée sous forme d'articles scientifiques. Les chapitres 2, 4, 5 et 6 correspondent à des articles rédigés en anglais, conformément aux exigences des revues et des conférences ciblées. Les autres sections de la thèse sont, quant à elles, rédigées en français.

Je suis l'auteur principal de ces articles, avec la contribution de mon directeur de thèse, la Professeure Carmen Mihaela Neculita, et de mes codirecteurs, les Professeurs Marouen Jouini, Mostafa Benzaazoua et Thomas Pabst, qui apparaissent en tant que coauteurs. Par ailleurs, Dr. Josianne Lefebvre est également coauteure des articles [A2] et [A3], en reconnaissance de sa contribution et collaboration précieuse dans l'analyse des données minéralogiques et de son aide lors de la révision de ces deux publications.

Cette thèse reflète les efforts de recherche menés tout au long de mon parcours doctoral, grâce à la contribution et au soutien de plusieurs partenaires scientifiques.

L’ensemble de ces travaux est présenté ci-dessous.

Articles publiés et/ou acceptés et/ou soumis dans une revue avec comité de lecture

[A1] **Mehdaoui, H.Y.**, Guesmi, Y., Jouini, M., Neculita, C.M., Pabst, T., Benzaazoua, M. (2023) Passive treatment residues of mine drainage: Mineralogical and environmental assessment, and management avenues. *Minerals Engineering* 204: 108362. https://doi.org/https://doi.org/10.1016/j.mineng.2023.108362

[A2] Mehdaoui, H.Y., Jouini., M., Lefevbre, J., Neculita, C.M., Pabst, T., Benzaazoua, M. (2025) Geochemical stability of As-rich residues from a 20-year-old passive field biofilter used for neutral mine drainage treatment. *Ecological Engineering* 216: 107618. https://doi.org/10.1016/j.ecoleng.2025.107618

[A3] Mehdaoui, H.Y., Jouini., M., Lefebvre, J., Neculita, C.M., Pabst, T., Benzaazoua, M., submitted. Stability of As-rich residues from passive pilot biofilters for contaminated neutral mine drainage treatment: Laboratory vs field testing. *Journal of Hazardous Materials* (soumis le 21/03/2025).

Article accepté pour conférence avec comité de lecture

[AC1] Mehdaoui, H.Y., Neculita, C.M., Pabst, T., Benzaazoua, M. (2024) Environmental assessment of post-treatment residues from contaminated neutral drainage: Field case study of Wood-Cadillac biofilter, Quebec, Canada. In: Proc. of the *13th International Conference on Acid Rock Drainage - ICARD*, Halifax, Nova Scotia, Canada, September 16–20.

Présentations de conférences

[C1] Mehdaoui, H.Y., Guesmi, Y., Jouini, M., Neculita, C.M., Pabst, T., Benzaazoua, M. (2024) Passive treatment residues of mine drainage: Mineralogical and environmental assessment, and management avenues. In: *Proc. of the 5th Edition of world Congress on Geology & Earth Science*, Lisbon, Portugal, September 09–11.

[C2] Mehdaoui, H.Y., Neculita, C.M., Pabst, T., Benzaazoua, M. (2024) Environmental assessment of post-treatment residues from contaminated neutral drainage: Field case study of Wood-Cadillac biofilter, Quebec, Canada. In: *Proc. of the 13th International Conference on Acid Rock Drainage - ICARD*, Halifax, Nova Scotia, Canada, September 16–20.

Présentation de séminaires

[S1] Mehdaoui, H.Y., Neculita, C.M., Pabst, T., Benzaazoua, M., (2024) Étude de la stabilité environnementale des résidus de post-traitement du drainage neutre contaminé en As : Étude de cas – Biofiltre Wood-Cadillac, Québec, Canada. *Colloque IRME*, UQAT, Rouyn-Noranda, QC, Canada, 07 novembre.

CHAPITRE 1 INTRODUCTION

1.1 Cadre général du projet

L'activité minière est un des principaux piliers de l'économie du Québec. En même temps elle est à l'origine de plusieurs enjeux environnementaux dus aux différents rejets solides et liquides produits au fil du temps (Bussière and Guittonny, 2021). Les sites miniers abandonnés, considérés comme un défi majeur pour le gouvernement, sont générateurs de différents types de drainage minier, notamment le drainage minier acide (DMA) et le drainage minier neutre contaminé (DNC) (Turcotte et al., 2021).

Durant les dernières décennies, beaucoup d'efforts de recherche ont été consacrés pour l'étude du DMA (Aubertin et al., 2015). Une compréhension des différents mécanismes de génération ainsi qu'une connaissance des meilleures options existante de systèmes de traitement a été acquise (Neculita et al., 2021). Des études récentes ont même déterminé les conditions de gestion recommandées pour les solides issus du traitement passif d'un DMA ferrière en climat froid (Jouini et al., 2021). En revanche, à ce jour, les connaissances sur le traitement passif du DNC-As et la stabilité des solides de post-traitement passif contaminés en As sont limitées.

Un DNC est caractérisé par un pH neutre à légèrement basique (6,5-9) et des concentrations faibles en métaux et métalloïdes excédant les règlementations en vigueur (Nordstrom et al., 2015). Un DNC-As est caractérisé par des concentrations en As excédant les critères imposés par les législations provinciales (D019; MELCCFP, 2025) et fédérales (REMMD; Ministère de Justice, 2025). Des mesures préventives/réparatrices sont ainsi nécessaires pour acquérir une meilleure compréhension des voies de traitement permettant la gestion et le traitement du DNC-As.

Les systèmes de traitement passif (PTSs), ayant l'avantage de leurs faibles coûts d'installation et leur pseudo-autonomie, ont démontré leur efficacité pour les sites miniers abandonnés et éloignés en voie de restauration (Neculita et al., 2021). L'efficacité des PTSs pour l'enlèvement de l'As a été déjà confirmée dans la littérature à l'échelle du laboratoire (Calugaru et al., 2019; Dabrowska et al., 2021; Lee et al., 2018), à l'échelle pilote (Sekula et al., 2018) et à l'échelle de terrain (Germain and Gagnon, 2013; Libero, 2007). Cette efficacité dépend de plusieurs facteurs à savoir la chimie de l'effluent, les conditions du site et les critères de design des systèmes, en particulier le temps de résidence hydraulique (TRH). Ce dernier doit être bien choisi un afin de permettre un

traitement efficace de l'effluent sans détériorer trop rapidement les propriétés hydrauliques des matériaux de remplissage utilisés (Neculita et al., 2021).

Les PTSs, y compris les biofiltres, produisent inévitablement des résidus de post-traitement en quantités significatives, dont la stabilité peut varier. Une gestion responsable de ces résidus est essentielle afin de prévenir tout risque de contamination future (McCann and Nairn, 2022; Mehdaoui et al., 2023). La caractérisation environnementale de ces résidus est dument nécessaire pour évaluer leurs stabilité et décider les meilleures méthodes de gestion. Par ailleurs, des résidus riches en métaux issus des réacteurs passifs biochimiques (RPB) ont été considérés comme non dangereux et stables sur le plan environnemental (Jong and Parry, 2005). De même, les solides extraits des bassins d'oxydation utilisés dans les traitements passifs ont été classés comme non dangereux (McCann and Nairn, 2022). En revanche, les résidus issus des substrats alcalins dispersés à base de MgO (MgO-DAS) présentent un risque élevé de lixiviation, nécessitant leur stockage dans un environnement sec afin de limiter leur impact potentiel (Macias et al., 2012). Plusieurs études ont montré l'instabilité des résidus générés par les RPB lors du traitement d'un DMA riche en Fe et ont recommandé leur entreposage sous une colonne d'eau ou dans un milieu à pH neutre afin d'atténuer leur capacité de lixiviation (Genty et al., 2012). Par ailleurs, les résidus métalliques issus des RPB, susceptibles de libérer du Cu, Fe, Mn, Ni et Zn, doivent impérativement être stabilisés avant tout stockage ou réutilisation afin de limiter leur impact sur l'environnement (Jouini et al., 2020).

Ainsi, bien que les PTSs constituent une approche efficace et économique pour la gestion du DNC-As, la stabilité des résidus de post-traitement demeure un enjeu crucial. Une caractérisation approfondie de ces résidus est nécessaire afin d'évaluer leur potentiel de lixiviation et d'identifier les meilleures stratégies de gestion à long terme. Dans ce contexte, il est essentiel de mieux comprendre les mécanismes de rétention de l'As dans les PTS et d'anticiper le comportement des solides générés. La section suivante exposera la problématique de cette étude en mettant en lumière les lacunes scientifiques et les défis à relever.

1.2 Problématique du projet

À présent, bien que plusieurs études aient été orientées sur l'efficacité des PTSs face à un DNC contaminé en métaux, peu d'études ont été réalisées concernant le DNC-As. Aucune de ces dernières n'a examiné l'efficacité des biofiltres passifs face à un DNC-As réel en allant de l'échelle

du laboratoire jusqu'à celle du terrain. L'objectif principal du présent projet est l'évaluation et la quantification des proportions relatives des mécanismes d'enlèvement de l'As (précipitation, sorption, complexation, échange ionique), la stabilité chimique des résidus du post-traitement passif et leur comportement environnemental.

1.3 Originalité du projet

La contribution originale de ce projet se situe au niveau de (1) la comparaison rigoureuse des phases minérales porteuses de l'As dans les résidus issus des biofiltres ayant traité le DNC-As à différentes échelles : laboratoire, pilote de terrain et biofiltre réel de terrain, (2) l'approfondissement des connaissances quant aux mécanismes d'enlèvement de l'As dans les biofiltres passifs en climat froid ainsi que la stabilité des solides de post-traitement, (3) la réalisation de la première étude qui porte sur un biofiltre passif de terrain (Wood-Cadillac) traitant un DNC-As pour plus que 20 ans.

1.4 Hypothèses de recherche

Les hypothèses de la présente étude sont les suivantes :

1. Les résidus de post-traitement une fois excavés pourraient générer de la contamination.
2. Le TRH et les concentrations d'As, de Fe et des sulfates influencent les mécanismes d'enlèvement (sorption vs (co)-précipitation) de l'As dans les biofiltres passifs.
3. La nature des phases minérales porteuses de l'As dans les résidus de post-traitement est influencée par l'effet d'échelle (laboratoire vs pilote de terrain vs pleine échelle).
4. La stabilité des résidus de post-traitement peut être influencée par l'échelle du biofiltre.

1.5 Objectifs

1.5.1 Objectif général

L'objectif général du projet vise d'évaluer et quantifier la contribution relative des mécanismes d'enlèvement de l'As et sa mobilité potentielle à partir des biofiltres passifs traitant un DNC-As à différentes échelles (laboratoire, pilote et terrain).

1.5.2 Les objectifs spécifiques

Pour atteindre l'objectif principal, les objectifs spécifiques (OS) sont les suivants:

OS1- Évaluer et quantifier les mécanismes et les processus qui régissent l'immobilisation de l'As dans les biofiltres passifs à différentes échelles.

OS2- Évaluer la stabilité des solides de post-traitement passif contaminés en As.

OS3- Évaluer l'effet de l'échelle du biofiltre sur la nature des phases minérales porteuses d'As, sur la stabilité des résidus et sur le potentiel de lixiviation à court terme.

1.6 Contenu de la thèse

Cette thèse s'articule autour de huit chapitres, dont quatre sont présentés sous forme d'articles scientifiques publiés ou soumis à des revues (trois) et conférences (un) avec comité de lecture.

Le chapitre introductif expose le cadre général ainsi que la problématique liée aux résidus de post-traitement générés en fin de cycle de vie à partir des biofiltres passifs dédiés au traitement du DNC-As. Une synthèse des principaux systèmes de traitement passif du drainage minier et en particulier du DNC a été brièvement rappelée. Par ailleurs, une discussion succincte concernant la gestion et la stabilité des résidus post-traitement a été réalisée. Cette première section a également permis de définir la problématique générale, de souligner l'originalité du projet, de formuler les hypothèses de recherche, de préciser les objectifs globaux et spécifiques de l'étude, ainsi que de présenter la structure générale du manuscrit.

Le deuxième chapitre a été rédigé sous forme d'article scientifique et publié dans la revue *Minerals Engineering* (2023). Il présente une synthèse de la littérature récente et pertinente sur le traitement du DNC-As, tout en soulignant le nombre relativement limité d'études de terrain consacrées à cette problématique spécifique. La caractérisation des résidus de post-traitement issus du traitement du DMA et du DNC-As est également abordée, avec une attention particulière aux facteurs influençant leur stabilité environnementale. Une analyse approfondie a été menée pour identifier les phases minérales porteuses d'As et comprendre leur rôle dans les mécanismes de rétention de ce dernier et dans la limitation de sa remobilisation à partir des résidus post-traitement sous diverses conditions environnementales. Enfin, les différentes stratégies de valorisation, de réutilisation et

de disposition des résidus de post-traitement sont présentées en tenant compte des contraintes liées à leur gestion et les risques environnementaux associés.

Le troisième chapitre décrit la démarche méthodologique mise en œuvre dans le cadre de ce projet, soit une revue de la littérature approfondie, l'échantillonnage des résidus post-traitement issus des biofiltres passifs étudiés, la caractérisation physicochimique et minéralogique des résidus collectés, et enfin, les essais de lixiviation statiques. Par ailleurs, une attention particulière a été accordée au transfert des connaissances acquises à partir du site de référence Wood-Cadillac pour l'application de ces solutions à d'autres sites ayant la problématique du DNC-As.

Le quatrième chapitre, présenté sous forme d'un article de conférence scientifique et qui a été publié dans les comptes-rendus de la conférence *ICARD 2024*, est lié aux objectifs spécifiques OS1 et OS2 de la présente thèse pour le site de référence Wood-Cadillac. Dans ce chapitre, l'étude porte sur la variation verticale des propriétés physicochimiques et environnementales des résidus de post-traitement. Les résultats ont montré que le biofiltre a permis la rétention des contaminants avec des concentration importantes de contaminants en particulier d'As (2,3 g/kg) de Fe (41,5 g/kg) et d'Al (19,5 g/kg). Il a été constaté que les couches superficielles (A : 0-30 cm et B : 30-60 cm) sont plus riches en métaux et en As comparant à la couche du fonds (C : 60-90 cm). Les résultats des essais statiques (TCLP et SPLP), en se référant aux réglementations de l'USEPA, ont montré que les résidus étaient non-dangereux et que leurs lixiviats ne présentent pas un potentiel de contamination des eaux de surface. Toutefois, ces résidus ont échoué les concentrations d'As selon la directive D019. Également, des écart-types élevés ont été trouvés suggérant une variation horizontale des propriétés des résidus de post-traitement dans chaque unité étudiée (A, B et C). Il a été recommandé de réaliser une caractérisation physico-chimique et environnementale de tous les échantillons pour détecter les variations entre les placettes tout en la combinant avec une caractérisation minéralogique permettant de révéler les phases minérales porteuses d'As et quantifier les mécanismes d'enlèvement.

Le cinquième chapitre, présenté sous forme d'un article scientifique sous presse dans la revue *Ecological Engineering* (2025), est la continuité du chapitre 4, traitant les objectifs spécifiques OS1 et OS2 de la thèse avec un focus sur les résidus de post-traitement du biofiltre Wood-Cadillac. Ce chapitre discute particulièrement :

- La caractérisation physicochimique et minéralogique des résidus de post-traitement avec un focus sur la variation horizontale des propriétés entre les placettes du chaque horizon
- L'évaluation des mécanismes d'enlèvement d'As au sein du biofiltre Wood-Cadillac et l'identification des phases minérales porteuses d'As
- La prédiction du comportement environnemental des résidus de post-traitement et les risques de lixiviation d'As.

Les résultats ont confirmé les observations du chapitre 4 quant aux concentrations des contaminants dans les résidus de post-traitement. Il a été constaté que les oxyhydroxydes métalliques (Fe, Al) ont été prépondérants dans les couches superficielles du biofiltre (0-60 cm) tandis que les sulfures métalliques et les sulfures d'As se concentrent principalement au fonds du système (60-90 cm). Cette répartition des phases minérales a permis de confirmer l'enlèvement de l'As via la sorption sur les oxyhydroxydes métalliques (mécanisme de rétention principal) dans la partie supérieure du biofiltre, ainsi que la précipitation sous forme de sulfures d'As dans les couches du bas caractérisées par un milieu réducteur. D'un point de vue environnemental, aucun des résultats issus des tests TCLP et SPLP n'a dépassé les seuils réglementaires établis par les directives de l'USEPA, indiquant ainsi une faible mobilité potentielle de l'As et permettant de classer les résidus comme non dangereux. Toutefois, 66 % des concentrations mesurées lors des essais TCLP et 20 % lors des tests SPLP ont échoué les recommandations de 0,1 mg/L fixé par la directive D019 pour les effluents miniers. Ces dépassements suggèrent qu'en cas de modifications physico-chimiques du milieu (acidification ou changement de pH), une mobilisation partielle de l'As dans les résidus de post-traitement pourrait survenir, posant un risque pour l'environnement. De plus, les analyses FLT_m ont révélé un potentiel élevé de lixiviation de l'As, avec des concentrations supérieures à 1 mg/L. Il est recommandé d'éviter le séchage et le concassage de ces résidus avant leur disposition finale. Ces résultats contribueront à l'optimisation des stratégies de gestion des résidus contenant des concentrations élevées en As.

Le sixième chapitre, présenté également sous forme d'un article scientifique, soumis pour une publication potentielle dans la revue *Journal of Environmental Management*, traite les objectifs spécifiques OS1, OS2 et OS3 de la thèse, et s'intéresse spécifiquement aux résidus de post-traitement du biofiltre de laboratoire et des biofiltres pilotes de terrain :

- La caractérisation physico-chimique et minéralogique des résidus de post-traitement collectés à partir de biofiltres
- La quantification des mécanismes d'enlèvement d'As
- La prédiction du comportement environnemental des résidus de post-traitement via des essais statiques et l'évaluation des conditions de stabilité à court terme
- La comparaison de la nature des phases minérales prépondérantes et des mécanismes d'enlèvement d'As à entre l'échelle du laboratoire et du pilote de terrain versus le biofiltre de terrain de référence Wood-Cadillac.

Les résultats de la composition chimique des résidus de post-traitement ont montré des teneurs élevés en contaminants (As, Al, Fe, S) confirmant l'efficacité des biofiltres pour le traitement du DNC-As. Les oxyhydroxydes métalliques et les silicates étaient les principales phases observées dans les trois biofiltres étudiés. Dans le biofiltre de laboratoire, la rétention de l'As était principalement gouvernée par des mécanismes d'adsorption sur les oxyhydroxydes de fer (Fe(III)). L'enlèvement de l'As à l'échelle pilote s'effectuait par précipitation sous forme d'arsénopyrite (FeAsS) dans le fonds du biofiltre, ainsi que par coprécipitation avec des oxyhydroxydes métalliques (Fe et Al), tandis que les mécanismes d'adsorption semblaient prédominants dans les couches supérieures du biofiltre principalement au tour des entrées du système. Des traces de sulfures métalliques ont été également observés dans ces résidus post-traitement dans les couches profondes principalement à proximité de l'exutoire. L'ensemble des tests statiques (TCLP, SPLP et FLT) respectait les seuils réglementaires définis par l'USEPA, permettant de classer les résidus comme non dangereux et permettant d'envisager leur co-disposition avec les déchets municipaux. Également, les résultats du TCLP n'ont pas dépassé les recommandations de table T1-AII de la D019, classifiant les résidus à faible risque. Les prochains travaux devraient se concentrer sur la stabilité à long terme des résidus de post-traitement en utilisant des tests cinétiques.

Le septième chapitre propose une discussion générale et intégrée des principaux résultats obtenus au cours de cette étude, en mettant en lumière les aspects clés développés tout au long de la thèse. Cette analyse prend en compte plusieurs paramètres déterminants : l'influence de l'échelle du biofiltre (laboratoire vs pilote vs terrain), les conditions spécifiques des tests statiques (nature de la solution de lixiviation, pH et la durée des essais), les seuils réglementaires de concentration d'As, la composition du mélange de remplissage utilisé dans les biofiltres, la durée des expériences, les

concentrations initiales d'arsenic dans DNC-As, la co-présence d'autres contaminants et les conditions oxydo-réductrices qui influencent les mécanismes de rétention et de précipitation. Ce chapitre vise ainsi à fournir une vue d'ensemble des performances des biofiltres passifs face à un DNC-As tout en identifiant les facteurs pouvant améliorer la gestion des résidus post-traitement contaminés à l'As.

Enfin, le huitième chapitre expose les conclusions générales tirées des travaux menés au cours de cette étude, en mettant de l'avant les contributions scientifiques et pratiques apportées par cette recherche. Ce chapitre propose également des recommandations pour l'amélioration des biofiltres à différentes échelles, ainsi que des perspectives visant à optimiser la gestion des résidus post-traitement contaminés à l'As et à orienter les recherches futures dans ce domaine.

1.7 Organisation de la thèse

Cette thèse est structurée en trois parties visant à évaluer le potentiel de lixiviation de l'As des résidus post-traitement du DNC-As issus de quatre biofiltres : un installé sur site (Wood-Cadillac), un en laboratoire et deux pilotes expérimentaux sur le terrain (Newmont-Éléonore) (Figure 1.1).

La première partie consiste en une revue détaillée de la littérature scientifique relative au sujet, permettant de mieux cerner la problématique et d'identifier les besoins de recherche.

La deuxième partie de l'étude visait le site de Wood-Cadillac avec la préparation d'un plan d'échantillonnage représentatif couvrant l'ensemble de la surface et de la profondeur du biofiltre. Cette partie inclut la récupération des résidus post-traitement, suivie d'une caractérisation détaillée physicochimique, minéralogique et environnementale de ces résidus.

La troisième partie visait la mise en place, la contribution au suivi et au démantèlement du biofiltre de laboratoire ainsi que des deux biofiltres pilotes de terrain. Tous les échantillons ont ensuite fait l'objet d'une caractérisation physicochimique, minéralogique et environnementale.

À noter que tous les résidus post-traitement récupérés des différents biofiltres ont été soumis à la même démarche de caractérisation. D'abord, la caractérisation physicochimique consistait à déterminer le pH de la pâte, l'humidité, la teneur en métaux, le carbone total (CT), le carbone inorganique (CI), le carbone organique (CO), le soufre total (ST), le soufre sulfate et l'azote total (NT). Ensuite, la caractérisation minéralogique via la spectroscopie photoélectronique aux rayons X (XPS) a servi pour l'identification les phases minérales présentes en particulier celles porteuses

de l'As, ainsi que pour déterminer l'état d'oxydation des éléments et quantifier les mécanismes d'enlèvement de l'As. Finalement, la mobilité potentielle de l'As a été étudié via trois essais de lixiviation statiques : TCLP, SPLP et FLT, et FLT_m. Les trois essais ont été réalisés en batch unique, avec une variation des pH de la solution de lixiviation, de la nature de la solution de lixiviation et de la durée de contact. Ces essais ont permis d'évaluer non seulement les risques de lixiviation de l'As, mais aussi classier les résidus (dangereux ou non-dangereux), de déterminer les meilleures options de stockage, et de déterminer les risques de lixiviation en cas de conditions extrêmes (pluie acides).

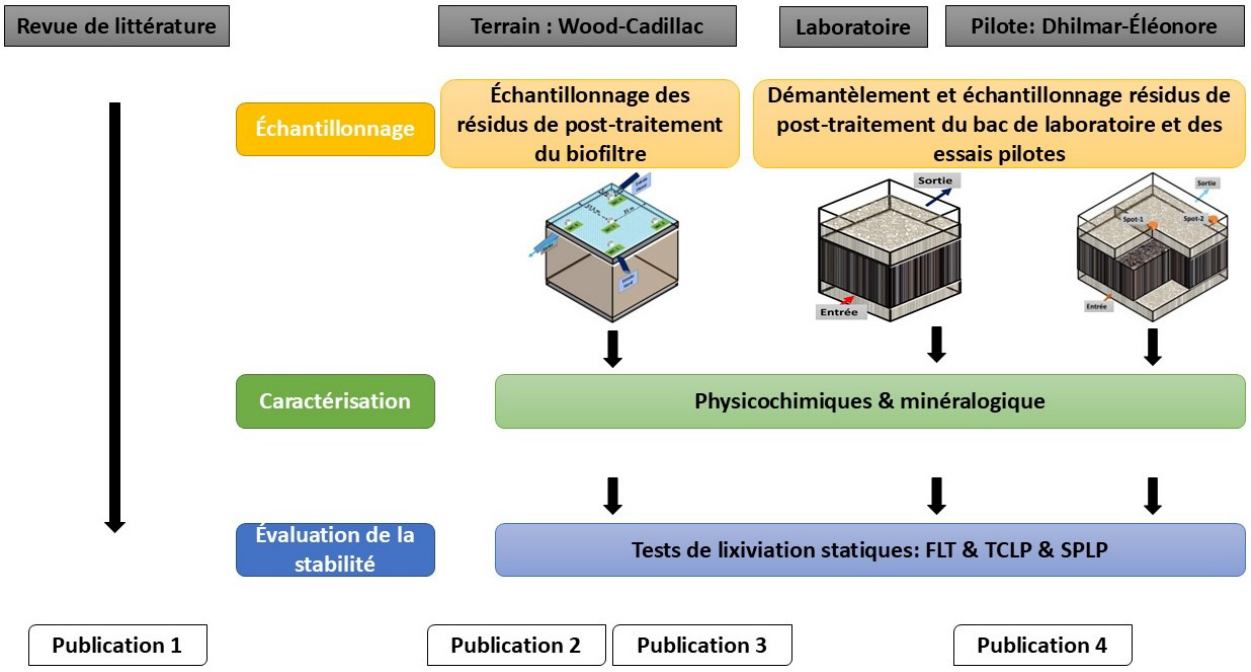

Figure 1.1 Méthodologie du projet de thèse

CHAPITRE 2 ARTICLE 1 _ PASSIVE TREATMENT RESIDUES OF MINE DRAINAGE: MINERALOGICAL AND ENVIRONMENTAL ASSESSMENT, AND MANAGEMENT AVENUES[1]

Hsan Youssef Mehdaoui[1], Youssef Guesmi[1], Marouen Jouini[1], Carmen Mihaela Neculita[1,2,*], Thomas Pabst[1,3] and Mostafa Benzaazoua[1,4]

[1] Research Institute on Mines and Environment (RIME), Université du Québec en Abitibi-Témiscamingue (UQAT), Rouyn-Noranda, QC J9X 5E4, Canada

[2] Canada Research Chair - Treatment and Management of Mine Water, RIME, UQAT, Rouyn-Noranda, QC J9X 5E4, Canada

[3] Civil, Geological and Mining Engineering Department, RIME, Polytechnique Montreal, QC H3T 1J4, Canada

[4] University Mohammed VI Polytechnic (UM6P), Geology and Sustainable Mining Institute (GSMI), Lot 660 Hay Moulay Rachid, 43150, Ben Guerir, Morocco

*Corresponding author email: Carmen Mihaela Neculita

Article publié le 16 septembre 2023 dans la revue *Minerals Engineering*

2.1 Abstract

Passive treatment systems (PTSs) are effective for mine drainage (MD) treatment through chemical and biological processes. The by-products of PTSs represent potential environmental contaminants, but they are also secondary sources for recovering several elements of interest. A literature review on PTSs was conducted, with a focus on the chemical–mineralogical characterization and environmental assessment of PTSs residues and their management options. Precipitation is confirmed as the main mechanism in chemical systems that are more suitable for the treatment of acid mine drainage (AMD). For the treatment of contaminated neutral drainage (CND), characterized by low contaminant concentrations, sorption mechanisms are dominant. Inconsistent prediction of the stability of PTSs residues was reported depending on the type of leaching test, the extracting agent, the duration of the test, the presence of oxygen, and the

---

[1]Mehdaoui, H.Y., Guesmi, Y., Jouini, M., Neculita, C.M., Pabst, T., Benzaazoua, T., 2023. Passive treatment residues of mine drainage: Mineralogical and environmental assessment, and management avenues. *Minerals Engineering*, 204, 108362. https://doi.org/10.1016/j.mineng.2023.108362

regulatory criteria. The combination of chemical–mineralogical characterization with leaching tests was suggested to provide a more realistic prediction of the environmental behavior of PTSs residues. Several options for PTSs residues management were identified. Further studies are needed to select the appropriate leaching tests that assess the mobility of contaminants from PTSs residues and better predict their fate. Techno-economic analyses are also required to evaluate the reprocessing of PTSs residues for their sustainable management.

Keywords: Acid mine drainage, contaminated neutral drainage, post-treatment residues, environmental behavior, waste management.

2.2 Highlights

- Biochemical and geochemical PTSs are efficient for AMD and CND treatment.
- Contaminated residuals from PTSs require a proper assessment of their stability.
- Mineralogy combined with leaching tests gives a good prediction of PTSs residues stability.
- Management options of PTSs residues favor abandonment or their dumping.

2.3 Introduction

Mine drainage (MD) is one of the key environmental challenges facing the mining industry worldwide. MD is usually generated from mining residues and by-products found in active mines or abandoned mine sites that are unrehabilitated (Nordstrom et al., 2015). MD is generated by the oxidation of sulfide minerals in mining waste through chemical, physical, and biological interactions, as well as galvanic processes (Johnson and Hallberg, 2005). Depending on the water chemistry, MD could be acidic (acid mine drainage: AMD), near-neutral (contaminated neutral drainage: CND), or net alkaline (AlkD). Several hazardous metal(loid)s can be found in MD, such as Fe, Al, Cu, Zn, As, and Ni. The accumulation of these contaminants in MD leads to several ecological problems for aquatic life and for the surrounding environment. Passive treatment systems (PTSs) have been developed as a cost-effective and low-maintenance solution for the treatment of MD at abandoned mine sites (Skousen et al., 2017). These systems are based on natural chemical and biological processes, allowing pH increase and removal of metals and metalloids through similar mechanisms relative to semi-passive or active treatment (Skousen et al., 2017; Kleinmann et al., 2023). The treatment process generates contaminated residues/solids containing

the removed contaminants. These solids must be discharged for cleaning or dismantled at the end of the treatment system's life (McCann and Nairn, 2022). The disposed contaminated residues could be a source of further contamination in the case of mismanagement.

Over the past two decades, rising concerns about MD issues have increased environmental restrictions for the discharge of solid and liquid mine waste. Several reviews have been published on MD. Various topics were reviewed, including MD occurrence, prevention options, and conventional treatment strategies (Ben Ali et al., 2019; Johnson and Hallberg, 2005; Kleinmann et al., 2023; Simate and Ndlovu, 2014; Skousen et al., 2017, 2019).

More recently, new trends for AMD treatment methods have been reported (Du et al., 2022). Sustainable approaches for the remediation of AMD have been extensively evaluated (Moodley et al., 2018; Rezaie and Anderson, 2020). A special focus on alternative treatment technologies for water reuse and resource recovery from AMD (Naidu et al., 2019) as well as phytoremediation and bioremediation methods were also reported (Anekwe and Isa, 2023; Thomas et al., 2022). The co-treatment opportunity of MD with other wastewater streams (e.g., industrial, agricultural, domestic) as organic substrates for sulfate reduction in the treatment of AMD was also discussed (Rakotonimaro et al., 2017). Most of the available and reviewed papers were focused on MD occurrence and treatment. However, the assessment of post-treatment residues of MD as well as their proper management were rarely investigated. For example, conventional management options for mine waste were reviewed more than fifteen years ago (Zinck, 2006). Opportunities for the valorization of active treatment sludge were reported (Macías et al., 2017), while the management of waste sludge generated from passive treatment was briefly addressed (Jouini et al., 2021; Rakotonimaro et al., 2018). Recent results about the potential for rare earth elements (REEs) recovery from mine drainage (Royer-Lavallée et al., 2020) and mine residues were also reviewed, with less attention paid to residues generated from passive treatment systems (Costis et al., 2021). A comprehensive study of the contaminated residues, combining mineralogical and environmental assessment, is deemed necessary to select an appropriate sustainable management option (Jouini et al., 2021; Lounate et al., 2021; McCann and Nairn, 2022). In this context, this review aims to fill the gap of literature on this topic, giving insights into this step of the performance of MD treatment for the purpose of proper management of the contaminated residues. A framework to select the assessment plans and the appropriate disposal method for contaminated residues will be also presented.

The first part of the study provides an overview of the main PTSs with a focus on the biochemical systems. The paper then explores the prospective and current methods that are available for the chemical–mineralogical and environmental characterizations of contaminated residues. The environmental assessment of residues generated from these systems is also critically reviewed. The reported management options for contaminated residues and the prediction/evaluation of their economic feasibility and sustainable potential are finally addressed.

2.4 Passive treatment of mine drainage

PTSs are known to be ecofriendly with limited requirements in terms of maintenance after installation (Ben Ali et al., 2019; Ness et al., 2014). They mimic natural biochemical processes to remediate contaminated effluents (Neculita et al., 2021). Commonly, PTSs selection is based on site characteristics and water chemistry, and must also consider other factors including economic costs, flow rate, local topography, targeted contaminants, and environmental requirements (Ben Ali et al., 2019). A methodological approach based on progressive upscaling from small (a few mL) to full scale (hundreds to thousands of m^3) is required for the design of PTSs. For both AMD and CND treatment, the hydraulic residence time (HRT) is the most critical parameter in PTSs design. A long HRT (≥4 days) favors precipitation and coprecipitation of contaminants, while a shorter HRT (a few hours to one day) favors sorption, which is more suitable for the treatment of contaminants with low concentrations, such as in the case of CND (Neculita et al., 2021; Vasquez et al., 2016). The PTSs are commonly divided into two main categories: biochemical systems that rely on bacterial activity stimulated by the presence of organic matter, and chemical systems that are mostly applied for moderately to highly contaminated AMD (Skousen et al., 2017). Multi-step systems were also designed, constructed, and monitored for their performance in the treatment of highly contaminated AMD (for several metallic elements, including Fe and Al) on several mine sites (Genty et al., 2016; Macías et al., 2012). They combine biological, geochemical, and physicochemical processes, in successive units operated under aerobic or anaerobic conditions with an aim to increase water treatment efficiency and extend the lifespan of treatment system (Genty et al., 2016; Skousen et al., 2017). Those treatment systems showed satisfactory results for CND as well (Table 2.1).

A selection of the most used PTSs for AMD and CND treatment is summarized in Figure 2.1 and discussed in detail in the following sections.

2.4.1 Biochemical systems

Biochemical systems are filled with reactive mixtures composed of sulfate-reducing bacteria (SRB) inoculum, organic matter, a structuring agent, and a neutralizing agent (Neculita et al., 2007). The latter component is usually removed for CND treatment (El Kilani et al., 2021). They are classified in surface reactors (passive biochemical reactors), subsurface engineered trenches (permeable reactive barrier), or shallow surface ponds with selected plants (constructed wetlands) (Table 2.2) (Johnson and Hallberg, 2005).

2.4.1.1 Passive biochemical reactors (PBRs)

Passive biochemical reactors (PBRs), also known as bioreactors, are an efficient technology for the treatment of AMD and CND (Neculita et al., 2007; Sekula et al., 2018). For AMD, bioreactors aim to increase the pH (and alkalinity) and favor the precipitation of dissolved metals, mainly in the form of sulfides. Precipitation of oxyhydroxides and carbonates and adsorption of metals also contribute to contaminant removal (Skousen et al., 2017). Because of the low contaminant charge in CND, other removal mechanisms such as sorption, coprecipitation, and ion exchange are also present (Ben Ali et al., 2019).

Performance and long-term efficiency of bioreactors depend mainly on the quality of the inlet water to the treatment system, the depletion rate of organic matter, and weather conditions (e.g., temperature) (Logan et al., 2005; Yim et al., 2015). Bioreactors remain effective PTSs for the removal of contaminants (e.g., Fe, Ni, As, sulfates) and produce a small quantity of generated by-product residues compared to other systems. Post-treatment residues resulting from PBRs are basically metal-rich sludge with varying stability.

2.4.1.2 Permeable reactive barriers (PRBs)

Permeable reactive barriers (PRBs) are engineered systems aiming for the removal of dissolved contaminants from MD based on both physicochemical and biological mechanisms. They consist of a trench filled with a mixture of organic and inorganic materials that react with the inlet water to remove metals and metalloids (Blowes et al., 2000; USEPA, 2014). The selection of the reactive media is based on the nature of the contaminants, the chemistry of the inlet water, and the treatment target (De Repentigny et al., 2018). In PRB systems, removal of contaminants mainly occurs via

precipitation and adsorption, resulting in post-treatment residues consisting of immobilized contaminants in the form of precipitates, and coated reactive materials.

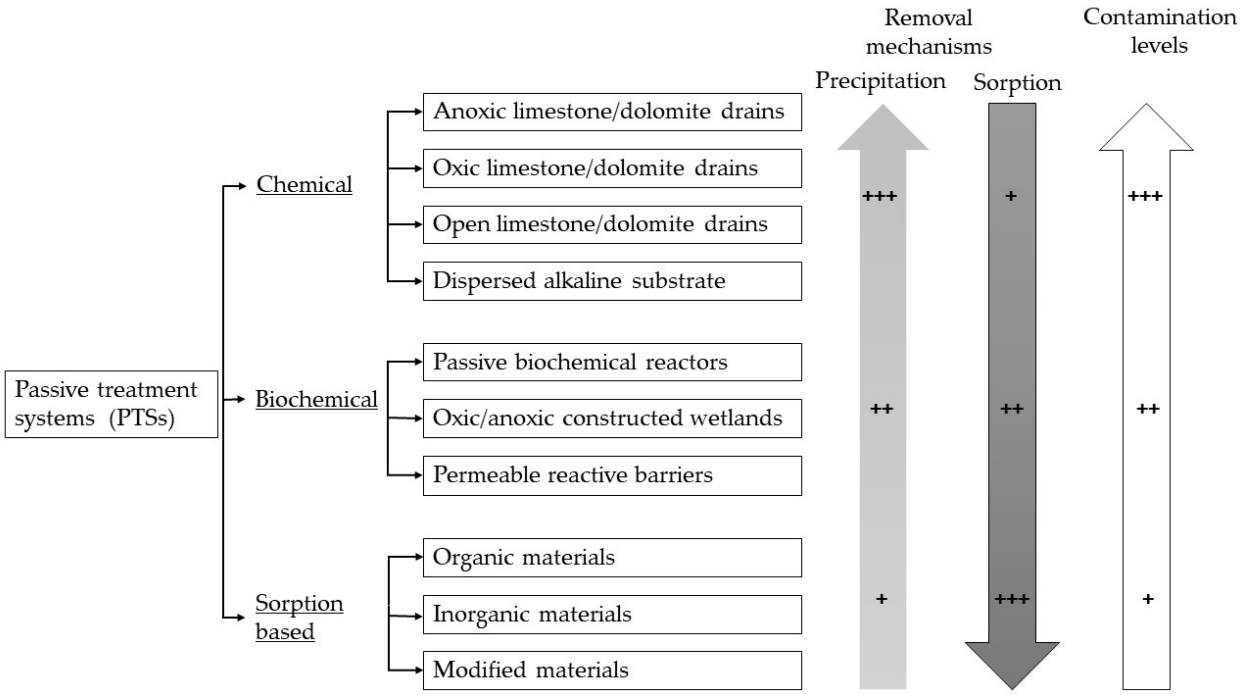

Figure 2.1 Passive treatment systems (PTSs) for acid mine drainage (AMD) and contaminated neutral drainage (CND) as well as the main involved mechanisms discussed

2.4.1.3 Constructed wetlands (CWs)

Constructed wetlands (CWs) are efficient and sustainable technologies for MD treatment, when operated in oxic or anoxic conditions (USEPA, 2014). They involve a combination of several biogeochemical processes such as plant uptake, biological reduction, filtration, oxidation, precipitation, and adsorption to remove contaminants (Ness et al., 2014). Oxic CWs are designed for net alkaline water treatment, while anoxic CWs are more suitable for net acidic waters (Johnson and Hallberg, 2005; Skousen and Ziemkiewiez, 2005; Taylor et al., 2005). Oxic CWs provide a longer retention time for ferrous (Fe^{2+}) to ferric (Fe^{3+}) iron oxidation and its subsequent precipitation as hydroxides. Anoxic CWs rely on organic-rich substrates that remove the oxygen from the water, creating anaerobic conditions. Post-treatment residues in CWs consist of contaminated sediments originating from decaying plants and inorganic precipitates.

2.4.2 Chemical systems

Chemical systems rely on neutralizing materials (e.g., limestone, dolomite) to increase the alkalinity and pH and enhance metals precipitation. Depending on the system hydraulics and filling materials, adsorption and ion exchange may contribute to metal removal. The efficiency and performance of chemical systems are very sensitive to climatic conditions (Skousen et al., 2017). A drop in temperature and freeze/thaw cycles may change the hydraulic properties inside those systems and, in consequence, influence contaminant removal rates (El Kilani et al., 2021). Anoxic limestone/dolomite drains, oxic limestone/ dolomite drains, oxic limestone/dolomite channels, and dispersed alkaline substrates are the most frequently applied systems. Chemical systems generate considerable amounts of limestone/dolomite materials associated with metal oxyhydroxides. Thus, the management of such residues may be problematic.

2.4.2.1 Anoxic limestone drains (ALDs)/anoxic dolomite drains

Anoxic limestone drains (ALDs) are widely used for MD treatment, mainly for AMD rich in Fe. ALDs are composed of engineered anoxic trenches filled with limestone/dolomite through which flows the influent. Those trenches are usually encapsulated in a plastic liner and covered with clay or compacted soil to prevent the entry of oxygen (USEPA, 2014). Inside the ALD, the dissolution of limestone/dolomite increases the pH and alkalinity, thus contributing to the precipitation of metals following the oxidation of Fe^{2+} to Fe^{3+} at the output of the drain (Iii and Trahan, 1999). The performance of ALDs depends on the properties of the filling materials (i.e., grain size, reactivity, purity), dissolved oxygen concentration and the quality of the influent (Neculita et al., 2021; Taylor et al., 2005).

2.4.2.2 Oxic limestone drains (OLDs)/oxic dolomite drains and oxic limestone channels (OLCs)

Unlike ALDs, oxic limestone drains (OLDs) and oxic limestone channels (OLCs) are designed to treat AMD in the presence of O_2. OLDs allow AMD to flow through the drain, while the design of OLCs favors the percolation of water on the surface of the reactive material. In both cases, acidity neutralization and metal oxidation of AMD occur within the system, contributing to the precipitation of metal hydroxides and sulfates (Genty et al., 2012a; Skousen et al., 2017). OLDs

Table 2-1 Examples of multi-step treatment systems.

Multistep system			**Removal efficiency (%)**	**References**
Effluent (Contaminants)	**Scale (Location)**	**Units**		
AMD (Fe, Mn, SO_4^{2-})	Pilot-scale (Columbia)	Unit 1: Dispersed alkaline substrate Unit 2: Three open passive biochemical reactors Unit 3: Three closed passive biochemical reactors	Fe (80), Mn (60), SO_4^{2-} (91)	Vasquez et al. (2022)
AMD (As, Cu, Fe, Mo, Ni, Zn)	Full-scale (Spain)	Unit 1: Natural Fe-oxidizing lagoon Unit 2: Two reactive tanks (CaO-DAS) Unit 3: Decantation ponds	Unit 1: As (60); Fe (17); Mo (83); Sb (100) Unit 2: As (100); Al (100); Cu (70); Ni (70) Unit 3: Fe (12); Zn (23)	Orden et al. (2021)
AMD (Fe)	Full-scale (Canada)	Unit 1: Sulfate-reducing passive biofilter 1 Unit 2: Wood ash unit Unit 3: Sulfate-reducing passive biofilter 2	Fe (70); SO_4^{2-} (57)	Jouini et al. (2020b); Genty et al. (2016)
CND (As, Se)	Pilot-scale (Slovakia)	Unit 1: Settling reactor Unit 2: Reactor with Fe fillings	As (89); Sb (84)	Sekula et al. (2018)
AMD (As, Cu, Fe, Mn, Zn)	Pilot-scale (USA)	Unit 1: Rock-lined aeration channel Unit 2: Sedimentation tank Unit 3: Peat biofilter Unit 4: SRB reactor Unit 5: Re-aeration limestone drain	Unit 3: As (20); Cu (34); Ni (27) Unit 4: Mn (64); Zn (31)	Clyde et al. (2016)

AMD = Acid Mine Drainage; DAS =Dispersed Alkaline Substrate; CND =Contaminated Neutral Drainage; SRB =Sulfate-Reducing Bacteria.

and OLCs are common choices for low-cost AMD treatment but require ongoing maintenance to maintain their efficiency (Ouakibi et al., 2013; Taylor et al., 2005).

2.4.2.3 Dispersed alkaline substrate (DAS)

Dispersed alkaline substrate (DAS) is a new passive treatment system designed for highly contaminated AMD (Rötting et al., 2008). The primary upgrade of DAS systems (vs limestone/dolomite drains) is the intense dissolution rate of the small grains of neutralizing substances, which delays the passivation of materials and maintains the hydraulic parameters of the DAS system (Ayora et al., 2013). This technology can be integrated into individual units: CaO-DAS reactors, MgO-DAS reactors (Orden et al., 2021) or wood-ash-DAS reactors (Rakotonimaro et al., 2016). The filling mixture of DAS-based systems consists of the combination of a coarse inert matrix (e.g., wood chips) and fine-grained alkaline reagents (e.g., calcite-$CaCO_3$, magnesia-MgO, wood ash) separated by aeration and settling ponds (Macías et al., 2012; Rötting et al., 2008; Rakotonimaro et al., 2016). The first component provides high porosity to delay clogging issues, while the second provides a highly reactive surface and complete dissolution prior to passivation of the surface (Ayora et al., 2013; Orden et al., 2021). DAS systems are more effective when coupled with other biological and/or abiotic treatment units. When used alone, the DAS lifetime is reduced (Ayora et al., 2013; Macías et al., 2012).

Biochemical and chemical PTSs are efficient for MD treatment. However, the selection of the appropriate system requires sufficient knowledge of the effluent chemistry and treatment objective, selection of the appropriate materials (geotechnical and mineralogical composition), and consideration of the climatic conditions (Figure 2.2). The environmental behavior and geochemical stability of PTSs residues also remain critical aspects that helps to better anticipate the residues fate.

Table 2-2 Examples of passive treatment biochemical systems for acid mine drainage (AMD) and contaminated neutral drainage (CND).

Treatment system				Removal efficiency		
Type	**Effluent**	**Scale**	**Location**	**(%)**	**Mechanisms**	**References**
Bioreactor	AMD, CND	Laboratory columns	Canada	Cu (99), Fe (90), Ni (99), SO_4^2(99)	Precipitation, sorption	Ben Ali et al. (2020)
Bioreactor	CND	Field-pilot	Slovakia	As (89); Sb (84)	Precipitation, co-precipitation, sorption	Sekula et al. (2018)
Permeable reactive barrier	AMD	Laboratory weathering cell	China	Cu (99), Zn (100)	Precipitation	Hu et al. (2022)
Permeable reactive barrier	AMD	Field	Spain	Al (96), Cu (98), Zn (95)	Precipitation, co-precipitation, sorption	Gibert et al. (2011)
Permeable reactive barrier	AMD	Field	Canada	Fe (90), Ni (99), SO_4^{2-}(99)	Precipitation	Benner et al. (2002); Benner et al. (1999)
Constructed wetland	AMD	Laboratory columns	China	Cu (99), Cd (97), Cr (93), Fe (76), Zn (94)	Precipitation, adsorption, complexation, cation exchange	Chang et al. (2022)
Oxidizing system and slag leaching beds	CND	Field-pilot	New Zealand	Fe (82–96), Mn (99)	Precipitation, sorption	Trumm and Pope (2015)

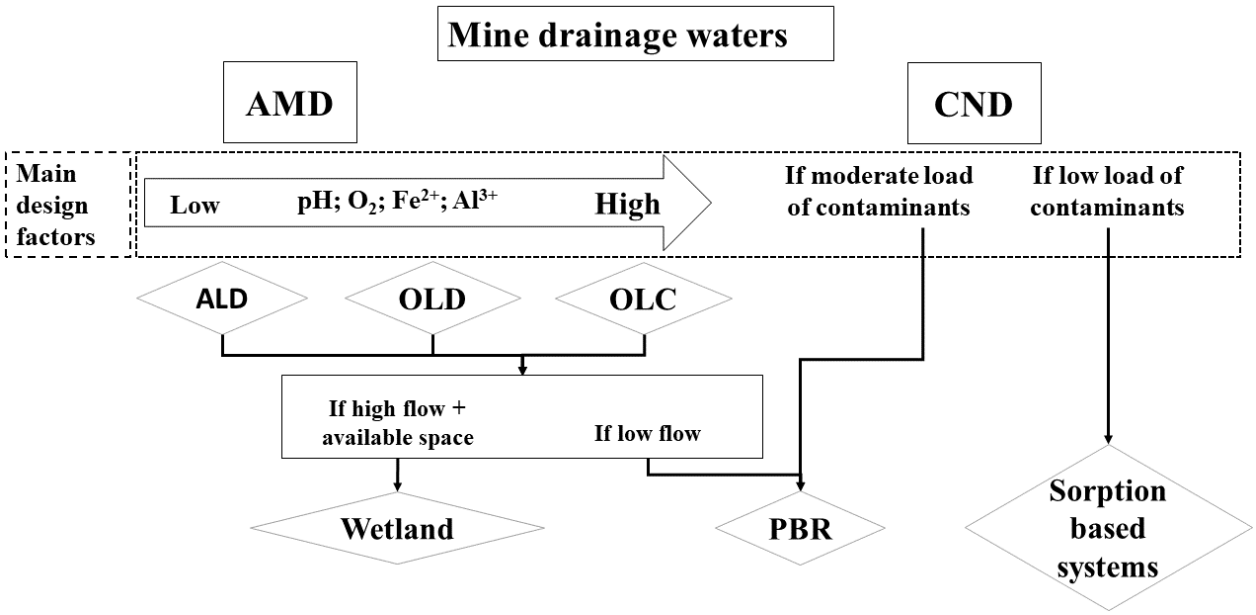

Figure 2.2 Flowchart for selecting passive treatment systems (PTSs) discussed in this paper. AMD = Acid Mine Drainage; CND = Contaminated Neutral Drainage; ALD = Anoxic Limestone Drain; OLD = Oxic Limestone Drain; OLC = Oxic Limestone Channel; PBR = Passive Biochemical Reactor.

2.5 Mineralogical and environmental characterization of passive treatment systems (PTSs) residues

2.5.1 Mineralogical characterization

The mineralogical characterization of the newly formed minerals in the residues is required for several purposes. A mineralogical assessment during periodic monitoring of the treatment systems, in addition to the chemical composition analysis, provides the needed information to optimize remediation design. Current studies consider a mineralogical assessment essential for predicting the long-term stability and potential economic benefits of the generated residues (Jouini et al., 2021). Characterization of the mineralogical composition of the solid samples is crucial to provide input data for geochemical simulations (e.g., PHREEQC) and to predict the quality of mine drainage (Alpers et al., 1999). Moreover, the mineralogical analysis could provide information about removal mechanisms during the treatment process. Oxyhydroxide adsorption of metals and metalloids (Xie et al., 2018).

An accurate and meaningful mineralogical assessment requires the consideration of several factors from the field/lab sampling step to sample preparation. The sampling process should be carefully planned and executed to ensure representative samples of the PTSs residues. Proper sample preservation is crucial to prevent oxidation or other chemical reactions that may alter the minerals present in the sample. Samples should be preserved in a cold environment, and it may be necessary to store them under such conditions until they are analyzed (Wilkin, 2006). The sample preparation for mineralogical assessment depends on the type of analysis that will be performed. Following specific drying procedures is mandatory for samples that need to be dried before analysis. For instance, oven drying is not recommended, as it may affect the sample's crystallinity. Moreover, air drying should be conducted in a glove box or glove bag supported by a continuous supply of dry, oxygen-free nitrogen or argon gas to prevent oxidation (Roy et al., 1992).

A summary of characterization tools used for the mineralogical assessment of post-treatment residues is presented in Table 2.3. A short description of the most widely used techniques and main minerals found in PTSs residues is given hereafter.

2.5.1.1 Characterization methods: Conventional tools vs synchrotron-based X-ray techniques

X-ray diffraction (XRD) is a routine technique used for the mineralogical characterization of post-treatment residues. XRD provides a fast and cost-effective evaluation with few requirements for sample preparation and is often chosen because of its availability and its non-destructive aspect. Several mineral phases can be detected by XRD in post-treatment residues. The detection of gypsum, silicate minerals, and carbonates (e.g., magnesium carbonate and siderite) was reported (Jouini et al., 2020b). Some mineral phases require a longer time for nucleation and growth and, consequently, their detection with XRD is strongly dependent on the working duration of the treatment system (Jouini et al., 2019b). In addition, XRD techniques might present detection limitations for some amorphous minerals (e.g., oxyhydroxides) commonly associated with AMD. The coupling of the XRD method with other characterization tools is recommended to improve identification (Gagliano et al., 2004). Among them, X-ray photoelectron spectroscopy (XPS) is often used to assess the surface chemistry and bonding structure of elements with a probing depth of approximately 10 nm. The XPS has been used to determine the chemical oxidation state of metals contained in post-treatment residues of passive biochemical reactors (Jouini et al., 2020b).

Table 2-3 Case studies of mineralogical characterizations of contaminated residues.

Residues origins			Mineralogical characterizations		References
Influent (contaminants)	**Treatment system**	**Scale**	**Techniques**	**Phases**	
AMD (As, Fe)	Biological oxidative reactors	Field pilot	XRD	Amorphous ferric arsenate and schwertmannite, jarosite	Diaz-Vanegas et al. (2022)
AMD (Al, Cu, Zn)	Dispersed Alkaline Substrate (DAS)	Lab	XRD	Malachite, calcite, gypsum	Schwarz et al. (2020)
AMD (Fe)	Multi-units: 2PBRs+WA	Field	XRD, XPS	Hematite, goethite, magnetite	Jouini et al. (2020)
AMD (Fe)	Multi-units: PBR + 2DAS	Lab	XRD, SEM	Hematite, magnetite, carbonates, silicate	Jouini et al. (2019)
CND (As, Sb)	Bioreactor (Iron fillings)	Field pilot	TEM, XRD	Ferrihydrite, goethite	Sekula et al. (2018)
AMD (As, Fe)	Bioreactor (based on the oxidation of iron by bacteria)	Field pilot	XRD	Tooeleite, Amorphous-Fe-As phase	Fernandez-Rojo et al. (2019)
AMD (Al, Co, Fe, Mn, Ni, Zn)	DAS	Field	XRD, EPMA	Schwertmannite, goethite, basaluminite, gypsum	Caraballo et al. (2011)
AMD (Al, Fe, Mn, Zn)	MgO-DAS	Field pilot	XRD, synchrotron radiation (μ-XRF, μ-XRD, XAS, EPMA)	Hydrozincite, loseyite	Nieva et al. (2021)

AMD = acid mine drainage; XRD = X-Ray Diffraction; DAS = Dispersed Alkaline Substrate; WA = Wood Ash; XPS = X-Ray Photoelectron Spectroscopy; PBR = Passive Biochemical Reactor; SEM = Scanning Electron Microscopy; CND = contaminated neutral drainage; TEM = Transmission Electron Microscopy; μ-XRF = micro X-Ray Fluorescence; XAS = X-ray Absorption Spectroscopy; EPMA = Electron Probe Microanalysis.

Scanning electron microscopy (SEM) and transmission electron microscopy (TEM) coupled with energy-dispersive X-ray spectroscopy (EDX or EDS) were considered useful in supporting X-ray diffraction results (Jouini et al., 2019b). With high-resolution images, SEM and TEM allow a better characterization of the surface morphology of the investigated samples. In addition, EDS could provide microanalysis or elemental mapping of the chemical composition in a specific sample area, which is useful for acquiring compositional data or verifying the identification of particles (Table 2.3). SEM-EDS was used to characterize residues of biochemical reactors after treatment of AMD and CND. The SEM images (secondary electron mode or even backscattered electron mode) described well the surface morphology, and the gypsum particles were easy to observe. Meanwhile, EDS analysis confirmed the presence of several metals in the amorphous precipitates, without a clear identification of the formed mineral phases (Ben Ali et al., 2020). Electron probe microanalyzer (EPMA) is another tool that can be used to determine the chemical composition of solid materials with better sensitivity and accuracy than SEM-EDS. EPMA provides imaging data and a full qualitative and quantitative analysis of micron-sized volumes of the material's surface (Zhou and Thompson, 2017). The EPMA analysis was successfully correlated with XRD results to assess the mineralogical evolution of solids from a DAS system at the Mina Esperanza mine (SW Spain) (Caraballo et al., 2011). Time-of-flight secondary ion mass spectrometry (TOF-SIMS) is another surface analysis technique that can be used for the mineralogical assessment of PTSs residues. TOF-SIMS uses high-energy ions to generate secondary ions from the surface of the sample. These secondary ions are then analyzed using a mass spectrometer to provide detailed information on the surface's chemical composition and molecular structure (Chehreh-Chelgani and Hart, 2014). Combining TOF-SIMS with other analytical techniques provided complementary information on the sample analyzed (Stevie et al., 2014).

Synchrotron-based X-ray techniques can be used to identify amorphous minerals and have several advantages over the limitations of the conventional mineralogical characterization tools described above (Sarret et al., 2013). Synchrotron-based X-ray techniques are particularly adapted to study chemical speciation, transport, and reactions of metal(loid)s, even at trace levels (Opio, 2013). The special features of synchrotron sources come from their capacity to produce radiation with a brightness several orders of magnitude greater than a conventional X-ray tube. With highly micro-focused X-ray probes, synchrotron facilities possess a combination of properties that allow X-ray scattering, absorption, and diffraction experiments, making it possible to quantify the abundance

and speciation of minute quantities of elements and assess mineralogy in amorphous samples. Micro X-ray fluorescence (μXRF) and X-ray absorption spectroscopy (XAS) are particularly adapted for mapping elemental abundances and the chemical speciation of trace elements in residues (Sarret et al., 2013). XAS is commonly used to determine the oxidation state of elements through X-ray absorption near-edge structure (XANES) analysis and to investigate the surrounding of the studied atom (e.g., the interatomic distance, neighbor species) through extended X-ray absorption fine structure (EXAFS) analysis (Yano and Yachandra, 2009). For instance, the speciation of arsenic in gold ores and their process tailings was examined using XAS. XANES analysis revealed that arsenic was present in the form of As(V) in all the studied samples, whereas EXAFS was utilized to determine the interatomic distances between As–Fe (Paktunc et al., 2004). EXAFS was used with conventional tools to characterize several compounds of ferric-arsenate-sulfate. EXAFS was mainly used to explore the surrounding species and interatomic distances among Fe, O, As, and S atoms in the studied compounds (Paktunc et al., 2013). Additionally, the combination of XAS and XRF provides a powerful tool for accurately characterizing trace elements (Nieva et al., 2021).

The use of synchrotron-based X-ray tools has proved efficient for the mineralogical assessment of amorphous materials in many studies (Opio, 2013). However, the limited number of synchrotron radiation facilities as well as their restricted accessibility and the necessity of additional data to interpret results (e.g., reference spectra and/or crystallographic information for XAS) remain the main limitations of this technology.

In summary, conventional techniques such as XRD, XPS, SEM-EDX, and EPMA can be used to analyze solid samples. A combination of several techniques could be used to identify several mineral phases and provide qualitative chemical analysis and imaging of the micro-morphology of the residues (Table 2.3). The main limitations of these techniques are a low detection limit and the analysis requirements (e.g., XPS and EPMA require a vacuum, XRD and TEM require a dried sample or specific preparation requirement).

Synchrotron-based microanalytical techniques are favored when a deep and accurate mineralogical assessment is required. These methods provide complementary information to the results obtained with conventional techniques. The synchrotron also permits the detection of trace

minerals/elements in poorly crystalline residues and the gathering of other information (e.g., oxidation state, neighbor species).

2.5.1.2 Mineralogy of passive treatment systems (PTSs) residues

Residues generated by PTSs are in the form of solids, which contain hydrated minerals with poor crystallinity. The mineral composition of these residues varies according to the treatment process and the involved removal mechanisms (Table 2.3). Residues generated from MgO passive treatment of Zn-AMD confirmed the existence of hydrozincite ($Zn_5(CO_3)_2(OH)_6$) as a major mineral phase together with loseyite ($(Mn, Zn)_7 (CO_3)_2 (OH)_{10}$) as a minor phase (Pérez-Lòpez et al., 2011). A mineralogical assessment of constructed wetland residues showed schwertmannite [$Fe_8O_8(OH)_{4.8}(SO4)_{1.6}$] and goethite (α-FeOOH) with an average Fe content of 585 g/kg (Gagliano et al., 2004). For residues collected from PTSs composed of anaerobic and aerobic units for the treatment of AMD, characterization results showed that the precipitation of minerals occurred according to pH and redox conditions inside the system. A high proportion of goethite (84.8 wt%) with minor amounts of jarosite ($KFe_3(SO_4)_2(OH)_6$; 8.3 wt%) and hematite (Fe_2O_3; 3.32 wt%) were detected in the top layer of the system associated with the higher oxidation rate and low pH. However, gypsum ($CaSO_4{\cdot}2H_2O$; 23.15 wt%) and metal sulfides (7.91 wt%) were reported in the bottom layer of the system, attributed to microbial sulfate reduction (Mashalane et al., 2018) or up to 15% (Neculita et al., 2008). Residues from passive biological treatment systems might contain metallic sulfides, hydroxides, carbonates, and contaminant-bearing organic matter (Neculita et al., 2007). Native sulfur was also detected in PBRs for Fe-AMD treatment (Jouini et al., 2019b). Lime-based systems yielded vast amounts of sludge with a solid content greater than 25%. Residues produced by these systems contain Fe-oxyhydroxides in the form of goethite and might include Al and other elements, depending on the provenance of the mine drainage (Hedin, 2003; Taylor et al., 2005). Solid phases associated to AMD at the Tharsis mines (IPB, Spain) indicated the dominance of Fe, Al, and Mn sulfates. A variety of soluble Al sulfates including alunogen ($NaAl(SO_4)_2{\cdot}6H_2O$), tamarugite ($Al_2(SO_4)_3{\cdot}17H_2O$), and minerals from the halotrichite-pickeringite group were detected. For Mn minerals, they occurred mainly in the form of the heptahydrate mallardite ($MnSO_4{\cdot}7H_2O$) (Valente et al., 2013). Further details about the composition and mineral phases found in contaminated residues of PTSs are provided elsewhere (Jouini et al., 2019b; Neculita et al., 2007, 2008).

As a result, the mineral composition of the PTSs residues is largely dependent on the type of technology used and the quality of the MD. The newly formed minerals may contain metallic sulfides, metal-rich hydroxides/oxyhydroxides, and carbonates, among others. The stability of the formed residues depends on various factors, including the type of contaminants occurring, the treatment process, and the conditions (e.g., pH, Eh, temperature) in which the residues will be stored. Hence, it is important to assess the stability of the residues to prevent any potential environmental impacts and find out more about the management options, including the required disposal/storage conditions.

2.5.2 Environmental characterization

2.5.2.1 Leaching tests

Mining environmental legislation requires an assessment of the stability of PTSs residues and their potential environmental risks (Macías et al., 2012). A wide range of leaching tests were proposed to simulate the natural leaching of contaminants from PTSs residues (Jouini et al., 2020b; Jouini et al., 2019a; Macías et al., 2012; Tiwari et al., 2015). A single test cannot provide an accurate understanding of the leaching behavior for all types of residues and different scenarios (e.g., climatic, management, reclamation stage). Therefore, the combination of several tests leads to more reliable results (Jouini et al., 2020b; Tiwari et al., 2015). A common classification of leaching methods divides them into two categories: static tests, which include a single addition of the leaching fluid, and dynamic (or semi-dynamic) tests, in which the leaching solution is periodically renewed (Tiwari et al., 2015).

2.5.2.2 Static Tests

Static tests may include one or more leaching steps (Hageman et al., 2015). A selection of the most used tests to evaluate the stability of PTSs residues is summarized in Table 2.4. The leaching tests are either a regulatory method approved by government agencies, such as the Toxicity Characteristic Leaching Procedure (TCLP), the Synthetic Precipitation Leaching Procedure (SPLP), the pH-dependent leaching test (pHstat), and the Field Leaching Test (FLT), or developed methods used by scientists to solve a specific problem, such as the Sequential Extraction Procedure

(SEP) and the Non-Sequential Extraction Procedure (N-SEP) (CEAEQ, 2012; Macías et al., 2012; Rakotonimaro et al., 2021; Turunen et al., 2016).

2.5.2.3 Single-step leaching tests

In practice, single-step leaching tests involve adding a selected leaching liquid for a defined time, which makes them the simplest leaching tests. Usually, the solid/liquid ratio is 1/20, although exceptions can be found depending on the experimental protocols (Table 2.4).

Toxicity Characteristic Leaching Procedure (TCLP). The TCLP, known also as Method 1311 of the United States Environmental Protection Agency (USEPA), is mainly used to assess the potential mobility of contaminants in waste. The TCLP test is considered the most used method among the regulatory leaching tests. It allows a classification of the residues depending on their metal concentrations through leachate analysis (USEPA, 1992). Despite its efficiency (Table 2.4), the TCLP also presents several limitations. Mistaken use of this test may generate inaccurate results and fail to simulate the natural leaching process (Hageman et al., 2015). A misclassification of Mn-Zn mine residues was also noted between the TCLP, the SPLP, and the SEP (Akhavan and Golchin, 2021). Moreover, the TCLP reliability might be affected by a high metals content. Acetic acid in the TCLP favors metal complexation and thus increases metal mobility (Jouini et al., 2019a). For instance, post-treatment residues from a DAS system were classified as hazardous according to EN 12457–2 leaching tests, while they were classified as inert according to the TCLP (Macías et al., 2012). More recent research also showed that the leaching behavior of PTSs residues from AMD was underestimated based on the TCLP. For example, residues classified as 'low risk' showed a high release of several contaminants (Ba, Cu, Mn, and Zn) that exceeded regulations (Jouini et al., 2019a). In addition, Mn-Zn mine tailing residues were usually misclassified when using the TCLP (Akhavan and Golchin, 2021). Another concern about the TCLP is that the concentrations of As and Fe are significantly underestimated in the presence of oxygen due to their precipitation during the extraction step. Hence, it is recommended to perform the TCLP under nitrogen to avoid precipitation of secondary Fe phases considered as suitable adsorption sites for As (Jong and Perry, 2004). Finally, coupling the TCLP test with other static tests (e.g., pH_{stat} and SEP) is necessary for a more reliable prediction of the leaching behavior of PTSs residues (Jouini et al., 2019a).

Synthetic Precipitation Leaching Procedure (SPLP). Also known as Method 1312 of USEPA, the SPLP protocol is almost the same as the TCLP except for the use of extraction reagents

simulating the leaching of inorganic species after acidic rain (USEPA, 1994). The main limitation of this test is the presence of sulfate in the leaching fluid, which may influence the dissolution of sulfate-bearing minerals (Jouini et al., 2019a).

pH-dependent leaching test (pH_{stat}). Also known as Method 1313 of USEPA, this method is used to evaluate the leaching behavior of waste under different pH conditions (acid, neutral, and alkaline) and to study the chemical speciation of contaminants (USEPA, 2012). The pH_{stat} test was used to evaluate the potential leaching of contaminants from PTSs residues of AMD and confirm the results of other static tests for a better waste classification (Jouini et al., 2019c; Jouini et al., 2019a).

Field Leaching Test (FLT). The FLT was developed by the United States Geological Survey (USGS) and is considered the simplest test among all the static leaching tests. Using deionized water as a reagent and a short shaking time (5 min), the FLT aims to give a preliminary evaluation of the mobility of readily soluble contaminants (Hageman, 2007). The main advantage of this test is the use of the same S/L (solid/ liquid) ratio as the TCLP and the SPLP, thus allowing a direct comparison of the results and some complementarity between the leaching tests (McCann and Nairn, 2022). The FLT is effective for short-term and long-term prediction of the ABA (acid base accounting) behavior of PTSs residues (Hageman et al., 2015).

2.5.2.3.1.1 Multi-step leaching tests

Sequential Extraction Procedure (SEP). The SEP is a widely used technique to evaluate the potential mobility of contaminants under different simulated environmental conditions. Among several available methods, a standardized method elaborated by the European Community Bureau of References (BCR-SEP) is the most accepted (Macías et al., 2012). The SEP uses different chemical reagents through several sequenced extraction steps to assess the operational speciation of definite phases allowing the prediction of contaminant mobility (Caraballo et al., 2018). The SEP involves the extraction of five fractions: water-soluble, acid-extractable, reducible, oxidizable, and residual (Consani et al., 2019; Dold, 2003; Macías et al., 2012). The sum of these five fractions is compared to the total content determined by total digestion (Kim et al., 2015). Like other tests, the SEP may be unreliable in some cases. The incomplete dissolution of some metal-bearing minerals in the studied samples often leads to an underestimation of the mobility of these metals. However, the complete dissolution of other phases during the SEP steps can lead to an

overestimation of total concentration (calculated as the sum of each individual step and might lead to a recovery rate greater than 100%) vs total digestion results (considered as 100%). The SEP is based on the selection of a specific reagent for each fraction of the contaminant. If the selected reagent fails to fully extract the target contaminant, the remaining fraction is likely to be dissolved in subsequent steps, thereby altering the results (Caraballo et al., 2018). The incomplete dissolution of pyrite can lead to the poor prediction of the mobility of toxic elements (e.g., As) (Caraballo et al., 2018). The compatibility of extraction reagents with the targeted phases is also very important. Ascorbic acid and oxalate, effective in extracting metalloids (e.g., As) associated with amorphous Fe (oxy)hydroxide phases, are unable to extract metalloids associated with well-crystallized ferric phases. The combination of reducing and chelating agents (dithionite + EDTA) allows the extraction of 90% of well-crystallized ferric phases. The SEP could be more reliable than other static tests, such as the TCLP, but leaching reagents should be carefully selected depending on the mineralogy of the PTSs residues.

Non-Sequential Extraction Procedure (N-SEP). The N-SEP, known as the parallel extraction procedure, aims to overcome the limitations of the conventional SEP, particularly concerning Fe-rich residues and/or As-bearing residues (Rakotonimaro et al., 2021). The N-SEP is intended to study the operational speciation of metals/metalloids in mine tailings and PTSs residues. The N-SEP was developed for the study of As-contaminated PTSs residues by Turunen et al. (2016) and improved by Rakotonimaro et al. (2021). This procedure defines four different fractions: exchangeable, poorly crystallized oxyhydroxides, well-crystallized oxyhydroxides, and residual. Fractions are distinguished according to their crystallinity, which influences the release of contaminants. The N-SEP also takes into consideration the risk of re-adsorption of metals/metalloids. During the strong extractions, even the phases leached with the weaker reagents will be dissolved. Therefore, the amount of each fraction is obtained by subtracting the concentrations obtained during the weaker dissolutions that precede it (Turunen et al., 2016). The N-SEP proposed by Rakotonimaro et al. (2021) divides the fractions associated with “well-crystallized oxyhydroxides” into two subfractions: the fraction absorbed to “well-crystallized oxyhydroxides” and the fraction coprecipitated with “well-crystallized oxyhydroxides”. This distinction ensures a better understanding of the mechanisms of contaminant removal in the PTSs (Rakotonimaro et al., 2021).

Consequently, the N-SEP test is highly recommended for PTSs residues with high contents of metalloids such as As (Rakotonimaro et al., 2021). In practice, however, the use of a separate beaker for each reagent during the N-SEP test leads to more sample consumption. This could be a possible drawback compared to the SEP, where a unique sample is used for all the extraction steps.

To summarize, static leaching tests are a quick tool to assess the short-term water quality and evaluate the stability of PTSs residues (Jouini et al., 2019a). The reliability of those tests is influenced by several factors, such as: i) the pH of the extraction, ii) the interference of dissolved phases complexing the reagents, and iii) oxidoreduction potential and neutralization processes that may occur during the lixiviation phases (Jouini et al., 2020b; Tiwari et al., 2015). To overcome the limits of static tests, they are often coupled with a wide range of dynamic tests to predict more precisely the reactivity of residues and anticipate their long-term leaching behavior (Jouini et al., 2019a).

2.5.2.3.1.2 Dynamic Tests

Among dynamic tests, weathering cells (WCs) and columns are the most used. They consist of continuous/intermittent leaching for a defined time (weeks to years) and sampling on a periodic basis to mimic natural weathering (Hageman et al., 2015). Dynamic tests were used to predict the environmental behavior of PTSs residues from Fe-AMD (Jouini et al., 2020b; Jouini et al., 2019a), As-rich desulfurized mine residues (Rakotonimaro et al., 2021), sulfide-rich residues (Bouzahzah et al., 2014), and PTSs residues from As-AMD (Jong and Parry, 2005). They allow the prediction of CND generation from PTSs residues and sorption capacities for dissolved contaminants (Jouini et al., 2020b; Plante et al., 2011).

WCs require small quantities of materials and less time (a few weeks), while column tests are designed for a longer duration (up to several months). These tests are also statistically repeatable (Demers et al., 2011; Tiwari et al., 2015). Nevertheless, experimental conditions should be carefully monitored because of their influence on sample reactivity (Bouzahzah et al., 2014). The long-term stability of residues generated from a laboratory-scale multi-step PTSs (wood ash, wood chips, and calcite) used for the treatment of Fe-AMD was investigated (Jouini et al., 2019a).

Table 2-4 A selection of static leaching tests used to evaluate residue stability.

Test	Extraction / leaching				Advantages	Limits	References
	Pre-selection	Steps	Reagents	Solid / liquid			
TCLP	Yes	Single	Fluid 1 (H_2O + CH_3COOH + NaOH) Fluid 2 (H_2O + CH_3COOH)	1/20 1/20	• Estimate the mobility of metals/metalloids • Select the most appropriate discharge medium and conditions to maintain residue stability • Allow the determination of whether a pre-treatment is required • Classify contamination potential of wastes (non-hazardous vs hazardous).	• Do not consider other contaminants such as Fe, Zn, and Al • Risk of precipitation of metals during extraction.	CEAEQ (2012); USEPA (1992)
SPLP	No	Single	H_2O + HNO_3 + H_2SO_4	1/20	• Allow the determination of the potential of contaminants from a solid waste to leach into groundwater.	• Presence of sulfates in the leaching solution could limit the dissolution of sulfate-bearing minerals • Absence of standard regulatory limits to compare results.	CEAEQ (2012); USEPA (1994)

Table 2.4 A selection of static leaching tests used to evaluate residues stability (suite)

Test	Extraction / leaching				Advantages	Limits	References
	Pre-selection	**Steps**	**Reagents**	**Solid / liquid**			
pH_{stat}	Yes	Single	H_2O + HNO_3 H_2O + KOH	1/10	• Allow the determination of the most appropriate manner of waste discharge under different pH conditions (e.g. mine waste, soil, sludge, combustion residues, sediments, stabilized materials, demolition debris) • Determine the potential recovery of elements from waste.	• Largely dependent on the buffering capacity of the residues • Absence of standard regulatory limits to compare results.	USEPA (2012); Jouini et al. (2019)
FLT	No	Single	H_2O	1/20	• Allows a preliminary field estimation of the mobility of metals and metalloids.	• Needs to be complemented by other leaching tests.	Hageman (2007); McCann and Nairn (2022)
SEP	No	Multi	Step 1= H_2O Step 2 = CH_3COOH Step 3 = $NH_2OH{\cdot}HCl$ Step 4 = H_2O_2 Step 5 = HNO_3 + HCl	1/50 * ** *** ****	• Investigate the speciation of metals/metalloids.	• Incomplete dissolution of some metal-bearing minerals leads to an underestimation of contaminant mobility.	Macías et al. (2012); Caraballo et al. (2018); Dold (2003)

Table 2.4 A selection of static leaching tests used to evaluate residues stability (suite)

Test	Extraction / leaching				Advantages	Limits	References
	Pre-selection	**Steps**	**Reagents**	**Solid / liquid**			
N-SEP	No	Multi	Step 1 = NH_4-Ac; $CH_3CO_2NH_4$ Step 2 = NH_4-Ox; $(NH_4)_2C_2O_4$ Step 3 = NH_4-Ox; $(NH_4)_2C_2O_4$ + $C_6H_8O_6$ Step 3' = NH_4-Ox; $(NH_4)_2C_2O_4$ + $C_2H_2O_4$ Step 4 = HNO_3 + Br_2 + HF + HCl	1/60 1/100 1/25 1/25 1/15	• Investigate the operational speciation of metals/metalloids • Take into consideration the risk of re-adsorption of metalloids during extraction.	• Requires sacrificial samples • Involves more samples and reagents.	Turunen et al. (2016); CEAEQ (2020); Rakotonimaro et al. (2021)

*40 mL of reagent to be added to the residue from Step 1; **40 mL of reagent to be added to the residue from Step 2;

***10 mL of reagent to be added to the residue from Step 3; ****10 mL of reagent to be added to the residue from Step 4;

TCLP = Toxicity Characteristic Leaching Procedure; SPLP = Synthetic Precipitation Leaching Procedure; pHstat = pH-dependent leaching test; FLT = Field Leaching Test; SEP = Sequential Extraction Procedure; N-SEP = Non-Sequential Extraction Procedure

The results of kinetic tests revealed the leaching behavior of those residues and the potential release of several contaminants such as Fe, Ni, Cu, Mn, and Zn. In addition, the residues were evaluated as a potential source for CND generation. The findings exhibited some discrepancies between kinetic tests and TCLP results in terms of residue classification. Such results were explained mainly by the leaching medium, the S/L ratio, and the presence/absence of O_2 (Jouini et al., 2019a). The mobility of contaminants from Fe-rich residues was evaluated with a kinetic test in mini-columns. Results showed that a kinetic test is still mandatory to better anticipate the long-term stability of post-treatment residues (Jouini et al., 2020b).

In summary, kinetic tests provide a reliable overview of the leaching behavior of PTSs residues despite limitations such as long testing time, large sample quantities, and high costs. A good balance between static and kinetic tests should be considered in experimental research. Knowledge of each test limitation and a combination of several tests are recommended to generate a more realistic prediction of the leaching behavior of PTSs residues with optimal cost.

2.5.2.4 Chemical stability of passive treatment systems (PTSs) residues

The long-term geochemical stability of PTSs residues is influenced by several factors, including the effluent quality (pH, Eh, type of contaminants (metals, metalloids, non-metals)), the site conditions (temperature, flow rate, degree of saturation), the characteristics of the PTSs (HRT, nature of the filling material and presence of organic matter, dimensions), the mineralogy and crystallinity of the resulting precipitates, and the ageing of the PTSs (Coudert et al., 2020; Jouini et al., 2021; McCann and Nairn, 2022). Such factors should be carefully considered to classify PTSs residues and to have an accurate prediction of their stability (Jouini et al., 2021). Metal-rich residues from PBRs were classified as non-dangerous with relative stability (Jong and Parry, 2005), while other residues generated from a MgO-DAS showed a high leaching risk and were recommended to be stored in a dry environment (Macías et al., 2012). Another study has shown the instability of PBR residues from Fe-AMD and recommended their storage under water or in a neutral pH environment to prevent the release of contaminants (Genty et al., 2012b). The disposal of residues generated from a semi-passive PBR in an oxidizing environment promoted a high risk of metal leaching, including Fe, Mn, Ni, and Zn (Lounate et al., 2020b). Moreover, metal-rich residues from a PBR (laboratory scale and field scale) showed high leaching behavior for Cu, Fe, Mn, Ni, and Zn. The authors recommended the stabilization/solidification of those residues before

any storage or reuse (Jouini et al., 2020b). Furthermore, those residues should be stored under anoxic conditions in the presence of water to prevent further leaching of contaminants. Indeed, residues showed high leaching of metals and sulfates with the possibility of the generation of newly formed CND (Jouini et al., 2020b; Jouini et al., 2019a, 2019b). Similar observations were found for metal-rich (Cu, Fe, Ni, and Zn) PBR residues, where a mandatory pre-treatment before any disposal in the environment was suggested (Kousi et al., 2018). In addition, the stability of aged PTSs residues contaminated with As and other metals was studied (Pantuzzo and Ciminelli, 2010). The study confirmed that the stability of residues was dependent on the oxidation state of As and the Fe/As ratio. The combination of the predominance of As(V) and a Fe/As ratio greater than four allowed better stability. However, it has been reported that, with the ageing of the tailings, the stability of Fe-oxyhydroxides at neutral to slightly acidic pH was low. These minerals tend to transform into more stable ferrihydrites with an improved As sorption capacity (Pantuzzo and Ciminelli, 2010; Parviainen et al., 2012). Through the various leaching tests, the environmental assessment provides a clear insight about the potential environmental impacts of PTSs residues and their disposal requirements. Considering mineralogical and environmental assessments, it is crucial to decide the suitable management strategies for these residues.

2.6 Management of contaminated residues from passive treatment systems (PTSs)

The generated solids from PTSs are accumulated on the surface or downstream, which decreases the performance of the treatment process. Once the effectiveness of the passive system becomes too low, the system is subjected to cleaning or dismantling and reconstruction. Removed residues might be hazardous because of the elevated content of toxic metals, such as As, Cd, Cr, Cu, Mn, Ni, and Pb, and the mobility of these contaminants. For instance, residues of several PTSs displayed variable stability levels, which could potentially result in the leaching of contaminants (Jouini et al., 2020b; Vasquez et al., 2022). Thus, the management and disposal of these metal-rich waste can be complex, as they can be a source of secondary contamination. Traditional management methods consider residues from PTSs as output that should be disposed of at minimal cost. However, residues can also present an opportunity for the potential recovery of metals and other precious elements (Macías et al., 2012; Vass et al., 2019; Vaziri-Hassas et al., 2022). Three main potential options should be considered according to the characteristic of the residues: i) reduce their

environmental impact, ii) reuse for other purposes, or iii) recycle for resource recovery (Zinck and Griffith, 2005). Through the three options identified, this strategy aims to minimize the environmental footprint of pollutants, maintain primary resources, and preserve recoverable resources with minimal resource consumption. Over the past few decades, various management options for PTSs residues have been reported (Jouini et al., 2021; Rakotonimaro et al., 2017; Zinck, 2006). These included the reuse of residues as admixtures with tailings to prevent AMD generation (Demers et al., 2015). The recovery of rare earth elements (REEs) (i.e., fifteen lanthanide elements plus Sc and Y), saleable iron oxide (Ayora et al., 2016; Hedin, 2003), and pigment resources (Kirby et al., 1999) has also been reported. Some processes were considered to have promising economic benefits, and the design of treatment facilities was suggested to preclude the need for additional treatment of the accumulated residues (Kirby et al., 1999; Vaziri-Hassas et al., 2022). The use of residues to backfill mines or to support underground works is another interesting management option (Zinck, 2006). To do this, paste backfill is prepared by mixing PTSs residues with water and a binder (Benzaazoua et al., 2006). The binder (e.g., ordinary or sulfate-resistant Portland cement, slags, fly ash) is usually chosen according to the desired requirement in the mine, including mechanical strength and chemical stability. Economic aspects, together with mechanical behavior and metal leachability, are critical in this approach (Benzaazoua et al., 2002, 2006). The stabilization/solidification (S/S) process was also proposed as a sustainable management option to minimize contaminant leaching, thus limiting the environmental impact (Jouini et al., 2020a, 2021). The appropriate management option for PTSs residues depends on several factors, including the composition and characteristics of the residues, the environmental and human health risks posed by the residues, and the availability of resources for management and disposal. Based on the results of the mineralogical and environmental assessment, the different management options are evaluated for their feasibility, cost, and environmental impact. REEs recovery from PTSs has only gained significant attention in recent years, while S/S is a well-established and proven technology for preventing the leaching of contaminants from residues. The following sub-sections provide an overview of these two strategies to explore their effectiveness as two important management options for PTSs residues.

2.6.1 Recovery of rare earth elements

REEs are the most critical materials in modern industry, required for use in electronic devices, in renewable energy generation, and as catalysts (Balaram, 2019; Miranda et al., 2022). The main sources of REEs are carbonates, phosphate minerals, and other alkaline magmatic intrusive rocks (Ettoumi et al., 2021). Extraction and recovery of REEs from mining waste as a secondary source, especially phosphogypsum, is considered a promising alternative avenue (Costis et al., 2021). REE weathering occurs under low pH conditions, making them more available in AMD than CND. During AMD treatment, the scavenging inclusion of REEs in secondary Fe-, Al-, and/or Mn-minerals restrains their mobility (Royer-Lavall´ee et al., 2020; Costis et al., 2021). The use of PTSs residues as a REEs resource is a promising approach, which has the potential to provide a sustainable solution for MD while also supporting the circular economy and helping to offset treatment costs. The most recent studies on REEs extraction from contaminated PTSs residues versus phosphogypsum, which is one of the main secondary sources of REEs recovery are summarized in Table 2.5. Considering the values found in phosphogypsum, PTSs residues have proven to be a potentially interesting secondary source for the recovery of REEs. From a chemical standpoint, PTSs residues are amorphous and easily break down. Consequently, REE recovery from these sources does not require specific/complex preparation (no crushing or milling) or chemical reagent input for the leaching process, thereby representing a cost-effective path compared to primary and other secondary sources. Although the environmental benefits and impacts of REEs recovery are of interest, the feasibility of the process for PTSs residues in terms of cost and effectiveness has not been well assessed. A relatively recent study investigated the technical and economic performance of REEs extraction from Mn- and Al-rich residues from PTSs in the Appalachian coal basin (Fritz et al., 2021). The study was based on an estimate of the cost of processing, including transportation, chemical reagents, and energy consumption, in relation to revenue. The findings showed that the process needs subsidy, and its profitability is dependent on i) the concentrations and distribution of REEs in the PTSs residues, ii) the processing steps, namely transportation and extraction, and iii) reagent consumption. Recovery of REEs and other precious elements from AMD treatment sludge in the Lower Kittanning coal seam, PA, USA, was also reported (Vaziri-Hassas et al., 2022). A three-stage selective precipitation process can achieve high-grade products (up to 99% recovery rate) of Al, REEs, and Co-Mn.

Table 2-5 Typical studies of rare earth elements (REEs) recovery from passive treatment systems (PTSs) residues and phosphogypsum.

Localization / Type of mine	Source of REEs; PTSs/phosphogypsum	Extraction process	Efficiency (%)	REEs content in contaminated residues (ppm)/ formed REEs-bearing minerals	References
Spain (IPB) – Monte Romero Mine / Zn, Pb	CaO-DAS and MgO-DAS (PTSs)	SEP	100	0.016–12.05 * / basaluminite	Ayora et al. (2016)
Spain (IPB) – Almagrera Mine / Zn, Pb, Cu	CaO-DAS and MgO-DAS (PTSs)	SEP	100	0.015–2.20 * / basaluminite	
USA – Appalachian Basin/ Coal	Open limestone drain (PTSs)	Leaching and solvent extraction	80	29−1,286 /N.A.	Fritz et al. (2021)
USA (Pennsylvania)- Lower Kittanning/ Coal	Open limestone ponds (PTSs)	Leaching and precipitation	99	1,043–2,788 / adamsite-(Y)	Vaziri Hassas et al. (2022)
Portugal – Jales Mine	Open limestone channel and wetlands (PTSs)	N.A.	-	0.307–37.4 /ochre-precipitates	Prudêncio et al. (2017)
USA (Florida)/Phosphate	phosphogypsum	Leaching and extraction	100	0.17 / N.A	Laurino et al. (2019)
Tunisia (Sfax)/Phosphate	phosphogypsum	Leaching and precipitation	84	350 / precipitates of quartz-calcite-sodium carbonate sulfate	Hammas-Nasri et al. (2019)

IPB = Iberian Pyrite Belt; SEP = Sequential extraction procedure; DAS = Dispersed alkaline substrate; PTSs = Passive treatment system; *µmol/ g; N.A.=Not applicable

This process was deemed cost-effective because of the high purity and recovery rate of the target elements despite the simplicity of the system. Such studies are rare (Table 2.5), and more research data is required to determine whether this approach is efficient for the large scale. Several parameters seem crucial to ensure the profitability of the process, including the system design, the concentration and value of the targeted REEs, the amount and composition of the PTSs residues, and addressing the economic challenge posed by the necessary reagents, such as acids, for the recovery process. A country's policies towards waste management and their need to address REEs supply shortages are also key factors in the decision of launching a large-scale system for REEs recovery.

2.6.2 Stabilization/solidification (S/S)

Stabilization/solidification (S/S) is a process for the management of solid waste containing unstable contaminants prior to potential use, transportation, or landfill. This method is generally based on the use of cementitious materials or other stabilizers to prevent or slow down the leaching of hazardous materials from residues through chemical and physical interactions (Touite et al., 2022). Contaminant stabilization might occur through i) chemical pathways, including reactions of neutralization and complexation, cementitious and pozzolanic solidification reactions, and ii) physical pathways, such as adsorption on the surface or in pores (Conner and Hoeffner, 1998). Portland cement is the most used binder in the S/S process due to its availability and versatility. The residual water in the contaminated residues chemically reacts with the Portland cement, generating several compounds, including ettringite, calcium silicate hydrates (C-S-H), and aluminate, which ensure the chemical fixation of contaminants (Bates and Hills, 2015; Jouini et al., 2020a). The formed phases serve to immobilize metals through several mechanisms, including isomorphic substitutions, precipitation, and complexation. The hydration reaction with Portland cement allows the stiffening and densification of the cemented matrices by binding solids, including the target residues, to form the monolithic solid block "concrete". The physical separation of contaminants occurs during the solidification process through encapsulation inside solid matrices. The S/S process has been extensively used to prevent the leaching of contaminants in various residues, including organic radioactive waste (Touite et al., 2022), sewage sludge (Zhou et al., 2022), contaminated soil (Wang et al., 2021), and for mining tailings management (Benzaazoua et al., 2004). However, the use of S/S technology for contaminated PTSs residues has

been rarely documented. The S/S process was tested to limit contaminant leaching from residues generated from a PTSs for AMD at a reclaimed mine site in Lorraine, Quebec, Canada (Jouini et al., 2020a). Different formulations between unstable residues, Portland cement, wood ash, sand, and pozzolanic additives, including ground blast furnace slag and fly ash, were prepared to assess the mechanical and environmental behavior of stabilized samples over time. The Portland cement-based mixtures had the best mechanical strength regardless of the curing time. In addition, concentrations of contaminants (As, Ba, Cr, Cu, Fe, Ni, and Zn) were found to be within the USEPA limits, and it was recommended to proceed to landfill disposal without restrictions. Meanwhile, Ba concentrations were higher than the thresholds set in Quebec's provincial guidelines. The stability of the metals was explained by physical and chemical processes entailed by the cement hydration products, such as encapsulation, fixation within C–S–H phases, and precipitation or coprecipitation as hydroxides through the formation of mixed Al-Si metal phases (Jouini et al., 2021; Jouini et al., 2020a). The stabilization of residues issued from sulfate-reducing bioreactors mixed with several alkaline amendments (e.g., biomass ash, aluminum red mud, lime kiln dust, and hydroxyapatite) was evaluated. Results showed that aluminum red mud and lime kiln dust are efficient materials for maintaining a near-neutral pH and preventing acidity generation from residues. However, the leaching behavior of metals was influenced by the storage conditions (Lounate et al., 2020a; Lounate et al., 2021). The S/S process is still considered a cost-effective and efficient method for managing PTSs residues. The process allows the management of a large volume of waste in a small space, which resolves some disposal problems (Zhou et al., 2022). However, the S/S process is still unable to ensure the appropriate stability of all contaminants, and the stability of the treated contaminants could be reduced over time depending on the storage conditions (Lounate et al., 2021). More research is being conducted for the purpose of exploring more efficient materials as amendments and/or stabilizers according to the target residues (Long et al., 2023; Luo et al., 2022). Alternative materials to Portland cement are receiving more attention to make the process more sustainable (Long et al., 2023). The management of PTSs residues is an ongoing challenge and developing standardized guidelines that consider both environmental and economic aspects can help to ensure that residues are managed in a consistent and sustainable manner. The environmental performance of the valorization options of PTSs residues may be assessed using tools like Life Cycle Analysis (LCA) that allow the estimation of the cumulative environmental impacts resulting from all stages in the product life cycle. The decision-making

process for the remediation of the PTSs residues produced by the MD treatment can be supported by this innovative technique (Moreno-Gonzalez et al., 2023).

2.7 Conclusion and research needs

The objective of this study was to provide an overview of PTSs for AMD and CND, the options for evaluating the stability of PTSs residues, and the challenges facing their management. Both biochemical and chemical treatment systems showed high efficiency for AMD remediation, while CND treatment is mainly remediated with biochemical systems. Nevertheless, the selection of the appropriate PTSs requires sufficient knowledge of the effluent chemistry, operating costs, and treatment targets. At the end of their lifetime, PTSs generate considerable quantities of post-treatment residues requiring careful characterization to evaluate their long-term stability and to better anticipate their fate in a sustainable way. The main mineralogical tools and leaching tests used in PTSs residue characterization were discussed. Finally, the review identified recovery of critical and strategic metals and stabilization/solidification as prospective avenues for responsible management of PTSs residues. The S/S ensures sustainable reuse at the end of the mine life cycle, while the recovery and reuse of elements of interest could reduce treatment costs.

The main conclusions from this study are as follows:

•Significant concentrations of metal(loid)s (e.g., Al, As, Fe, Zn) were found in post-treatment residues, while non-negligeable amounts of critical metals (e.g., REEs, Co, Ni) were confirmed.

•Post-treatment residues had a high residual neutralization potential.

•Depending on the type of treatment system and the MD, post-treatment residues showed the presence of carbonates, oxides, oxyhydroxides, sulfur, sulfides, and sulfates.

•Advanced mineralogical analysis techniques such EXAFS and XANES are needed to better understand the retention mechanisms in passive treatment systems.

•Static tests showed several drawbacks, including: i) inconsistent prediction of the environmental behavior and classification of metal rich residues between single- vs. multi-step leaching tests, ii) interference with extracting reagents, and iii) pH dependency.

•The leaching pH, the presence of a chelating agent (e.g., organic acid), the S/L ratio, the leaching time, and the presence of dry/wet.

Declaration of Competing Interest

The authors declare that they have no known competing financial interests or personal relationships that could have appeared to influence the work reported in this paper.

Data availability

No data was used for the research described in the article.

Acknowledgments

This research was funded by the Natural Sciences and Engineering Research Council of Canada (NSERC), Canada Research Chairs Program, Mitacs and RIME UQAT-Polytechnique industrial partners, including Agnico Eagle, Canadian Malartic Mine, Iamgold, Raglan Mine–Glencore, Newmont, and Rio Tinto.

References

Akhavan, A., Golchin, A., 2021. Estimation of arsenic leaching from Zn–Pb mine tailings under environmental conditions. Clean. Prod. 295, 126477 https://doi.org/ 10.1016/j.jclepro.2021.126477. Alpers, N., Nordstrom, D.K., 1999. Geochemical modeling of water–rock interactions in mining environments. In: The environmental geochemistry of mineral deposits, Plumlee, G. S., Logsdon, M.J., Eds. Society of Economic geologists, 6, pp. 289–323.

Anekwe, I.M.S., Isa, Y.M., 2023. Bioremediation of acid mine drainage – Review. Alex. Eng. J. 65, 1047–1075. https://doi.org/10.1016/j.aej.2022.09.053.

Ayora, C., Caraballo, M.A., Macias, F., Rötting, T.S., Carrera, J., Nieto, J.M., 2013. Acid mine drainage in the Iberian Pyrite Belt: 2. Lessons learned from recent passive remediation experiences. Environ. Sci. Pollut. Res. 20, 7837–7853. https://doi.org/ 10.1007/s11356-013-1479-2.

Ayora, C., Macías, F., Torres, E., Lozano, A., Carrero, S., Nieto, J.-M., Pérez-López, R., Fernández-Martínez, A., Castillo-Michel, H., 2016. Recovery of rare earth elements and yttrium from passive-remediation systems of acid mine drainage. Environ. Sci. Tech. 50 (15), 8255–8262. https://doi.org/10.1021/acs.est.6b02084.

Balaram, V., 2019. Rare earth elements: A review of applications, occurrence, exploration, analysis, recycling, and environmental impact. Geosci. Front. 10 (4), 1285–1303. https://doi.org/10.1016/j.gsf.2018.12.005.

Bates, E., Hills, C., 2015. Stabilization and solidification of contaminated soil and waste: A manual of practice. Hygge Media, p. 603, 2015. https://clu-in.org/download/tech focus/stabilization/S-S-Manual-of-Practice.pdf. (Accessed 21 June 2023).

Ben Ali, H.E., Neculita, C.M., Molson, J.W., Maqsoud, A., Zagury, G.J., 2019. Performance of passive systems for mine drainage treatment at low temperature and high salinity: A review. Miner. Eng. 134, 325–344. https://doi.org/10.1016/j. mineng.2019.02.010.

Ben Ali, H.E., Neculita, C.M., Molson, J.W., Maqsoud, A., Zagury, G.J., 2020. Salinity and low temperature effects on the performance of column biochemical reactors for the treatment of acidic and neutral mine drainage. Chemosphere 243, 125303. https:// doi.org/10.1016/j.chemosphere.2019.125303.

Benner, S.G., Blowes, D.W., Gould, W.D., Herbert, R.B., Ptacek, C.J., 1999. Geochemistry of a permeable reactive barrier for metals and acid mine drainage. Environ. Sci. Tech. 33 (16), 2793–2799. https://doi.org/10.1021/es981040u.

Benner, S.G., Blowes, D.W., Ptacek, C.J., Mayer, K.U., 2002. Rates of sulfate reduction and metal sulfide precipitation in a permeable reactive barrier. Appl. Geochem. 17 (3), 301–320. https://doi.org/10.1016/S0883-2927(01)00084-1.

Benzaazoua, M., Belem, T., Bussière, B., 2002. Chemical factors that influence the performance of mine sulphidic paste backfill. Cem. Concr. Res. 32 (7), 1133–1144. https://doi.org/10.1016/S0008-8846(02)00752-4.

Benzaazoua, M., Marion, P., Picquet, I., Bussière, B., 2004. The use of pastefill as a solidification and stabilization process for the control of acid mine drainage. Miner. Eng. 17 (2), 233–243. https://doi.org/10.1016/j.mineng.2003.10.027.

Benzaazoua, M., Fiset, J.-F., Bussière, B., Villeneuve, M., Plante, B., 2006. Sludge recycling within cemented paste backfill: Study of the mechanical and leachability properties. Miner. Eng. 19 (5), 420–432. https://doi.org/10.1016/j. mineng.2005.09.055.

Blowes, D.W., Ptacek, C.J., Benner, S.G., McRae, C.W.T., Bennett, T.A., Puls., R.W., 2000. Treatment of inorganic contaminants using permeable reactive barriers. Contam. Hydrol. 45(1–2), 123–137. doi:10.1016/S0169-7722(00)00122-4.

Bouzahzah, H., Benzaazoua, M., Bussière, B., Plante, B., 2014. Prediction of acid mine drainage: Importance of mineralogy and the test protocols for static and kinetic tests. Mine Water Environ. 33 (1), 54–65. https://doi.org/10.1007/s10230-013-0249-1.

Caraballo, M.A., Macías, F., Nieto, J.M., Castillo, J., Quispe, D., Ayora, C., 2011. Hydrochemical performance and mineralogical evolution of a dispersed alkaline substrate (DAS) remediating the highly polluted acid mine drainage in the full-scale passive treatment of Mina Esperanza (SW Spain). Am. Mineral. 96 (8–9), 1270–1277. https://doi.org/10.2138/am.2011.3752.

Caraballo, M.A., Serna, A., Macías, F., Pérez-López, R., Ruiz-Cánovas, C., Richter, P., Becerra-Herrera, M., 2018. Uncertainty in the measurement of toxic metals mobility in mining/mineral wastes by standardized BCR®SEP. J. Hazard. Mater. 360, 587–593. https://doi.org/10.1016/j.jhazmat.2018.08.046.

CEAEQ (Centre d'expertise en analyse environnementale du Québec), 2012. Protocole de Lixiviation Pour les Espèces Inorganiques. MA. 100–Lix.com.1.1, Rév. 1, Ministère du Développement Durable, l'Environnement, la Faune des Parcs du Québec, Québec, QC, Canada, Volume 7, pp. 1–17.

CEAEQ, 2020. Méthode d'analyse MA. 200 – M´et. 1.2 2020-05-21. Rév. 7; Ministère du Développement Durable, l'Environnement, la Faune des Parcs du Québec, Québec, QC, Canada, pp. 1–35.

Chang, J., Deng, S., Li, X., Li, Y., Chen, J., Duan, C., 2022. Effective treatment of acid mine drainage by constructed wetland column: Coupling walnut shell and its biochar product as the substrates. Water Process Eng. 49, 103116 https://doi.org/10.1016/j. jwpe.2022.103116.

Chehreh-Chelgani, S., Hart, B., 2014. TOF-SIMS studies of surface chemistry of minerals subjected to flotation separation – A review. Miner. Eng. 57, 1–11. https://doi.org/ 10.1016/j.mineng.2013.12.001.

Clyde, E.J., Champagne, P., Jamieson, H.E., Gorman, C., Sourial, J., 2016. The use of a passive treatment system for the mitigation of acid mine drainage at the Williams Brothers Mine (California): Pilot-scale study. J. Clean. Prod. 130, 116–125. https:// doi.org/10.1016/j.jclepro.2016.03.145.

Conner, J.R., Hoeffner, S.L., 1998. A critical review of stabilization/solidification technology. Crit. Rev. Environ. Sci. Technol. 28 (4), 397–462. https://doi.org/ 10.1080/10643389891254250.

Consani, S., Ianni, M.C., Dinelli, E., Capello, M., Cutroneo, L., Carbone, C., 2019. Assessment of metal distribution in different Fe precipitates related to acid mine drainage through two sequential extraction procedures. Geochem. Explor. 196, 247–258. https://doi.org/10.1016/j.gexplo.2018.10.010.

Costis, S., Mueller, K.K., Coudert, L., Neculita, C.M., Reynier, N., Blais, J.-F., 2021. Recovery potential of rare earth elements from mining and industrial residues: A review and cases studies. Geochem. Explor. 221, 106699 https://doi.org/10.1016/j. gexplo.2020.106699.

Coudert, L., Bondu, R., Rakotonimaro, T.V., Rosa, E., Guittonny, M., Neculita, C.M., 2020. Treatment of As-rich mine effluents and produced residues stability: Current knowledge and research priorities for gold mining. J. Hazard. Mater. 386, 121920 https://doi.org/10.1016/j.jhazmat.2019.121920.

De Repentigny, C., Courcelles, B., Zagury, G.J., 2018. Spent MgO-carbon refractory bricks as a material for permeable reactive barriers to treat a nickel- and cobalt-contaminated groundwater. Environ. Sci. Pollut. Res. 25 (23), 23205–23214. https://doi.org/10.1007/s11356-018-2414-3.

Demers, I., Bussière, B., Aachib, M., Aubertin, M., 2011. Repeatability evaluation of instrumented column tests in cover efficiency evaluation for the prevention of acid mine drainage. Water Air Soil Pollut. 219 (1), 113–128. https://doi.org/10.1007/ s11270-010-0692-6.

Demers, I., Benzaazoua, M., Mbonimpa, M., Bouda, M., Bois, D., Gagnon, M., 2015. Valorisation of acid mine drainage treatment sludge as remediation component to control acid generation from mine wastes, part 1: Material characterization and laboratory kinetic testing. Miner. Eng. 76, 109–116. https://doi.org/10.1016/j. mineng.2014.10.015.

Diaz-Vanegas, C., Casiot, C., Lin, L., De Windt, L., Hery, M., Desoeuvre, A., Bruneel, O., Battaglia-Brunet, F., Jacob, J., 2022. Performance of semi-passive systems for the biological treatment of high-as acid mine drainage: Results from a year of monitoring at the Carnoules mine (Southern France). Mine Water Environ. 41 (3), 679–694. https://doi.org/10.1007/s10230-022-00885-4.

Dold, B., 2003. Speciation of the most soluble phases in a sequential extraction procedure adapted for geochemical studies of copper sulfide mine waste. Geochem. Explor. 80 (1), 55–68. https://doi.org/10.1016/S0375-6742(03)00182-1.

Du, T., Bogush, A., Mašek, O., Purton, S., Campos, L.C., 2022. Algae, biochar and bacteria for acid mine drainage (AMD) remediation: A review. Chemosphere 304, 135284. https://doi.org/10.1016/j.chemosphere.2022.135284.

El Kilani, M.A., Jouini, M., Rakotonimaro, T.V., Neculita, C.M., Molson, J.W., Courcelles, B., Dufour, G., 2021. In-situ pilot-scale passive biochemical reactors for Ni removal from saline mine drainage under subarctic climate conditions. Water Process Eng. 41, 102062 https://doi.org/10.1016/j.jwpe.2021.102062.

Ettoumi, M., Jouini, M., Neculita, C.M., Bouhlel, S., Coudert, L., Taha, Y., Benzaazoua, M., 2021. Characterization of phosphate processing sludge from Tunisian mining basin and its potential valorization in fired bricks making. Clean. Prod. 284, 124750 https://doi.org/10.1016/j.jclepro.2020.124750.

Fernandez-Rojo, L., Casiot, C., Laroche, E., Tardy, V., Bruneel, O., Delpoux, S., Desoeuvre, A., Grapin, G., Savignac, J., Boisson, J., Morin, G., Battaglia-Brunet, F., Joulian, C., Héry, M., 2019. A field-pilot for passive bioremediation of As-rich acid mine drainage. Environ. Manag. 232, 910–918. https://doi.org/10.1016/j. jenvman.2018.11.116.

Fritz, A.G., Tarka, T.J., Mauter, M.S., 2021. Technoeconomic assessment of a sequential step-leaching process for rare earth element extraction from acid mine drainage precipitates. Sustain. Chem. Eng. 9 (28), 9308–9316. https://doi.org/10.1021/ acssuschemeng.1c02069.

Gagliano, W.B., Brill, M.R., Bigham, J.M., Jones, F.S., Traina, S.J., 2004. Chemistry and mineralogy of ochreous sediments in a constructed mine drainage wetland. Geochim. Cosmochim. Acta 68 (9), 2119–2128. https://doi.org/10.1016/j. gca.2003.10.038.

Genty, T., Bussière, B., Potvin, R., Benzaazoua, M., Zagury, G.J., 2012a. Dissolution of calcitic marble and dolomitic rock in high iron concentrated acid mine drainage: application to anoxic limestone drains. Environ. Earth Sci. 66, 2387–2401. https:// doi.org/10.1007/s12665-011-1464-3.

Genty, T., Neculita, C.M., Bussière, B., Zagury, G.J., 2012b. Environmental behaviour of sulphate-reducing passive bioreactor mixture. In: Proc. of the 9th International Conference on Acid Rock Drainage, Ottawa, Canada.

Genty, T., Bussière, B., Paradis, M., Neculita., C.M., 2016. Passive biochemical treatment of ferriferous mine drainage: Lorraine mine site, Northern Québec, Canada. In: Proc. of the IMWA, Leipzig, Germany, pp. 790–795. http://www.mwen.info/docs/imwa_ 2016/IMWA2016_Genty_10.pdf.

Gibert, O., Rötting, T., Cortina, J.L., de Pablo, J., Ayora, C., Carrera, J., Bolzicco, J., 2011. In-situ remediation of acid mine drainage using a permeable reactive barrier in Aznalcóllar (SW Spain). J. Hazard. Mater. 191 (1), 287–295. https://doi.org/ 10.1016/j.jhazmat.2011.04.082.

Hageman, P.L., Seal, R.R., Diehl, S.F., Piatak, N.M., Lowers, H.A., 2015. Evaluation of selected static methods used to estimate element mobility, acid-generating and acid-neutralizing potentials associated with geologically diverse mining wastes. Appl. Geochem. 57, 125–139. https://doi.org/10.1016/j.apgeochem.2014.12.007.

Hageman, P.L., 2007. "U.S. Geological Survey Field Leach Test for Assessing Water Reactivity and Leaching Potential of Mine Wastes, Solids, and Other Geologic and Environmental Materials," U.S. Geological Survey Techniques and Methods, Vol. 5, Ch. D3, Department of the Interior, Reston, VA.

Hammas-Nasri, I., Horchani-Naifer, K., Férid, M., Barca, D., 2019. Production of a rare earths concentrate after phosphogypsum treatment with dietary NaCl and Na2CO3 solutions. Miner. Eng. 132, 169–174. https://doi.org/10.1016/j. mineng.2018.12.013.

Hedin, R.S., 2003. Recovery of marketable iron oxide from mine drainage in the USA. Land Contam. Reclam. 11 (2), 93–97. https://doi.org/10.2462/09670513.802.

Hu, X., Peng, M., Sheng, X., Shi, H., Zhang, J.S., Liu, J., Yang, L., Shao, P., Luo, X., Hong, M., Liu, T., 2022. Continuous and effective treatment of heavy metal in acid mine drainage based on reducing barrier system: A case study in North China. J. Hazard. Mater. Adv. 8, 100152 https://doi.org/10.1016/j.hazadv.2022.100152.

Iii, C.A.C., Trahan, M.K., 1999. Limestone drains to increase pH and remove dissolved metals from acidic mine drainage. Appl. Geochem. 14, 581–606. https://doi.org/ 10.1016/S0883-2927(98)00066-3.

Johnson, D.B., Hallberg, K.B., 2005. Acid mine drainage remediation options: a review. Sci. Total Environ. 338 (1), 3–14. https://doi.org/10.1016/j.scitotenv.2004.09.002. Jong, T., Parry, D.L., 2004. Heavy metal speciation in solid-phase materials from a bacterial sulfate reducing bioreactor using sequential extraction procedure combined with acid volatile sulfide analysis. Environ. Monit. 6 (4), 278–285.

Jong, T., Parry, D.L., 2005. Evaluation of the stability of arsenic immobilized by microbial sulfate reduction using TCLP extractions and long-term leaching techniques. Chemosphere 60 (2), 254–265. https://doi.org/10.1016/j. chemosphere.2004.12.046.

Jouini, M., Benzaazoua, M., Neculita, C.M., Genty, T., 2020a. Performances of stabilization/solidification process of acid mine drainage passive treatment residues: Assessment of the environmental and mechanical behaviors. J. Environ. Manage. 269, 110764 https://doi.org/10.1016/j.jenvman.2020.110764.

Jouini, M., Neculita, C.M., Genty, T., Benzaazoua, M., 2020b. Environmental behavior of metal-rich residues from the passive treatment of acid mine drainage. Sci. Total Environ. 712, 136541 https://doi.org/10.1016/j.scitotenv.2020.136541.

Jouini, M., Benzaazoua, M., Neculita, C.M., 2021. Stabilization/solidification of acid mine drainage treatment sludge. In: Wang, L., Tsang, C.W. (Eds.), Low Carbon Stabilization and Solidification of Hazardous Wastes. Elsevier, pp. 175–199.

Jouini, M., Neculita, C.M., Genty, T., Benzaazoua, M., 2019c. Environmental assessment of residues from multi-step passive treatment of Fe-AMD: Field case study of the Lorraine mine site, Quebec, Canada. In: Proceedings of Tailings and Mine Waste, Vancouver, BC, Canada.

Jouini, M., Rakotonimaro, T.V., Neculita, C.M., Genty, T., Benzaazoua, M., 2019b. Prediction of the environmental behavior of residues from the passive treatment of acid mine drainage. Appl. Geochem. 110, 104421 https://doi.org/10.1016/j. apgeochem.2019.104421.

Jouini, M., Rakotonimaro, T.V., Neculita, C.M., Genty, T., Benzaazoua, M., 2019c. Stability of metal-rich residues from laboratory multi-step treatment system for ferriferous acid mine drainage. Environ. Sci. Pollut. Res. 26 (35), 35588–35601. https://doi.org/10.1007/s11356-019-04608-1.

Kim, E.J., Lee, J.-C., Baek, K., 2015. Abiotic reductive extraction of arsenic from contaminated soils enhanced by complexation: Arsenic extraction by reducing agents and combination of reducing and chelating agents. J. Hazard. Mater. 283, 454–461. https://doi.org/10.1016/j.jhazmat.2014.09.055.

Kirby, C.S., Decker, S.M., Macander, N.K., 1999. Comparison of color, chemical and mineralogical compositions of mine drainage sediments to pigment. Environ. Geol. 37 (3), 243–254. https://doi.org/10.1007/s002540050382.

Kleinmann, R., Sobolewski, A., Skousen, J., 2023. The evolving nature of semi-passive mine water treatment. Mine Water Environ. 42, 170–177. https://doi.org/10.1007/ s10230-023-00922-w.

Kousi, P., Remoundaki, E., Hatzikioseyian, A., Korkovelou, V., Tsezos, M., 2018. Fractionation and leachability of Fe, Zn, Cu and Ni in the sludge from a sulphate-reducing bioreactor treating metal-bearing wastewater. Environ. Sci. Pollut. Res. 25 (36), 35883–35894. https://doi.org/10.1007/s11356-018-1905-6.

Laurino, J.P., Mustacato, J., Huba, Z.J., 2019. Rare earth element recovery from acidic extracts of Florida phosphate mining materials using chelating polymer 1-octadecene, polymer with 2,5-furandione, sodium salt. Minerals 9 (8). https://doi.org/ 10.3390/min9080477.

Logan, M.V., Reardon, K.F., Figueroa, L.A., McLain, J.E., Ahmann, D.M., 2005. Microbial community activities during establishment, performance, and decline of bench-scale passive treatment systems for mine drainage. Water Res. 39, 4537–4551. https://doi. org/10.1016/j.watres.2005.08.013.

Long, L., Zhao, Y., Lv, G., Duan, Y., Liu, X., Jiang, X., 2023. Improving stabilization/ solidification of MSWI fly ash with coal gangue based geopolymer via increasing active calcium content. Sci. Total Environ. 854, 158594 https://doi.org/10.1016/j. scitotenv.2022.158594.

Lounate, K., Coudert, L., Genty, T., Mercier, G., Blais, J.-F., 2020a. Geochemical behavior and stabilization of spent sulfate-reducing biofilter mixtures for treatment of acid mine drainage. Sci. Total Environ. 718, 137394 https://doi.org/10.1016/j. scitotenv.2020.137394.

Lounate, K., Coudert, L., Genty, T., Mercier, G., Blais, J.-F., 2020b. Performance of a semi-passive sulfate-reducing bioreactor for acid mine drainage treatment and prediction of environmental behavior of post-treatment residues. Mine Water Environ. 39 (4), 769–784. https://doi.org/10.1007/s10230-020-00702-w.

Lounate, K., Mueller, K.K., Coudert, L., Genty, T., Potvin, R., Mercier, G., Blais, J.-F., 2021. Stabilization and management of sulfate-reducing bioreactor residues after acid mine drainage treatment. Water Air Soil Pollut. 232 (10), 404. https://doi.org/ 10.1007/s11270-021-05325-7.

Luo, Z., Zhi, T., Liu, L., Mi, J., Zhang, M., Tian, C., Si, Z., Liu, X., Mu, Y., 2022. Solidification/stabilization of chromium slag in red mud-based geopolymer. Constr. Build. Mater. 316, 125813 https://doi.org/10.1016/j.conbuildmat.2021.125813.

Macías, F., Caraballo, M.A., Nieto, J.M., 2012. Environmental assessment and management of metal-rich wastes generated in acid mine drainage passive remediation systems. Hazard. Mater. 229–230, 107–114.

Macías, F., Pérez-López, R., Caraballo, M.A., Cánovas, C.R., Nieto, J.M., 2017. Management strategies and valorization for waste sludge from active treatment of extremely metal-polluted acid mine drainage: A contribution for sustainable mining. J. Clean. Prod. 141, 1057–1066. https://doi.org/10.1016/j.jclepro.2016.09.181.

Mashalane, T.B., Novhe, O.N., Yibas, B., Coetzee, H., Wolkersdorfer, C., 2018. Metal removal from mine water using integrated passive treatment system at Witkrantz discharge point in the Ermelo coalfields, Mpumalanga. In: Proc. of the 11th ICARD/ IMWA/MWD Conf Risk to Opportunity, Pretoria, South Africa.

McCann, J.I., Nairn, R.W., 2022. Characterization of residual solids from mine water passive treatment oxidation ponds at the tar creek superfund site, Oklahoma, USA: Potential for reuse or disposal. Cleaner Waste Syst. 3, 100031 https://doi.org/ 10.1016/j.clwas.2022.100031.

Miranda, M.M., Bielicki, J.M., Chun, S., Cheng, C.-M., 2022. Recovering rare earth elements from coal mine drainage using industrial byproducts: environmental and economic consequences. Environ. Eng. Sci. 39 (9), 770–783. https://doi.org/ 10.1089/ees.2021.0378.

Moodley, I., Sheridan, C.M., Kappelmeyer, U., Akcil, A., 2018. Environmentally sustainable acid mine drainage remediation: Research developments with a focus on waste/by-products. Miner. Eng. 126, 207–220. https://doi.org/10.1016/j. mineng.2017.08.008.

Moreno- González, R., Macías, F., Meyer, A., Schneider, P., Nieto, J.M., Olías, M., Cánovas, C.R., 2023. Life cycle assessment of management/valorisation practices for metal-sludge from treatment of acid mine drainage. Environ. Impact Assess. Rev. 99, 107038 https://doi.org/10.1016/j.eiar.2023.107038.

Naidu, G., Ryu, S., Thiruvenkatachari, R., Choi, Y., Jeong, S., Vigneswaran, S., 2019. A critical review on remediation, reuse, and resource recovery from acid mine drainage. Environ. Pollut. 247, 1110–1124. https://doi.org/10.1016/j. envpol.2019.01.085.

Neculita, C.M., Zagury, G.J., Bussière, B., 2007. Passive treatment of acid mine drainage in bioreactors using sulfate-reducing bacteria: Critical review and research needs. Environ. Qual. 36 (1), 1–16. https://doi.org/10.2134/jeq2006.0066.

Neculita, C.M., Zagury, G.J., Bussière, B., 2008. Effectiveness of sulfate-reducing passive bioreactors for treating highly contaminated acid mine drainage: II. Metal removal mechanisms and potential mobility. Appl. Geochem. 23 (12), 3545–3560. https:// doi.org/10.1016/j.apgeochem.2008.08.014.

Neculita, C.M., Zagury, G.J., Bussière, B., 2021. Passive treatment of acid mine drainage at the reclamation stage. In: Bussière, B., Guittonny, M. (Eds.), Hard Rock Mine Reclamation: From Prediction to Management of Acid Mine Drainage. CRC Press, pp. 271–296.

Ness, I., Janin, A., Stewart, K., 2014. Passive treatment of mine impacted water in cold climates: A review. Yukon College, Yukon Research Centre, p. 56.

Nieva, N.E., Garcia, M.G., Borgnino, L., Borda, L.G., 2021. The role of efflorescent salts associated with sulfide-rich mine wastes in the short-term cycling of arsenic: Insights from XRD, XAS, and μ-XRF studies. J. Hazard. Mater. 404, 124158 https://doi.org/ 10.1016/j.jhazmat.2020.124158.

Nordstrom, D.K., Blowes, D.W., Ptacek, C.J., 2015. Hydrogeochemistry and microbiology of mine drainage: an update. Appl. Geochem. 57, 3–16. Opio, F.K., 2013. Investigation of Fe (III)-As (III)

bearing phases and their potential for arsenic disposal. Queen's University, Kingston, Ontario, Canada. PhD.

Orden, S., Macías, F., Cánovas, C.R., Nieto, J.M., Pérez-López, R., Ayora, C., 2021. Eco-sustainable passive treatment for mine waters: Full-scale and long-term demonstration. J. Environ. Manage. 280, 111699 https://doi.org/10.1016/j. jenvman.2020.111699.

Ouakibi, O., Loqman, S., Hakkou, R., Benzaazoua, M., 2013. The Potential use of phosphatic limestone wastes in the passive treatment of AMD: A laboratory study. Mine Water Environ. 32 (4), 266–277. https://doi.org/10.1007/s10230-013-0226-8.

Paktunc, D., Foster, A., Heald, S., Laflamme, G., 2004. Speciation and characterization of arsenic in gold ores and cyanidation tailings using X-ray absorption spectroscopy. Geochim. Cosmochim. Ac. 68 (5), 969–983. https://doi.org/10.1016/j. gca.2003.07.013.

Paktunc, D., Majzlan, J., Palatinus, L., Dutrizac, J., Klementová, M., Poirier, G., 2013. Characterization of ferric arsenate-sulfate compounds: Implications for arsenic control in refractory gold processing residues. Am. Mineral. 98 (4), 554–565. https://doi.org/10.2138/am.2013.4342.

Pantuzzo, F.L., Ciminelli, V.S.T., 2010. Arsenic association and stability in long-term disposed arsenic residues. Water Res. 44 (19), 5631–5640. https://doi.org/10.1016/ j.watres.2010.07.011.

Parviainen, A., Lindsay, M.B.J., Pérez-López, R., Gibson, B.D., Ptacek, C.J., Blowes, D.W., Loukola-Ruskeeniemi, K., 2012. Arsenic attenuation in tailings at a former Cu–W–As mine. SW Finland. Appl. Geochem. 27 (12), 2289–2299. https://doi.org/10.1016/j. apgeochem.2012.07.022.

Pérez-Lòpez, R., Macías, F., Caraballo, M.A., Nieto, J.M., Román-Ross, G., Tucoulou, R., Ayora, C., 2011. Mineralogy and geochemistry of Zn-rich mine-drainage precipitates from an MgO passive treatment system by synchrotron-based X-ray analysis. Environ. Sci. Tech. 45 (18), 7826–7833. https://doi.org/10.1021/es201667n.

Plante, B., Benzaazoua, M., Bussière, B., 2011. Kinetic testing and sorption studies by modified weathering cells to characterize the potential to generate contaminated neutral drainage. Mine Water Environ. 30 (1), 22–37. https://doi.org/10.1007/ s10230-010-0131-3.

Prudêncio, M.I., Valente, T., Marques, R., Braga, M.A.S., Pamplona, J., 2017. Rare earth elements, iron and manganese in ochre-precipitates and wetland soils of a passive treatment system for acid

mine drainage. Procedia Earth Planet. Sci. 17, 932–935. https://doi.org/10.1016/j.proeps.2017.01.024.

Rakotonimaro, T.V., Neculita, C.M., Bussière, B., Zagury, G.J., 2016. Effectiveness of various dispersed alkaline substrates for the pre-treatment of ferriferous acid mine drainage. Appl. Geochem. 73, 13–23. https://doi.org/10.1016/j. apgeochem.2016.07.014.

Rakotonimaro, T.V., Neculita, C.M., Bussière, B., Benzaazoua, M., Zagury, G.J., 2017. Recovery and reuse of sludge from active and passive treatment of mine drainage-impacted waters: a review. Environ. Sci. Pollut. Res. 24 (1), 73–91. https://doi.org/ 10.1007/s11356-016-7733-7.

Rakotonimaro, T.V., Guittonny, M., Neculita, C.M., 2018. Stabilization of hard rock mines tailings with organic amendments: pore water quality control and revegetation-a review. Desalin. Water Treat. 112, 53–71. https://doi.org/10.5004/ dwt.2018.22395.

Rakotonimaro, T.V., Guittonny, M., Neculita, C.M., 2021. Compaction of peat cover over desulfurized gold mine tailings changes: Arsenic speciation and mobility. Appl. Geochem. 128, 104923 https://doi.org/10.1016/j.apgeochem.2021.104923.

Rezaie, B., Anderson, A., 2020. Sustainable resolutions for environmental threat of the acid mine drainage. Sci. Total Environ. 717, 137211 https://doi.org/10.1016/j. scitotenv.2020.137211.

Rötting, T.S., Caraballo, M.A., Serrano, J.A., Ayora, C., Carrera, J., 2008. Field application of calcite dispersed alkaline substrate (calcite-DAS) for passive treatment of acid mine drainage with high Al and metal concentrations. Appl. Geochem. 23 (6), 1660–1674. https://doi.org/10.1016/j.apgeochem.2008.02.023.

Roy, W.R., Krapac, I.G., Chou, S.F.J., Griffin, R.A., 1992. Technical Resource Document: Batch-type Procedures for Estimating Soil Adsorption of Chemicals. Cincinnati, OH, Washington, D.C.

Royer-Lavallée, A., Neculita, C., Coudert, L., 2020. Removal and potential recovery of rare earth elements from mine water. Ind. Eng. Chem. 89 https://doi.org/10.1016/j. jiec.2020.06.010.

Sarret, G., Smits, E.A.H.P., Michel, H.C., Isaure, M.P., Zhao, F.J., Tappero, R., 2013. Chapter one - Use of synchrotron-based techniques to elucidate metal uptake and metabolism in plants. In: Advances in Agronomy. Sparks, D.L. (Ed.), Academic Press, 119, pp. 1-82.

Schwarz, A., Nancucheo, I., Gaete, M.A., Muñoz, D., Sanhueza, P., Torregrosa, M., Rötting, T., Southam, G., Aybar, M., 2020. Evaluation of dispersed alkaline substrate and diffusive exchange system technologies for the passive treatment of copper mining acid drainage. Water 12 (3), 854 https://www.mdpi.com/2073-4441/12/3/ 854.

Sekula, P., Hiller, E., Šottník, P., Jurkovič, Ľ., Klimko, T., Vozár, J., 2018. Removal of antimony and arsenic from circum-neutral mine drainage in Poproč, Slovakia: A field treatment system using low-cost iron-based material. Environ. Earth Sci. 77 (13), 518. https://doi.org/10.1007/s12665-018-7700-3.

Simate, G.S., Ndlovu, S., 2014. Acid mine drainage: Challenges and opportunities. Environ. Chem. Eng. 2 (3), 1785–1803. https://doi.org/10.1016/j.jece.2014.07.021.

Skousen, J., Ziemkiewicz, P.F., 2005. Performance of 116 passive treatment systems for acid mine drainage. In: In: Proc. of the National Meeting of the American Society of Mining and Reclamation (ASMR), pp. 1100–1133. https://doi.org/10.21000/ JASMR05011100.

Skousen, J.G., Ziemkiewicz, P.F., McDonald, L.M., 2019. Acid mine drainage formation, control and treatment: Approaches and strategies. Extr. Ind. Soc. 6 (1), 241–249. https://doi.org/10.1016/j.exis.2018.09.008.

Skousen, J., Zipper, C.E., Rose, A., Ziemkiewicz, P.F., Nairn, R., McDonald, L.M., Kleinmann, R.L., 2017. Review of passive systems for acid mine drainage treatment. Mine Water Environ. 36 (1), 133–153. https://doi.org/10.1007/s10230-016-0417-1.

Stevie, F.A., Sedlacek, L., Babor, P., Jiruse, J., Principe, E., Klosova, K., 2014. FIB-SIMS quantification using TOF-SIMS with Ar and Xe plasma sources. Surf. Interface Anal. 46 (S1), 285–287. https://doi.org/10.1002/sia.5483.

Taylor, J., Pape, S., Murphy, N., 2005. A summary of passive and active treatment technologies for acid and metalliferous drainage (AMD). In: Proc. of the 5th Australian Workshop on Acid Mine Drainage, Fremantle, Western Australia, August 29-31.

Thomas, G., Sheridan, C., Holm, P.E., 2022. A critical review of phytoremediation for acid mine drainage-impacted environments. Sci. Total Environ. 811, 152230 https:// doi.org/10.1016/j.scitotenv.2021.152230.

Tiwari, M.K., Bajpai, S., Dewangan, U.K., Tamrakar, R.K., 2015. Suitability of leaching test methods for fly ash and slag: A review. JRRAS 8 (4), 523–537. https://doi.org/ 10.1016/j.jrras.2015.06.003.

Touite, A., Labied, S., El ghailassi, T., Guedira, T., 2022. Treatment of organic radioactive waste by stabilization/solidification into a cement/alumina based mortar. Mater. Today: Proc. 58, 1485–1489. https://doi.org/10.1016/j. matpr.2022.02.567.

Trumm, D., Pope, J., 2015. Passive treatment of neutral mine drainage at a metal mine in New-Zealand using an oxidizing system and slag leaching bed. Mine Water Environ. 34 (4), 430–441. https://doi.org/10.1007/s10230-015-0355-3.

Turunen, K., Backnäs, S., Neitola, R., Pasanen, A., 2016. Factors controlling the migration of tailings-derived arsenic: A case study at the Yara Siilinjärvi site. Mine Water Environ. 35 (4), 407–420. https://doi.org/10.1007/s10230-016-0393-5.

USEPA, 1994. Method 1312: Synthetic precipitation leaching procedure. DC, USA, Washington.

USEPA, 2012. Method 1313: Liquid–solid partitioning as a function of extract pH using a parallel batch extraction procedure. DC, USA, Washington.

USEPA (US Environmental Protection Agency), 1992. Method 1311: Toxicity characteristic leaching procedure. Washington, DC, USA.

USEPA, 2014. Reference guide to treatment technologies for mining-influenced water. EPA 542-R-14-001. Washington, DC: EPA, USA.

Valente, T., Grande, J.A., De la Torre, M.L., Santisteban, M., Cerón, J.C., 2013. Mineralogy and environmental relevance of AMD-precipitates from the Tharsis mines, Iberian Pyrite Belt (SW, Spain). Appl. Geochem. 39, 11–25. https://doi.org/ 10.1016/j.apgeochem.2013.09.014.

Vasquez, Y., Escobar, M.C., Neculita, C.M., Arbeli, Z., Roldan, F., 2016. Biochemical passive reactors for treatment of acid mine drainage: Effect of hydraulic retention time on changes in efficiency, composition of reactive mixture, and microbial activity. Chemosphere 153, 244–253. https://doi.org/10.1016/j. chemosphere.2016.03.052.

Vasquez, Y., Neculita, C.M., Caicedo, G., Cubillos, J., Franco, J., Vásquez, M., Hernández, A., Roldan, F., 2022. Passive multi-unit field-pilot for acid mine drainage remediation: Performance

and environmental assessment of post-treatment solid waste. Chemosphere 291, 133051. https://doi.org/10.1016/j. chemosphere.2021.133051.

Vass, C.R., Noble, A., Ziemkiewicz, P.F., 2019. The occurrence and concentration of rare earth elements in acid mine drainage and treatment by-products: Part 1—initial survey of the northern Appalachian coal basin. Mining Metall. Explor. 36 (5), 903–916. https://doi.org/10.1007/s42461-019-0097-z.

Vaziri Hassas, B., Shekarian, Y., Rezaee, M., Pisupati, S.V., 2022. Selective recovery of high-grade rare earth, Al, and Co-Mn from acid mine drainage treatment sludge material. Miner. Eng. 187, 107813 https://doi.org/10.1016/j.mineng.2022.107813.

Wang, F., Xu, J., Yin, H., Zhang, Y., Pan, H., Wang, L., 2021. Sustainable stabilization/ solidification of the Pb, Zn, and Cd contaminated soil by red mud-derived binders. Environ. Pollut. 284, 117178 https://doi.org/10.1016/j.envpol.2021.117178.

Wilkin, R.T., 2006. Mineralogical preservation of solid samples collected from anoxic subsurface environments. US EPA, National Risk Management Research Laboratory, p. 8.

Xie, Y., Lu, G., Yang, C., Qu, L., Chen, M., Guo, C., Dang, Z., 2018. Mineralogical characteristics of sediments and heavy metal mobilization along a river watershed affected by acid mine drainage. PLoS One 13 (1), e0190010.

Yano, J., Yachandra, V.K., 2009. X-ray absorption spectroscopy. Photosynth. Res. 102 (2), 241. https://doi.org/10.1007/s11120-009-9473-8.

Yim, G., Ji, S., Cheong, Y., Neculita, C.M., Song, H., 2015. The influences of the amount of organic substrate on the performance of pilot-scale passive bioreactors for acid mine drainage treatment. Environ. Earth Sci. 73, 4717–4727. https://doi.org/ 10.1007/s12665-014-3757-9.

Zhou, X., Thompson, G.E., 2017. Electron and Photon Based Spatially Resolved Techniques. In Reference Module in Materials Science and Materials Engineering; Elsevier: New York, NY, USA, pp. 1–30.

Zhou, Y.-F., Cai, G., Cheeseman, C., Li, J., Poon, C.S., 2022. Sewage sludge ash-incorporated stabilisation/solidification for recycling and remediation of marine sediments. J. Environ. Manage. 301, 113877 https://doi.org/10.1016/j. jenvman.2021.113877.

Zinck, J., Griffith, W., 2005. CANMET Mining and Mineral Sciences Laboratories. MEND (Mine Environment Neutral Drainage) Report 3.43.1, 1–60.

Zinck, J., 2006. Disposal, reprocessing and reuse options for acidic drainage treatment sludge. In: Proc. of the 7th ICARD, ASMR, St. Louis Missouri, USA.

CHAPITRE 3 DÉMARCHE MÉTHODOLOGIQUE

La méthodologie générale du présent projet de doctorat est la suivante :

- Revue de littérature
- Échantillonnage des résidus de post-traitement du biofiltre passif de terrain Wood-Cadillac
- Caractérisation physicochimique et minéralogique des résidus de post-traitement de Wood-Cadillac
- Réalisation des essais de lixiviation statique (TCLP, SPLP et FLT_m) sur les résidus de post-traitement de Wood-Cadillac
- Échantillonnage des matériaux disponibles (tourbe et boue de géotube issue du traitement actif du DMA) pour le mélange de remplissage des biofiltres de laboratoire et pilote de terrain sur le site minier Éléonore-Newmont
- Caractérisation physicochimique de la tourbe et de la boue de géotube
- Caractérisation minéralogique de la boue de géotube
- Réalisation des essais de lixiviation statique (TCLP, SPLP et FLT) sur la tourbe et la boue de géotube
- Contribution dans la mise en place, le suivi et le démantèlement du biofiltre de laboratoire et des deux biofiltres pilotes de terrain
- Échantillonnage des résidus de post-traitement du biofiltre de laboratoire et des deux biofiltres pilotes de terrain
- Caractérisation physicochimique et minéralogique des résidus de post-traitement du biofiltre de laboratoire et les deux biofiltres pilotes de terrain
- Caractérisation environnementale (TCLP, SPLP et FLT) des résidus de post-traitement du biofiltre de laboratoire et les deux biofiltres pilotes de terrain

Les travaux de suivi qui portent sur le biofiltre passif de Wood-Cadillac représentent une continuité des travaux antérieurs déjà réalisés portant surtout sur le suivi de la qualité des eaux (Figure 3.1) :

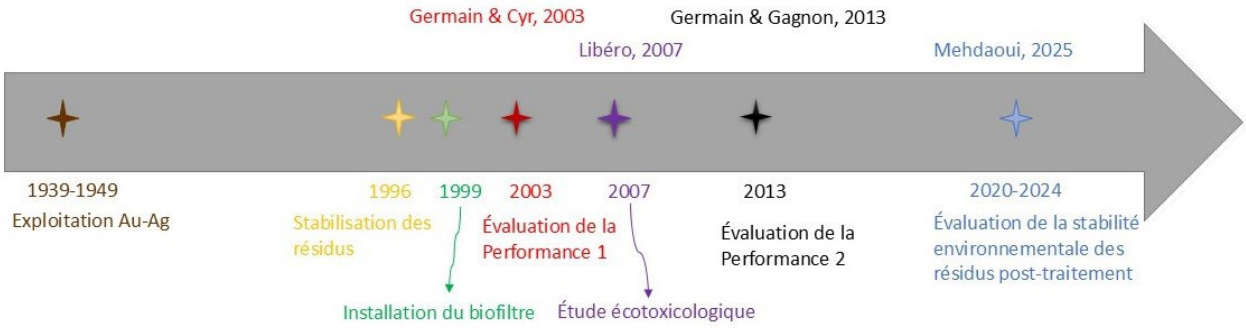

Figure 3.1 Schéma sommatif de l'historique des travaux sur le site minier abandonné Wood-Cadillac

Les caractérisations physicochimique, environnementale et minéralogique des résidus de post-traitement du biofiltre Wood-Cadillac ont été faites selon les étapes suivantes :

- Échantillonnage des résidus de post-traitement du biofiltre passif de terrain Wood-Cadillac à cinq placettes distinctes permettant de couvrir les deux entrées, la sortie, le milieu et le coin stagnant. Dans l'ensemble 10 carottes (d'environ 100 cm chaque) ont été récupérées dont chacune a été divisée en 3 sous unités (A = 0–30 cm, B = 30–60 cm et C = 60–90 cm) pour avoir 30 échantillons au total
- Caractérisation physicochimique des résidus post-traitement échantillonnés : pH de pâte, teneur en eau, teneur en métaux, carbone total, carbone organique, carbone inorganique, soufre total, sulfates Sobek, azote total, etc.
- Caractérisation minéralogique par XPS des résidus de post-traitement de Wood-Cadillac
- Évaluation du comportement environnemental des résidus de post-traitement via des essais statiques (TCLP, SPLP et FLT_m)
- Analyse et discussions des résultats et rédaction des articles 2 et 3.

La méthodologie détaillée adoptée dans cette partie et l'ensemble des résultats obtenus sont présentés dans les chapitres 4 et 5. Dans le chapitre 4, l'objectif était de fournir un aperçu des caractéristiques des résidus ainsi que leur comportement environnemental. Une attention particulière a été porté à la variation verticale en considérant les valeurs moyennes par unité. Toutefois, il a été observé que les écart-types étaient élevés pour les résultats des caractérisations physico-chimique et environnementale. Dans le chapitre 5, il a été décidé de faire l'analyse

approfondie de l'ensemble des échantillons, avec présentation des résultats pour chaque placette, divisées par unité (A, B, et C). Ceci a permis une meilleure interprétation des résultats. Également, considérant les discordances entre les résultats préliminaires des essais statiques (TCLP et SPLP) présentés dans le chapitre 4, il a été décidé d'ajouter d'un troisième test FLT_m pour valider ces résultats et évaluer des scénarios alternatifs de gestion des résidus.

Selon les résultats obtenus dans les chapitres 4 et 5, le transfert des connaissances a permis d'identifier les propriétés hydrauliques et les proportions des composantes du mélange de remplissage utilisées sur le site Wood-Cadillac pour concevoir et mettre en place des biofiltres pilote au laboratoire et sur le terrain. Après une période de suivi de trois mois, les biofiltres ont été démantelés et les résidus post-traitement ont été caractérisés en suivant les étapes ci-dessous :

- Échantillonnage des résidus post-traitement sur quatre niveaux différents :
    - Biofiltre de laboratoire : quatre échantillons composites, aux profondeurs suivantes : I-1 (18–23 cm), A (23–33 cm), B (33–43 cm) et I-2 (43–48 cm)
    - Deux biofiltres pilote de terrain : huit échantillons, de chaque biofiltre, à deux placettes distinctes ciblant quatre profondeurs différentes : I-1 (15–25 cm), A (25–55 cm), B (55–80 cm) et I-2 (80–90 cm)
- Caractérisation physicochimique des résidus échantillonnés (pH de pâte, teneur en eau, teneur en métaux, carbone total, carbone organique et inorganique, soufre total, sulfates Sobek, azote total, etc.)
- Caractérisation minéralogique par XPS des résidus de post-traitement
- Étude de la stabilité chimique des résidus de post-traitement via des essais statiques (TCLP, SPLP et FLT)
- Analyse et discussions des résultats et rédaction de l'article 4.

Plus de détails concernant la mise place des biofiltres, le démantèlement, les protocoles d'échantillonnage, et la méthodologie sont fournis dans le chapitre 6, ainsi que les résultats obtenus.

CHAPITRE 4 ARTICLE 2 _ ENVIRONMENTAL ASSESSMENT OF POST-TREATMENT RESIDUES FROM CONTAMINATED NEUTRAL DRAINAGE: FIELD CASE STUDY OF WOOD-CADILLAC BIOFILTER, QUEBEC, CANADA[2]

Hsan Youssef Mehdaoui[1], Carmen Mihaela Neculita[1,2,*], Thomas Pabst[1,3] and Mostafa Benzaazoua[1,4]

[1] Research Institute on Mines and Environment (RIME), Université du Québec en Abitibi-Témiscamingue (UQAT), Rouyn-Noranda, QC J9X 5E4, Canada

[2] Canada Research Chair - Treatment and Management of Mine Water, RIME, UQAT, Rouyn-Noranda, QC J9X 5E4, Canada

[3] Civil, Geological and Mining Engineering Department, RIME, Polytechnique Montreal, QC H3T 1J4, Canada

[4] University Mohammed VI Polytechnic (UM6P), Geology and Sustainable Mining Institute (GSMI), Lot 660 Hay Moulay Rachid, 43150, Ben Guerir, Morocco

*Corresponding author email: Carmen Mihaela Neculita

Article publié le 16 septembre 2024 dans les comptes-rendus de la conférence *ICARD 2024*.

4.1 Abstract

Arsenic-rich contaminated neutral mine drainage (CND-As) is a rising environmental concern because of a worldwide increasing trend of extracting gold and silver from refractory and As bearing ores. Passive biofilters have shown promising results in the treatment of CND-As, but they also generate significant quantities of residues when exhausted/dismantled. This research evaluated the environmental behaviour of the residues generated from a field-scale passive system for CND-As treatment. Thirty (30) residue samples were collected from a 20-year-old biofilter on the rehabilitated Wood-Cadillac mine site, in northwest Quebec, Canada. Depth profile samples were collected from five locations covering the two inlets and the outlet of the field system. A physicochemical characterization was performed on these samples, and the potential mobility of the contaminants was assessed via the Toxicity Characteristic Leaching Procedure (TCLP) and the

---

[2]Mehdaoui, H.Y., Neculita, C.M., Pabst, T., Benzaazoua, T., 2024. Environmental assessment of post-treatment residues from contaminated neutral drainage: Field case study of Wood-Cadillac Biofilter, Quebec, Canada. In: Proc. of the *13th International Conference on Acid Rock Drainage - ICARD*, Halifax, Nova Scotia, Canada, Sept. 16–20.

Synthetic Precipitation Leaching Procedure (SPLP) tests. Residues contained high contents of metals (up to 2.3 g/kg of As, 41.1 g/kg of Fe, 19.5 g/kg of Al). Metal concentrations in the upper layer were nearly two times greater than in the bottom layer. The results of TCLP classified the residues as nonhazardous according to USEPA criteria. Furthermore, none of the SPLP results exceeded USEPA guidelines, reducing the potential of groundwater contamination from residue leachates. However, the residues were considered leachable for As according to Quebec regulations (D019). Further environmental and mineralogical characterizations are necessary. Future work should focus on As speciation of the residues and its removal mechanisms, to understand the As-phase stability and suggest novel concept-design of other efficient passive biofilters.
Key Words: arsenic, contaminated neutral mine drainage, passive treatment, leaching behaviour.

4.2 Introduction

Contaminated neutral mine drainage (CND), characterized by circumneutral pH and contaminant concentration that slightly exceed standards, represents a complex environmental problem due to the high mobility of some metal(loid) (e.g. As) at neutral pH (Sekula et al., 2018). Passive treatment systems (PTSs) are considered an efficient solution for the treatment of both acid rock drainage (ARD) and CND at closed and abandoned mine sites. They rely on natural biochemical processes to promote contaminant removal (Neculita et al., 2021; Ness et al., 2014). Contaminant load is a critical parameter in PTSs selection. Thus, biochemical systems are preferred for CND treatment (Neculita et al., 2021). Passive biochemical reactors (PBRs), also known as biofilters, showed high efficiency to remediate CND rich in As (Sekula et al., 2018; Turcotte et al., 2021), Sb (Sekula et al., 2018), Cu, Fe and Ni (Ben Ali et al., 2020). Often, a mixture of neutralizing material, organic matter, sulfate-reducing bacterial inoculum and structuring agents (e.g. gravel) is used for contaminant removal (Neculita et al., 2021). Despite their efficiency, biofilters produce considerable amounts of post-treatment residues which exhibit various degrees of stability and unpredictable environmental behaviour. Depending on effluent quality and the type of the PTSs, residues collected at the end of the lifespan of systems have been classified as non-hazardous (Jong and Parry, 2005; McCann and Nairn, 2022), or hazardous and leachable (Jouini et al., 2019a; Genty et al., 2012; Macías et al., 2012). These solids require proper management to avoid further contamination of the environment.

Considering those aspects, the present study aimed to investigate the potential mobility of arsenic from residues generated by a field biofilter and to predict their environmental behaviour.

4.3 Materials and methods

4.3.1 Field study site

A passive biofilter was constructed in the 2000s on the reclaimed Wood-Cadillac mine site, located 6 km east of Cadillac in north-western Quebec (Figure 4.1a), where a former mine operated from 1939 to 1949 to extract Au and Ag. The operations left behind 350,000 tones of tailings spread over 21 ha. The site has been monitored since 1995 mainly for its As concentrations. Between 1996 and 1997, the tailings were stabilized with a layer of gravel and vegetation islands. Since 1999, the CND-As generated by the tailings has been treated with a biofilter measuring 50 m×57 m by 1 m depth (Figure 4.1b, 4.1c). The biofilter was primarily made from yellow birch bark chips (forest residues) (Germain and Cyr, 2003; Germain and Gagnon, 2013). Over the past two decades, the biofilter has shown high efficiency (≥ 80%) for As removal and reduced the concentrations of contaminants below the required limits (Table 4.1) (Germain and Gagnon, 2013; Turcotte et al., 2021).

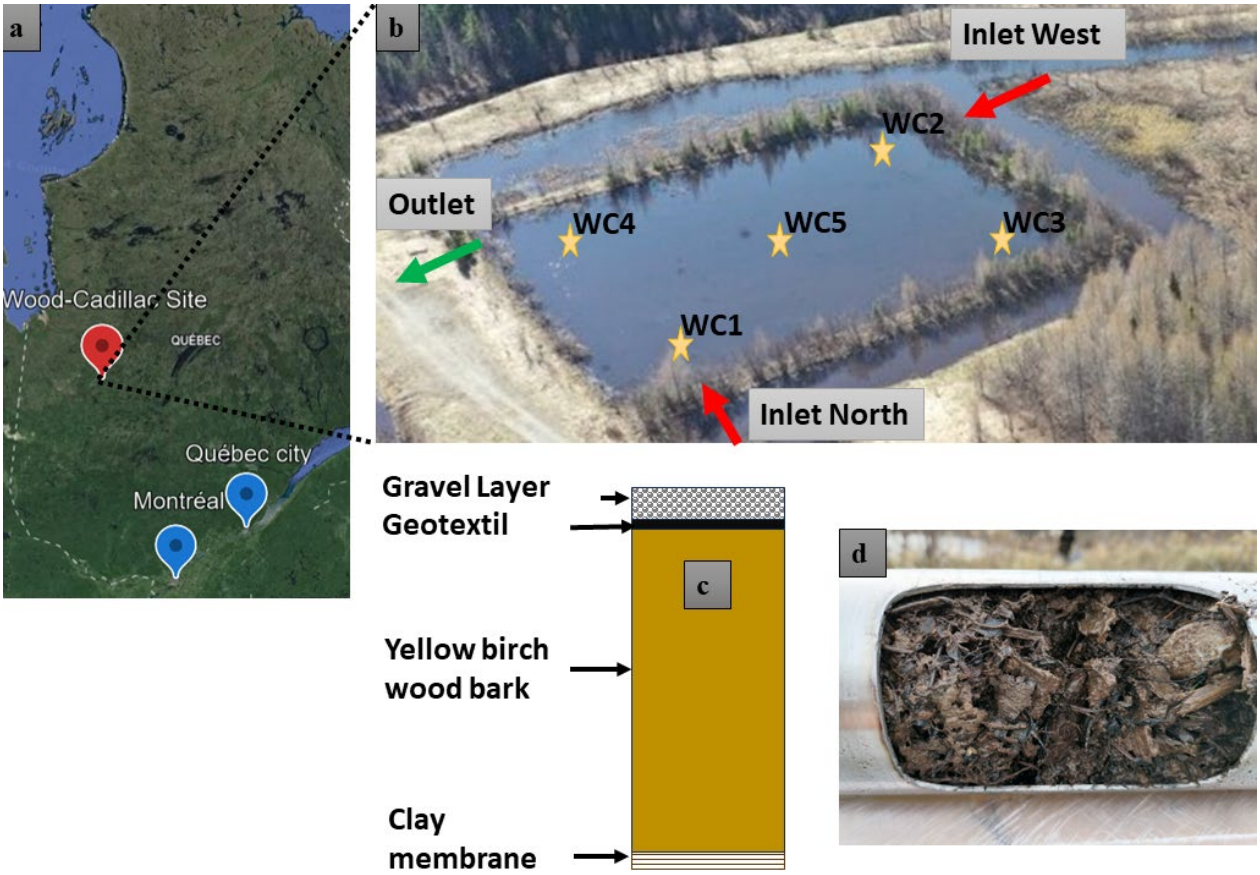

Figure 4.1 a) Location of the Wood-Cadillac mine site (GoogleMaps); b) Aerial view of Wood-Cadillac biofilter (https://mrnf.gouv.qc.ca/); c) Cross section of the biofilter; d) Fresh residues

4.3.2 Sampling protocols

Post-treatment organic residues (partially to totally decomposed wood chips) were sampled in October 2022. A total of 30 samples were collected using a manual core drilling device from five (5) locations across the surface of the biofilter: one positioned in the middle of the biofilter, and the other four (4) located 5 m from the edges of the biofilter. Two cores were taken at each sampling location, that were divided into three (3) individual targeted sub-samples: A: top (0-30 cm), B: middle (30-60 cm) and C: bottom (60-100 cm) to investigate vertical variations in the biofilter. Prior to their analyses, all residue samples were vacuum-packed in sealed containers and stored in the dark at 4°C.

Table 4-1 Physicochemical characterization of CND-As (Inlets vs. Outlet) at Wood-Cadillac mine site (2002, 2012 and 2022)

		pH	Eh (mV)	EC (µS/cm)	Acidity (mg/L $CaCO_3$)	Alkalinity (mg/L $CaCO_3$)	As (mg/L)	Fe (mg/L)	SO_4^{2-} (mg/L)
D019		6<>9.5	N/A	N/A	N/A	N/A	0.2	3	N/A
Inlet North	2002*	6.3	N/A	882		54.2	0.14	0.4	392
	2012*	6.7	N/A	148	17	39.7	0.48	4.2	21.7
	2022**	6.6	95.2	36	6.2	14.6	0.35	2	11
Inlet West	2002*	5.6	N/A	955	N/A	48.2	0.24	<0.2	456
	2012*	7	N/A	390	13.4	48.6	0.11	1	22.3
	2022**	6.9	124.8	161	5.7	30.6	0.07	0.5	61
Outlet	2002*	6.3	N/A	842	N/A	288	0.05	0.2	194
	2012*	6.5	N/A	275	66.2	89.9	0.11	1	39.2
	2022**	6.5	-141.7	57	21.1	28.6	0.08	1.9	10

D019 = Directive 019 pertaining to the Mining Industry in Quebec

*Water quality monitoring data for the Wood-Cadillac mine site was made available by MRNF

**Data were collected for this study; N/A= Not available

4.3.3 Physicochemical characterization of residues

Physicochemical characterization consisted of determining the paste pH, elemental composition, total carbon (TC), organic carbon (OC), total sulfur (TS), total nitrogen (TN) and sulfate concentration.

The paste pH was determined using a solid to liquid (deionized water) ratio of 1:10 (ASTM International, 1995). Prior to conducting chemical analyses, samples were homogenized, oven dried (60°C) and pulverized (<150 µm). Metal contents were determined after acid digestion (HNO_3, Br_2, HCl and HF) via ICP-AES (USEPA, 2007). The TS and TC were determined under oxygen atmosphere by combustion in an induction furnace at 1360°C. The OC and TN were determined according to Zimmerman et al. (1997). $S_{sulfate}$ was determined according to Sobek (1978). Inorganic carbon (IC) was determined by the difference between the TC and OC. Similarly, S_{sulfur} was calculated by the difference between TS and $S_{sulfate}$.

4.3.4 Leaching tests

To evaluate contaminant leachability, two static tests were performed on wet residues from different layers of each sample. Toxicity characteristic leaching procedure tests (TCLP) were used to classify the residues (hazardous, high risk, low risk or leachable). The TCLP required a pretest (5 g of sample + 3.5 mL of 1N HCl + 96.5 mL of deionized water at 50°C) to select the suitable leaching medium for the residues. Thus, the leaching medium 1 (NaOH dissolved in deionized water and glacial acetic acid; pH 4.93) was chosen for all Wood-Cadillac samples. The TCLP tests were conducted in a liquid to solid (L/S) ratio of 20:1, then stirred in a rotary tumbler (30±2 rpm) for 18 h at room temperature (20±2°C) (CEAEQ, 2012; USEPA, 1992). After the test, leachates were filtered (0.45 µm) then analyzed for pH (double junction electrode Orion GD9156BNWP of Thermo Scientific coupled with a VWR SympHony SB90M5 multimeter) and metal concentrations (ICP-AES on 2% HNO_3 acidified samples). Due to the lack of current guidelines for TCLP and SPLP in Quebec, results of metal concentrations were compared to: 1) TCLP limits according to USEPA guidelines, including TCLP limits and the Land Disposal Restrictions (LDR) regulations, and 2) final effluent discharge requirements according to Directive 019 pertaining to the Mining Industry in Québec (D019).

Synthetic precipitation leaching procedure tests (SPLP) were conducted in accordance with USEPA Method 1312 (USEPA, 1994). SPLP tests were carried out to identify any possible leaching from interaction with acid rain. To prepare the extraction medium, 1 mL of sulfuric acid/nitric acid (60:40 w/w) was added to deionized water until the pH of 4.2 was reached. The same steps as for TCLP were then used to prepare, rotate, filter, and store the samples (CEAEQ, 2012; USEPA, 1994). Metal concentration results were then compared to two sets of guidelines: 1) SPLP limits according to USEPA, and 2) final effluent discharge requirements according to D019.

4.4 Results

4.4.1 Physicochemical characterization of post-treatment residues

All residues had a circumneutral paste pH ranging from 6.2 to 7, averaging 6.6 in the middle and upper layers, and 6.5 at the bottom (Table 4.2). TC was high at the top (19.2%) and middle (17.9%) and almost twice as much at the bottom (35.5%). Likewise, the OC showed the same trend and represented 88% of TC in all samples. The high OC content in the residues was mainly due to the decomposition of wood chips used in the reactive mixture of the biofilter. Similar observations were found for the post-treatment residues from the Lorraine reclamation mine site (Genty et al., 2012; Jouini et al., 2019a). Moreover, IC was concentrated in the bottom layer due to a possible accumulation of calcite particles in the bottom of the biofilter because of their larger density compared to organic matter (OM). TS was higher at the bottom (0.7%), compared to ~0.4% in the top and middle layers (Table 2.2). This result may be due to the retention of sulfur or the formation of sulfide minerals in the bottom layer (i.e. layer C) (Jouini et al., 2019b). During the sampling campaign, the bottom layer showed bigger wood chips compared to the smaller or absent wood chips at the top. This observation may suggest the existence of a reducing environment at the bottom.

The elemental composition of the residues is summarized in Table 4.2. Levels of Ca and Zn were almost constant in all residues. Al, As, Fe, K and Mg levels were higher in the upper layers, whereas the S level was higher at the bottom. This could indicate a high removal efficiency of those elements via precipitation/sorption in the biofilter layers. The As concentration was lowest at the

bottom at the WC3 position near the west inlet while the highest concentration was observed at WC3 and WC1 in the top and middle layers near the inlets (Figure 4.2).

Both Fe (Figure 4.2) and Al (Table 4.2) showed the same trend as As with Fe/As ratio between 15 and 36. In the top and middle layers, the highest concentrations of the three elements (i.e. As, Fe and Al) were recorded at the two inlets, decreasing gradually toward the outlet. In fact, efficient retention of arsenic will probably occur in and around of the inlets; after this, the contamination concentration drops as the contaminated water flows through the biofilter. Furthermore, the flow exposes the residues to continuous leaching near the outflow.

Table 4-2 Physicochemical parameters and metal concentrations in Wood-Cadillac mine site post-treatment residues

Physicochemical parameters								
	Paste pH	**TC (%)**	**OC (%)**	**IC (%)**	**TS (%)**	**$S_{sulfate}$ (%)**	**S_{sulfur} (%)**	**TN (%)**
Top	6.6±0.05	19.2±9	17±8	2.2	0.4±0.2	0.06±0.03	0.3	0.9±0.1
Middle	6.6±0.07	17.9±7	15.9±5	2	0.3±0.2	0.07±0.02	0.3	0.9±0.1
Bottom	6.5±0.2	35.5±6	31.2±2	4.4	0.7±0.2	0.1±0.04	0.6	0.6±0.1
Metals (g/kg)								
	Al	**As**	**Ca**	**Fe**	**K**	**Mg**	**S**	**Zn**
Top	20.5±5	2.3±0.9	10.6±1.8	38.3±11	1.7±0.4	6.6±2	3.6±2	0.2±0.03
Middle	19.5±7	2.3±0.8	10.1±1	41.1±9	1.8±0.4	6.9±2	3.5±1	0.2±0.03
Bottom	8.7±4	1.4±0.7	10.4±3	18±7	0.7±0.3	3.1±1	6.5±3	0.1±0.05

With respect to TS variation, the S concentration was highest at the bottom in WC4, WC5 and WC1 locations (Figure 4.2). The retention of As seemed mainly related to Fe, Al and Mg in the form of metal oxyhydroxides at the top and in the middle layers and in the form of sulfide (metal sulfides, arsenic sulfides) at the bottom of the biofilter. The retention of As in the biofilter residues may be also enhanced by sorption and surface precipitation.

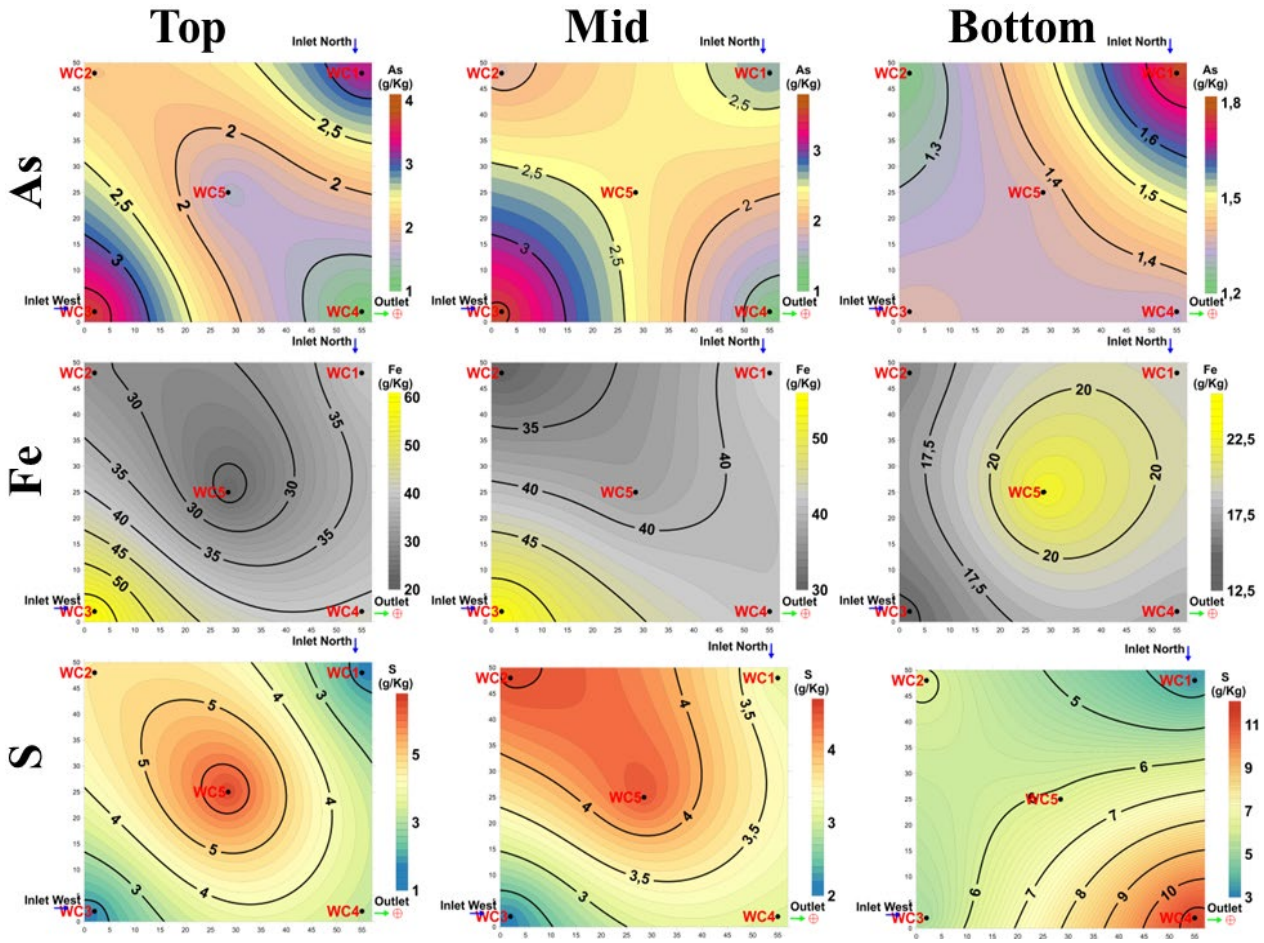

Figure 4.2 Elemental concentrations of As, Fe and S in Wood-Cadillac residues

4.4.2 Assessment of the leaching potential of As from post-treatment residues

TCLP tests were carried out on Wood-Cadillac post-treatment residues to evaluate the mobility and the release of contaminants. The final pH of the leachates was ~5. According to D019, none of the TCLP results exceeded the allowable limits, except As (≥0.2 mg/L). In total, 20 out of 30 samples showed leachable behaviour for As. The As concentrations in the leachates were between 0.09 and 0.66 mg/L. The leached As concentration varied between sample location and depth (Figure 4.3). It was unexpected that residues with the highest As concentration did not have a high leaching potential (Figure 4.2; 4.3). In such samples, the presence of Fe and As could have generated As minerals less prone to leaching. Conversely, residues with a high As leaching potential had high sulfur content. This could be explained by the difference in the chemical composition, the mineral phases bearing As and the composition of pore water.

All residues in the bottom layer had a high potential to leach As, according to D019, with the highest potential in the outlet sample (WC4) (Figure 4.3); residues in the upper layers did not release As. Similarly, no leachable behaviour was observed at the inlet WC1 position in the middle layer (Figure 4.3). Based on the USEPA criterion (5 mg/L for As), all residues had a low environmental risk and qualified as non-hazardous material for landfill disposal. However, according to D019, 66% of residues may be considered as leachable for As. In contrast, none of the SPLP results exceeded the USEPA standards, that reduces the risk of leached residues contaminating groundwater. Moreover, the results of TCLP are sometimes inconsistent in the presence of Fe and As (Jong and Parry, 2005). It is recommended to combine several environmental tests in order to produce reliable results and evaluate the leaching potential of the biofilter residues (Mehdaoui et al., 2023). Further environmental and mineralogical characterization are required to properly evaluate the environmental stability of the Wood-Cadillac residues.

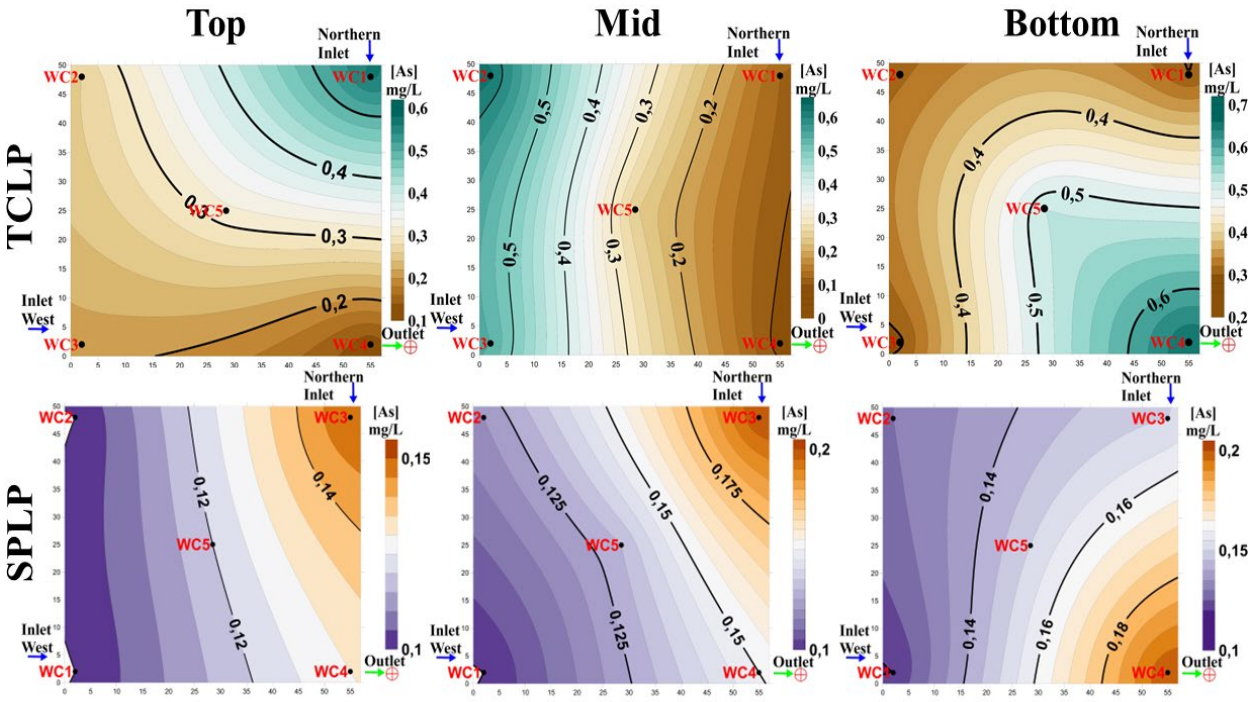

Figure 4.3 Arsenic concentrations in the TCLP and SPLP leachates

4.5 Conclusion

The main objective of this study was to assess the environmental behaviour of post-treatment CND-As residues collected from a field biofilter. Residues sampled in the treatment system showed high concentrations of As, Al, Fe and S, thus establishing evidence of efficient removal of contaminants

from the CND-As influent containing from 0.07 to 0.35 mg/L As in 2022. Based on USEPA TCLP regulations, the residues were categorized as non-hazardous wastes. Moreover, none of the SPLP results exceeded USEPA limits, reducing the risk of groundwater contamination from the leachates. But, 66% of the residues failed the Quebec directive D019 for As. A combination of mineralogical and environmental investigations is recommended to better access the mechanisms of As removal and the As mineral speciation in the Wood-Cadillac biofilter residues and to predict long-term stability of the biofilter.

Acknowledgements

This research was funded by the Natural Sciences and Engineering Research Council of Canada (NSERC), Canada Research Chairs Program, Mitacs and RIME UQAT-Polytechnique industrial partners, including Agnico Eagle, Canadian Malartic Mine, Iamgold, Raglan Mine–Glencore, Newmont, and Rio Tinto. The authors would like to thank MRNF for their on-site support during the sampling campaign and for providing the historical monitoring data. They also acknowledge the guidance and support received from Professor Eric Rosa, Dr. Étienne Bélanger, Dr. Félix Legendre and Dr. Youssef Guesmi during the collection of field samples and laboratory experiments. The authors are thankful to the two reviewers who reviewed the manuscript twice and improved its readability and scope.

References

ASTM International (American Society for Testing and Materials)., 1995. D4972-95a: Standard test method for pH of soils. Dans Annual book of ASTM standards. Vol. 4, p. 27-28.

Ben Ali, H.E., Neculita, C.M., Molson, J.W., Maqsoud, A., Zagury, G.J., 2020. Salinity and low temperature effects on the performance of column biochemical reactors for the treatment of acidic and neutral mine drainage. Chemosphere, 243, 125303. https://doi.org/10.1016/j.chemosphere.2019.125303

CEAEQ (Centre d'Expertise en Analyse Environnementale du Québec)., 2012. Protocole de lixiviation pour les espèces inorganiques, MA. 100 – Lix.com. 1.1, Rév. 1, Ministère du Développement Durable, de l'Environnement, de la Faune et des Parcs du Québec, Québec, Canada, Volume 7, 17p.

Genty, T., Neculita, C.M., Bussière, B., Zagury, G.J., 2012. Environmental behaviour of sulphate-reducing passive bioreactor mixture. In, Proceedings of the 9th International Conference on Acid Rock Drainage, May 20-26, 2012, Ottawa, Canada.

Germain, D., Cyr, J., 2003. Evaluation of biofilter performance to remove dissolved arsenic: Wood Cadillac. In: Proc. of Mining and the Environment, Mai 25-28, 2003, Sudbury, Ontario.

Germain, D., Gagnon, A., 2013. Site minier Wood Cadillac: Évaluation de la performance du biofiltre et de la qualité des eaux du ruisseau Pandora. Direction de la restauration des sites minier – Ministère des Ressources Naturelles, CI121.0, 40 p.

Jong, T., Parry, D.L., 2005. Evaluation of the stability of arsenic immobilized by microbial sulfate reduction using TCLP extractions and long-term leaching techniques. Chemosphere, 60 (2), 254-265. https://doi.org/10.1016/j. chemosphere.2004.12.046

Jouini, M., Neculita, C.M., Genty, T., Benzaazoua, M., 2019a. Environmental assessment of residues from multi-step passive treatment of Fe-AMD: Field case study of the Lorraine mine site, Quebec, Canada. In, Proceeding of Tailings and Mine Waste, November 17-20, 2019, Vancouver, BC, Canada.

Jouini, M., Rakotonimaro, T.V., Neculita, C.M., Genty, T., Benzaazoua, M., 2019b. Stability of metal rich residues from laboratory multi-step treatment system for ferriferous acid mine drainage. Environmental Science and Pollution Research, 26 (35), 35588-35601. https://doi.org/10.1007/s11356-019-04608-1

Macías, F., Caraballo, M.A., Nieto, J.M., 2012. Environmental assessment and management of metal-rich wastes generated in acid mine drainage passive remediation systems. Hazardous Materials, 229–230, 107–114. https://doi.org/10.1016/j.jhazmat.2012.05.080

McCann, J.I., Nairn, R.W., 2022. Characterization of residual solids from mine water passive treatment oxidation ponds at the tar creek superfund site, Oklahoma, USA. Potential for reuse or disposal. Cleaner Waste Systems, 3, 100031. https://doi.org/ 10.1016/j.clwas.2022.100031

Mehdaoui, H.Y., Guesmi, Y., Jouini, M., Neculita, C.M., Pabst, T., Benzaazoua, M., 2023. Passive treatment residues of mine drainage: Mineralogical and environmental assessment, and management avenues. Minerals Engineering, 204, 108362. https://doi.org/https://doi.org/10.1016/j.mineng.2023.108362

Neculita, C.M., Zagury, G.J., Bussière, B., 2021. Passive treatment of acid mine drainage at the reclamation stage. Hard Rock Mine Reclamation: From Prediction to Management of Acid Mine Drainage. Bussière, B., Guittonny, M, CRC Press, pp. 271-296.

Ness, I., Janin, A., Stewart, K., 2014. Passive treatment of mine impacted water in cold climates: A review. Yukon College, Yukon Research Centre, 56 p.

Sekula, P., Hiller, E., Šottník, P., Jurkovič, Ľ., Klimko, T., Vozár, J., 2018. Removal of antimony and arsenic from circum-neutral mine drainage in Poproč, Slovakia: A field treatment system using low-cost iron-based material. Environmental Earth Sciences, 77 (13), 518. https://doi.org/10.1007/s12665-018-7700-3

Sobek, A.A., 1978. Field and laboratory methods applicable to overburdens and minesoils. Industrial Environmental Research Laboratory, Office of Research and Development, US Environmental Protection Agency.

Turcotte, S., Trépanier, S., Bussière, B., 2021. Restauration des sites miniers abandonnés au Québec: Un état de la situation et revue des solutions appliquées. In, Proceeding of Symposium 2021 sur l'Environnement et les Mines, Juin 14-16, 2021, Rouyn-Noranda, Québec.

USEPA (US Environmental Protection Agency), 2007. Method 3051A (SW-846): Microwave assisted acid digestion of sediments, sludges, and oils. Revision 1. Washington, DC, USA.

USEPA, 1992. Method 1311. Toxicity characteristic leaching procedure. Washington, DC, USA.

USEPA, 1994. Method 1312. Synthetic precipitation leaching procedure. Washington, DC, USA.

Zimmerman, C.F., Keefe, C.W., Bashe, J., 1997. Method 440.0 Determination of carbon and nitrogen in sediments and particulates of estuarine/coastal waters using elemental analysis. U.S. Environmental Protection Agency, Washington, DC, USA, EPA/600/R-15/009.

CHAPITRE 5 ARTICLE 3 _ GEOCHEMICAL STABILITY OF AS-RICH RESIDUES FROM A 20-YEAR-OLD PASSIVE FIELD BIOFILTER USED FOR NEUTRAL MINE DRAINAGE TREATMENT[3]

Hsan Youssef Mehdaoui[1], Marouen Jouini[2], Josianne Lefebvre[3], Carmen Mihaela Neculita[1,*], Thomas Pabst[4] and Mostafa Benzaazoua[2]

[1] Research Institute on Mines and Environment (RIME), Université du Québec en Abitibi-Témiscamingue (UQAT), Rouyn-Noranda, QC J9X 5E4, Canada

[2] University Mohammed VI Polytechnic (UM6P), Geology and Sustainable Mining Institute (GSMI), Lot 660 Hay Moulay Rachid, 43150, Ben Guerir, Morocco

[3] Materials Surface Analyses Laboratory, Engineering Physics Department, Polytechnique Montréal, 2500, chemin de Polytechnique, Montréal, QC H3T 1J4

[4] Norwegian Geotechnical Institute (NGI), Sandakerveien 140, 0484 Oslo, Norway

*Corresponding author email: Carmen Mihaela Neculita

Article soumis le 26 novembre 2024 dans la revue *Ecological Engineering*

5.1 Abstract

Arsenic-rich contaminated neutral mine drainage (As-CND) is a major environmental problem frequently faced during gold and silver mining of As-bearing ores. Passive treatment systems, particularly passive biofilters, have proven to be a promising technique for As-CND treatment. However, these systems generate significant quantities of residues at the end of their operational lifespan with variable geochemical stabilities and environmental impacts that involve several parameters (e.g., water quality, treatment mechanism, leaching test, and regulatory criteria). This study evaluated the environmental behaviour of residues from a 20-year-old biofilter installed for the treatment of As-CND at the rehabilitated Wood-Cadillac mine site in northwest Quebec, Canada. Thirty samples of post-treatment residues were collected from five different locations within the system, including two within the inlets, the outlet, and at various depths (0–30 cm, 30–60 cm, and 60–90 cm). Physicochemical and mineralogical characterizations were undertaken to

---

[3]Mehdaoui, H.Y., Jouini, M., Lefebvre, J., Neculita, C.M., Pabst, T., Benzaazoua, T., 2025. Geochemical stability of As-rich residues from a 20-year-old passive field biofilter used for neutral mine drainage treatment. *Ecological Engineering* 216, 107618. https://doi.org/10.1016/j.ecoleng.2025.107618

understand the As removal mechanisms in the biofilter. The potential mobility of metals was assessed via static leaching tests including TCLP, SPLP, and FLTm. The results showed that the residues were characterized by high metal contents (up to 2.3 g/kg of As, 41.1 g/kg of Fe, and 19.5 g/kg of Al), mainly concentrated in the upper layers of the biofilter. Metals were precipitated in the form of oxyhydroxides in the upper and mid layers and as secondary sulfides at the bottom. Arsenic was predominantly removed through sorption onto Fe and Al oxyhydroxides in the upper layers; in contrast, reducing conditions at the bottom facilitated the precipitation of amorphous As sulfides (FeAsS and AsS). None of the TCLP and SPLP release results exceeded USEPA guidelines, and the residues could therefore be classified as non-hazardous with no potential risk of groundwater contamination from leachates. However, 66% of TCLP and 20% of SPLP concentrations exceeded D019 guidelines for As (0.2 mg/L). Additionally, FLT_m results indicated a high leaching potential for As (>1 mg/L). Consequently, these residues should not be crushed or dried during ultimate disposal. These findings will contribute to improving the management strategy for As-rich residues.

Key Words: arsenic removal, As-CND, passive treatment, static leaching tests, environmental behaviour.

5.2 Graphical Abstract

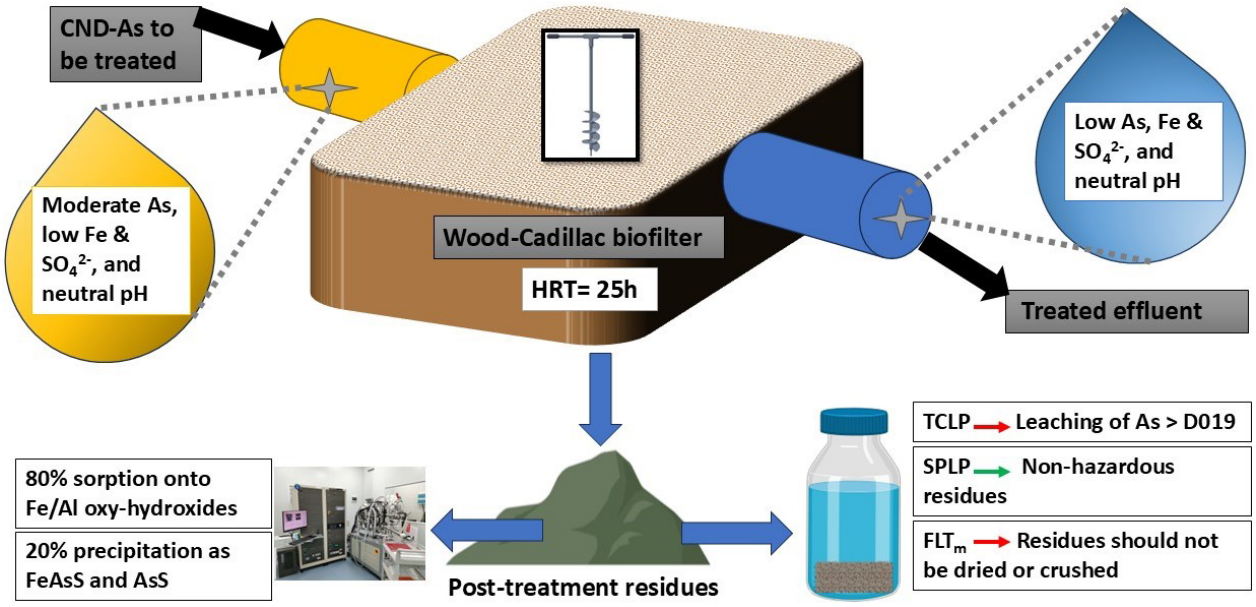

5.3 Highlights

- Characteristics and stability of passive post-treatment residues from CND-As were assessed.
- As removal involved sorption onto Fe(III) oxyhydroxides and metal sulfides.
- Environmental characterization revealed inconsistent classification.
- Further assessment of the CND-As residues is needed to determine a management plan.

5.4 Introduction

Contaminated neutral mine drainage (CND), characterized by circumneutral pH and moderate contaminant contents, poses a challenging environmental concern considering the high mobility of several metallic elements at neutral pH (Skousen et al., 2017; Sekula et al., 2018). CND is generated under specific conditions such as (i) the presence of neutralizing minerals capable of buffering the acidity produced by the oxidation of sulfide minerals over time; (ii) the leaching of metals/metalloids from non-acid-generating mine tailings; and (iii) acid mine drainage (AMD) remediation and control facilities (Nordstrom et al., 2015, Jouini et al., 2021). Passive treatment systems (PTSs) are considered as a viable option for treating CND at closed and abandoned mine sites: they employ natural chemical, biological, and biochemical processes to remove contaminants (Ness et al., 2014; Neculita et al., 2021). Biofilters require minimal energy and resource inputs, making them cost-effective and suitable for large-scale applications, particularly at closed and abandoned mine sites. So far, the vast majority of PTSs have focused on AMD treatment. However, full-scale PTSs designed specifically for CND and particularly for CND-As have barely been discussed (Masindi et al., 2022; Mehdaoui et al., 2023).

Constructed wetlands have been used for As removal from contaminated waters (Rahman et al., 2011; Schwindaman et al., 2014). High removal efficiency of contaminants from CND has been reported for permeable reactive barriers (De Repentigny et al., 2018), peatlands (Eberle et al., 2021), and passive biochemical reactors (PBRs) (Sekula et al., 2018; El Kilani et al., 2021; Turcotte et al., 2021). These PBRs, also known as biofilters, showed excellent efficiency for the treatment of As-rich CND (Sekula et al., 2018; Turcotte et al., 2021), Sb (Sekula et al., 2018), Cu, Fe, and Ni (Ben Ali et al., 2020; El Kilani et al., 2021). Typically, a combination of neutralizing material,

organic matter (OM), sulfate-1 reducing bacteria inoculum, and structuring agents is used to remove contaminants (Neculita et al., 2021).

The long-term performance of biofilters relies mainly on the quality of inlet waters, the availability of OM, the meteoric conditions, and the evolution of hydraulic residence time (Yim et al., 2015; Neculita et al., 2021). For CND with moderate to high contaminant concentrations, PBRs primarily adjust the pH to promote the precipitation of dissolved metals, predominantly as secondary sulfides. Additional removal mechanisms, such as the precipitation of oxyhydroxides and carbonates, along with metal adsorption, also play an important role in the fixation process (Skousen et al., 2017). In contrast, for CND with lower contaminant concentrations, other processes including sorption, co-precipitation, and ion exchange may contribute to contaminant removal (Ben Ali et al., 2019). Overall, contaminant removal is primarily achieved through precipitation and adsorption mechanisms, leading to post-treatment residues composed of immobilized contaminants as precipitates and coated reactive material (Mehdaoui et al., 2023).

While most of the research has focused on the treated water to highlight the removal efficiency of contaminants, the stability of post-treatment solids requires more attention to evaluate long-term performance and management of these residues after end-of-life of these systems. Regardless of their efficiency, PTSs including biofilters generate a significant quantity of post-treatment residues with varying stability. These solids must be properly managed to prevent future contamination (McCann and Nairn, 2022; Mehdaoui et al., 2023). Leaching tests used to assess residue stability are generally classified into two categories: static tests, which involve a single application of the leaching fluid, and dynamic (or semi-dynamic) tests, where the leaching solution is periodically refreshed (Hageman et al., 2015; Mehdaoui et al., 2023). The reliability of those tests depends on several parameters such as: the medium pH, the interference with the reagents, the leaching time, the solid/liquid ratio, and the temperature. Thus, the combination of several leaching tests is highly recommended for more reliable prediction of the leaching behaviour of contaminants from PTS residues after dismantling (Mehdaoui et al., 2023).

As-, Fe-, and S-rich waste from PBRs were determined to be non-hazardous and environmentally stable (Jong and Parry, 2005). Similar findings were observed for solids from passive treatment oxidation ponds, classifying them as non-hazardous (McCann and Nairn, 2022). On the other hand, it was recommended to store the residues from MgO-type dispersive alkaline substrate (MgO-

DAS) in a dry environment because of its significant leaching potential (Macias et al., 2012). Various studies have demonstrated the great instability of PBR residues from Fe-AMD and recommended their storage under water or in a neutral pH environment to reduce the leaching potential (Genty et al., 2012). Moreover, metal-rich residues from PBRs were classified as leachable for Cu, Fe, Mn, Ni, and Zn and their stabilization/solidification was determined to be mandatory before disposal or reuse to limit the environmental impact (Jouini et al., 2020a). Subsequently, to avoid the possibility of newly generated residues, keeping them under anoxic conditions with a water cover is highly suggested (Jouini et al., 2019a, 2019b, 2020a). Comparable findings have been reported for metal-rich (Cu, Fe, Ni, and Zn) PBR waste, where pre-treatment was recommended prior to disposal in the natural environment (Kousi et al., 2018).

To the authors' best knowledge, the environmental behaviour of post-treatment residues of As-CND derived from a field biofilter has barely been discussed. The Wood-Cadillac biofilter has proven its efficiency for As removal (Turcotte et al., 2021), but the generated residues have never been sampled or characterized. Previous studies, based on water analyses and modeling, predicted that As removal in the Wood-Cadillac biofilter occurred via precipitation in the form of orpiment (As_2S_3) (Germain and Cyr, 2003). The aim of this study is to investigate the As removal mechanisms in a 20-year-old passive field biofilter designed for As-CND treatment and to assess post-treatment residues chemical stability to better anticipate their fate after dismantling. To do so, a comprehensive characterization of post-treatment residues collected from the biofilter was conducted. Then, to predict chemical stability and the environmental behavior of the post-treatment residues, static leaching tests were performed.

5.5 Materials and Methods

5.5.1 Field study site

The Wood-Cadillac mine site is located 6 km east of the Cadillac district of Rouyn-Noranda in northwestern Quebec (Figure 5.1.a); it was in operation between 1939 and 1949, producing gold and silver. These mining operations left behind a tailings pile covering an area of 21 ha with 350,000 tonnes of As-rich residues (Figure 5.1.b). Site reclamation, conducted between 1996 and 1997, focused on the mechanical stabilization of the tailings with a layer of gravel and vegetation cover. Subsequently, a biofilter measuring 50 m x 57 m by 1 m depth was constructed in 1999 to

treat the As-CND generated from the waste. The system was made of yellow bark chips and designed to allow vertical flow with a hydraulic residence time (HRT) of 25 h (Germain and Cyr, 2003; Germain and Gagnon, 2013). Drainage water from the tailings pond is carried to the biofilter via two channels, one to the north (inlet north) and one to the west (inlet west) (Figure 1b and Figure 1c). The biofilter showed high efficiency for As removal (≥80%) and maintained the SO_4^{2-} concentrations below 200 mg/L (Turcotte et al., 2021; Mehdaoui et al., 2024).

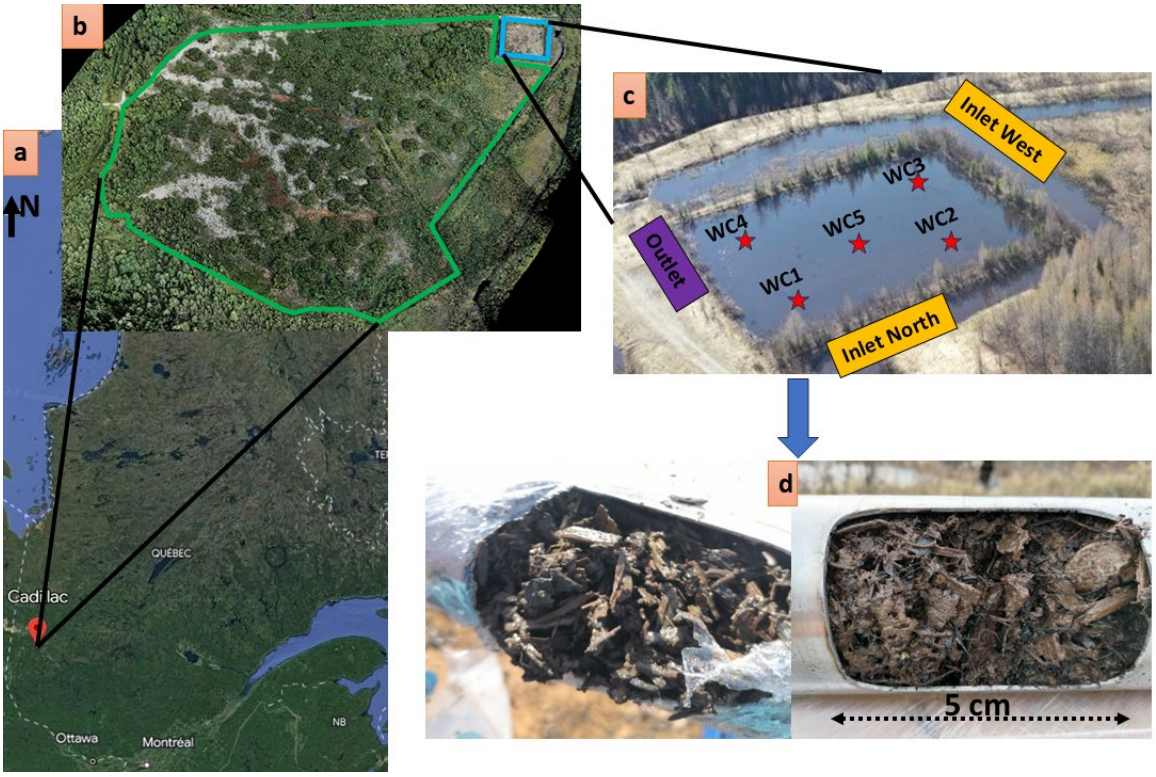

Figure 5.1 a) Location of Wood-Cadillac reclaimed mine site (Google Earth); b) Aerial view of Wood-Cadillac reclaimed mine site (in green; IRME); c) Wood-Cadillac biofilter (in blue; https://mrnf.gouv.qc.ca); d) Freshly sampled residues.

5.5.2 Sampling protocols

Post-treatment residues were collected after 23 years of As-CND treatment. Five locations were chosen to ensure representative sampling (Figure 5.1c and Figure 5.2), with four located 5 metres from the edges of the biofilter (WC1–4) and one positioned in the center of the treatment system (WC5). Each core (2 per sampling spot) was split into three targeted depths (A = 0–30 cm, B = 30–60 cm, and C = 60–90 1 cm) (Fig. 5.2). A total of 30 samples were collected, vacuum-packed in

sealed plastic containers, and stored in the dark at 4°C until analysis to ensure integrity. The chemical composition and mineralogy of the residues were determined to characterize the solids and to confirm the chemical state of As and other metals. Leaching tests were performed to evaluate the mobility of As in the residues.

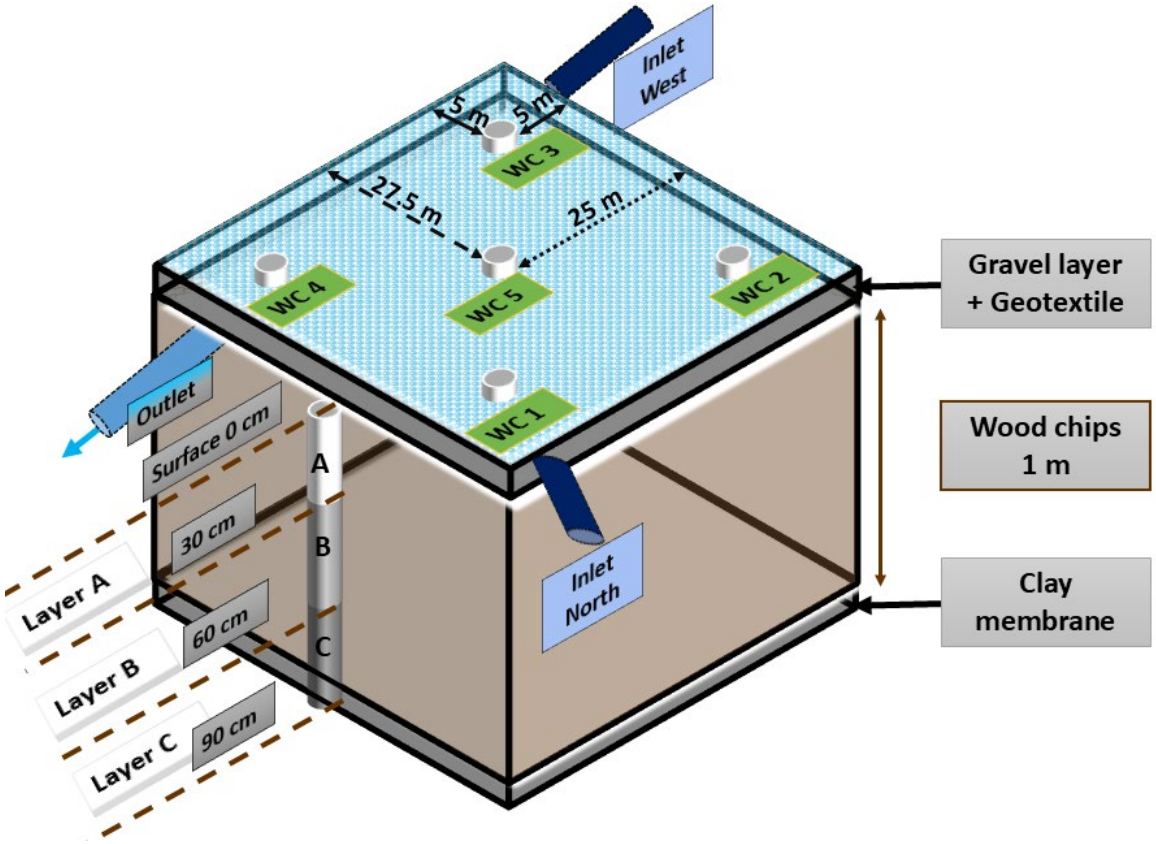

Figure 5.2 Model and sampling points of the passive treatment system installed on the Wood-Cadillac mine site.

5.5.3 Physicochemical characterization of post-treatment residues

Post-treatment residues were characterized for their paste pH, total carbon (TC), organic carbon (OC), total sulfur (TS), total nitrogen (TN), sulfates concentration, and elemental composition. The paste pH was measured in duplicate using a double junction electrode Orion GD9156BNWP from Thermo Scientific 1 paired with a VWR SympHony SB90M5 multimeter with a solid-to-liquid (deionized water) ratio of 1:10 (ASTM International, 2019). Samples were homogenized, oven dried (60°C), and pulverized (150 µm) prior to all chemical analyses. In total, 15 samples were analysed, covering the five selected locations and the targeted depths. For each analysis, one

location was randomly selected and analyzed in triplicate to ensure representativity. The TS and TC were determined under an oxygen atmosphere by combustion in an induction furnace at 1,360°C. The OC and TN were determined according to Zimmerman et al. (1997), while $S_{sulfates}$ was determined according to Sobek (1978). The inorganic carbon (IC) and the S_{sulfur} were calculated by the difference between the TC and OC and the difference between TS and $S_{sulfates}$, respectively. Metal contents were determined via inductively coupled plasma atomic emission spectroscopy (ICP-AES; Varian Vista Pro CCD) following acid digestion (HNO_3, Br_2, HCl, and HF) (USEPA, 2007).

5.5.4 Mineralogical characterization

Mineralogical characterization was conducted on 15 selected samples using X-ray photoelectron spectroscopy (XPS). XPS was used to identify the chemical oxidation state of metals and oxyanions in the residues and to determine their speciation within the neoformed mineral phases. To limit oxidation, samples were dried under inert conditions (N_2) in a glovebox at room temperature prior to analysis. XPS analyses were conducted at the Laboratory for the Analysis of the Surface of Materials (Polytechnique Montreal) using a VG ESCALAB 250Xi (Thermo Fisher Scientific) with monochromated Al Kα radiation at 1,486.86 eV; the detection limit was 0.1% atomic. Standard charge compensation with low energy electrons and Ar^+ ions was used. The pressure in the chamber during analysis was around 10-8 mbar. Survey spectra were 1 acquired at a pass energy of 150 eV and a step size of 1.0 eV; high-resolution spectra were acquired at a 40 eV pass energy and a step size of 0.1 eV. For these samples, high-resolution spectra acquisition was necessary to obtain accurate elemental quantification considering various peak overlaps, especially at low elemental concentrations (<0.5 % at.). Specimens were analysed at an emission angle of 0˚ with respect to surface normal. Data processing was performed using Avantage v6.5.0 (Thermo Fisher Scientific). XPS is a surface analysis technique that is sensitive to a maximum depth of 10 nm; this enhances the concentration of whatever is located on the surface relative to the bulk in cases where a non-homogeneous distribution of elements exists. All elements present on the surface (except H and He, which are not detected by XPS) were identified from survey spectra: their atomic concentrations were calculated using integral peak intensities and the sensitivity factors supplied by the manufacturer. Binding energies were referenced to the C1s peak at 284.8 eV for aliphatic hydrocarbons.

5.5.5 Leaching tests

A combination of three static tests was performed, including toxicity characterization leaching procedure (TCLP), synthetic precipitation leaching procedure (SPLP), and modified field leaching test (FLTm). The leaching tests were conducted in duplicate from the three sampled layers (A = 0–30, B = 30–60 and C = 60–90 cm). After each test, leachates were filtered (0.45 µm) and tested for pH and metal concentrations (ICP-AES on samples acidified with 2% HNO_3).

5.5.5.1 Toxicity characterization leaching procedure (TCLP)

TCLP was applied on wet preserved samples to determine the leachability of contaminants and classify the residues (hazardous, high risk, low risk, or leachable). Leaching medium (NaOH dissolved in deionized water and glacial acetic acid; pH 4.93±0.05) was applied for all samples after the pre-test (5 g of sample + 3.5 mL of HCl 1N + 96.5 mL of deionized water at 50°C for 10 minutes). The TCLP tests used a 20:1 liquid-to-solid ratio and were agitated in a rotary tumbler (30±2 rpm) for 18 h at room temperature (20±2°C) (USEPA, 1992; CEAEQ, 2012).

5.5.5.2 Synthetic precipitation leaching procedure (SPLP)

SPLP tests were conducted to determine potential leaching that originates from acidic rain contact. The extraction medium was prepared by the addition of a stock made of 1 mL of sulfuric acid/nitric acid (60:40 w/w) to deionized water until a pH of 4.20±0.05 was attained. The wet residues were extracted at room temperature (20±2°C) using a 20:1 liquid-to-solid ratio and were agitated in a rotary tumbler (30±2 rpm) for 18 h (USEPA, 1994; CEAEQ, 2012).

5.5.5.3 Modified field leaching test (FLT_m)

The modified field leaching test (FLT_m) was applied to evaluate the worst-case leaching scenario in contact with water. The original FLT test aims to quickly assess and predict the leachate geochemistry using a 20:1 leaching ratio of pure water (1 L) and air-dried residues (particle size less than 2 mm). The slurry sample was hand mixed for 5 minutes then permitted to settle for 20 minutes (Hagemann, 2007). The FLT_m followed the modification of McCann and Nairn (2022). In addition, samples were oven dried and pulverized to expose all surfaces of the residues and to assess the most conservative leaching scenario.

5.6 Results and discussion

5.6.1 Physicochemical characterization of post-treatment residues

Analyses showed that all residues had circumneutral pH values ranging from 6.2 to 7.0, exhibiting an average of 6.6±0.1 for layers A and B and 6.5±0.1 for layer C (Figure 5.3). The TC in layer C (35.5±1.7%) was almost twice that in layers A (19.2±8%) and B (17.9±5%). Similar results were also observed for the post-treatment residues of Fe-AMD at the reclaimed Lorraine mine site (Genty et al., 2012; Jouini et al., 2019a). OC, accounting for around 88% of the TC in all samples, followed the same trend as TC; the decrease in OC from layer A to C was mainly due to the decomposition of wood chips used in the reactive mixture of the biofilter. The availability of oxygen for bacteria was more significant on the surface, which explains the increased degradation of OM in the upper layers. It is important to note that the highest contents of TC and OC for all layers were recorded in WC2, indicating a stagnating confined zone with limited water flow and therefore favouring carbon fixation. Nevertheless, due to the permanent leaching with the entry flow and the transport of dissolved carbon away from the western inlet, location WC3 showed a unique behaviour with no significant variation between layers for both TC and OC. TS behaved similarly to TC, with a high concentration of sulfur in layer C (0.7±0.2%) as compared to layers A (0.4±0.1%) and B (0.3±0.1%) (Figure 5.3). Layer C contained ~83% of the secondary sulfides in the unit; this outcome might be attributed to the retention of sulfur or the formation of sulfur-based minerals in the bottom layer (Jouini et al., 2019b). During the collection of the samples, layer C had coarser wood fragments compared to the top layers (i.e., layers A and B), where they were more degraded and occasionally absent. This finding might point to the presence of a strongly reducing environment in layer C. Interestingly, the western inlet (WC3) followed the same pattern for TS distribution as mentioned for TC. This confirms the hypothesis of steady feeding spreading in all layers at this location, preventing the establishment of a strongly reducing environment. In terms of TN, layers A and B showed similar contents (0.87±0.1%), which slightly decreased with depth (0.66±0.1%). The presence of TN could be explained by the biological activity in the woodland tailings pile. The slow decomposition of wood bark in layer C compared to the upper layers may explain the contrast in TN content.

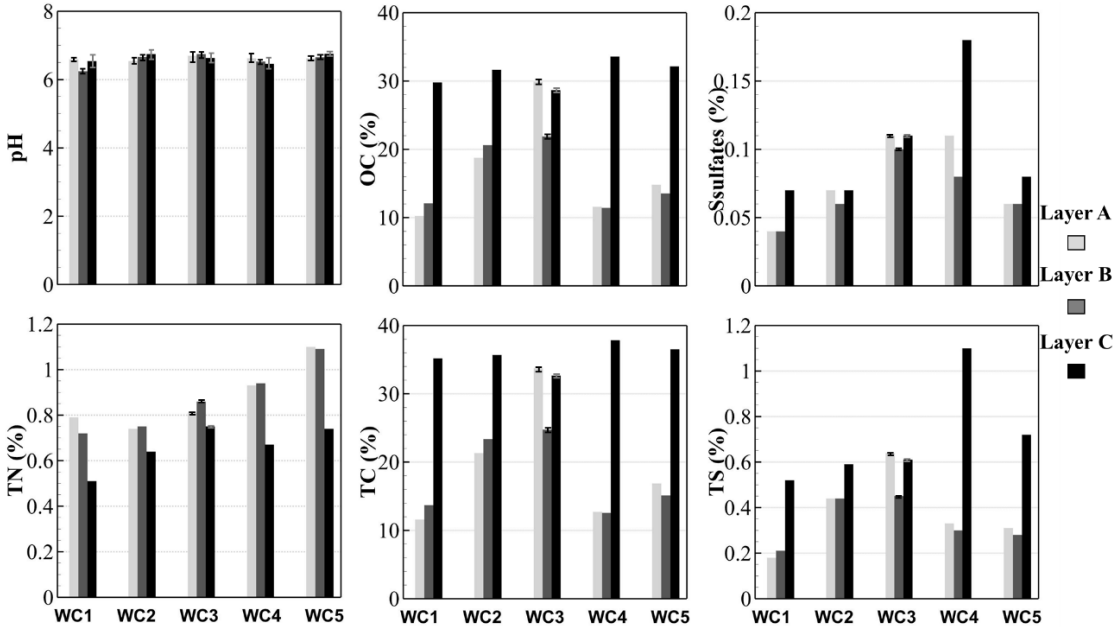

Figure 5.3 Physicochemical characterization of post-treatment residues.

The Ca and Zn concentrations were relatively stable (respectively 10.3±2 g/kg and 0.2±0.03 g/kg) across all samples (Table 5.3; Supplementary Material). The results also showed that Al, As, Fe, K, and Mg were mainly encountered in layers A and B, whereas S was concentrated at the bottom (Figure 5.4 and Table 5.3). This could suggest highly efficient removal of those elements via precipitation/sorption in the biofilter layers (Mehdaoui et al., 2024). As and Fe showed a similar distribution across the biofilter with an Fe/As ratio between 15 and 36. In layers A and B, the highest concentrations of both Fe and As were recorded near the north inlet (WC1; 57.9 g/kg and 3.7 g/kg, respectively), decreasing gradually toward the outlet (WC4; 41.0 g/kg and 1.1 g/kg, respectively). Indeed, high retention was expected near the inlets due to contaminant concentrations in the As-CND and enhanced reactivity. The load of contaminants subsequently decreased due to spreading inside the biofilter, resulting in a decrease in contaminant contents in the post-treatment solids. The same tendency was observed for Al concentrations at the bottom (i.e., layer C), whereas the highest Al concentrations were mostly found close to the outlet (WC4) in the upper layers. Layer C had the lowest metals content with a particular accumulation in the center of the biofilter (WC5). Lower metal contents in this layer could be explained by the slow decomposition of OM and the reducing environment at the bottom of the biofilter, limiting the formation of metal oxides, hydroxides, and oxyhydroxides (Eberle et al., 2021). In contrast, the sulfur distribution within the biofilter produced the lowest S concentrations near the inlets (1.7 g/kg for WC1; Figure 5.4), while

the highest S concentrations were detected at the bottom of the biofilter (11.38 g/kg for WC4), confirming the TS distribution. A considerable horizontal variation was noted in the bottom layer—at the sampling point WC4—that showed a sulfur content four times higher than in the rest of the biofilter.

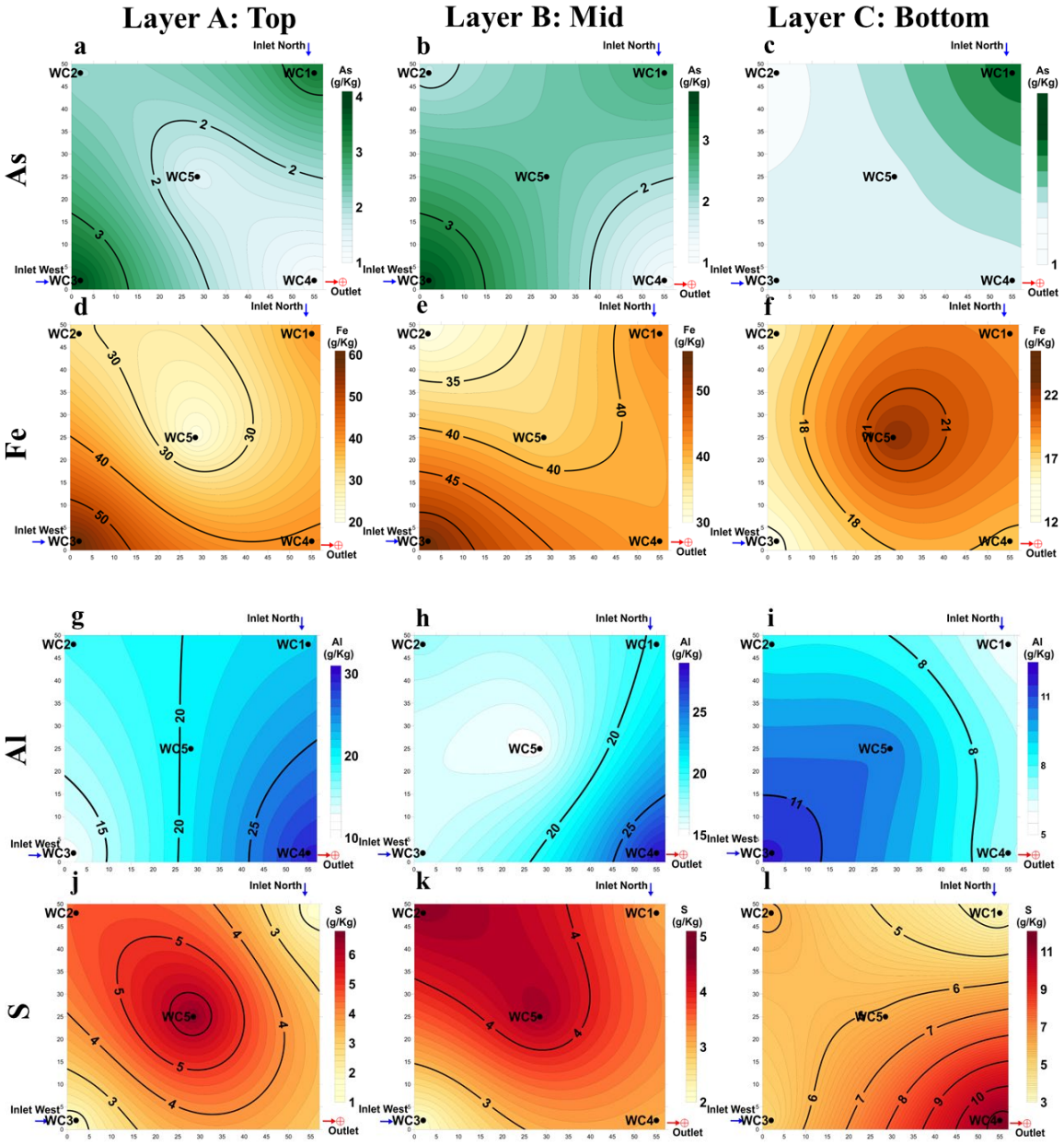

Figure 5.4 Total elemental composition in the post-treatment residues: As (a = top, b = middle, and c = bottom layers), Fe (d = top, e = middle, and f = bottom layers), Al (g = top, h = middle, and i = bottom layers) and S (j = top, k = middle, and l = bottom layers).

This suggests a strongly reducing environment at this location, contributing to the retention of As in the form of As sulfide. The other analysed metals (i.e., K, Mn, and Zn) showed a homogeneous distribution across the biofilter (Mehdaoui et al., 2024). Based on the results discussed above, As retention seemed mainly correlated with metals in the form of metal oxyhydroxides (Fe, Al, and Mg) in layers A and B and in the form of metal sulfides (e.g., As sulfides) in layer C. Therefore, an adequate mineralogical characterization was required to confirm the As removal mechanisms and As-bearing mineral phases that participated in the retention of As in the biofilter residues.

5.6.2 Mineralogical properties of post-treatment residues

XPS was used to determine the oxidation states of the element of interest and to identify As-bearing mineral phases. XPS survey spectra (0–1,350 eV) for all tested samples are presented in the Supplementary Material (Figure A 1) where peaks of special interest ($As2p_{3/2}$, Fe2p, O1s, C1s, S2p, Al2p and As3d) are labeled. XPS survey spectra were used to identify the elements present on the surface of the samples, but high-resolution spectra were necessary to identify chemical or oxidation state information: Al2p, Si2p, K2p, Ca2p, Mg1s, As3d, S2p, C1s, N1s, O1s, and Fe2p high-resolution spectra were collected. Al2p at a binding energy (BE) of 74.8 eV, Si2p at BE = 103.2 eV, $K2p_{3/2}$ at BE = 293.5 eV, $Ca2p_{3/2}$ at BE = 347.7 eV, and Mg 1s at BE = 1,305.0 eV (Figure A 2) were consistent with these elements being in oxyhydroxide and/or silicate phases. High-resolution spectra peak fitting was performed with symmetrical, convoluted Gaussian/Lorentzian functions. Peak fitting components for any element and orbital were constrained to identical full-width-half-maximum (FWHM) except for Fe2p. Each fitting component was related to a chemical group or chemical state for the element based on its BE; the concentration was calculated from the component peak area. It is worth noting that the C 1s and N 1s peak fits (Figures A 3 and A 4) revealed the presence of component peaks C1s at BE = 286.5 and 288.0 eV, indicative of the presence of C-O or C-O-C and O-C-O groups, respectively, which are thought to be mainly related to the decomposition of wood chips (Sasaki et al., 2009). N1s at BE = 400.0 eV indicates bonding of N to carbon such as in amine or amide groups. O1s (Figure A 3 and A 4) was fitted using four component peaks: (i) at BE = 530.6 eV for metal oxides, (ii) at BE = 531.6 eV for metal hydroxides and sulfates, (iii) at BE = 532.6 eV for silicates and C-O species, and (iv) at BE = 533.5 eV for O-C-O species. The Al2p signal (74.6 eV) suggested the formation of Al oxyhydroxides mainly in the upper layer and all over the west inlet (WC3). Similar findings

were reported previously during passive treatment of AMD (Jouini et al., 2019b; Macias et al., 2012).

Selected XPS high-resolution spectra for As3d, Fe2p, and S2p regions are presented in Figure 5.5, Figure 5.6, and Figure 5.7, respectively. Peak fitting of $As2p_{3/2}$ (upper left panel of Figure 5.5) found As in AsS or FeAsS forms at BE = 1,323.7 eV, As(III) at BE = 1,325.7 eV, and As(V) at BE = 1,326.9 eV. Peak fitting of As3d (lower left panel of Figure 5.5) also required fitting of Ca3s at BE = 44.2 eV and overlapped the As3d region. Peak position and FWHM for Ca3s were obtained from sample WC2 in layer C, in which no As was detected (no signal contribution to $As2p_{3/2}$); these fit parameters were fixed for all other samples. The intensity of the Ca3s component peak was also constrained to yield the same relative atomic percentage of Ca from quantification with Ca3s or Ca2p. The remainder of the As3d spectrum intensity was attributed to As in AsS or FeAsS with $As3d_{5/2}$ at BE = 40.9 eV, As(III) at BE = 43.2 eV, and As(V) at BE = 44.7 eV. Spin-orbit splitting and relative peak intensity between $As3d_{3/2}$ and $As3d_{5/2}$ were fixed to 0.6 eV and 0.674 eV, respectively. The right panel of Figure 5.5 presents $As2p_{3/2}$ spectra for samples from all three layers (A (top), B (middle), and C (bottom)) at the biofilter's west inlet (WC3), outlet (WC4), and center (WC5). The spectra were scaled and offset to facilitate comparison of shape differences, thereby providing a visual way to observe changes in As chemical speciation as a function of depth in the biofilter (more to less oxidizing conditions). The upper panel reveals a similar distribution of As species in layers A and B at the inlet, but lower concentrations of As(III) and As(V) species relative to FeAsS or AsS in the bottom layer of the biofilter. A similar behaviour was observed at the outlet where a progressive decrease in As(V), and to a lesser extent As(III), species relative to AsS or FeAsS species was observed from the top to the bottom layer. On the other hand, the center of the biofilter presents a stable distribution of As species along the depth. The lower left panel of Figure 5.7 shows the distribution of As species to total As averaged over WC1 to WC5 as a function of depth, where it is readily observed that As(V) dominated the As species at the top of the biofilter and decreased with depth, while As(III) slightly increased with depth and the least oxidized As species were relatively uniformly distributed.

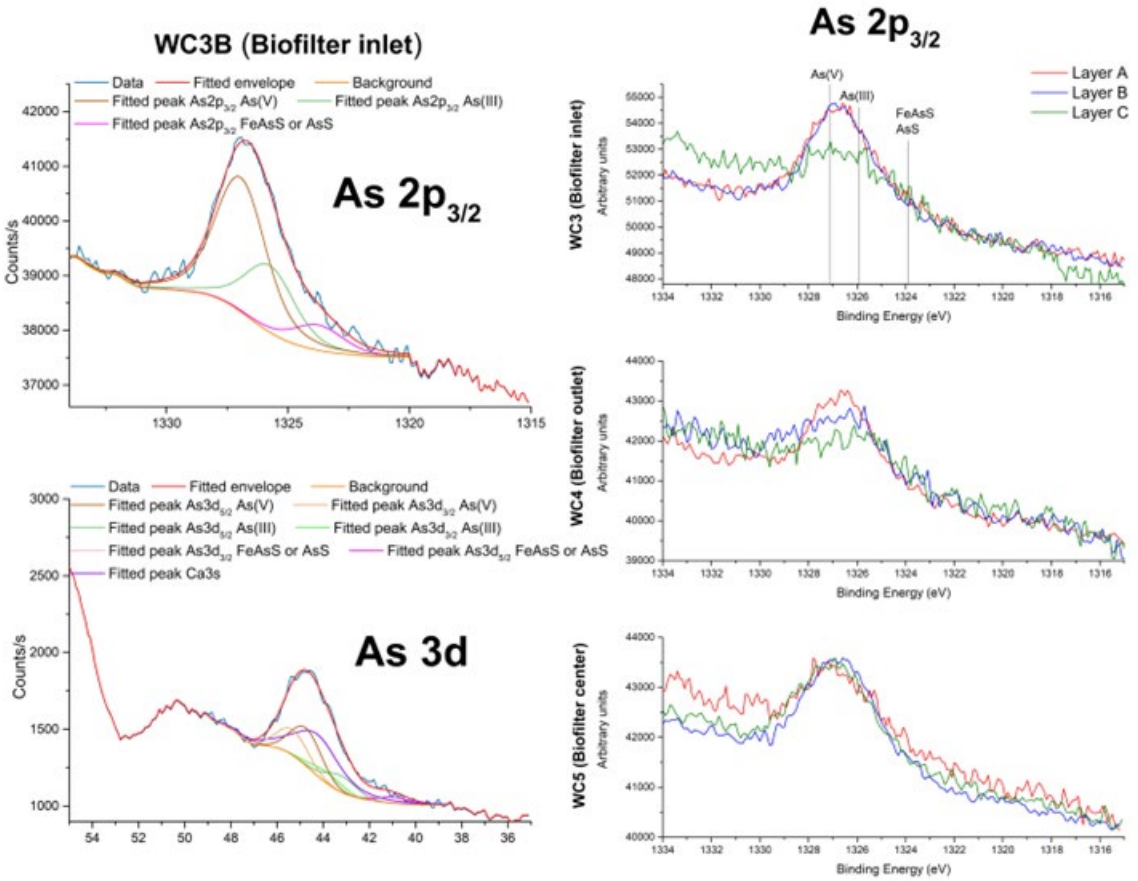

Figure 5.5 High-resolution As2p$_{3/2}$ (upper left panel) and As3d (lower left panel) peak fitting example from data for layer B at the west biofilter inlet (WC3). As2p$_{3/2}$ high-resolution spectra (scaled and offset) for layers A, B, and C at locations WC3 (upper right), WC4 (middle right), and WC5 (lower right panel).

Fe2p typically has a non-symmetrical line shape due to multiplet splitting and shake up peaks, which renders peak intensity assignment to specific mineral phases or even oxidation state arduous in the presence of mixed phase samples. Generally, we expect the form of hematite (Fe_2O_3, 710.8 eV) and goethite (FeOOH, 711.3 eV). Similar phases were previously found in post-treatment residues from the passive treatment of Fe-AMD (Jouini et al., 2019a). Moreover, the precipitation of Fe-oxyhydroxides is a common mechanism during the passive treatment of CND (Sekula et al., 2018). Previously, it was reported that Fe-oxyhydroxides are a main sink for As removal via co-precipitation, surface precipitation, and sorption (Benzaazoua et al., 2004; Coussy et al., 2011; Lizama et al., 2011; Sekula et al., 2018). The high ratio of Fe/As shown above (15 to 36; Figure

5.4), the availability of oxygen, and the pseudo-neutral pH of As-CND created an ideal environment for the co-removal of Fe and As.

Peak fitting of Fe2p is presented in the upper left panel of Figure 6 for the west inlet, layer B. Component peaks in this fit do not bear physical meaning with regards to Fe2p multiplets or shake up peaks, nor to separation of Fe_2O_3 and FeOOH phases. However, it is expected that Fe2p intensity below 710 eV is indicative of the presence of Fe(II) while intensity between 710 eV and 720 eV is dominated by Fe(III) species in iron oxide and iron oxyhydroxide. Peak fitting was performed to determine if the concentration of Fe(II) to Fe(III) species varied across the biofilter.

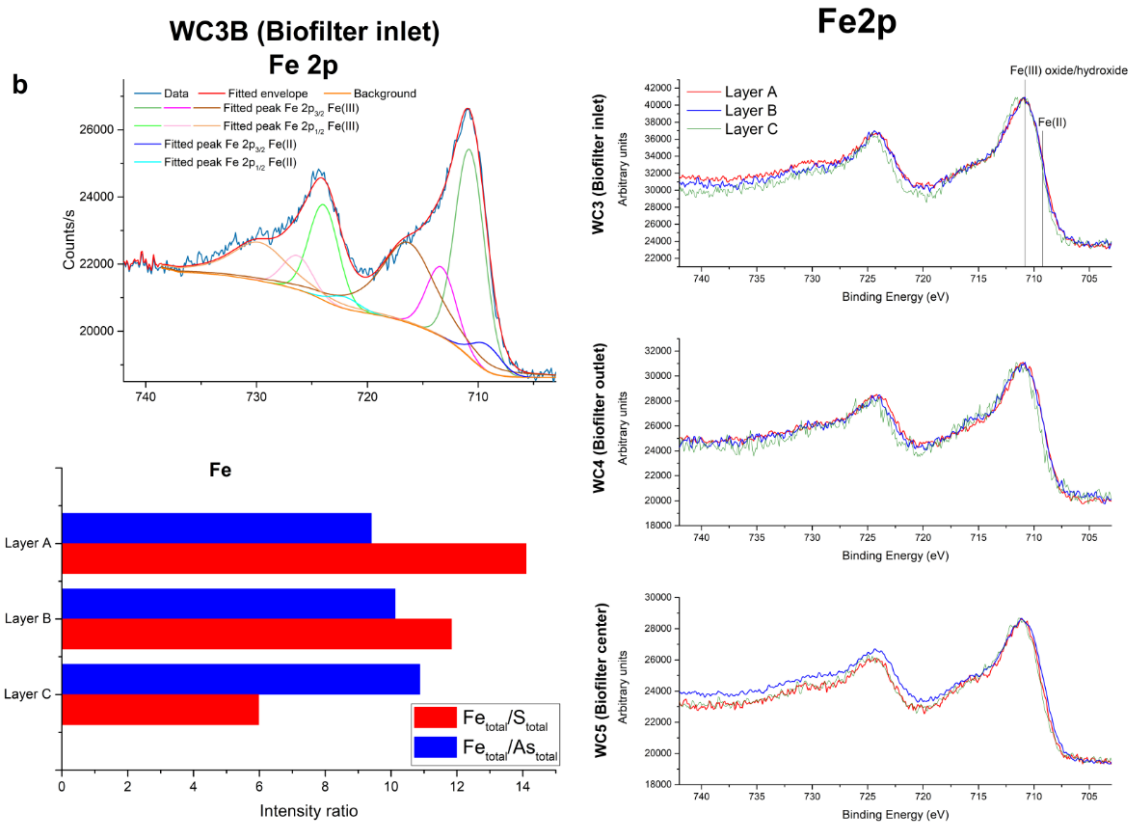

Figure 5.6 High-resolution Fe2p (upper left panel) peak fitting example from data for layer B at the west biofilter inlet. Fe2p high-resolution spectra (scaled and offset) for layers A, B, and C at locations WC3 (upper right), WC4 (middle right), and WC5 (lower right panel). Lower left panel: Ratio of total Fe to total S and As concentrations averaged over locations WC1–WC5 obtained from XPS quantification.

The scaled and offset spectra in the right panel of Figure 6 confirm that Fe(II) vs Fe(III) concentration variations were subtle, but both peak fitting and visual spectral inspection agree that: (i) at the west inlet (WC3) and at the outlet (WC4), lower Fe(II)/Fe(III) concentrations were found in the bottom layer; and (ii) in the biofilter's center (WC5), the concentration of Fe(II)/Fe(III) was highest in layer B and similar in the top and bottom layers. The enhanced presence of highly oxidized species in the upper layers of the west inlet and outlet was similarly observed in As species. As(V) is known to be more prone to sorption onto Fe(III) oxyhydroxides present in the upper layers of the system comparing to other As species.

S2p peak fitting was performed using four doublet components with spin-orbit splitting of 1.18 eV and relative $S2p_{1/2}$ to $S2p_{3/2}$ intensity of 0.511 (Figure 5.7), and with $S2p_{3/2}$ at BE = 162.2, 163.6, 167.7, and 169.0 eV attributed to metal sulfides (M-S), carbon-sulfur (C-S) groups (Jouini et al., 2019b), sulfites, and sulfates, respectively (Kim et al., 2014; Wu et al., 2018). In the right panel of Figure 5.7, scaled and offset S2p spectra permit direct observation of the lower concentration of oxidized sulfur species (sulfite and sulfate) relative to non-oxidized C-S and M-S species in the bottom layers of the west inlet, and at the outlet (WC4) where a significant enhancement of C-S and M-S species was observed. The center of the biofilter exhibited higher concentrations of C-S and M-S species relative to sulfite and sulfate species in the middle layer compared to the top and bottom layers. Once again, this distribution of oxidized and non-oxidized or less oxidized species was also observed in Fe and As. Furthermore, relative to total sulfur concentration and averaged over WC1–WC5, SO_3 and SO_4 species, as well as metal sulfides, dominated in layers A and B, while C-S species dominated at the bottom of the biofilter (Figure 5.7, lower left panel).

The elemental composition presented in Table A 1 found Fe/As ratios between 15 and 36. Meanwhile, disregarding chemical state, XPS analyses determined Fe/As ratios around 10 (Figure 5.6, lower left panel), which increased with depth when averaged over the WC1–WC5 biofilter locations. A lower Fe/As ratio determined by XPS as compared to the bulk elemental composition presented in Table A 1 is an indication that As may have been located predominantly on the surface of iron particles rather than homogeneously within the iron particles. Further evidence of this is provided by $Fe2p/As3d_{5/2}$ vs $Fe2p/As2p_{3/2}$ intensity ratios. Indeed, $As3d_{5/2}$ at a low binding energy around 44 eV has an information depth of 7 nm, while $As2p_{3/2}$ at a binding energy of 1,325 eV is more surface sensitive with an information depth of 1.5 nm.

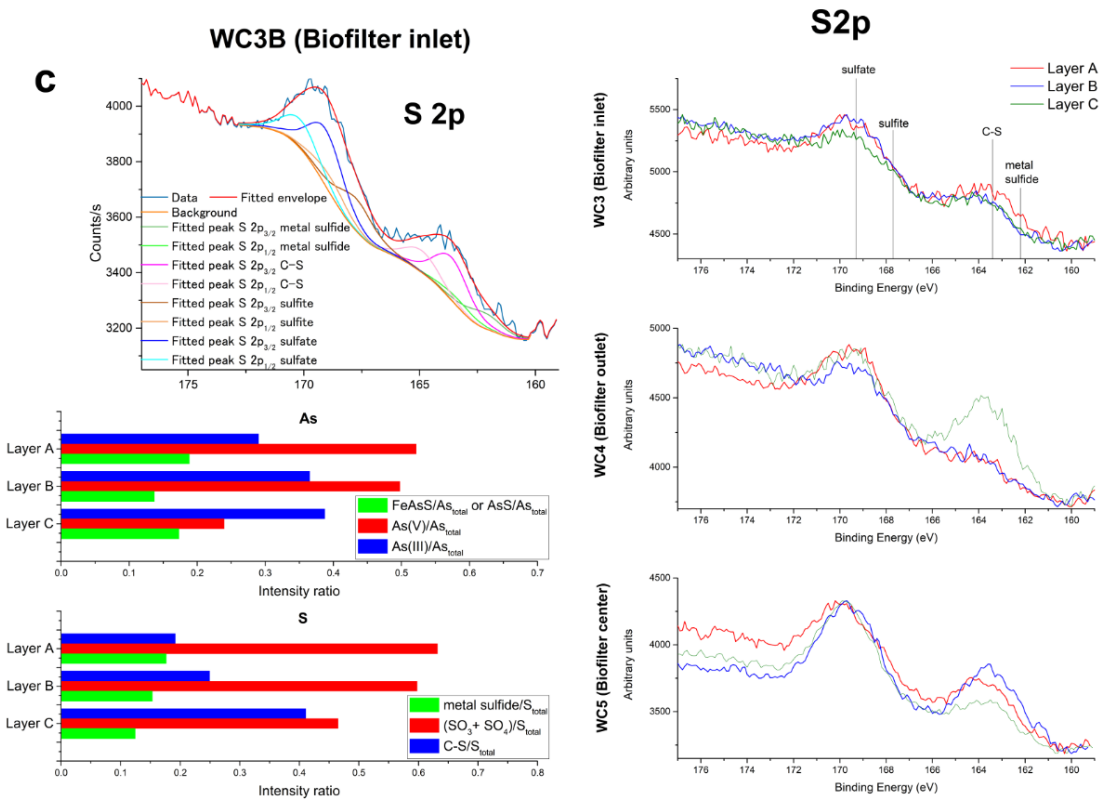

Figure 5.7 High-resolution S2p (upper left panel) peak fitting example from data for layer B at the west biofilter inlet. S2p high-resolution spectra (scaled and offset) for layers A, B, and C at locations WC3 (upper right), WC4 (middle right), and WC5 (lower right panel). Lower left panel: Ratio of As species and S species to total As and S concentrations, respectively, averaged over WC1–WC5 locations obtained from XPS quantification.

As a consequence, a concentration ratio of Fe2p/As2p$_{3/2}$ lower than Fe2p/As3d$_{5/2}$ is indicative of As being mostly located on the surface of iron particles, while a ratio closer to 1 indicates a homogeneous distribution of As throughout the iron particles and supports the mechanism of As precipitation or coprecipitation into more stable phases. As Table 5.1 shows, all Fe2p/As2p$_{3/2}$ concentration ratios were 1.3 to 2.0 times the Fe2p/As3d$_{5/2}$ concentration ratios, except in the bottom layer at the west inlet where a ratio closer to 1 was observed and the bottom layer of WC2 where no As was detected. Therefore, sorption (e.g., adsorption) was the main removal mechanism. Further consistency between the XPS quantification results and the elemental composition presented in Table A 1 was observed in the sulfur distribution, which varied along the depth of the

biofilter as seen in Figure 5.4, and in the decreasing total Fe/S concentration ratios with depth (Figure 5.6).

Overall, results suggest the following possible mechanisms of As removal: (i) sorption of As onto metallic oxyhydroxides (mainly Fe and Al) in the upper layers, and onto metallic sulfides in the bottom layer; (ii) co-precipitation with metal oxyhydroxides (e.g., Fe, Al) in the upper layer; and (iii) precipitation in the form of FeAsS and AsS throughout, especially in the bottom layer.

Table 5-1 Intensity ratios of As peaks (As3d5/2 to As2p3/2).

Samples		**Chemical species**		
		FeAsS or AsS	**As (III)**	**As (V)**
Layer A (Top)	WC1	0.47	0.93	0.44
	WC2	0.64	0.56	0.70
	WC3	0.62	0.68	0.89
	WC4	0.93	0.91	0.60
	WC5	0.70	0.78	0.28
Layer B (Mid)	WC1	0.68	0.57	0.81
	WC2	0.53	0.99	0.78
	WC3	0.52	0.53	0.60
	WC4	0.61	0.31	1.12
	WC5	0.71	0.39	0.95
Layer C (Bottom)	WC1	0.70	0.69	0.67
	WC2	Not detected	Not detected	Not detected
	WC3	0.73	1.05	1.04
	WC4	0.42	0.64	Not detected
	WC5	0.71	0.69	0.69

5.6.3 Environmental assessment of post-treatment residues

The Wood-Cadillac residues were subjected to various leaching scenarios to evaluate As mobility. Results obtained after different leaching tests (TCLP, SPLP, and FLT_m) were compared to Directive 019 (2012) guidelines and the USEPA's Water Quality Criteria (1992, 1994). The As concentrations in TCLP, SPLP, and FLT_m leachates are presented in Figures 5.8 and 5.9, while metal concentrations in each sample are provided in Tables A 5, Table A 6, and Table A 7. Among the three tests, FLT_m showed the highest As release, followed by TCLP and SPLP.

Results of TCLP showed a weakly acidic pH of 4.9±0.2, which was almost the same pH as the leaching medium (4.93). All samples met the USEPA's criteria for As (5 mg/L for As) and were

considered stable and non-hazardous materials suitable for landfill disposal given their low environmental risk. In contrast, the residues exhibited an increasing leaching behaviour with depth, with concentrations exceeding the D019 guidelines limits (>0.2 mg/L of As) (MELCCFP, 2012). Indeed, 66% of leachate samples exceeded the D019 limits for As with the highest concentrations in the bottom layer (1.06 mg/L at WC4; Table A 5). The findings revealed an unexpected pattern, where samples with the highest As content did not correspond to those with significant As leaching (Figure 5.4a and Figure 5.8). It appears that, in the upper layers, the co-presence of Fe and As led to co-precipitation of As onto Fe(III) oxyhydroxides that were less prone to leaching. However, locations with high As leaching were situated at the bottom, which were typically rich in sulfur-bearing minerals such as realgar (AsS), arsenopyrite (FeAsS), and metal sulfides. Once oxidized, those phases were more susceptible to As leaching.

The SPLP leachates showed a slightly acidic pH of 5.9±0.3. Metal concentrations were below the USEPA's criteria; thus, the risk of groundwater contamination through leachate formation was excluded. However, regarding D019 guidelines, only six samples qualified as leachable for As (Figure 5.8 and Table A 6). It is worth noting that samples from the biofilter center (WC5) were leachable for As after TCLP and SPLP according to D019 guidelines. This result could be explained by the presence of FeAsS and/or AsS in the residues from the biofilter center. Indeed, these minerals are known to be unstable under oxidizing conditions, thus exhibiting high As leaching.

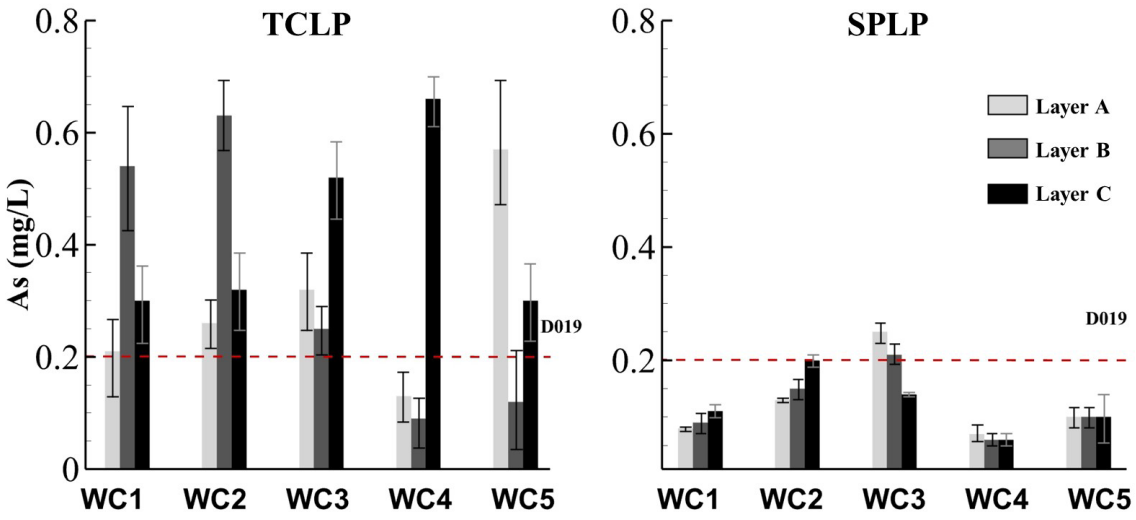

Figure 5.8 Arsenic concentrations in TCLP and SPLP leachates.

The FLT_m leachates exhibited a slightly acidic pH of 5.9±0.4, which was close to the pH of the demineralized water used in the test (~5.7). The concentrations of metals released in the FLT_m, particularly As (Figure 5.9 and Table A 7) were greater than those leached in the TCLP and SPLP tests (Fig. 5.8, Table A 5 and Table A 6). This was probably caused by the reduction in particle size, providing more exposed surfaces and thus enhancing As release (Akhavan and Golchin, 2021). In addition, the residues were dried prior to the FLT_m test, which accelerated their reactivity. The highest concentrations in leachates were associated with the upper layer, particularly at the biofilter center. The dissolution of Fe(III) oxyhydroxides at pH ≥ 6 may enhance the desorption of As, thus increasing the leaching potential (Rakotonimaro et al., 2021). Hence, at the end of the biofilter lifespan, it is recommended to store the residues under water.

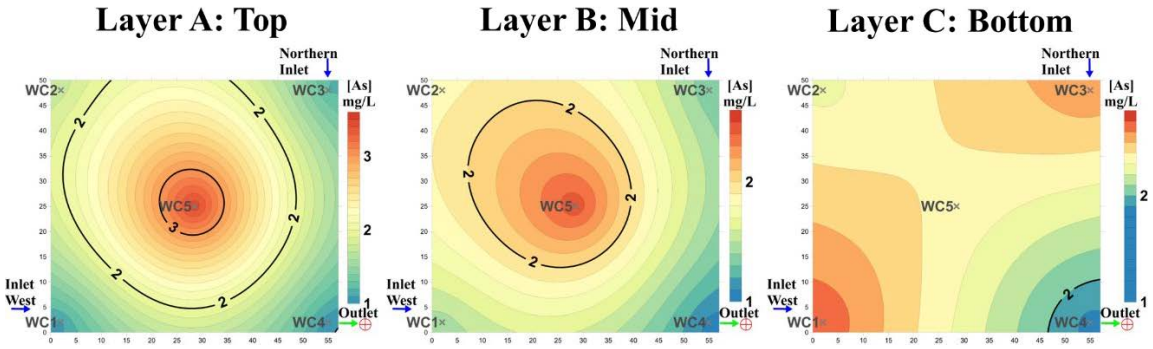

Figure 5.9 Arsenic concentration in modified FLT leachates in the field biofilter.

Overall, results showed inconsistent residue stability: USEPA criterion classified them as non-hazardous while D019 guidelines confirmed their leachable behaviour for As. The discrepancy in post-treatment residues classification after the FLT_m test is explained by differences in the stringency of regulatory levels (D019 vs USEPA). The pH of the extractions (4.93 vs 4.20 vs 5.70), the interference with the reagents (glacial acetic acid vs sulfuric acid + nitric acid vs demineralized water), and the short reaction time (less than 24 h) are some of the variables that affect the reliability of static tests (Mehdaoui et al., 2023). It is therefore suggested that dynamic tests (e.g., columns) be performed as previously recommended for post-treatment residues from Fe-AMD to confirm the behaviour of residues under static tests and to anticipate their fate at the end of the lifespan of the biofilter (Jouini et al., 2019c, 2020b).

5.7 General discussion

The Wood-Cadillac biofilter demonstrated high efficiency in treating As-CND, with results indicating that all residues contained elevated concentrations of metals (As, Al, Fe, and S). The highest levels of TC, OC, and TS were observed in the bottom of the biofilter, confirming the existence of a reducing environment at depth. The upper layers (i.e., top, and mid layers) contained only half of the TC and TS content as compared to the bottom. Furthermore, Fe and Al were mainly concentrated in the upper layers while the highest concentrations of S were measured in the bottom. The mineralogical composition showed a heterogeneous distribution between the upper layers and those at depth. Arsenic removal during As-CND treatment in the biofilter occurred via sorption onto Fe-oxyhydroxides and/or Al-oxyhydroxides, as well as through precipitation in the form of As sulfides (FeAsS or AsS). The high ratio of Fe/As (>15) favoured the co-removal of As with Fe. Additional mechanisms such as co-precipitation or surface precipitation were also possible. Regardless of the As-bearing mineral phases, differences in As leaching were observed between TCLP, SPLP, and FLT_m (Table 5.2). Arsenic sulfides exhibited the highest leaching potential, followed by metal sulfides and then metal oxyhydroxides. The leaching behaviour was significantly influenced by the type of leaching medium, the pH, and the particle size of the post-treatment residues (specifically, an increase in an element's solubility after grinding, as observed under FLT_m tests). Furthermore, most TCLP leachates did not comply with D019 guidelines, and could be considered as leachable according to provincial regulations in Quebec. In addition, at the end of the operational lifespan of PTS, an effective management of post-treatment residues, particularly As-rich materials, is necessary to ensure long-term stability and prevent contaminants leaching. Several factors may alter contaminant dynamics, such as oxidation, which may lead to mobilization; redox induced instability of Fe-bound arsenic; sulfate release; and variations in pore water pH (Yamaguchi et al., 2011; Eberle et al., 2021). To mitigate As remobilization, storing residues under anoxic conditions or submerging them in water is recommended (Jouini et al., 2019a; 2020a). Management strategies could include stabilization/solidification with lime or phosphate amendments, secure encapsulation in engineered facilities, or repurposing residues in construction materials (Macias et al., 2012; Kousi et al., 2018; Jouini et al., 2020b). However, these approaches must be carefully evaluated for long-term effectiveness.

Table 5-2 Summary of the environmental behaviour of Wood-Cadillac post-treatment residues.

Test	Leaching conditions							Observations
	Sample	**Reagents**	**pH**	**Time**	**Temperature**	**Solid /Liquid**	P_{80} (μm)	
TCLP	Wet	H_2O + CH_3COOH + NaOH	4.93	18 h	20±2°C	1/20	2,700 ~ 5,600	Residues were classified as nonhazardous 66% are leachable for As according to D019
SPLP	Wet	H_2O + HNO_3 + H_2SO_4	4.20	18 h	20±2°C	1/20	2,700 ~ 5,600	No potential leaching of contaminants from residues into groundwater. 20% of samples qualified as leachable for As according to D019
FLTm	Dried	H_2O	5.70	5 min	20±2°C	1/20	<100	All samples were leachable for As according to D019 Residues should not be dried or crushed at the end of biofilter lifespan

5.8 Conclusion

This study aimed to enhance the understanding of As removal mechanisms in a 20-year-old field passive biofilter treating As-CND and assess the stability of post-treatment residues. The results showed high levels of contaminants (As, Al, Fe, and S) in the residues, indicating effective retention of the contaminants within the biofilter system. XPS analyses demonstrated that As removal occurred primarily through sorption onto metal oxyhydroxides (mainly Fe and Al) in the upper layers. Reducing conditions at the bottom of the biofilter promoted the precipitation of As sulfide (FeAsS and AsS) and metal sulfide minerals. The environmental behaviour of post-treatment As-CND was evaluated using several static tests. According to the results from TCLP and SPLP, the residues were classified as non-hazardous with respect to USEPA regulations. However, 66% of TCLP leachates and 20% of SPLP results exceeded D019 guidelines limits for As. Additionally, all residues were found to be leachable for As according to FLT_m results, indicating that residues should not be dried or crushed. Overall, the study suggested that residues should be left onsite to ensure their stability. While storage under water could be considered as a management option, future research should focus on developing a more suitable environmental assessment framework to evaluate management plans.

Acknowledgments

This research was funded by the Natural Sciences and Engineering Research Council of Canada (NSERC), Canada Research Chairs Program, Mitacs and RIME UQAT-Polytechnique industrial partners, including Agnico Eagle, Canadian Malartic Mine, Iamgold, Raglan Mine–Glencore, Newmont, and Rio Tinto. The authors would like to thank MRNF for their on-site support during the sampling campaign and for providing the historical monitoring data. They also acknowledge the guidance and support received from Professor Eric Rosa, Dr. Étienne Bélanger, Dr. Félix Legendre and Dr. Youssef Guesmi during the collection of field samples and laboratory experiments.

References

Akhavan, A., Golchin, A., 2021. Estimation of arsenic leaching from Zn–Pb mine tailings under environmental conditions. Clean. Prod., 295, 126477. https://doi.org/10.1016/j.jclepro.2021.126477

American Society for Testing and Materials (ASTM), 2019. D4972-19: Standard test method for pH of soils. Book of Standards 04 (08), West Conshohocken, PA. 10.1520/D4972-19

Ben Ali, H.E., Neculita, C.M., Molson, J.W., Maqsoud, A., Zagury, G.J., 2019. Performance of passive systems for mine drainage treatment at low temperature and high salinity: A review. Miner. Eng., 134, 325–344. https://doi.org/10.1016/j. mineng.2019.02.010

Ben Ali, H.E., Neculita, C.M., Molson, J.W., Maqsoud, A., Zagury, G.J., 2020. Salinity and low temperature effects on the performance of column biochemical reactors for the treatment of acidic and neutral mine drainage. Chemosphere, 243, 125303. https:// doi.org/10.1016/j.chemosphere.2019.125303

Benzaazoua, M., Marion, P., Picquet, I., Bussière, B., 2004. The use of pastefill as a solidification and stabilization process for the control of acid mine drainage. Miner. Eng. 17 (2), 233–243. https://doi.org/10.1016/j.mineng.2003.10.027

Centre d'Expertise en Analyse Environnementale du Québec (CEAEQ), 2012. Protocole de lixiviation pour les espèces inorganiques, MA. 100 – Lix.com. 1.1, Rév. 1, Ministère du Développement Durable, de l'Environnement, de la Faune et des Parcs du Québec, Québec, Canada, Volume 7, pp. 1–17.

Coussy, S., Benzaazoua, M., Blanc, D., Moszkowicz, P., Bussière, B., 2011. Arsenic stability in arsenopyrite-rich cemented paste backfills: a leaching test-based assessment. Hazard. Mater., 185 (2-3), 1467-1476. https://doi.org/10.1016/j.jhazmat.2010.10.070

De Repentigny, C., Courcelles, B., Zagury, G.J., 2018. Spent MgO-carbon refractory bricks as a material for permeable reactive barriers to treat a nickel- and cobalt- contaminated groundwater. Environ. Sci. Pollut. Res., 25(23), 23205–23214. https://doi.org/10.1007/s11356-018-2414-3

Eberle, A., Besold, J., León-Ninin, J.M., Kerl, C.F., Kujala, K., Planer-Friedrich, B., 2021. Potential of high pH and reduced sulfur for arsenic mobilization – Insights from a Finnish peatland treating mining waste water. Sci. Total Environ., 758, 143689. https://doi.org/10.1016/j.scitotenv.2020.143689

El Kilani, M.A., Jouini, M., Rakotonimaro, T.V., Neculita, C.M., Molson, J.W., Courcelles, B., Dufour, G., 2021. In-situ pilot-scale passive biochemical reactors for Ni removal from saline mine

drainage under subarctic climate conditions. Water Process Eng., 41, 102062. https://doi.org/10.1016/j.jwpe.2021.102062

Genty, T., Neculita, C.M., Bussière, B., Zagury, G.J., 2012. Environmental behaviour of sulphate-reducing passive bioreactor mixture. In: Proc. of the 9th International Conference on Acid Rock Drainage, Ottawa, Canada, May 20–26.

Germain, D., Cyr, J., 2003. Evaluation of biofilter performance to remove dissolved arsenic: Wood Cadillac. In: Proc. of the Mining and the Environment, Sudbury, Ontario, May 25–28.

Germain, D., Gagnon, A., 2013. Site minier Wood Cadillac: Évaluation de la performance du biofiltre et de la qualité des eaux du ruisseau Pandora. Direction de la restauration des sites minier – Ministère des Ressources Naturelles, 40 p.

Hageman, P.L., Seal, R.R., Diehl, S.F., Piatak, N.M., Lowers, H.A., 2015. Evaluation of selected static methods used to estimate element mobility, acid-generating and acid- neutralizing potentials associated with geologically diverse mining wastes. Appl. Geochem., 57, 125–139. https://doi.org/10.1016/j.apgeochem.2014.12.007

Hageman, P.L., 2007. U.S. Geological survey field leach test for assessing water reactivity and leaching potential of mine wastes, solids, and other geologic and environmental materials. U.S. Geological Survey Techniques and Methods, Vol. 5, Ch. D3, Department of the Interior, Reston, VA.

Jong, T., Parry, D.L., 2005. Evaluation of the stability of arsenic immobilized by microbial sulfate reduction using TCLP extractions and long-term leaching techniques. Chemosphere, 60(2), 254–265. https://doi.org/10.1016/j. chemosphere.2004.12.046

Jouini, M., Neculita, C.M., Genty, T., Benzaazoua, M., 2019a. Environmental assessment of residues from multi-step passive treatment of Fe-AMD: Field case study of the Lorraine mine site, Quebec, Canada. In: Proc. of Tailings and Mine Waste, Vancouver, BC, Canada, November 17–20.

Jouini, M., Rakotonimaro, T.V., Neculita, C.M., Genty, T., Benzaazoua, M., 2019b. Stability of metal rich residues from laboratory multi-step treatment system for ferriferous acid mine drainage. Environ. Sci. Pollut. Res., 26(35), 35588–35601. 10.1007/s11356-019-04608-1

Jouini, M., Rakotonimaro, T.V., Neculita, C.M., Genty, T., Benzaazoua, M., 2019c. Prediction of the environmental behavior of residues from the passive treatment of acid mine drainage. Appl. Geochem., 110, 104421. https://doi.org/10.1016/j.apgeochem.2019.104421

Jouini, M., Neculita, C.M., Genty, T., Benzaazoua, M., 2020a. Environmental behaviour of metal-rich residues from the passive treatment of acid mine drainage. Sci. Total Environ., 712, 136541. https://doi.org/10.1016/j.scitotenv.2020.136541

Jouini, M., Neculita, C.M., Genty, T., Benzaazoua, M., 2020b. Freezing/thawing effects on geochemical behavior of residues from acid mine drainage passive treatment systems. Water Process Eng., 33, 101087. https://doi.org/10.1016/j.jwpe.2019.101087

Jouini, M., Benzaazoua, M., Neculita, C.M., 2021. Stabilization/solidification of acid mine drainage treatment sludge. In: Wang, L., Tsang, C.W. (Eds.), Low carbon stabilization and solidification of hazardous wastes, 175–199.

Kim, E.J., Yoo, J-C., Baek, K., 2014. Arsenic speciation and bioaccessibility in arsenic-contaminated soils: Sequential extraction and mineralogical investigation. Environ. Pollut., 186, 29–35. https://doi.org/10.1016/j.envpol.2013.11.032

Kousi, P., Remoundaki, E., Hatzikioseyian, A., Korkovelou, V., Tsezos, M., 2018. Fractionation and leachability of Fe, Zn, Cu and Ni in the sludge from a sulphate-reducing bioreactor treating metal-bearing wastewater. Environ. Sci. Pollut. Res., 25 (36), 35883–35894. https://doi.org/10.1007/s11356-018-1905-6

Lizama, K., Fletcher, T.D., Sun, G., 2011. Removal processes for arsenic in constructed wetlands. Chemosphere, 84 (8), 1032–1043. https://doi.org/10.1016/j.chemosphere.2011.04.022

Macías, F., Caraballo, M.A., Nieto, J.M., 2012. Environmental assessment and management of metal-rich wastes generated in acid mine drainage passive remediation systems. Hazard. Mater., 229–230, 107–114. https://doi.org/10.1016/j.jhazmat.2012.05.080

Masindi, V., Foteinis, S., Renforth, P., Ndiritu, J., Maree, J.P., Tekee, M., Chatzisymeon, E., 2022. Challenges and avenues for acid mine drainage treatment, beneficiation, and valorisation in circular economy: A review. Ecol. Eng. 183, 106740. https://doi.org/10.1016/j.ecoleng.2022.106740

McCann, J.I., Nairn, R.W., 2022. Characterization of residual solids from mine water passive treatment oxidation ponds at the tar creek superfund site, Oklahoma, USA: Potential for reuse or disposal. Cleaner Waste Syst., 3, 100031. https://doi.org/ 10.1016/j.clwas.2022.100031

Mehdaoui, H.Y., Guesmi, Y., Jouini, M., Neculita, C.M., Pabst, T., Benzaazoua, M., 2023. Passive treatment residues of mine drainage: Mineralogical and environmental assessment, and management avenues. Miner. Eng., 204, 108362. https://doi.org/https://doi.org/10.1016/j.mineng.2023.108362

Mehdaoui, H.Y, Neculita, C.M., Pabst, T., Benzaazoua, M., 2024. Environmental assessment of post-treatment residues from contaminated neutral drainage: Field case study of Wood-Cadillac biofilter, Quebec, Canada. In: Proc. of the 13th International Conference on Acid Rock Drainage, Halifax, Nova Scotia, Canada, September 16-20.

Ministère de l'Environnement, de la Lutte contre les Changements Climatiques, de la Faune et des Parcs (MELCCFP), 2012. Directive 019 sur l'industrie minière. Québec's Government, QC, Canada, 978-2-550- 64507-8, 105 p.

Neculita, C.M., Zagury, G.J., Bussière, B., 2021. Passive treatment of acid mine drainage at the reclamation stage. In: Bussière, B., Guittonny, M. (Eds.), Hard Rock Mine Reclamation: From Prediction to Management of Acid Mine Drainage. CRC Press, 271–296.

Ness, I., Janin, A., Stewart, K., 2014. Passive treatment of mine impacted water in cold climates: A review. Yukon College, Yukon Research Centre, 56 p.

Nordstrom, D.K., Blowes, D.W., Ptacek, C.J., 2015. Hydrogeochemistry and microbiology of mine drainage: an update. Appl. Geochem., 57, 3–16. https://doi.org/10.1016/j.apgeochem.2015.02.008

Rahman, K.Z., Wiessner, A., Kuschk, P., Van Afferden, M., Mattusch, J., Muller, R.A., 2011. Fate and distribution of arsenic in laboratory-scale subsurface horizontal-flow constructed wetlands treating an artificial wastewater. Ecol. Eng. 37 (8), 1214-1224. https://doi.org/10.1016/j.ecoleng.2011.02.016

Rakotonimaro, T.V., Guittony, M., Neculita, C.M., 2021. Compaction of peat cover over desulfurized gold mine tailings changes: Arsenic speciation and mobility. Appl. Geochem., 128, 104923. https://doi.org/10.1016/j.apgeochem.2021.104923

Sasaki, K., Nakano, H., Wilopo, W., Miura, Y., Hirajima, T., 2009. Sorption and speciation of arsenic by zero-valent iron, Colloids Surf. A: Physicochem. Eng. Asp. 347 (1–3), 8-17. https://doi.org/10.1016/j.colsurfa.2008.10.033

Schwindaman, J.P., Castle, J.W., Rodgers Jr., J.H., 2014. Fate and distribution of arsenic in a process-designed pilot-scale constructed wetland treatment system. Ecol. Eng. 68, 251-259. https://doi.org/10.1016/j.ecoleng.2014.03.049

Sekula, P., Hiller, E., Šottník, P., Jurkovič, Ľ., Klimko, T., Vozár, J., 2018. Removal of antimony and arsenic from circum-neutral mine drainage in Poproč, Slovakia: A field treatment system using low-cost iron-based material. Environ. Earth Sci., 77 (13), 518. https://doi.org/10.1007/s12665-018-7700-3

Skousen, J., Zipper, C.E., Rose, A., Ziemkiewicz, P.F., Nairn, R., McDonald, L.M., Kleinmann, R.L., 2017. Review of passive systems for acid mine drainage treatment. Mine Water Environ., 36 (1), 133–153. https://doi.org/10.1007/s10230-016-0417-1

Sobek, A.A., 1978. Field and laboratory methods applicable to overburdens and minesoils. Industrial environmental research laboratory, Office of research and development, US Environmental Protection Agency.

Turcotte, S., Trépanier, S., Bussière, B., 2021. Restauration des sites miniers abandonnées au Québec : Un état de la situation et revue des solutions appliquées. In. Proc. Symposium 2021 sur l'Environnement et les Mines, Rouyn-Noranda, Québec, Juin 14–16.

USEPA (United States Environmental Protection Agency), 2007. Method 3051A (SW-846): Microwave assisted acid digestion of sediments, sludges, and oils. Revision 1. Washington, DC, USA.

USEPA, 1992. Method 1311. Toxicity characteristic leaching procedure. Washington, D.C. https://www.epa.gov/sites/production/files/2015-12/documents/1311.pdf (last access August 23, 2024).

USEPA, 1994. Method 1312. Synthetic precipitation leaching procedure. Washington, DC, USA. https://www.epa.gov/sites/default/files/2015-12/documents/1312.pdf (last access August 23, 2024)

Yamaguchi, N., Nakamura, T., Dong, D., Takahashi, Y., Amachi, S., Makino, T., 2011. Arsenic release from flooded paddy soils is influenced by speciation, Eh, pH, and iron dissolution. Chemosphere 83, 7, 925-932. https://doi.org/10.1016/j.chemosphere.2011.02.044

Yim, G., Ji, S., Cheong, Y., Neculita, C.M., Song, H., 2015. The influences of the amount of organic substrate on the performance of pilot-scale passive bioreactors for acid mine drainage treatment. Environ. Earth Sci., 73, 4717–4727. https://doi.org/ 10.1007/s12665-014-3757-9

Wu, H., Zhu, Y., Bian, S., Ko, J.H., Li, S.F.Y., Xu, Q., 2018. H2S adsorption by municipal solid waste incineration (MSWI) fly ash with heavy metals immobilization, Chemosphere, 195, 40–47. https://doi.org/10.1016/j.chemosphere.2017.12.068

Zimmerman, C.F., Keefe, C.W., Bashe, J., 1997. Method 440.0 Determination of carbon and nitrogen in sediments and particulates of estuarine/coastal waters using elemental analysis. U.S. Environmental Protection Agency, Washington, DC, USA, EPA/600/R-15/009. style des titres de sections doit être Titre 2 (voir la saisie d’écran de la section 2.1).

CHAPITRE 6 ARTICLE 4 _ STABILITY OF As-RICH RESIDUES FROM PILOT BIOFILTERS FOR PASSIVE TREATMENT OF NEUTRAL MINE DRAINAGE: LABORATORY VS FIELD TESTING[4]

Hsan Youssef Mehdaoui[1], Marouen Jouini[2], Josianne Lefebvre[3], Carmen Mihaela Neculita[1,*], Thomas Pabst[4] and Mostafa Benzaazoua[2]

[1] Research Institute on Mines and Environment (RIME), Université du Québec en Abitibi-Témiscamingue (UQAT), Rouyn-Noranda, QC J9X 5E4, Canada

[2] University Mohammed VI Polytechnic (UM6P), Geology and Sustainable Mining Institute (GSMI), Lot 660 Hay Moulay Rachid, 43150, Ben Guerir, Morocco

[3] Materials Surface Analyses Laboratory, Engineering Physics Department, Polytechnique Montréal, 2500, chemin de Polytechnique, Montréal, QC H3T 1J4

[4] Norwegian Geotechnical Institute (NGI), Sandakerveien 140, 0484 Oslo, Norway

*Corresponding author email: Carmen Mihaela Neculita

Article soumis le 21 mars 2025 à la revue *Journal of Hazardous Materials*

6.1 Abstract

Passive biofilters efficiently treat As-rich contaminated neutral drainage (As-CND), while the management of contaminated residues remains uncertain. Environmental stability of As-CND post-treatment residues from 3 pilot-scale biofilters, lab vs field was assessed. Twenty solid samples were collected from four layers of each biofilter (I-1, A, B and I-2), while As removal mechanisms were assessed via physiochemical and mineralogical characterization. Environmental stability was evaluated using static leaching tests (TCLP, SPLP and FLT). Results showed highly contaminated residues, with concentrations of As up to 3.6 g/kg, and of Fe up to 86.3 g/kg. Metal oxyhydroxides and silicates were the main mineral phases in the three biofilters. The retention of As was controlled by sorption onto Fe (III)-oxyhydroxides in the laboratory biofilter, whereas in field-pilot biofilters As removal involved sorption in the upper layers but precipitation in the form of FeAsS and co-precipitation with metal (Fe and Al)-oxyhydroxides was found in the deeper layers. Static tests results showed compliance (USEPA) classifying the residues of as non-hazardous and suitable for

[4]Mehdaoui, H.Y., Jouini, M., Lefebvre, J., Neculita, C.M., Pabst, T., Benzaazoua, T. (2025) Stability of As-rich residues from pilot biofilters for passive treatment of neutral mine drainage: Laboratory vs field testing. *Journal of Hazardous Materials* (en évaluation)

potential co-disposal with municipal waste. The TCLP results also met Quebec's regulation on mine effluents classifying them as low risk. These findings indicate passive biofilters as promising for the control of As-CND.

Keywords: pilot biofilter, passive treatment, arsenic removal, residues stability, contaminated neutral drainage

List of abbreviations

AMD = Acid Mine Drainage; As-CND = Arsenic-rich Contaminated Neutral Drainage; CND = Contaminated Neutral Drainage; DAS = Dispersed Alkaline Substrate; D019 = Directive 019 (Guidelines) pertaining to the Mining Industry in Quebec, Canada; FLT = Field Leaching Test; HRT = Hydraulic Residence Time; MD-S = Mine drainage Sludge; OM = Organic Matter; PBRs = Passive Biochemical Reactors; PTSs = Passive Treatment Systems; SPLP = Synthetic Precipitation Leaching Procedure; TCLP = Toxicity Characteristic Leaching Procedure; USEPA = United States Environmental Protection Agency; XPS = X-ray Photoelectron Spectroscopy.

6.2 Graphical abstract

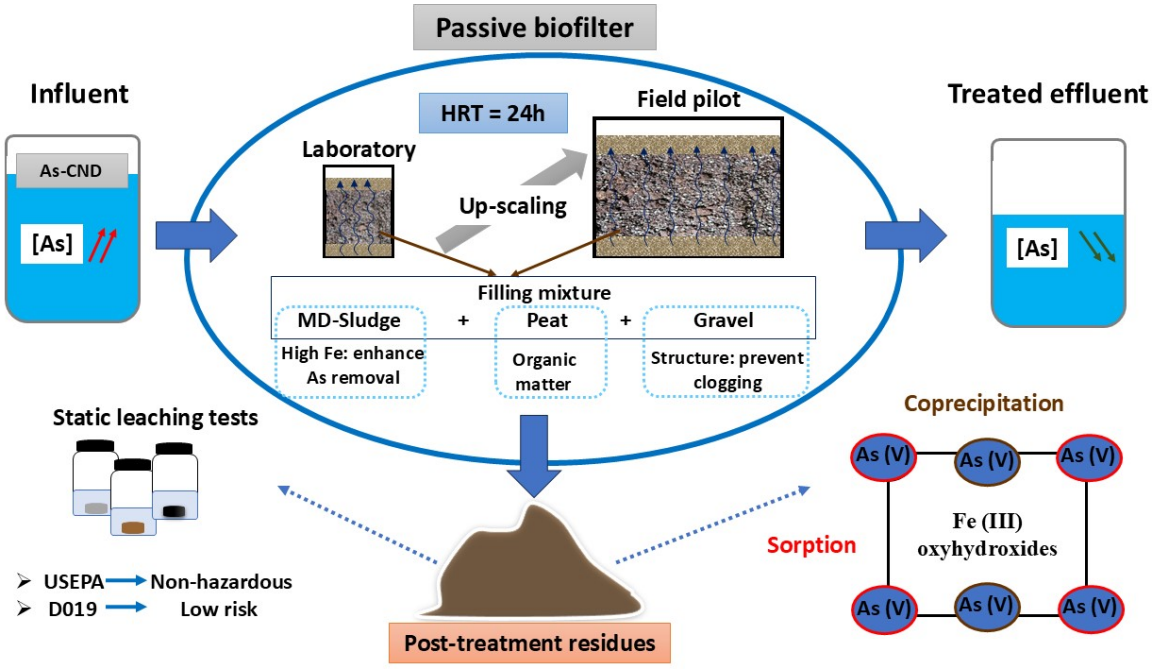

6.3 Highlights

- Lab vs field-pilot biofilters were operated for As-neutral mine drainage treatment.
- All pilot biofilters efficiently remove As via sorption onto Fe(III)-oxyhydroxides.
- As retention was enhanced by metals (Fe, Al, Mg) in filling mixture of biofilters.
- Post-treatment residues were classified as non-hazardous for their management.

6.4 Introduction

Contaminated neutral drainage (CND), also referred to neutral mine drainage, is a less documented type of mine drainage relative to acid mine drainage (Johnson and Hallberg, 2005). The CND is characterized by sulfates, metals and metalloids that exceed criteria and may have a detrimental impact on environment. These contaminants must be treated before releasing the water into the receiving environment. The As-CND is a type of contamination driven by the global increase in gold and silver extraction from refractory, As-bearing ores (Skousen et al., 2017). The common species of As in mine water are trivalent As(III) ($HAsO_2$) and pentavalent As(V) ($HAsO_4^{2-}$) (Smedley and Kinniburgh, 2002). At neutral pH, As (III) is more toxic and more mobile. Thus, precipitation of As in the form of As (V) is preferred (Wang and Mulligan, 2006).

Passive treatment is an efficient method to treat CND at abandoned and reclaimed mine sites (Ben Ali et al., 2019). Because of the high costs of conventional active treatment methods and the large number of abandoned mine sites, reliable, cost-effective, and sustainable passive treatment systems (PTSs) are still needed (Macias et al., 2012). Passive biochemical reactors (PBR) or biofilters are efficient PTSs (Neculita et al., 2007). They use a mixture of structuring agents, sorbants materials and organic matter (OM) to ensure the treatment of CND. The OM can be either natural (e.g., peat, wood ash, plant residues) or pseudo-natural (e.g., modified materials) (Neculita et al., 2007). Some Fe-rich inorganic materials such as sludge from active treatment of acid mine drainage (AMD) could be added to the mixture to enhance contaminants removal (Kawazoe et al., 2023). The efficiency of biofilters depends on CND quality, flow rate, hydraulic residence time (HRT) and the treatment objectives (Ben Ali et al., 2019). High removal of As (88%), Fe (75%), Cu (95%), Cd (90%), Sb (82%), Ni (74%) and Zn (89%) were recorded at field pilot and full scale biofilters

(Nielson et al., 2018; Sekula et al., 2018; Jouini et al., 2019a; El Kilani et al., 2021; Turcotte et al., 2021).

The As removal in biofilters is mainly related to the presence of Fe-oxyhydroxides (e.g. ferrihydrite, goethite) via sorption and co-precipitation (Sekula et al., 2018; Battaglia-Brunet et al., 2023; Mehdaoui et al., 2025). Metal oxyhydroxides are common minerals for As in PTSs treating CND (Sekula et al., 2018; Eberle et al., 2021). The presence of ferrihydrite and goethite ensured the co-removal of As and Sb mainly via co-precipitation and sorption (Sekula et al., 2018). Moreover, Fe(III) amorphous phases play a major role in As removal (>93%) at full scale passive multi-unit system including biofilters treating AMD (Jacob et al., 2022). Recently, residues from a full scale biofilter (Wood-Cadillac mine site, Canada) treating As-CND showed that metal [Fe(III), Al and Mg] oxyhydroxides were responsible for the removal of As via sorption (Mehdaoui et al., 2024; 2025). Several factors may influence As removal mechanisms. The pH and Eh of pore waters as well as the ratios of Fe/As and S/As are key factors influencing the type of As-bearing mineral phases and govern the removal mechanisms (Eberle et al., 2021). Under oxidizing conditions and adequate Fe/As ratio (> 6), As is mainly removed via sorption and co-precipitation to Fe(III)-oxyhydroxides. Under a reducing environment and the presence of sulfur, As will mainly precipitates in the form of As sulfides (Palmer et al., 2015; Heiderscheidt et al., 2020; Eberle et al., 2021). The type of As-bearing mineral phases has a direct influence on their environmental behavior and As leachability. An environmental characterization of the post-treatment residues is necessary to select their optimal management plan. Metal rich residues from PBR were qualified as non-hazardous and environmentally inert (Jong and Parry, 2005). Similarly, post-treatment residues of oxidation ponds were considered as non-hazardous and could be safely disposed of in natural ecosystems without posing environmental risks (McCann and Nairn, 2022). However, residues from a multi-step passive treatment system of Fe-AMD, on a mine site in Colombia, showed high leaching potential for Fe, Mn and Zn, preventing their storage under oxidizing conditions or any contact with water (Vasquez et al., 2022). Similarly, PBR metal-rich residues at Lorraine mine site, Canada showed stabilization/solidification as necessary to prevent contaminant leaching (Jouini et al., 2020a; 2020b). Consistently, the storage of dispersive alkaline substrate (DAS)-type residues, from passive treatment of AMD on mine sites in Spain, was recommended in a dry environment (Macias et al., 2012). Finally, post-treatment residues from a full scale

biofilter treating As-CND were deemed non-hazardous for the co-disposal with municipal waste, but leachable for As, especially once dried or crushed (Mehdaoui et al., 2024; 2025).

Therefore, despite their efficiency, the potential environmental impact of contaminated residues post-treatment from passive biofilters limit their management options. These solids show variable physicochemical characteristics, with respect to the quality of the mine drainage which ultimately governs their stability (Jouini et al., 2022).

In this predefined context, the present study performed a comprehensive characterization of post-treatment residues from three pilot-scale, laboratory vs field, passive biofilters. The main aim was to assess and quantify As removal mechanisms and long-term environmental stability of post-treatment contaminated solid residues.

6.5 Materials and Methods

6.5.1 Laboratory scale biofilter design, set-up and operation

The system setup was based on previous findings from batch tests which determined the optimal ratio of peat to mine drainage active treatment sludge (MD-S) and defined the appropriate hydraulic parameters. The results showed that a mixture proportion of 50/50 (w/w dry mass) peat and MD-S had the highest efficiency for As retention at 24h of contact time (Thevenot et al., 2024). A high density-polyethene barrel (48 cm x 41 cm x 55cm) was filled with 0.035 m^3 of a filling mixture composed of a 50/50 (w/w) mixture of peat and MD-S thoroughly homogenized with an equivalent volume of gravel. The filling mixture was placed between two layers of silica sand (5 cm each) to ensure uniform flow distribution at the inlet and to prevent the loss of fine particles at the outlet (Figure 6.1). Upward flow rate was set to maintain a 24h of hydraulic retention time (HRT), matching the 25h of HRT of the Wood-Cadillac field biofilter (Germain and Cyr, 2023; Mehdaoui et al., 2024). The system was initially fed with a synthetic As-CND (2.5 mg/L of As) for the first month (Figure 6.1). However, the concentration was decreased to 1 mg/L for the subsequent two months due a decline in the system efficiency (Thevenot et al., 2024). For three months operation, the system treated a total of 270 L of As-CND with a total load of 349 mg of As (Thevenot et al., 2025a). Results of the treated water are the following: pH (6.1 – 7.1), Eh (271.2–551.4 mV), As (up to 3.57 mg/L), Fe (up to 8.8 mg/L) and SO_4^{2-} (up to 52.5 mg/L).

6.5.2 Field pilot biofilter design, set-up and operation

The Dhilmar-Éléonore mine site, located in the Eeyou Istchee James Bay municipality in the province of Quebec, Canada (52◦42′ 16.49 N/76◦4′15.82W), provided the materials for the preparation of the filling mixture and workspace for installing the field-pilot biofilters.

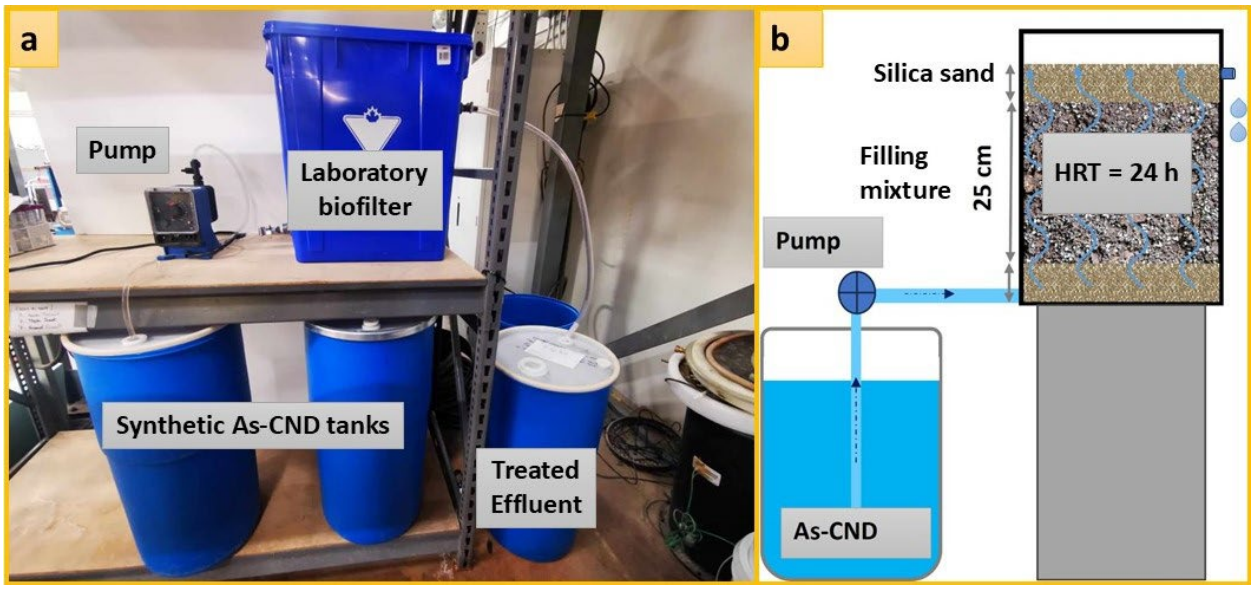

Figure 6.1 Laboratory experimental work: a) Biofilter; b) Schematic set-up

Two identical pilot biofilters (1 m^3; Pilot-field biofilters 1 and 2) were installed at the mine site (August to November 2023). The experiment was conducted during the summer to ensure the availability of sufficient As-CND to be treated. Both systems were fed by gravity, and the flow rate (200 L/d) was monitored weekly to ensure a 24 h of HRT (Figure 5.2 and Figure B1, Annexe B). In each biofilter, the inlet and outlet were covered with a geotextile to prevent materials loss. A 15 cm layer of gravel (P80 = 43 mm) was placed at the bottom to maintain a homogeneous distribution of the flow and prevent clogging. Approximately 65 cm of the filling mixture consisting of 85 kg of MD-S, 85 kg of peat, and an equivalent volume of gravel, were placed directly on the gravel layer. An additional 10 cm layer of gravel was placed at the top of the system to prevent material loss and provide a final polishing of treated water (Figure 5.2 and Figure B1). Biofilters were fed with As-CND on site. The quality of the inlet and treated waters were monitored on a weekly basis with the average quality is presented in Table B1. Each biofilter received approximately 15 g of As over three months (Thevenot et al., 2025b).

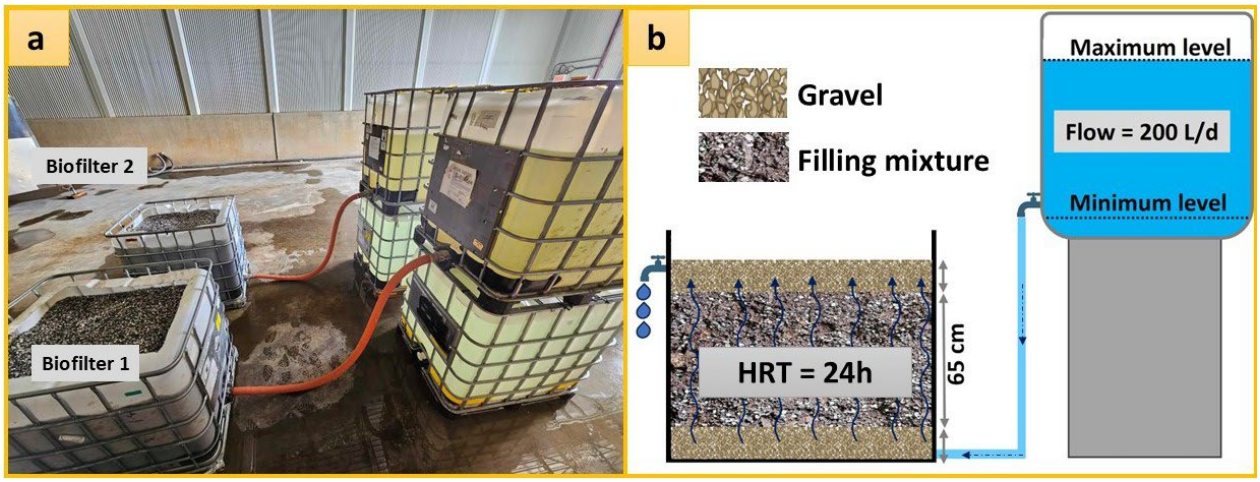

Figure 6.2 Field experimental work: a) Biofilters, b) Schematic set-up

During the 3 months of testing, biofilters showed high removal efficiency for As (> 91% for pilot 1 and >90% for pilot 2). The treated effluents met the guidelines of Directive 019 pertaining to the mining industry (D019, MELCCFP, 2025) and the Metal and Diamond Mining Effluent Regulations (MDMER, Minister of Justice, 2025). Both pilot biofilters, acting as duplicates, maintained their efficiency until dismantling (Table B 1).

6.5.3 Filling mixture characteristics

Fresh peat was sampled onsite and and combined with old peat, which was stored onsite since 2012. The MD-S and gravel were provided from the Dhilmar-Éléonore mine site. The first sampling campaign (September 2022) served for the preparation of the filling mixture for the laboratory biofilter. The second sampling campaign (August 2023) served for the set-up of field pilot biofilters. Peat and MD-S were characterized for their physicochemical parameters and environmental behavior (Table B2). Dried samples of MD-S were characterized for their mineralogy (Figure B3). The MD-S had close to neutral pH (8.0), low carbon content (5.2 %) and high concentrations of Al (15.3 g/kg), As (10.7 g/kg), Fe (172.9 g/kg), P (8.3 g/kg), and S (9.4 g/kg). The main mineral phases were Fe(III)-oxyhydroxides and sulfates. The static tests results (TCLP and SPLP) confirmed the hazardous and high-risk of the MD-S with As concentration exceeding both USEPA threshold's (> 5 mg/L for As) and the limit (> 5 mg/L for As for TCLP test, Table 1, Appendix II) of D019 guidelines. On the contrary, the peat showed high carbon content (46.4 %), low metal concentrations (0.8 g/kg Al; 2.1 g/kg Fe) and non-hazardous behavior (Table B 2).

6.5.4 Sampling protocols

To ensure consistency between the different scales, the same sampling protocol was followed (Mehdaoui et al., 2024), with a focus on the potential vertical variations. The sampled cores were divided into 4 layers: I1, A, B and I2. The upper and bottom layers (I1 and I2, respectively) were analyzed to evaluate removal mechanisms that may occur at the interference between gravel/silica and the filling mixture. The other two samples were collected directly in the filling mixture (layers A and B) allowing a better understanding of the processes responsible for the retention of contaminants (Figure B1 and Figure 6.3a, 6.3b). For the laboratory biofilter, four samples were collected from different depths, with one composite sample per each layer (Figure B2 and Figure 6.3a). For the pilot biofilters, eight samples were collected from each system to account for upscaling effect, with one sample taken from the center (spot 1; Figure 6.3b) and another from the corner at each depth (spot 2; Figure 6.3b). The aim was to assess any possible lateral variation in post-treatment residues. In total, twenty post-treatment residue samples were collected from three biofilters (laboratory biofilter, field pilot 1 and field pilot 2).

6.5.5 Physiochemical characterization of post-treatment residues

The twenty samples collected from laboratory and field pilot biofilters were analysed for their physicochemical parameters. For each biofilter, one layer was analyzed in triplicate to ensure the reliability, accuracy and reproducibility of results.

Samples were homogenized and characterized for their paste pH. Then, samples were oven dried (60 °C) and pulverized (150 µm) for analyses of total carbon (TC), organic carbon (OC), inorganic carbon (IC), total nitrogen (TN), total sulfur (TS), sulfates concentration ($S_{sulfates}$), sulfides concentration ($S_{sulfides}$), and chemical elemental composition. The paste pH was measured with a double junction electrode Orion GD9156BNWP of Thermo Scientific paired with a VWR SympHony SB90M5 multimeter using a solid to liquid (deionized water) ratio of 1:10 following the standard 4971-01 (ASTM, 1995). The TC and TS were measured under oxygen atmosphere by combustion in an induction furnace at 1360 °C. The $S_{sulfates}$ was determined according to Sobek (1978). The OC and TN were determined according to Zimmerman et al. (1997). The IC and the $S_{sulfides}$ concentrations deduced as the difference between the TC and OC and the difference between TS and $S_{sulfates}$, respectively. Metal contents were determined after acid digestion (HNO_3,

Br_2, HCl and HF) using inductively coupled plasma atomic emission spectroscopy (ICP-AES; Varian Vista Pro CCD) (USEPA, 2007).

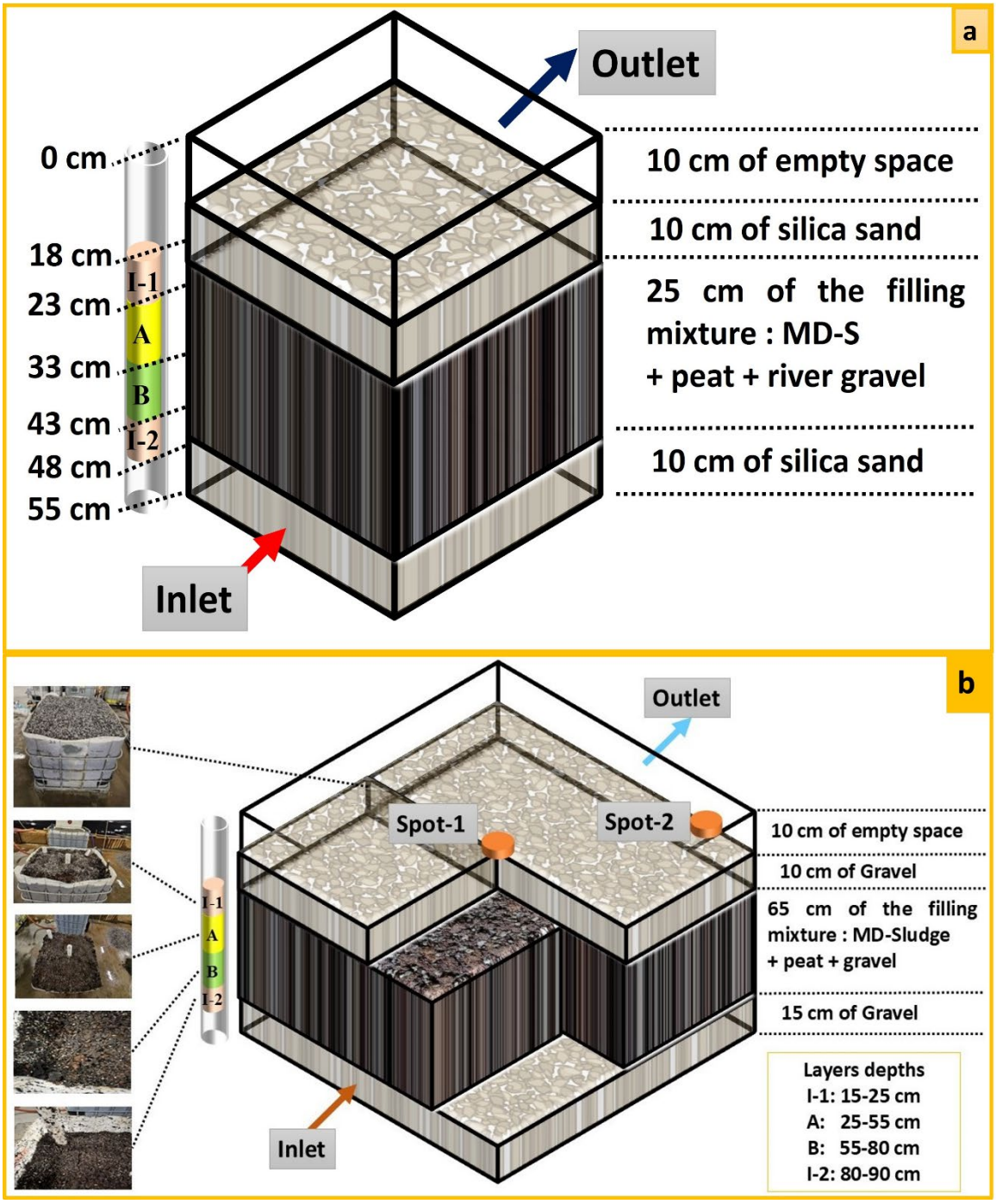

Figure 6.3 Sampling scheme: (a) laboratory biofilter, (b) field pilot biofilters

6.5.6 Mineralogical characterization

Elemental mineral speciation determination was undertaken on twelve selected samples (four from each system as follows: laboratory biofilter, field pilot biofilter 1 and field pilot biofilter 2) covering the four targeted layers for each biofilter using X-ray photoelectron spectroscopy (XPS). Prior to analysis, samples were dried in an inert nitrogen (N_2) atmosphere inside a glovebox at room temperature to minimize oxidation to avoid any sample alteration after dismantling. The objective of the XPS analysis was to determine the chemical oxidation states of metals and oxyanions within the residues and to identify their speciation in the newly formed mineral phases. Elements present on the surface of the samples were identified using XPS survey spectra, and high-resolution spectra were used to obtain information on chemical or oxidation states. High-resolution spectra for Al2p, Si2p, K2p, Ca2p, Mg1s, As3d, As2p, S2p, C1s, N1s, O1s, P2p, and Fe2p were collected. XPS measurements were conducted with an ESCALAB 250Xi (Thermo Scientific) using monochromated Al Kα radiation at an energy of 1486.86 eV, with a detection limit of 0.1% atomic. Standard charge compensation with low-energy electrons and Ar^+ ions was applied, and the pressure in the analysis chamber was maintained at approximately 10-8 mbar. Survey spectra were recorded at a pass energy of 150 eV with a step size of 1.0 eV, while high-resolution spectra were obtained at a pass energy of 40 eV and a step size of 0.1 eV. High-resolution spectra acquisition was essential for accurate elemental quantification, especially given peak overlaps and low elemental concentrations (<0.5% atomic). Samples were analyzed at a 0° emission angle relative to the surface normal. Data processing was performed using Avantage v6.5.0 (Thermo Fisher Scientific). Integral peak intensities and the manufacturer-provided sensitivity factors were used to determine the atomic concentration of the detected elements. The C1s peak at 284.8 eV for aliphatic carbon C-C groups served as reference for charge correction.

In addition, to better investigate the removal mechanism of As, two different As peaks with different surface sensitivities were studied. $As3d_{5/2}$ with a low binding energy around 44 eV giving an information depth of 7 nm, and $As2p_{3/2}$ at a binding energy of 1325 eV and enhanced surface sensitivity with an information depth of only 1.5 nm. Since As removal is mainly associated to Fe, As concentrations calculated from these two peaks and Fe2p was used to calculate the intensity ratios $Fe2p/As3d_{5/2}$ vs $Fe2p/As2p_{3/2}$. In this manner, a $Fe2p/As2p_{3/2}$ concentration ratio lower than $Fe2p/As\ 3d_{5/2}$ suggests that As is predominantly located on the surface of iron particles. In contrast,

ratios close to 1 indicate a more homogeneous distribution of As, consistent with the mechanism of As precipitation or co-precipitation into more stable mineral phases.

6.5.7 Leaching tests

Three different static leaching tests were used: toxicity characterization leaching procedure (TCLP), synthetic precipitation leaching procedure (SPLP) and field leaching test (FLT). In total, twenty samples were tested as follows: four samples from the laboratory biofilter (i.e., one sample from each layer), eight samples from each of field pilot biofilters 1 and 2 (i.e., two samples from each layer). To confirm repeatability, samples from layer A were tested in triplicates. Following the test, leachates were filtered (0.45 µm) before measuring the pH, redox potential (Eh), electronic conductivity (EC) and metal concentrations. The pH measurement was performed using a double junction electrode Orion GD9156BNWP of Thermo Scientific coupled with a VWR SympHony SB90M5 multimeter (relative accuracy ±0.01 pH). Metal concentrations were determined on acidified (2% HNO_3) samples using ICP-AES.

6.5.7.1 Toxicity characterization leaching procedure (TCLP)

To assess the leachability of contaminants and classify the residues (non-hazardous, hazardous, high risk, low risk, or leachable), the TCLP was carried out on wet preserved samples. Following a pretest (5 g of sample in contact with 3.5 mL of HCl 1N + 96.5 mL of deionized water at 50 °C for 10 minutes), the leaching medium 1 (NaOH dissolved in deionized water and glacial acetic acid; pH 4.93±0.05) was used for all samples. Using a 20:1 liquid to solid ratio, the experiments were run for 18 h at room temperature (20±2 °C) under agitation in a rotary tumbler (30±2 rpm) (USEPA, 1992; CEAEQ, 2012). The obtained leachates were filtered and analyzed for pH, and metal concentrations as previously described.

6.5.7.2 Synthetic precipitation leaching procedure (SPLP)

The aim of the SPLP test was to identify the potential leaching of contaminants that might occur after exposure of the post-treatment residues to acidic rain. To prepare the extraction medium, a 1 mL of sulphuric acid/nitric acid (60:40 w/w) stock was incorporated to deionised water until a pH of 4.20±0.05. The wet samples were extracted at room temperature (20±2 °C), using a 20:1 liquid to solid ratio under agitation for 18 h in a rotary tumbler (30±2 rpm) (USEPA, 1994; CEAEQ,

2012). The final, leachates were filtered and analyzed for pH, and metal concentrations as previously described.

6.5.7.3 Field leaching test (FLT)

The field leaching test (FLT) was performed to rapidly assess and predict the leachate geochemistry. It was performed using a 20:1 leaching ratio of pure water (1 L) on air-dried waste (particle size less than 2 mm). After 5 min of hand mixing, the slurry sample was allowed to settle for 20 min (Hagemann, 2007). The obtained leachates were filtered and analyzed for pH, and metal concentrations as previously described.

6.5.7.4 Classification criteria of residues

Results of the TCLP tests were compared to USEPA standards and D019 guidelines (Quebec's provincial regulation on mining effluents). According to USEPA standards, if the concentration of any metal in the TCLP leachate meets or exceeds the maximum contaminant level defined for the "toxicity" characteristic, the residue is classified as "hazardous" waste and cannot be co-disposed with municipal waste (USEPA, 1992). In addition, a residue is classified as "high risk" if the concentration of contaminant in the leachates exceeds the concentration established by D019 (T1-AII; MELCCFP, 2025). Results of the SPLP and FLT tests were compared to USEPA standards. If contaminant concentrations in the leachates exceed limits, residues are qualified as leachable under acidic rain conditions (USEPA, 1992; 1994).

6.6 Results and discussion

6.6.1 Physicochemical characterization

Laboratory biofilter post-treatment residues had slightly acidic paste pH (5.7–6.4). The TC was higher in the bottom (33.2 %, layers I2 and B) relative to the upper layers (28.7 %). The same pattern was observed for the OC that represents around 92% of the TC. This could be explained by the higher rate of organic matter decomposition in the upper layer due to its oxidation, when exposed to weathering. The presence of peat in the filling mixture and the oxygen availability could explain these results. No differences between layers were observed for TS (~ 0.23 %) and TN (0.85 ~ 0.96 %) (Figure 6.4; Tables B 3, B 4, B 5).

Residues from both field pilot biofilters showed similar properties (Figure. 6.4). The paste pH was neutral (7.4-7.7). The lowest TC content was found in the upper layer I-1 (11.1 % and 13.5 % for pilot 1 and for pilot 2, respectively) while the highest content was found in the middle layers (24.0 %, at layer B, for pilot 1; 24.9 %, at layer A, for pilot 2). Similar observations were found for field biofilters at the reclaimed mines sites Lorraine (Jouini et al., 2020a) and Wood-Cadillac (Mehdaoui et al., 2025), where the upper layers were almost depleted in carbon. High OC content (>90% of the TC) for both pilot biofilters could be explained by the high availability of organic matter in the filling mixture. The lowest OC content in the upper layers (11.8±1.9 %) could be attributed to their advanced degradation driven by the availability of oxygen, as previously mentioned. TS and $S_{sulfates}$ were relatively stable over biofilters layers with almost no variation were observed between layers (0.6±0.1 % and 0.4±0.1 % for TS and $S_{sulfates}$, respectively). The upper layer I-1 for all samples showed the lowest content for all elements as it served as a polishing layer.

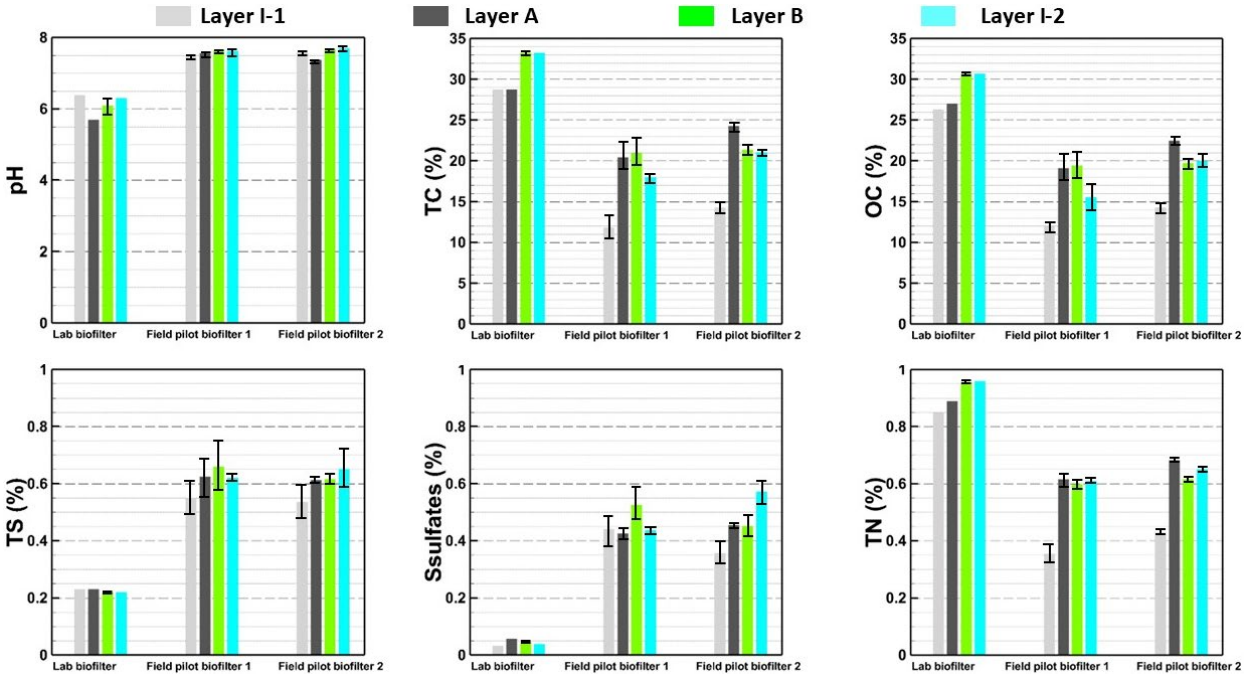

Figure 6.4 Physiochemical characterization of post-treatment residues from lab and field tests

The results showed high elements concentrations confirming the high removal efficiency of all biofilters (Figure 6.5). For laboratory biofilter, little variation in the elemental concentrations was observed across the layers, except for As, most probably due to the use of synthetic As-CND containing only As. Precisely, As showed distinct vertical distribution, indicating efficient removal

in the lower layers with concentrations gradually decreasing along the vertical flow toward the upper layers. An effective As retention was observed within the bottom layers (i.e., I2 and B) followed by a polishing in the mid and upper layers (i.e. A and I-1) (Figure 6.5).

The real As-CND led to a distinct distribution pattern of elements in the residues of field-pilot biofilters vs laboratory biofilter. Apart from Al and Mg, other contaminants (As, Fe, Ca, Na, P, S) showed a pronounced vertical distribution with higher concentrations in the bottom layer (I2) that progressively decreased towards the outlet in the top layer (I1) (Figure 6.5). This pattern suggests high retention of elements close to the inlet, where initial interaction with the filling mixture occurs probably via sorption mechanisms. For As, the availability of metals in the filling mixture, particularly Fe (Fe/As ratio > 15), allowed its efficient retention. A previous study reported that the use of a Fe-based mixture for the treatment of As-CND at pilot scale favored the co-removal of As and Sb for over 15 months (Sekula et al., 2018). This process likely occurs through sorption and/or co-precipitation of As. The formation of Al and Mg-oxyhydroxides generates new available sorption sites that may enhance As removal from CND in passive biofilters (Mehdaoui et al., 2025).

Overall, post-treatment residues showed high content in contaminants proving biofilter efficiency. Nevertheless, while most contaminants were retained at the bottom and mid-layers, Al and Mg behaved differently, showing a high concentration in the upper layers, probably due to a different redox condition. Hence, an investigation of the mineralogical composition of the post-treatment residues was deemed necessary to identify the main mineral phases bearing the As, as well as the other contaminants (e.g., Fe, Al).

6.6.2 Mineralogical characterization

6.6.2.1 XPS survey spectra

X-ray photoelectron spectroscopy (XPS) was used to determine the oxidation states of the target elements and to identify As-bearing mineral phases. The XPS survey spectra, spanning the energy range of 0–1,350 eV, for all analyzed samples with the peaks of particular interest labeled for clarity are presented in Figure 6.6. Metal oxyhydroxides and silicates were identified as the main phases, as confirmed based on peak binding energies (BE) for several elements.

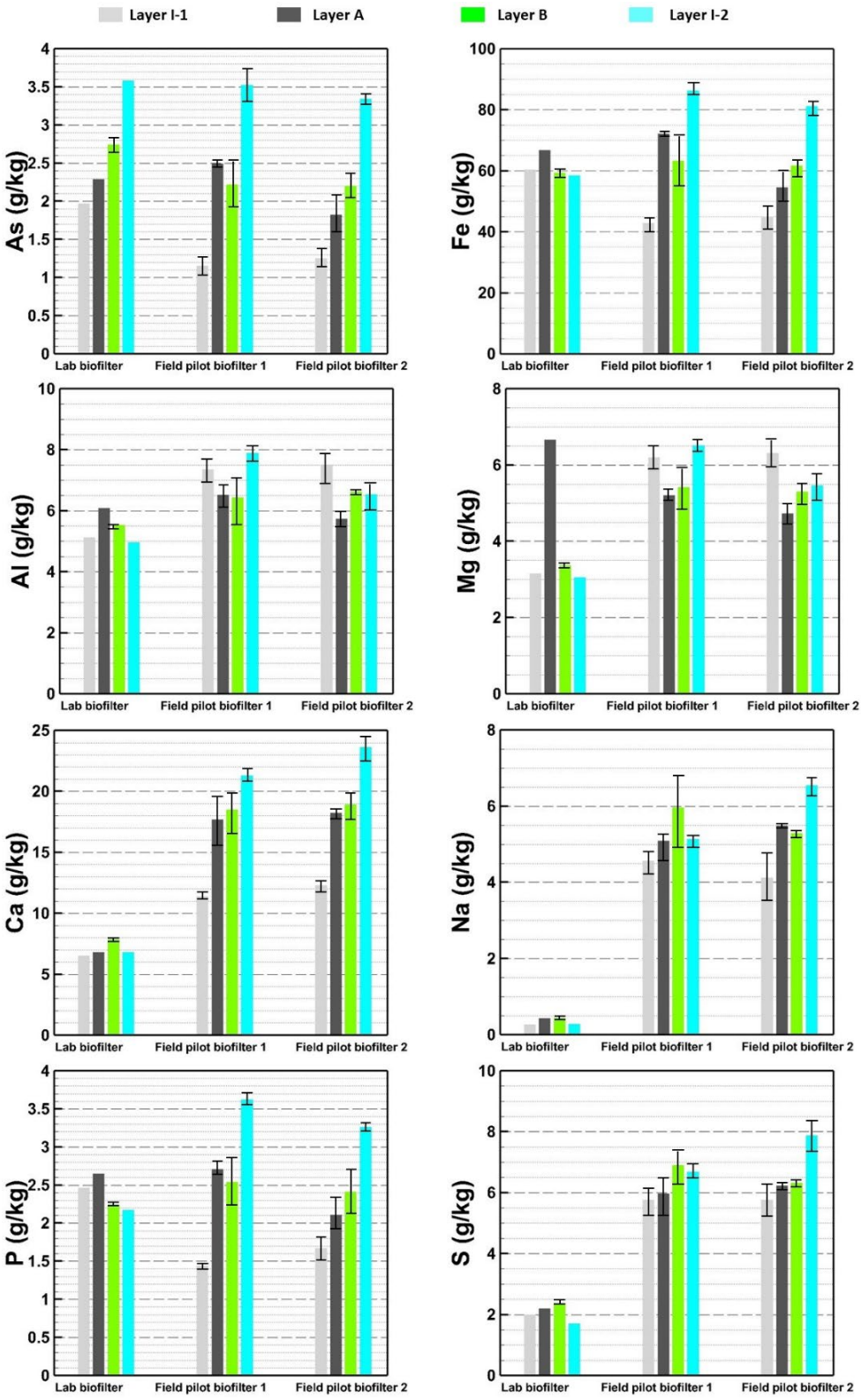

Figure 6.5 Chemical composition (Al, As, Fe, Mg, Ca, Na, P and S) of post-treatment residues from lab and field tests

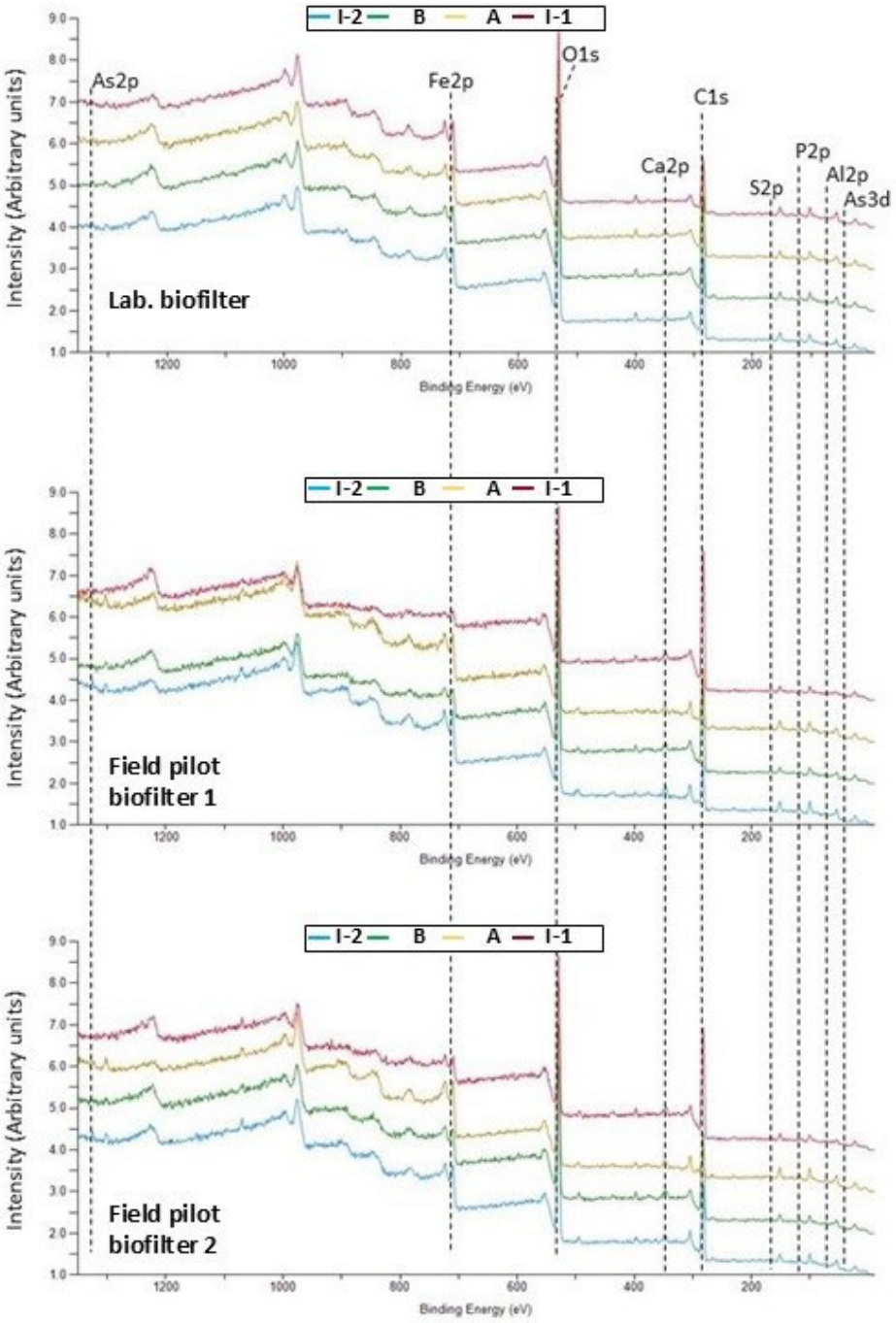

Figure 6.6 XPS survey scans. Peaks of special interest are labeled as follows: Al2p and Al2s (BE = 74 and 120 eV), Si2p and Si2s (BE = 103 and 153 eV), P2p (BE = 133.6 eV), Ca2p and Ca2s (BE = 348 and 439 eV), N1s (BE = 400 eV), Fe KLL Auger electron peaks (BE = 780–938 eV), O KLL (BE = 977–1013 eV), C KLL (BE = 1224 eV), and Mg1s (BE = 1306 eV). Spectra were offset vertically for clarity.

The Si2p peak at a BE = 103.0 eV confirmed the presence of silicates with a relative atomic proportion of 3.6~5.7 % in the lab biofilter residues and 2.3~8.5% in the pilot biofilter solids. The O1s spectrum (Figures B 4, B 5, B 6) was fitted using four peaks: (i) a peak at BE = 530.1 eV corresponding to metal oxides, (ii) a peak at BE = 531.2 eV associated with metal hydroxides, sulfates, and silicates, (iii) a peak at BE = 532.1 eV attributed to C-O species, and (iv) a peak at BE = 533.2 eV representing O-C-O species. The Al2p signal observed at 74.6 eV indicated the presence of Al-oxyhydroxides (1~3%) predominantly in the upper layer, specifically layers I1 and A, with the highest content in pilot biofilters residues compared to the laboratory biofilter. These results are consistent with previous studies on the passive treatment of AMD (Macias et al., 2012; Jouini et al., 2019c) and As-CND (Mehdaoui et al., 2025). The N1s peak (BE = 399.9 eV) indicated the presence of nitrogen bonded to carbon being characteristic of amine or amide functional groups. All residues showed high relative atomic proportion of carbon (11.9 to 42.4 %) mainly in the form of C-C, C-O or C-O-C and O-C-O groups at binding energies of 284.8 eV, 286.3 eV and 288.1 eV, respectively. These findings may be partially explained by peat decomposition in the filling mixture (Wu et al., 2023).

6.6.2.2 High-Resolution XPS Spectra for As

High-resolution XPS spectra for the As3d and As2p regions are shown in Figure 6.7a. Peak fitting of $As2p_{3/2}$ confirmed that As in the form of As(0), or FeAsS at BE = 1323.9 eV, As(III) at BE = 1326.2, and As(V) at BE = 1327.8 eV (Figure 6.7a).

The presence of As(III) and As(V) is confirmed by peak fitting of $As3d_{5/2}$ with components at BE at 43.5-44.0 eV and 45.0-45.5 eV, respectively (Figure 6.7b). Scaled and offset $As2p_{3/2}$ spectra did not show significant variation in shape as a function of sampling depth, indicating little differences in As species distribution with depth in the laboratory biofilter (Figure 6.7c). This supports the earlier interpretation on the chemical distribution of As in the post-treatment residues. Noteworthy, previous studies have indicated that As removal during the passive treatment of As-CND is influenced, among other factors, by the presence of Fe and S (Sekula et al., 2018; Lee et al., 2018; Turcotte et al., 2021; Mehdaoui et al., 2025). As(V) was the most abundant As species in the laboratory biofilter residues, with lower concentrations of As (III) present in the upper layers (i.e. I1 and A). A stagnant water layer on the top of the system after 4 weeks of operation may have limited O_2 availability leading to the formation of localized reducing conditions. This could explain

the presence of low content of As(III) in these layers comparing to its absence at the bottom (Thevenot et al., 2024). Residues from the field pilot biofilter 1 (Figure 7.7d) and field pilot biofilter 2 (Figure 7.7e) showed similar behaviour. The main As species were As(0) and/or As-metal. This distribution was high at the bottom of the systems (near in the inlet) for layers I-2 (green) and A (black) before decreasing progressively near the

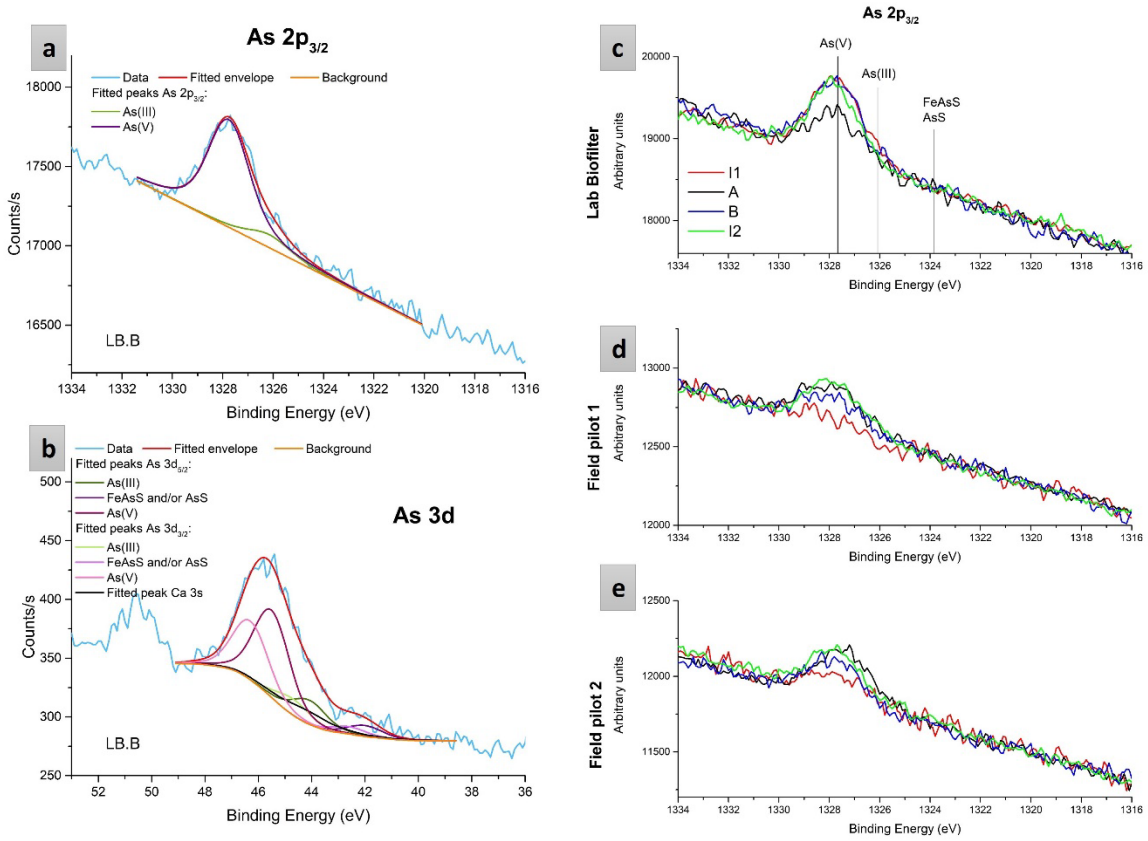

Figure 6.7 (a) High-resolution As2p3/2 and (b) high-resolution As3d peaks' fitting (data for layer B of laboratory biofilter), As2p3/2 high-resolution spectra (scaled and offset) for layers I1, A, B, and I2 for: (c) laboratory biofilter, (d) field pilot 1 and (e) field pilot 2

outlet in layers B (blue) and I1 (red). As both systems used vertical flow, higher retention of contaminants near the inlet (bottom) was expected, with the presence of a high amount of OC with a gradual decrease along the flow path. Residues from field pilot 1 showed a predominance of As(V) over As(III) species (Figure 7.7c,d,e; Table B 7). The upper layer I1 contained only As(V) confirming a more oxidizing environment at this level and a higher affinity for As to sorb onto metal oxyhydroxides, particularly those of Fe(III) (Sekula et al., 2018).

To better assess As removal mechanisms, two different levels of surface sensitivity were examined (Table 6.1). Almost all samples of the laboratory biofilter showed $As3d_{5/2}/As2p_{3/2}$ ratio <1 confirming sorption as main removal mechanism. On the contrary, layer I1 of both field pilot biofilters showed ratio close or strictly above 1 indicating possible mechanisms of (co)-precipitation of As with metal oxyhydroxides mainly Fe(III) and Al. Similarly, layer B samples of pilot biofilters showed ratios higher or close to 1, indicating possible precipitation of As in the form of FeAsS or a co-precipitation with metal oxyhydroxides.

Table 6-1 Intensity ratios of As peaks (As3d5/2 to As2p3/2)

Samples		As coordination states		
		As(0) or As-metal	**As (III)**	**As (V)**
Laboratory biofilter	I1	0.35	0.37	0.9
	A	0.35	0.48	1.19
	B	0.33	0.89	0.79
	I2	0.3	0.15	0.9
Field pilot biofilter 1	I1	1.52	ND*	2.88
	A	0.36	0.49	0.57
	B	0.55	0.7	1.11
	I2	0.51	0.44	0.73
Field pilot biofilter 2	I1	0.91	ND	1.79
	A	0.21	0.23	0.77
	B	0.47	1.07	0.94
	I2	0.28	0.85	0.78

*ND= Not Detected

6.6.2.3 High-Resolution XPS spectra for Fe

High-resolution XPS spectra for the Fe2p region is shown in Figure 6.8. The Fe2p region typically exhibited an asymmetric line shape due to multiplet splitting and the shake-up features, making it challenging to assign peak intensities to specific mineral phases or oxidation states, particularly in mixed-phase samples (Figure 6.8a). The formation of Fe-oxyhydroxides is a well-documented process during the passive treatment of AMD (Jouini at al., 2019c; 2020a) and CND (Sekula et al., 2018; Jacob et al., 2022; Mehdaoui et al., 2025). In particular, Fe(III)-oxyhydroxides play a significant role in As removal through different mechanisms such as co-precipitation, surface precipitation, and adsorption (Benzaazoua et al., 2004). The study of Fe phases and Fe/As ratio determination are necessary to understand As removal mechanisms. The elemental compositions

of the post-treatment residues for studied systems showed a Fe/As ratio, from 15 to 32 (Figure 6.5; Tables B 3, B 4, B 5). The XPS analyses showed lower Fe/As ratio, from 10 to 29, for both field pilot biofilters (Figure 6.8b; Table B 6). This Fe/As ratio likely contributes to the high efficiency of the systems in immobilizing As from As-CND.

Little variation of Fe-bearing minerals was observed between layers in laboratory biofilter residues confirming the homogenous distribution previously noted in the elementary composition (Figure 6.8c,d,e; Table B7). The Fe(II) and Fe(III) concentration variations for both field pilot biofilters confirmed the following observations: (i) the upper layer I1 (red line) contains the lowest content in Fe species, (ii) the highest content of Fe was in the bottom layers I2 (green line) and B (blue line), and (iii) Fe(III) is the main form of Fe in the residues (Table B7). These findings underscore the role of amorphous metallic phases, particularly those associated with MD-S, in As removal. The homogeneous distribution of Fe(III) in the residues suggests their amorphous origine from MD-S and critical role in binding and efficiently immobilizing As in biofilters, via adsorption and co-precipitation.

6.6.2.4 High-Resolution XPS spectra for S

High-resolution XPS spectra for the S2p region is shown in Figure 6.9. The S2p peak was deconvoluted through peak fitting into four doublet components with spin-orbit splitting of 1.18 eV and an intensity ratio of 0.511 between $S2p_{3/2}$ and $S2p_{1/2}$ (Figure 6.9a). The binding energies of $S2p_{3/2}$ were assigned as follows: 162.7 eV to metal sulfides (M-S), 163.5 eV to carbon-sulfur (C-S) and/or sulfur (S) groups, 166.2 eV to sulfites, and 168.7 eV to sulfates, consistent with previous studies (Kim et al., 2014; Wu et al., 2018; Jouini et al., 2019a; 2019c). For all samples, sulfates were the abundant form due to the oxidizing conditions in the systems. Featuring scaled and offset S2p spectra, clearly illustrated the predominance of oxidized S species, such as sulfites and sulfates, over other S forms (Figure 6.9b). A similar distribution pattern was observed for both Fe and As with the prevalence of oxidised species. Throughout the biofilter layers of field pilot 1, SO_3 and SO_4 species were found to dominate near the bottom close to the inlet layer (I-2), and in the upper layer (I-1), near the outlet, likely due to the availability of oxygen. In contrast, the middle layers (A and B) were characterized by a presence of C-S species accompanied by traces of metal sulfides. These findings may be explained either by the decomposition of the filling mixture or due to the presence of spots with reducing conditions (Figure 6.9c,d,e). Results showed some discrepancies

between biofilter scales. Residues of the laboratory biofilter showed high content of metal oxyhydroxides with As mainly removed via sorption mechanisms. Pilot biofilters showed similar behavior with variable removal mechanisms depending on the vertical distribution. The main possible removal mechanism of As for field pilot biofilters were: (i) co-precipitation of As(V) with metallic oxyhydroxides (mainly Fe(III) and Al) in layer I1 (upper layer near the outlet), (ii) sorption of As onto metallic oxyhydroxides over all biofilter layers, (iii) possible precipitation in the form of metallic sulfide in the bottom layers (i.e. B and I2), and (iv) possible precipitation in the form of FeAsS in some spots in the middle layers, mainly layer B. Sorption of As(V) onto MD-S amorphous metallic phases plays also an important role in the As removal.

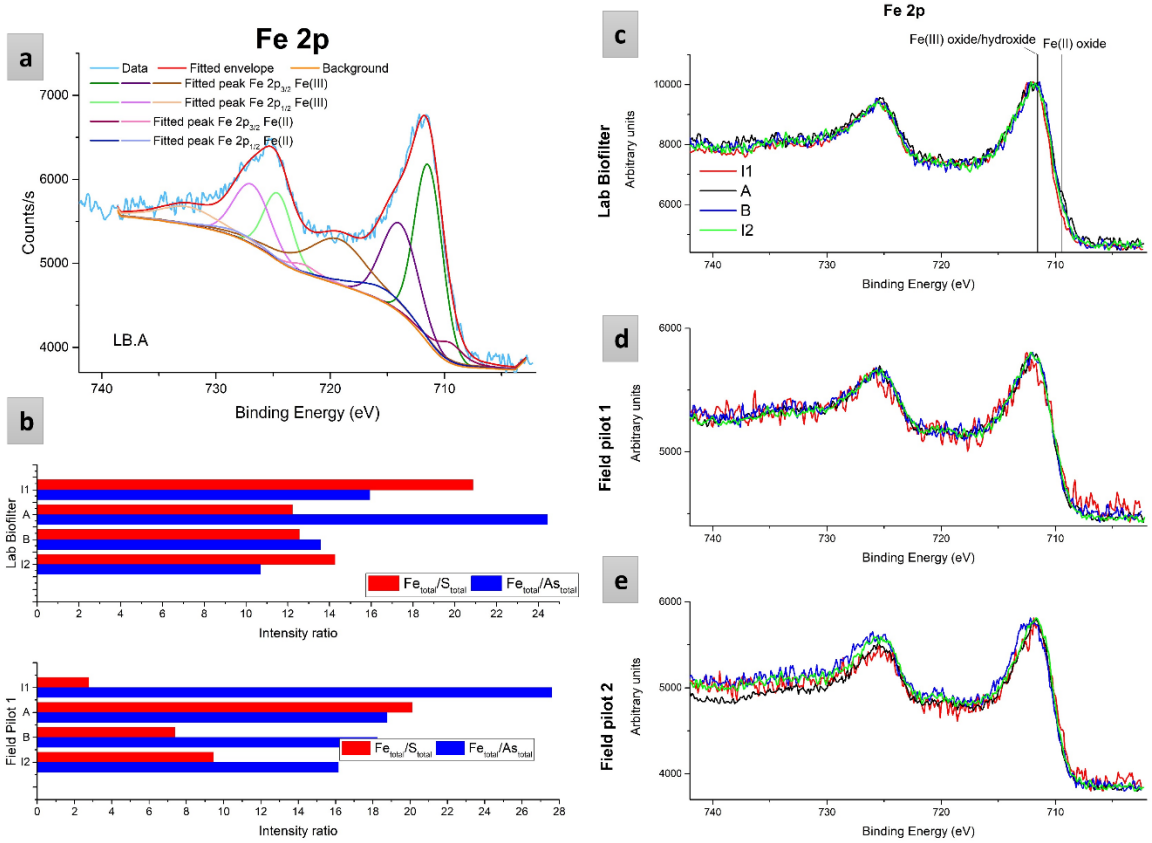

Figure 6.8 (a) High-resolution Fe2p, (b) Ratio of total Fe to total S and total As concentrations respectively for I1, A, B, and I2 from laboratory biofilter and field pilot 1 obtained from XPS quantification, Fe2p high-resolution spectra (scaled and offset) for layers I1, A, B, and I2 for: (c) laboratory biofilter, (d) field pilot 1 and (e) field pilot 2

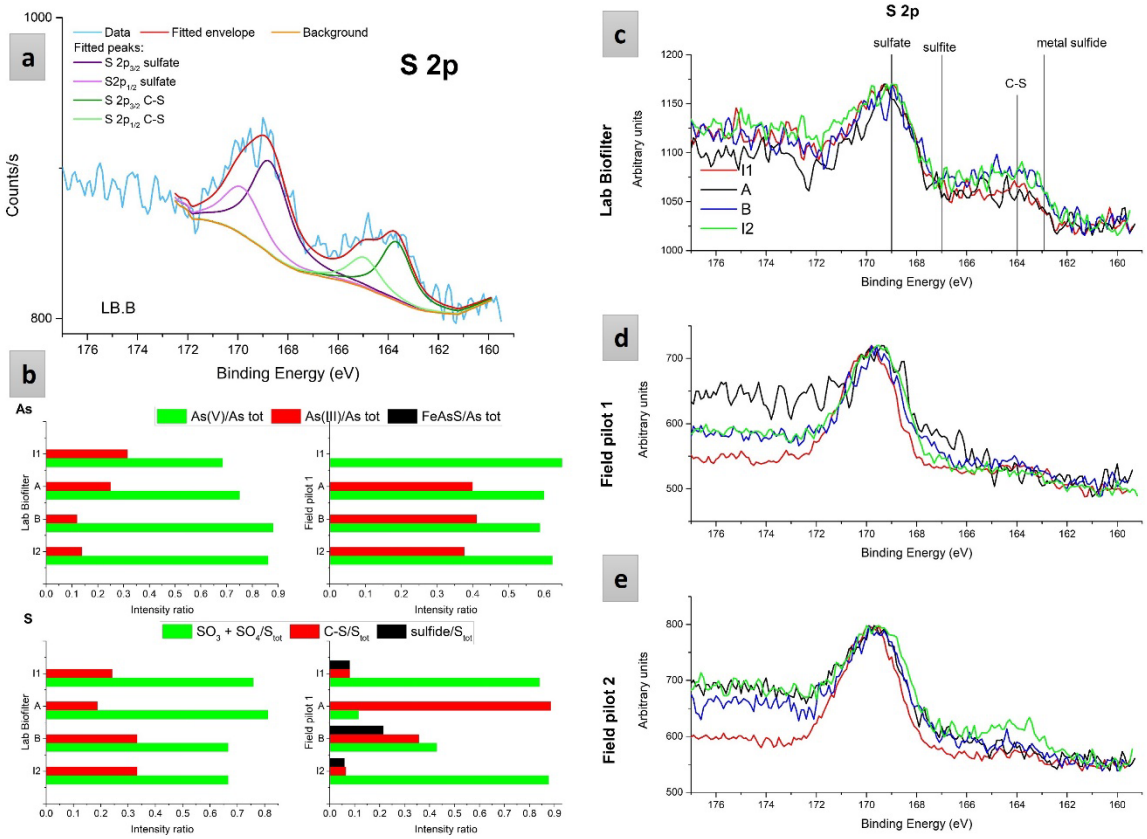

Figure 6.9 (a) High-resolution S2p, (b) Ratio of As species and S species to total As and S concentrations averaged over locations I1, A, B, and I2 from laboratory biofilter and field pilot 1 obtained from XPS quantification, S2p high-resolution spectra (scaled and offset) for layers I1, A, B, and I2 for: (c) laboratory biofilter, (d) field pilot 1 and (e) field pilot 2

6.6.3 Environmental behavior of post-treatment residues

Based on the pH of the leachates, discrepancies were noted among the three tests (Table 6.2). While TCLP showed acidic pH (~ 4.9) for all samples, SPLP and FLT results showed neutral pH (7.3-8.3) for pilot biofilters residues and slightly acidic for laboratory biofilter (5.6-6.4). The pH and the composition of the extraction fluid and its interaction with the residues could explain those results (Mehdaoui et al.,2025).

The results of TCLP test for the three biofilters showed that As concentrations did not exceed the regulation limits of T1-AII and TCLP (Tables 6.2, B 8, B 11, B 14). According to USEPA, residues

were classified as non-hazardous with potential co-disposal with municipal waste. The residues are also classified as low-risk according to D019 (T1-AII).

According to SPLP results and USEPA regulations, all the residues of laboratory biofilter and both pilot-biofilters met the requirements for all contaminants and do not present a risk of leaching contaminants after contact with acidic rain (Tables 6.2, B 9, B 12, B 15). Results of FLT tests confirmed those of TCLP and SPLP and met USEPA regulations (Tables 6.2, B 10, B 13, B 16). A recent study reported FLT results with a similar leaching concentrations comparing to those of SPLP for the characterization of post-treatment residues from oxidizing bonds (McCan and Nairn, 2022).

No metal concentration in leachates exceeded threshold set by USEPA guidelines, classifying them as non-hazardous for the three studied biofilters. The co-disposal with municipal waste seems a possible storage option. There is no risk of contaminants leaching upon exposure to acid rain. This could be explained by the predominance of Fe-oxyhydroxides in the post-treatment residues, which are highly stable under typical environmental conditions (oxidizing conditions, pH lower than the pHpzc (7 to 8) of Fe-oxyhydroxides). Thus, creates robust conditions that prevent the desorption of As or the dissolution of the bearing phases (Inam et al., 2021).

It worth to be noted that static tests are simple and quick methods to determine contaminants leachability which cannot simulate the behavior of materials in natural systems. The duration of these tests, the particle size, the chemistry of the leaching media and the agitation are key factors that influence the concentration of the contaminants in the leachates (McCann and Nairn, 2022). Dynamic tests may give a better simulation of the environmental behaviour of these residues as previously recommended for post-treatment residues of passive biofilters (Jouini et al., 2022).

6.7 General discussion

The present study shows biofilters with limited variability in terms of filling mixture and reducing/oxidizing conditions. The initiation of As removal in biofilters involves complex mechanisms. Previous studies showed that, under oxidizing conditions (biofilter exposed to atmosphere), As removal is primary associated with the precipitation of Fe-oxyhydroxides when high ratio of Fe:As is present (> 10) (Sekula et al., 2018).

Other results showed that As may precipitate in the form of metallic sulfides and As sulfides under reducing conditions in the presence of sulfur (Turcotte et al., 2021). These mechanisms may also involve biological processes (Thevenot et al., 2025a,b). In the present study, the chemical ratio of Fe:As was higher than 15 for all laboratory biofilter residues and ranged from 22 to 32 for field pilot 1 and 2 biofilters (Figure 6.10). The removal mechanism of As in field biofilters showed a vertical distribution depending on the oxidizing/reducing conditions. Near the surface, the availability of oxygen favored the precipitation of metal oxyhydroxides (e.g., Fe, Al and Mg) allowing the sorption and co-precipitation of As. However, near the bottom of the system, the limited availability of oxygen and the reducing condition in presence of sulfur favored the precipitation of As sulfides and metal sulfides bearing As. Sorption is the main removal mechanism for As primarily onto Fe-oxyhydroxides but also on other mineral phases such as Al-oxyhydroxides and metal sulfides.

All residues were classified as non-hazardous or low risk due to the stability of As-bearing mineral phases under leaching conditions. The limited leaching of As may be explained by the stability of Fe-oxyhydroxides at a wide range of oxidizing conditions and slightly acidic to neutral pH. The pH of the leachates during static tests varied among tests and samples (slightly acidic to neutral) and was below or close to the pH_{pzc} of Fe-oxyhydroxides (7~8) (Inam et al., 2021). Under the current pH conditions, thermodynamic stability of the residues appears to favor the presence of Fe-oxyhydroxides. According to XPS results, the As remained associated to Fe-oxyhydroxides via sorption and coprecipitation preventing its remobilization. The absence of As leaching in post-treatment residues may be due to crystal-chemical properties, thermodynamic stability of ferric phases, and physicochemical parameters (pH and Eh). These factors contributed to stabilize the Fe-oxyhydroxides and maintain As immobilized through adsorption and co-precipitation.

Table 6-2 Physicochemical parameters (pH, As and Fe) of the eluates after static tests (TCLP, SPLP and FLT)

		Final pH			Metal concentration (mg/L)					
					As			Fe		
		TCLP	**SPLP**	**FLT**	**TCLP**	**SPLP**	**FLT**	**TCLP**	**SPLP**	**FLT**
I-1	Field pilot biofilter 1	4.9±0.0	7.5±0.0	8.2±0.1	0.08±0.01	0.02±0.00	0.17±0.09	1.3±0.4	0.1±0.0	0.6±0.1
	Field pilot biofilter 2	4.9±0.0	7.5±0.0	7.6±0.0	0.05±0.00	0.02±0.00	0.09±0.00	0.6±0.1	0.1±0.0	0.1±0.0
	Laboratory biofilter	4.9	5.8	6.4	0.41	0.27	0.27	0.7	0.1	0.1
A	Field pilot biofilter 1	4.8±0.0	7.4±0.1	7.8±0.1	0.10±0.05	0.02±0.00	0.08±0.01	0.4±0.1	0.2±0.0	0.1 ±0.0
	Field pilot biofilter 2	4.9±0.0	7.4±0.1	7.3±0.0	0.07±0.01	0.03±0.01	0.05±0.01	0.3±0.0	0.2±0.0	0.0 ±0.0
	Laboratory biofilter	4.9±0.0	5.9±0.0	5.9±0.0	0.18±0.0	0.04±0.0	0.22±0.0	0.8±0.0	0.5±0.3	0.2±0.0
B	Field pilot biofilter 1	4.9±0.0	7.6±0.0	7.8±0.0	0.05±0.00	0.02±0.00	0.07±0.03	0.5±0.0	0.1±0.0	0.1±0.0
	Field pilot biofilter 2	4.9±0.0	7.4±0.1	7.8±0.0	0.06±0.00	0.03±0.00	0.10±0.00	0.7±0.2	0.2±0.0	0.1±0.0
	Laboratory biofilter	4.9	5.7	5.8	0.26	0.03	0.34	1.9	0.1	0.2
I-2	Field pilot biofilter 1	4.9±0.1	7.8±0.1	8.3±0.0	0.10±0.01	0.04±0.00	0.21±0.03	0.7±0.0	0.01±0.0	0.1±0.0
	Field pilot biofilter 2	4.9±0.0	7.6±0.0	8.1±0.2	0.07±0.00	0.02±0.01	0.20±0.02	0.6±0.2	0.01±0.0	0.1±0.0
	Laboratory biofilter	4.9	5.6	5.6	0.33	0.01	0.31	1.6	0.0	0.2
D019 T1-AII[a]					5	-	-			
USEPA[b,c]		-			5			-		

[a] Annex II (T1-AII) of D019 (MELCCFP, 2025)

[b] TCLP limits (USEPA, 1992)

[c] SPLP limits (USEPA, 1994)

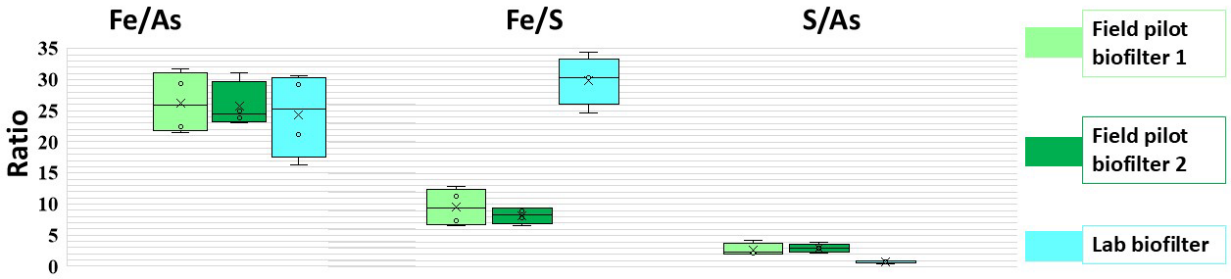

Figure 6.10 Ratio of main elements: Fe/As, Fe/S and S/As

6.8 Conclusion

This study evaluated As removal mechanisms in passive biofilters, at laboratory vs field scale, and the environmental behaviour of post-treatment residues. Results showed that the biofilters efficiently immobilized contaminants, as demonstrated by the high contaminant concentrations in all residues. While the MD-S maintained a high Fe:As ratio, the OM may contribute to biological processes that control As speciation and stability, potentially enhancing the long-term retention of As within the biofilter residues. Laboratory-scale residues showed little vertical variation, whereas field-scale pilot biofilters showed distinct vertical patterns with As and Fe contents being higher in the bottom layers near the inlet, and Al being predominantly present in the upper layers. The XPS analyses revealed that As removal occurred predominantly through sorption onto Fe (III)-oxyhydroxides across all biofilter layers. The Al-oxyhydroxides in the top layers also contributed to final polishing of the As-CND. The possible presence of reducing microenvironments in the middle layers facilitated the precipitation of As sulfide (FeAsS) and other metal sulfide minerals in trace amounts. As for the environmental behaviour of post-treatment residues, they were classified as non-hazardous with respect to USEPA regulations with no risk of contaminants leaching after contact with acidic rain. The residues are also considered as low risk according to D019. Further investigations should focus on long-term stability of post-treatment residues using kinetic tests.

Acknowledgments

This research was funded by the Natural Sciences and Engineering Research Council of Canada (NSERC), Canada Research Chairs Program, Mitacs and RIME UQAT-Polytechnique industrial partners, including Agnico Eagle, Canadian Malartic Mine, Iamgold, Raglan Mine–Glencore,

Dhilmar, and Rio Tinto. The authors would like to thank Dhilmar-Éléonore for their on-site support during the sampling, preparation, set-up and dismantling of field pilot biofilters as well as for providing the historical monitoring data.

References

American Society for Testing and Materials (ASTM), 2019. D4972-19: Standard test method for pH of soils. Book of Standards 04 (08), West Conshohocken, PA. 10.1520/D4972-19.

Battaglia-Brunet, F., Jacob, J., Duré, F., Huron, J., Gatellier, G., 2023. Passive treatment of mine seepage with high arsenic concentrations. In: Proc. IMWA, Newport, Wales, UK, July 17–21.

Ben Ali, H., Neculita, C.M., Molson, J.W., Maqsoud, A., Zagury, G.J., 2019. Performance of passive systems for mine drainage treatment at low temperature and high salinity: A review. Miner. Eng. 134, 325-344.

Benzaazoua, M., Marion, P., Picquet, I., Bussière, B., 2004. The use of pastefill as a solidification and stabilization process for the control of acid mine drainage. Miner. Eng. 17 (2), 233–243. https://doi.org/10.1016/j.mineng.2003.10.027.

Centre d'Expertise en Analyse Environnementale du Québec (CEAEQ), 2012. Protocole de lixiviation pour les espèces inorganiques, MA. 100 – Lix.com. 1.1, Rév. 1, Ministère du Développement Durable, de l'Environnement, de la Faune et des Parcs du Québec, Canada, Volume 7, pp. 1–17.

Eberle, A., Besold, J., León-Ninin, J.M., Kerl, C.F., Kujala, K., Planer-Friedrich, B., 2021. Potential of high pH and reduced sulfur for arsenic mobilization – Insights from a Finnish peatland treating mining waste water. Sci. Total Environ. 758, 143689. https://doi.org/10.1016/j.scitotenv.2020.143689.

El Kilani, M.A., Jouini, M., Rakotonimaro, T.V., Neculita, C.M., Molson, J.W., Courcelles, B., Dufour, G., 2021. In-situ pilot-scale passive biochemical reactors for Ni removal from saline mine drainage under subarctic climate conditions. Water Process Eng. 41, 102062. https://doi.org/10.1016/j.jwpe.2021.102062.

Germain, D., Cyr, J., 2003. Evaluation of biofilter performance to remove dissolved arsenic: Wood Cadillac. In: Proc. Mining and the Environment, Sudbury, Canada, May 25–28.

Hageman, P.L., 2007. U.S. Geological survey field leach test for assessing water reactivity and leaching potential of mine wastes, solids, and other geologic and environmental materials. U.S. Geological Survey Techniques and Methods, Vol. 5, Ch. D3, Department of the Interior, Reston, VA.

Heiderscheidt, E., Khan, U.A., Kujala, K., Ronkanen, A.K., Postila, H., 2020. Design, construction and monitoring of pilot systems to evaluate the effect of freeze-thaw cycles on pollutant retention in wetlands. Sci. Total Environ. 703, 134713. https://doi.org/10.1016/j.scitotenv.2019.134713.

Inam, M.A., Khan, R., Lee, K.H., Akram, M., Ahmed, Z., Lee, K.G., Wie, Y.M., 2021. Adsorption capacities of iron hydroxide for arsenate and arsenite removal from water by chemical coagulation: Kinetics, thermodynamics and equilibrium studies. Molecules 26(22), 7046. https://doi.org/10.3390/molecules26227046.

Jacob, J., Joulian, C., Battaglia-Brunet, F., 2022. Start-up and performance of a full-scale passive system including biofilters for the treatment of Fe, As and Mn in a neutral mine drainage. Water 14 (12), 1963. https://doi.org/10.3390/w14121963.

Johnson, D.B., Hallberg, K.B., 2005. Acid mine drainage remediation options: a review. Sci. Total Environ. 338(1), 3-14. https://doi.org/https://doi.org/10.1016/j.scitotenv.2004.09.002

Jong, T., Parry, D.L., 2005. Evaluation of the stability of arsenic immobilized by microbial sulfate reduction using TCLP extractions and long-term leaching techniques. Chemosphere 60(2), 254–265. https://doi.org/10.1016/j.chemosphere.2004.12.046.

Jouini, M., Neculita, C.M., Genty, T., Benzaazoua, M., 2019a. Environmental assessment of residues from multi-step passive treatment of Fe-AMD: Field case study of the Lorraine mine site, Quebec, Canada. In: Proc. Tailings and Mine Waste, Vancouver, BC, Canada, November 17–20.

Jouini, M., Rakotonimaro, T.V., Neculita, C.M., Genty, T., Benzaazoua, M., 2019b. Stability of metal-rich residues from laboratory multi-step treatment system for ferriferous acid mine drainage. Environ. Sci. Pollut. Res. 26 (35), 35588–35601. https://doi.org/10.1007/s11356-019-04608-1.

Jouini, M., Rakotonimaro, T.V., Neculita, C.M., Genty, T., Benzaazoua, M., 2019c. Prediction of the environmental behavior of residues from the passive treatment of acid mine drainage. Appl. Geochem. 110, 104421. https://doi.org/10.1016/j.apgeochem.2019.104421.

Jouini, M., Neculita, C.M., Genty, T., Benzaazoua, M., 2020a. Environmental behavior of metal-rich residues from the passive treatment of acid mine drainage. Sci. Total Environ. 712, 136541. https://doi.org/10.1016/j.scitotenv.2020.136541.

Jouini, M., Benzaazoua, M., Neculita, C.M., Genty, T., 2020b. Performances of stabilization/solidification process of acid mine drainage passive treatment residues: Assessment of the environmental and mechanical behaviors. J. Environ. Manage. 269, 110764. https://doi.org/10.1016/j.jenvman.2020.110764.

Jouini, M., Benzaazoua, M., Neculita, C.M., 2022. Stabilization/solidification of acid mine drainage treatment sludge. In: Low Carbon Stabilization and Solidification of Hazardous Wastes. Wang, L., Tsang, C.W. (Eds.), 175–199.

Kawazoe, Y., Kimura, K., Masaki, Y., Horiuchi, K., Hamai, T., Okibe, N., 2023. Re-use of passive treatment Fe-sludge for remediation of As-contaminated waters. Hydrometallurgy 221, 106123. https://doi.org/10.1016/j.hydromet.2023.106123

Kim, E.J., Yoo, J-C., Baek, K., 2014. Arsenic speciation and bioaccessibility in arsenic-contaminated soils: Sequential extraction and mineralogical investigation. Environ. Pollut. 186, 29–35. https://doi.org/10.1016/j.envpol.2013.11.032.

Macías, F., Caraballo, M.A., Nieto, J.M., 2012. Environmental assessment and management of metal-rich wastes generated in acid mine drainage passive remediation systems. Hazard. Mater. 229–230, 107–114. https://doi.org/10.1016/j.jhazmat.2012.05.080.

McCann, J.I., Nairn, R.W., 2022. Characterization of residual solids from mine water passive treatment oxidation ponds at the tar creek superfund site, Oklahoma, USA: Potential for reuse or disposal. Cleaner Waste Syst. 3, 100031. https://doi.org/10.1016/j.clwas.2022.100031.

Mehdaoui, H.Y., Guesmi, Y., Jouini, M., Neculita, C.M., Pabst, T., Benzaazoua, M., 2023. Passive treatment residues of mine drainage: Mineralogical and environmental assessment, and management avenues. Miner. Eng. 204, 108362. https://doi.org/https://doi.org/10.1016/j.mineng.2023.108362.

Mehdaoui, H.Y, Neculita, C.M., Pabst, T., Benzaazoua, M., 2024. Environmental assessment of post-treatment residues from contaminated neutral drainage: Field case study of Wood-Cadillac

biofilter, Quebec, Canada. In: Proc. of the ICARD, Halifax, Nova Scotia, Canada, September 16–20.

Mehdaoui, H.Y, Jouini., M., Lefebre, J., Neculita, C.M., Pabst, T., Benzaazoua, M., 2025. Geochemical stability of As-rich residues from a 20-year passive field biofilter used for neutral mine drainage treatment. Ecol. Eng. (accepted).

Minister of Justice, 2025. Metal and Diamond Mining Effluent Regulations (MDMER). Fisheries Act, SOR/2002-222. http://laws-lois.justice.gc.ca/PDF/SOR-2002-222.pdf

Ministère de l'Environnement, de la Lutte contre les Changements Climatiques, de la Faune et des Parcs (MELCCFP), 2025. Directive 019 sur l'industrie minière. Québec's Government, QC, Canada, 978-2-555-00464-1, 96 p.

Neculita, C.M., Zagury, G.J., Bussière, B., 2007. Passive treatment of acid mine drainage in bioreactors using sulfate-reducing bacteria: Critical review and research needs. J. Environ. Qual. 36(1), 1-16. https://doi.org/10.2134/jeq2006.0066

Nielsen, G., Hatam, I., Abuan, K.A., Janin, A., Coudert, L., Blais, J.F., Mercier, G., Baldwin, S.A., 2018. Semi-passive in-situ pilot scale biofilter successfully removed sulfate and metals from mine impacted water under subarctic climatic conditions. Water Res. 140, 268-279. https://doi.org/https://doi.org/10.1016/j.watres.2018.04.035.

Lee, G., Cui, M., Yoon, Y., Khim, J., Jang, M., 2018. Passive treatment of arsenic and heavy metals contaminated circumneutral mine drainage using granular polyurethane impregnated by coal mine drainage sludge. J. Clean. Prod. 186, 282–292. https://doi.org/10.1016/j.jclepro.2018.03.156.

Palmer, K., Ronkanen, A.K., Kløve, B., 2015. Efficient removal of arsenic, antimony and nickel from mine wastewaters in northern treatment peatlands and potential risks in their long-term use. Ecol. Eng. 75, 350–364. https://doi.org/10.1016/j.ecoleng.2014.11.045.

Sekula, P., Hiller, E., Šottník, P., Jurkovič, Ľ., Klimko, T., Vozár, J., 2018. Removal of antimony and arsenic from circum-neutral mine drainage in Poproč, Slovakia: A field treatment system using low-cost iron-based material. Environ. Earth Sci. 77 (13), 518. https://doi.org/10.1007/s12665-018-7700-3.

Skousen, J., Zipper, C.E., Rose, A., Ziemkiewicz, P.F., Nairn, R., McDonald, L.M., Kleinmann, R.L., 2017. Review of passive systems for acid mine drainage treatment. Mine Water Environ. 36(1), 133-153. https://doi.org/10.1007/s10230-016-0417-1

Smedley, P.L., Kinniburgh, D.G., 2002. A review of the source, behavior and distribution of arsenic in natural waters. Appl. Geochem. 17, 517-568. http://dx.doi.org/10.1016/S0883-2927(02)00018-5

Sobek, A.A., 1978. Field and laboratory methods applicable to overburdens and minesoils. Industrial Environmental Research Laboratory, Office of Research and Development, US Environmental Protection Agency (USEPA).

Thevenot, X.M., Neculita, C.M, Coudert, L., Rosa, E., 2024. Passive treatment of As-rich neutral mine drainage using natural organic and residual inorganic materials in a cold climate. In: Proc. of the ICARD, Halifax, Canada, September 16–20.

Thevenot, X.M., Roy, T., Pakostova, E., Rosa, E., Coudert, L., Neculita, C.M., 2025a. Effect of temperature and mixture composition on arsenic removal from neutral mine drainage in passive biofilters using iron-rich sludge and peat. Ecological Engineering, accepted.

Thevenot, X.M., Roy, T., Pakostova, E., Rosa, E., Coudert, L., Neculita, C.M., 2025b. Arsenic removal from neutral mine drainage using peat and Fe-rich sludge: Field-scale performance assessment of a passive treatment system under a subarctic climate. Science of the Total Environment (accepted).

Turcotte, S., Trépanier, S., Bussière, B., 2021. Restauration des sites miniers abandonnées au Québec : Un état de la situation et revue des solutions appliquées. In. Proc. of the Mines & Environment Symposium, Rouyn-Noranda, Canada, June 14–16.

USEPA (United States Environmental Protection Agency), 2007. Method 3051A (SW-846): Microwave assisted acid digestion of sediments, sludges, and oils. Revision 1. Washington, DC, USA.

USEPA, 1992. Method 1311. Toxicity characteristic leaching procedure. Washington, D.C. https://www.epa.gov/sites/production/files/2015-12/documents/1311.pdf (last access December 12, 2024).

USEPA, 1994. Method 1312. Synthetic precipitation leaching procedure. Washington, DC, USA. https://www.epa.gov/sites/default/files/2015-12/documents/1312.pdf (last access December 12, 2024)

Vasquez, Y., Neculita, C.M., Caicedo, G., Cubillos, J., Franco, J., Vasquez, M., Hernández, A., Roldan, F., 2022. Passive multi-unit field-pilot for acid mine drainage remediation: Performance and environmental assessment of post-treatment solid waste. Chemosphere 291, 133051. https://doi.org/10.1016/j. chemosphere.2021.133051.

Wang, S., Mulligan, C.N., 2006. Occurrence of arsenic contamination in Canada: Sources, behavior and distribution. Sci. Total Environ. 366(2), 701–721. 10.1016/j.scitotenv.2005.09.005

Wu, D., Lu, Y., Ma, L., Cheng, J., Wang, X., 2023. Preparation and molecular structural characterization of fulvic acid extracted from different types of peat. Molecules 28(19), 6780. https://doi.org/10.3390/molecules28196780.

Zimmerman, C.F., Keefe, C.W., Bashe, J., 1997. Method 440.0 Determination of carbon and nitrogen in sediments and particulates of estuarine/coastal waters using elemental analysis. USEPA, Washington, DC, USA, EPA/600/R-15/009.

CHAPITRE 7 DISCUSSSION GÉNÉRALE

Le DNC-As constitue une problématique environnementale croissante, notamment dans le contexte de l'extraction de l'or et de l'argent à partir de minerais riches en arsenic, en raison de la mobilisation accrue de l'arsenic sous des conditions de pH circumneutres. Ce type de drainage résulte de processus complexes impliquant la lixiviation des métaux et métalloïdes à partir des rejets miniers non acidogènes, la neutralisation des effluents acides par des minéraux carbonatés, ainsi que la formation de drainage minier secondaire dans des bassins de rétention ou des ouvrages de gestion des eaux minières. Contrairement au DMA qui est largement étudié, le DNC-As demeure peu documenté, en particulier en ce qui concerne les mécanismes gouvernant sa génération et son comportement environnemental (Nordstrom et al., 2015).

En l'absence de traitement adéquat, les rejets de DNC-As dans le milieu naturel peuvent engendrer des impacts durables sur les écosystèmes aquatiques et sur les ressources en eau potable. Bien que ces enjeux soient préoccupants, les recherches se sont majoritairement concentrées sur le traitement du DMA, laissant une importante lacune quant aux stratégies adaptées au DNC-As. Les biofiltres passifs, ou réacteurs biochimiques passifs (PBR), ont démontré une efficacité satisfaisante dans le traitement du DMA en exploitant des processus biologiques et géochimiques pour traiter les métaux et immobiliser les contaminants. Ces systèmes, caractérisés par une faible maintenance et des coûts d'exploitation réduits, sont particulièrement adaptés aux sites miniers abandonnés et isolés. Dans le cadre du DMA, les biofiltres passifs favorisent, d'une part, la précipitation des sulfures métalliques par l'action des bactéries sulfato-réductrices, et d'autre part, la coprécipitation et l'adsorption des métaux sur des phases oxyhydroxydes de Fe et d'Al. Cependant, bien que ces mécanismes soient largement documentés pour le traitement du DMA, leur application au DNC-As demeure peu exploré. L'application des biofiltres passifs au traitement du DNC-As représente ainsi une approche innovante, en exploitant la précipitation d'arséniures de Fe et de sulfures d'As ainsi que l'adsorption de l'As sur des minéraux ferriques amorphes (Sekula et al., 2018; Eberle et al., 2021; Neculita et al., 2021; Mehdaoui et al., 2023; Battaglia-Brunet et al., 2024).

L'un des défis majeurs liés à l'utilisation des biofiltres passifs pour le traitement des effluents miniers réside dans la gestion des résidus solides générés en fin de traitement. Ces résidus, composés principalement d'oxydes métalliques, de sulfures précipités et de matière organique (tourbe et écorces de bois), présentent une stabilité chimique variable en fonction des conditions

environnementales auxquelles ils sont exposés. Une gestion inadéquate de ces matériaux pourrait entraîner la remobilisation de l'arsenic et d'autres contaminants, compromettant ainsi l'efficacité à long terme des biofiltres (Jouini et al., 2021; McCann and Nairn, 2022; Mehdaoui et al., 2023). L'évaluation rigoureuse de la stabilité chimiques des résidus post-traitement s'avère cruciale pour estimer leur potentiel de relargage des contaminants et leurs impacts environnementaux. À cet effet, la combinaison des essais de lixiviation avec des analyses minéralogiques et géochimiques constitue une approche pertinente pour anticiper les scénarios de gestion optimaux. Toutefois, les connaissances sur la stabilité des résidus issus de biofiltres traitant le DNC-As demeurent limitées, soulignant l'importance des études approfondies sur ces enjeux (Mehdaoui et al., 2023; 2025).

Ce projet vise à évaluer la stabilité des résidus post-traitement du DNC-As dans les biofiltres passifs à différentes échelles : laboratoire (3 mois), pilote (3 mois) et terrain (22 ans). En adoptant une approche multi-échelle, cette recherche vise à approfondir la compréhension des mécanismes de rétention de l'As, à évaluer la stabilité environnementale des résidus générés et à optimiser les stratégies de gestion de ces résidus post-traitement. L'originalité de cette étude repose également sur l'analyse comparative entre les différentes échelles expérimentales, permettant de mieux appréhender l'effet d'échelle sur la performance des biofiltres et la nature des phases minérales formées. Cette approche intégrée et innovante contribuera à combler les lacunes scientifiques existantes en matière de traitement passif du DNC-As et à fournir des recommandations pratiques pour la gestion durable des résidus de traitement du DNC-As.

Pour ce faire, une combinaison des caractérisations physicochimique et minéralogique a permis d'identifier les phases minérales porteuses de l'As et de quantifier les mécanismes d'enlèvement de l'As dans les résidus de post-traitement. Ensuite, les tests de lixiviation statique ont permis d'évaluer le comportement environnemental des résidus et d'estimer les risques de lixiviation de l'As sous différentes conditions.

Ce chapitre fournit des éclaircissements sur les éléments brièvement abordés dans les chapitres antérieurs, en mettant en lumière les paramètres clés susceptibles d'influencer la stabilité des résidus de post-traitement issues des biofiltres passifs traitant le DNC-As.

7.1 Protocole d'échantillonnage et méthode de préservation des échantillons

Les protocoles d'échantillonnage mise en place durant cette thèse avaient pour objectif :

- D’assurer la représentativité des échantillons en tenant compte de toutes les variations verticales et horizontales possibles dans les biofiltres
- De permettre la conservation des échantillons, de leur prélèvement jusqu’à leur analyse.

De minimiser les délais entre l’échantillonnage et l’analyse afin de limiter toute altération des échantillons. Concernant le biofiltre de terrain de Wood-Cadillac, les résidus de post-traitement ont été collectés en octobre 2022, soit après 22 ans de traitement. Ce biofiltre composé de copeaux de bois de bouleau jaune, ayant les dimensions de 50 m x 57 mx 1 m, présente deux entrées (Nord et Ouest) et un seul exutoire. Ainsi, cinq différentes placettes ont été sélectionnées pour l’échantillonnage, couvrant les entrées, l’exécutoire, le centre et les différents coins du biofiltre (Figure 7.1). Au total, 10 carottes d’environ 100 cm de long ont été prélevées, soit deux par placette. Chaque carotte a été subdivisée en trois sous-unités (A = 0-30 cm, B = 30-60 cm et C = 60-90 cm), ce qui a permis d’obtenir un total de 30 échantillons. Cette subdivision a été réalisée afin de repérer la variation verticale des propriétés des résidus. Avant de les analyser, les résidus ont été bien identifiés et scellés dans des récipients plastiques sous vide pour minimiser le contact avec l’oxygène et prévenir toute altération. Ils ont ensuite été stockés à T < 4 ° C à l’obscurité. La caractérisation physicochimique a été réalisé dès après l’échantillonnage soit en novembre 2022, suivi de la caractérisation environnementale en décembre 2022. Une partie des échantillons a été séchée dans une boite à gant sous N_2 pour préserver l’état d’oxydation de l’As et des différents métaux, puis envoyée pour analyse minéralogique via XPS.

Les résidus de post traitement du biofiltre de laboratoire ont été récupérés à quatre profondeurs différentes permettant la collecte de quatre échantillons (octobre 2023) (Figure 6.3a; Figure 7.2a). La même démarche a été suivi pour les deux biofiltres pilote de terrain, avec la seule différence d’échantillonner deux placettes distinctes, ce qui a permis de recueillir huit échantillons pour chaque biofiltre pilote de terrain (novembre 2024) (Figure 6.3b; Figure 7.2a). Les échantillons, identifiés et stockés dans des sacs sous vide, ont été placés en obscurité et à T <4 ° C jusqu’à leurs caractérisation. Ensuite, ils ont été caractérisés, physico-chimique et environnemental. Par la suite, quatre échantillons de chaque système ont été analysé par XPS pour déterminer leur composition minéralogique et les états d’oxydation de l’As et d’autres métaux.

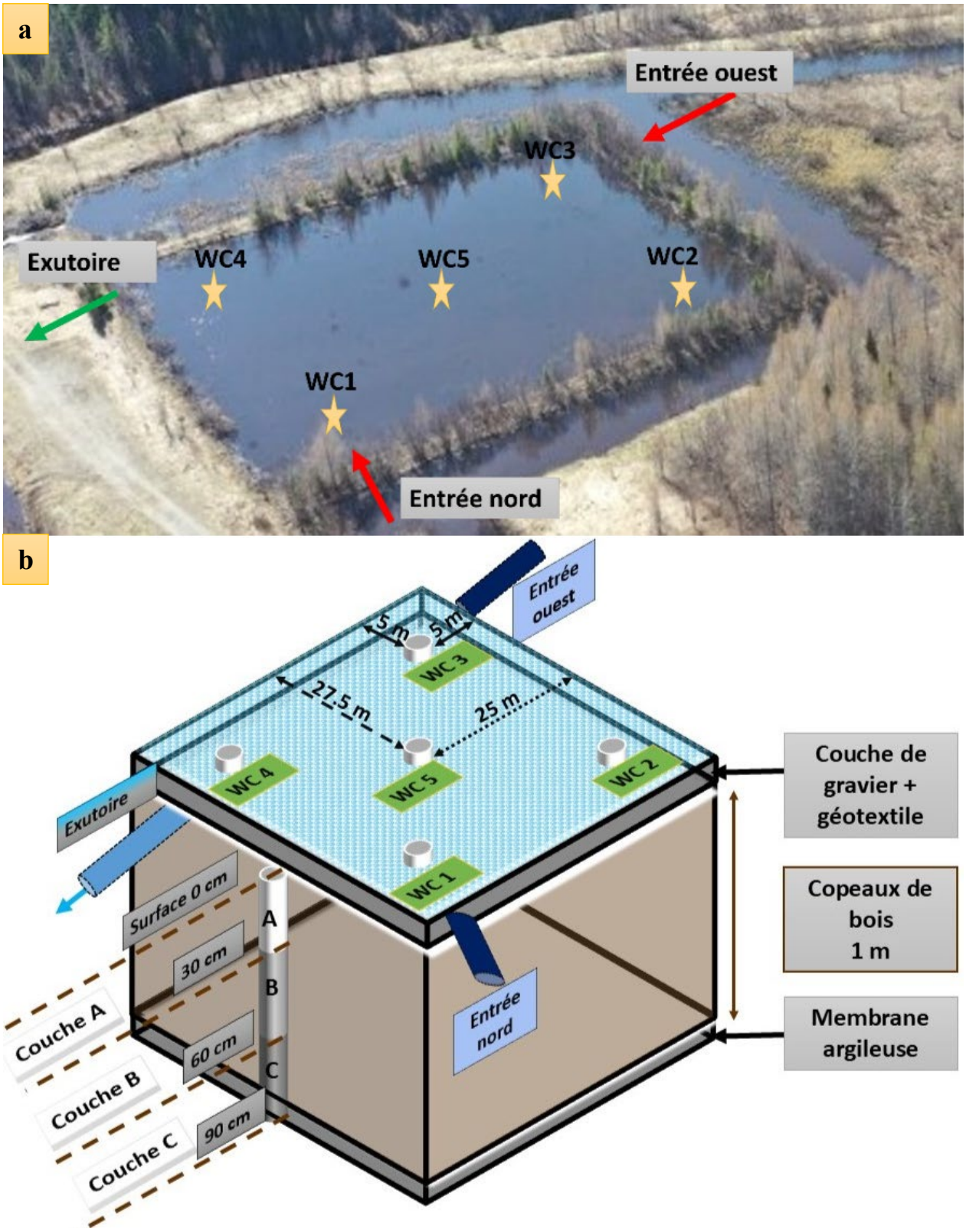

Figure 7.1 a) Vue aérienne du site Wood-Cadillac, b) Échantillonnage des résidus post-traitement du biofiltre Wood-Cadillac

Figure 7.2 Échantillonnage des résidus post-traitement: a) biofiltre de laboratoire, b) biofiltres pilotes de terrain

7.2 Caractérisation physico-chimique des résidus de post-traitement

Les résidus de post-traitement du biofiltre Wood-Cadillac ont montré des caractéristiques physico-chimiques qui varient en fonction de la localisation et de la profondeur.

Le pH de la pâte est pseudo-neutre (~6,6) avec une légère acidification observée en profondeur (couche C : 60 – 100 cm) probablement causé par les processus réducteurs et à la formation des sulfures métalliques. Les teneurs en CT et COT montrent une nette augmentation avec la profondeur. En profondeur, la concentration en CT est élevée (~35 %), mais elle diminue significativement dans les couches supérieures (~19 % et 18 %, respectivement pour les horizons A et B). Cette variation peut être attribuée à la dégradation progressive de la matière organique présente dans le mélange de remplissage et à l'activité microbienne qui consomme le carbone organique au fil du temps. De même, le ST était concentré au fonds du biofiltre avec une teneur non négligeable de 0,7% contre moins de 0,4% dans les couches supérieures. Les concentrations en métaux et métalloïdes (As, Al, Fe, Mg) varient également en fonction de la profondeur. L'As est principalement retenu dans les couches supérieures (jusqu'à 2,3 g/kg) et le Fe suit une distribution similaire (jusqu'à 41 g/kg), suggérant une forte interaction entre ces deux éléments (Tableau 7.1). L'Al et le Mg sont également concentrés en surface, ce qui souligne leur rôle dans l'adsorption et la coprécipitation des contaminants (McCann and Nairn, 2022). En résumé, les teneurs élevés en contaminants dans les différents échantillons témoignent de la rétention efficace des contaminants dans le biofiltre de Wood-Cadillac. Des observations similaires ont été trouvées

pour les résidus post-traitement passif du DMA dans le site Lorraine avec des concentration en métaux témoignant l'efficacité du traitement (Jouini et al., 2020). Contrairement aux résidus du biofiltre de Wood-Cadillac, le pH de la pâte des résidus issus du biofiltre de laboratoire est légèrement plus acide (5,7 – 6,4), ce qui pourrait favoriser une mobilisation plus importante de certains métaux. Les teneurs en CT et COT sont globalement similaires à celles observées dans les biofiltres de terrain, avec une dégradation plus marquée en surface. En revanche, aucune variation notable n'a été constatée pour le ST et pour l'ensemble des contaminants à l'exception de l'As. Ceci est probablement due à l'usage d'un effluent synthétique contaminé en As entrainant une rétention maximale à la base du système (au point d'alimentation) et qui diminue graduellement en allant vers l'exutoire (Tableau 7.1).

Les biofiltres pilotes de terrain montrent un comportement intermédiaire entre celui observé dans le laboratoire et celui de Wood-Cadillac. Le pH de pâte demeure stable oscillant entre 7,4 et 7,7. Les concentrations les plus élevées en CT et COT ont été trouvé dans les horizons intermédiaires (~21%) diminuant progressivement vers l'exutoire (11 – 17%). En revanche, les teneurs en ST (~0,6%) et en $S_{sulfates}$ (~0,4%) étaient relativement stables sans variation verticale notable. Les teneurs en contaminants, a l'exception de l'Al et du Mg, ont montré une variation verticale considérable avec des teneurs élevées à la base des biofiltres diminuant progressivement vers l'exutoire. Cette distribution suggère une rétention efficace des contaminants à l'entrée des systèmes. L'As suit la même tendance avec une rétention efficace dans les différentes couches des deux biofiltres pilotes probablement favorisée par un ratio Fe/As élevé (>15), indiquant un fort potentiel de coprécipitation ou d'adsorption sur les phases ferriques. La présence de l'Al et du Mg dans la couche I-1 (en surface) pourrait refléter un effet d'un polissage final du DNC-As assurant la capture des contaminants résiduels avant le sortie du système (Tableau 7.1).

7.3 Caractérisation minéralogique des résidus de post-traitement

Dans l'ensemble des biofiltres étudiés, l'As et le Fe présentent une corrélation étroite, indiquant que l'As est principalement stabilisé par les phases riches en Fe. Un rapport Fe/As élevé est ainsi associé à une immobilisation plus efficace de l'As, notamment via sorption et coprécipitation sur les oxyhydroxydes de Fe. La présence de la matière organique, constituant principal du mélange de remplissage, a été identifiée dans les différents échantillons, soulignant son rôle crucial dans la dynamique redox du système (Figure 7.3 et 7.4).

Tableau 7-1 Effet de l'échelle du biofiltre sur les propriétés physico-chimiques des résidus

	Biofiltre de laboratoire				**Biofiltre pilote de terrain nº1_ Dhilmar-Éléonore**				**Biofiltre pleine échelle de terrain _ Wood-Cadillac**		
	I-1	**A**	**B**	**I-2**	**I-1**	**A**	**B**	**I-2**	**A**	**B**	**C**
Nombre d'échantillons	1	1	2	1	2	2	4	2	10	10	10
pH de pate	6,4	5,6	6,1±0,2	6,3	7,4	7,6	7,6±0,1	7,6	6,6±0,05	6,6±0,07	6,5±0,2
CT (%)	28,75	28,78	33,22±0,3	33,21	11,84±0,2	20,42±0,5	20,93±0,3	17,96±0,4	19,2±9	17,9±7	35,5±6
COT (%)	26,29	26,99	30,69±0,4	30,66	11,68±0,1	19,09±0,4	19,42±0,5	15,53±0,7	17,0±8	15.9±5	31,2±2
NT (%)	0,85	0,89	0,95±0,08	0,96	0,35±0,1	0,61±0,18	0,59±0,09	0,61±0,17	0,9±0,1	0,9±0,1	0,6±0,1
ST (%)	0,23	0,23	0,22±0,02	0,22	0,55±0,08	0,61±0,1	0,66±0,13	0,62±0,14	0,4±0,2	0,3±0,2	0,7±0,2
$S_{sulfates}$ (%)	0,03	0,05	0,04±0,00	0,04	0,44±0,05	0,42±0,07	0,52±0,05	0,43±0,02	0,06±0,03	0,07±0,02	0,1±0,04
As (mg/L)	1,97	2,29	2,73±0,04	3,58	7,39±0,3	6,59±0,41	6,43±0,71	7,89±0,22	2,3±0,9	2,3±0,8	1,4±0,7
Al (mg/L)	5,13	6,09	5,44±0,05	4,96	1,15±0,14	2,49±0,04	2,22±0,29	3,52±0,22	20,5±5	19,5±7	8,7±4
Fe (mg/L)	60,44	66,85	59,47±0,5	58,45	42,85±2,3	72,19±0,17	63,32±9,61	86,32±1,75	38,3±11	41,1±9	18±7
Mg (mg/L)	3,15	6,66	3,36±0,02	3,05	5,29±0,25	5,19±0,15	5,41±1,22	6,50±0,12	6,6±2	6,9±2	3,1±1
S (mg/L)	1,99	2,20	2,37±0,02	1,70	5,75±0,35	5,97±0,35	6,90±0,52	6,46±0,35	3,6±2	3,5±1	6,5±3

L'analyse minéralogique du biofiltre Wood-Cadillac a révélé que l'As est majoritairement associé aux oxyhydroxydes de fer (goethite, hématite) dans les couches supérieures, où des conditions oxydantes favorisent la précipitation et l'adsorption. En effet, les oxyhydroxydes métalliques, en particulier de Fe(III) et d'Al, présentent des proportions variables selon les placettes et la profondeur (Figure 7.3). Ces phases ont joué un rôle crucial dans la fixation de l'As du DNC via des mécanismes combinés de sorption et coprécipitation limitant ainsi les risques de lixiviation des contaminants. La présence des sulfates était également observée en surface (<0.4%). En profondeur, sous des conditions plus réductrices, l'As précipite sous forme de sulfures amorphes (FeAsS et AsS), réduisant ainsi sa mobilité.

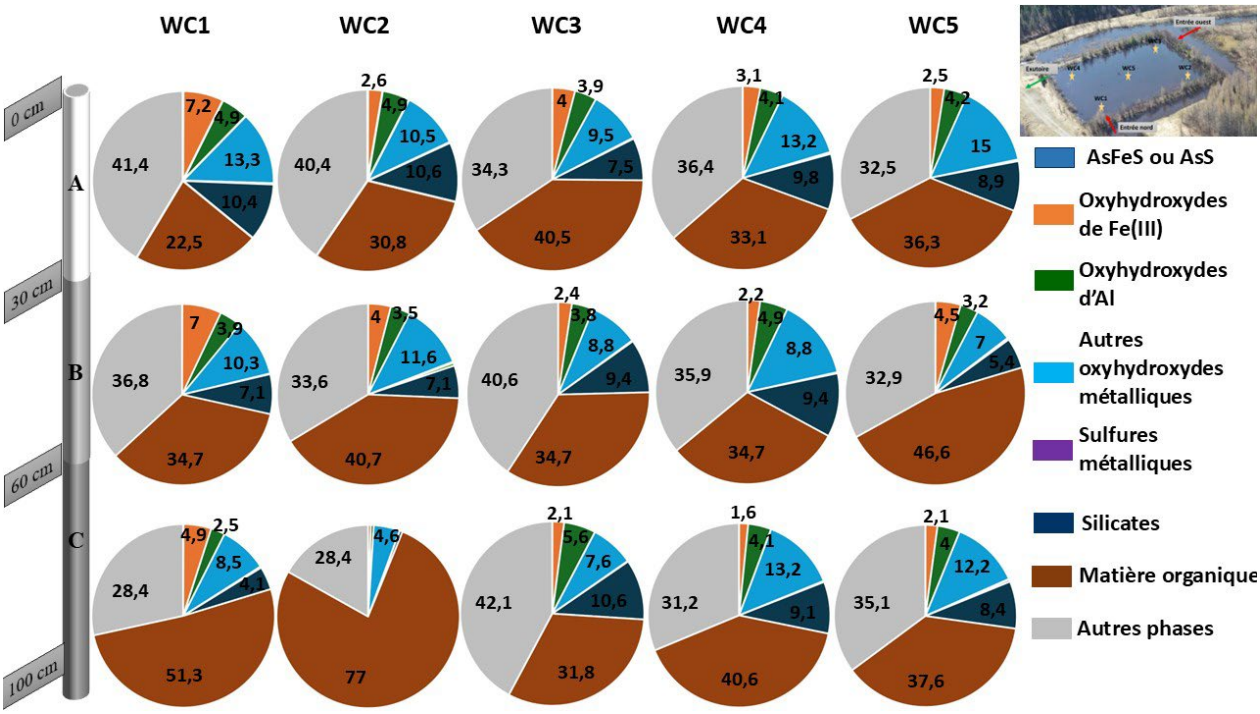

Figure 7.3 Composition minéralogique des résidus de post-traitement du biofiltre Wood-Cadillac

Dans les biofiltres de laboratoire, l'As est principalement fixé par adsorption, un mécanisme qui peut présenter une stabilité moindre à le long terme. Les oxyhydroxydes métalliques, principalement ceux de Fe (III), varient légèrement en fonction de la profondeur permettant ainsi une rétention efficace de l'As. Quant aux biofiltres de terrain, la rétention de l'As semble être influencée par deux mécanismes : la sorption et la coprécipitation, ce qui favorise une immobilisation plus durable. Une répartition similaire des oxyhydroxydes métalliques, incluant

ceux du Fe (III) et d'Al, a été observée dans les deux biofiltres pilotes avec une légère diminution de leurs pourcentages dans la couche superficielle I-1. La présence de ces phases minérales témoigne la rétention des différents contaminants dans les deux biofiltres pilotes (Figure 7.4).

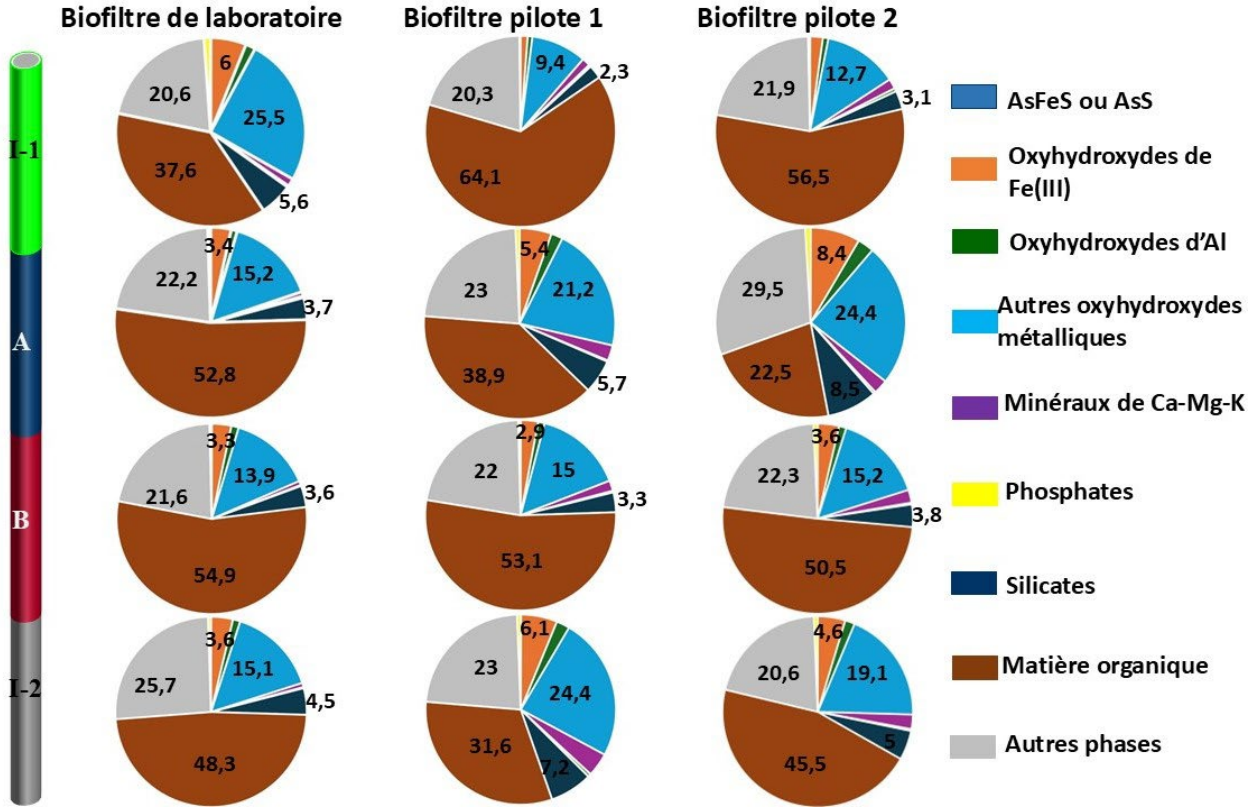

Figure 7.4 Composition minéralogique des résidus de post-traitement du biofiltre de laboratoire et des biofiltres pilotes de terrain

7.4 Comparaison entre les essais statiques : TCLP, SPLP et FLT

Concernant le biofiltre Wood-Cadillac, les valeurs de pH des lixiviats des essais TCLP, SPLP et FLT_m étaiement acides (moyennes de 4,9, 5,9 et 5,9, respectivement). L'acidité du pH peut favoriser la lixiviation des minéraux (ex. oxyhydroxydes métalliques) qui peuvent se dissoudre plus facilement dans des conditions acides. Par ailleurs, les résidus ont été classés comme non dangereux selon les critères de l'USEPA pour les différents tests statiques réalisés. Toutefois, les pourcentages respectifs des échantillons qui ont échoués la directive D019 pour la limite d'As étaient de 66% pour le TCLP, 20% pour le SPLP et 100% pour le FLT_m. En effet, la lixiviation de l'As dans les tests TCLP et SPLP ne dépassait pas 1% de la teneur élémentaire d'As. En revanche, un pourcentage considérable atteignant jusqu'à 5% des quantités d'As disponibles dans les résidus

a été lixivié par l'essai FLT_m. Ceci est probablement due à la réduction de la taille des particules et le séchage qui ont exposé davantage de surfaces réactives facilitant ainsi la lixiviation d'une fraction plus importante de l'As (Figure 7.4).

Quant aux autres biofiltres (laboratoire et pilotes), les valeurs de pH des lixiviats issus des essais statiques ont montré des discordances notables. Les lixiviats du TCLP étaient acides (~4,9) alors que ceux du SPLP et FLT étaient majoritairement neutres à légèrement basiques (7,3 – 8,3). Pour l'essai FLT, des résidus humides avec une granulométrie inférieure à 2 mm ont été utilisés. En revanche, lors du test FLTm, les résidus du biofiltre Wood-Cadillac ont été préalablement séchés et broyés afin de simuler un scénario extrême représentant la fin de vie du système. Ceci peut être dû aux caractéristiques du fluide d'extraction (i.e. pH, composition chimique). La quantité d'As lixivié n'a pas dépassé 1% des quantités d'As disponibles (Figure 7.5). Les résultats des tests ont permis de classer les résidus des 3 biofiltres comme non dangereux avec aucun risque de lixiviation de contaminants à la suite d'un contact avec des pluies acides selon les exigences de l'USEPA. En surplus, les résultats du TCLP respectent les recommandations du TII-AI de la directive D019 classifiant les résidus à risque faible. Ceci peut indiquer une certaine stabilité des phases minérales dans les conditions des tests. Toutefois, une extraction parallèle sera requise pour une meilleure évaluation des fractions échangeables.

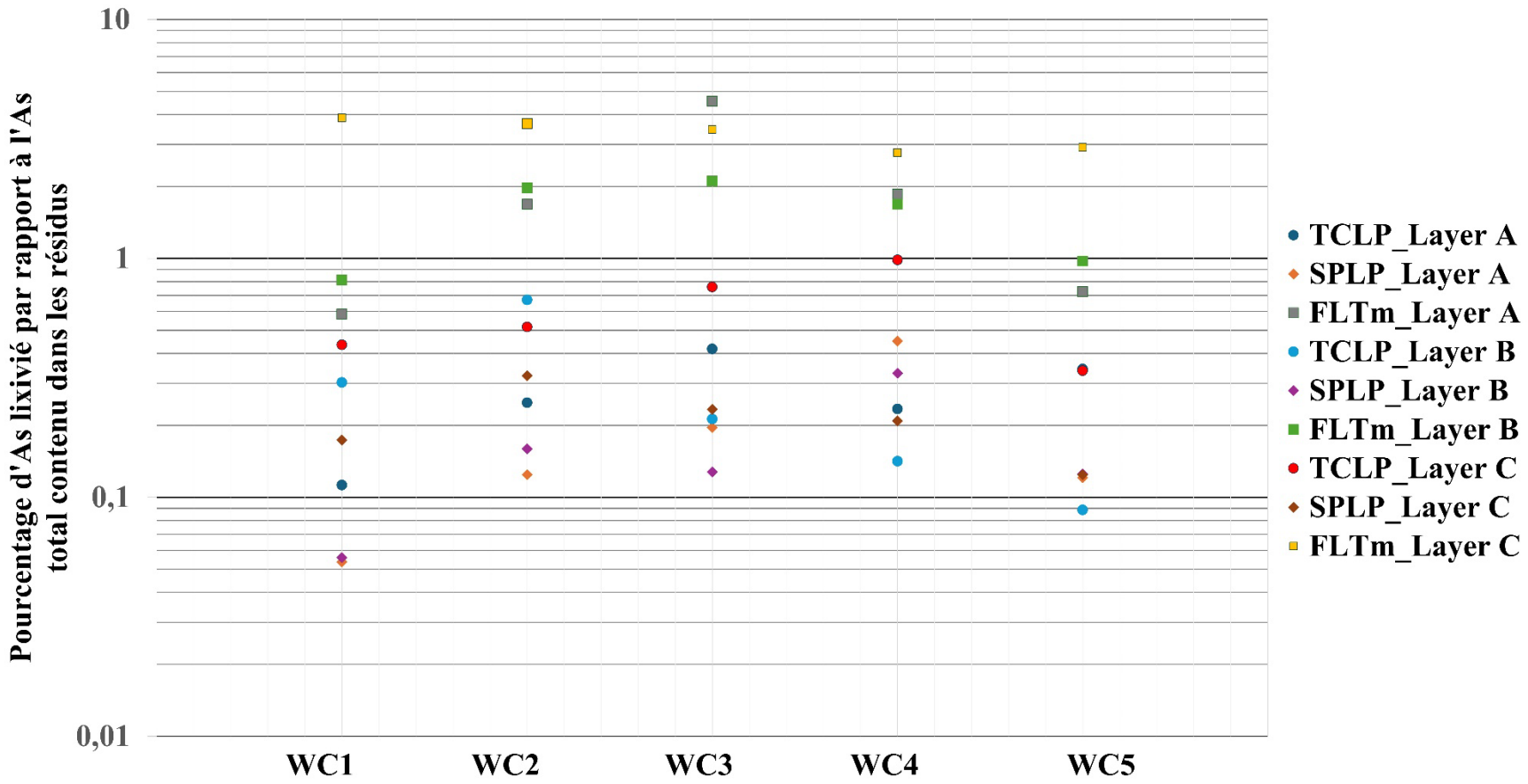

Figure 7.5 Proportion d'As lixivié durant les essais statiques par rapport à l'As total continu dans les résidus de post-traitement du biofiltre Wood-Cadillac

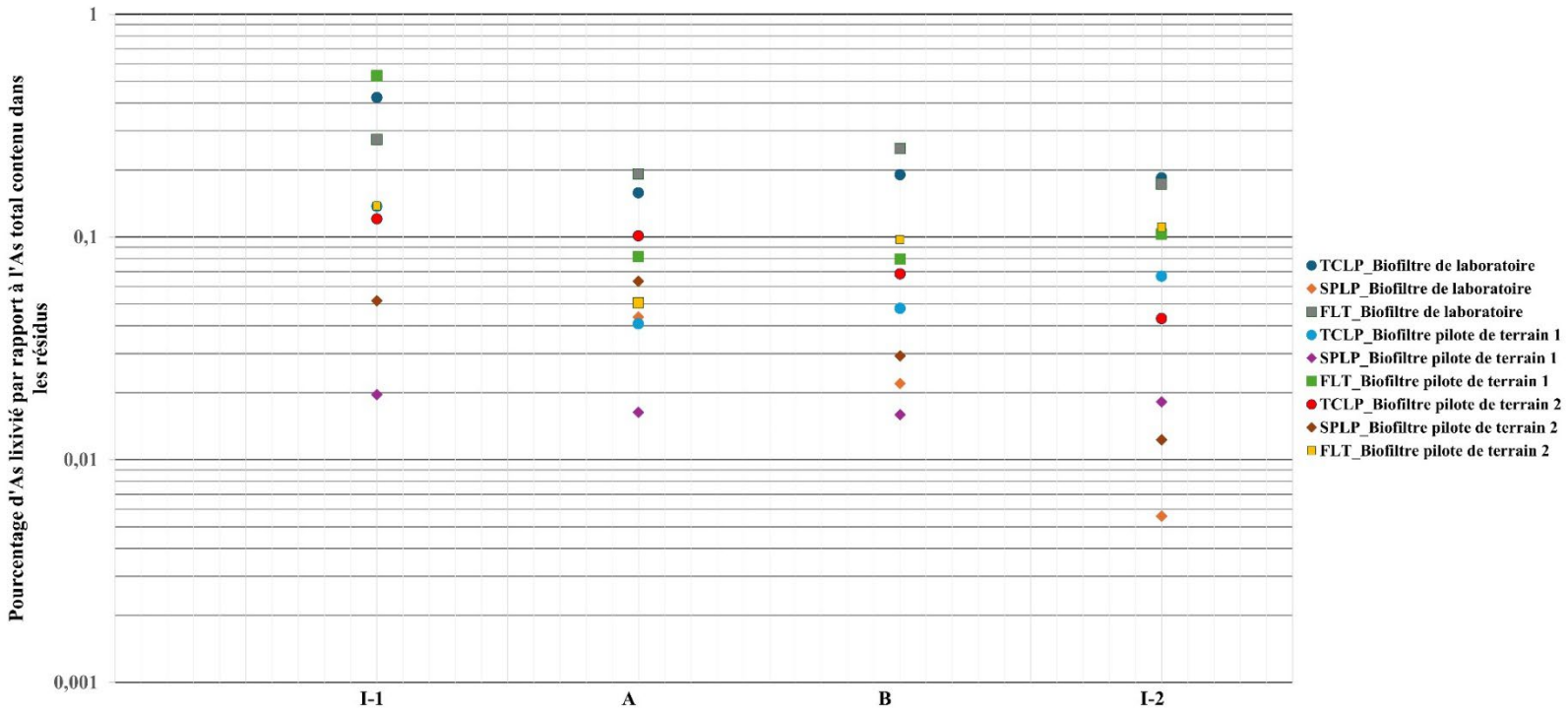

Figure 7.6 Proportion d'As lixivié durant les essais statiques par rapport à l'As total continu dans les résidus de post-traitement des biofiltres de laboratoire et pilotes de terrain

7.5 Transfert des connaissances pour le traitement du DNC-As : Wood-Cadillac exemple d'actualité

Le biofiltre Wood-Cadillac constitue un cas d'étude pertinent démontrant l'efficacité des traitements passifs à long terme. Son fonctionnement met en évidence :

- Une forte capacité d'adsorption et de précipitation des contaminants (As, Fe, S). La rétention de l'As est majoritairement contrôlée par l'adsorption sur les oxyhydroxydes de fer et d'aluminium, ainsi que par la coprécipitation sous forme de phases minérales stabilisées. Sous conditions réductrices (en profondeur), l'As précipite sous forme de sulfures amorphes (FeAsS et AsS).
- Une stabilité environnementale accrue par la présence de phases minérales bien cristallisées (Pantuzzo and Ciminelli., 2010). Les oxyhydroxydes de fer cristallins (hématite et goethite) et la formation de sulfures métalliques contribuent à la stabilisation de l'As en réduisant sa biodisponibilité et son potentiel de lixiviation.
- Une perspective de transfert des connaissances vers d'autres sites contaminés. L'efficacité du biofiltre Wood-Cadillac en tant que technologie passive peut être adaptée à d'autres contextes de contamination en ajustant les paramètres du réactif (composition, granulométrie, rapport Fe/As) et les conditions hydrogéochimiques du système

Le biofiltre Wood-Cadillac et les biofiltres pilotes démontrent une stabilisation plus efficace des contaminants comparativement aux biofiltres en laboratoire en raison de conditions hydrodynamiques et biogéochimiques plus représentatives des environnements réels. En effet, les biofiltres de terrain sont souvent de plus grande taille, avec une structure plus complexe et une hétérogénéité naturelle, ce qui favorise la formation de chemins d'écoulement préférentiels. Ces écoulements influencent fortement la répartition spatiale des contaminants ainsi que celles des phases minérales formées, créant des zones à conditions redox variées. Par conséquent, une diversité des mécanismes d'enlèvement peut être observée, notamment la coprécipitation, l'adsorption et ainsi que des processus de transformation comme la réduction, qui peuvent conduire à la précipitation de phases minérales stables telles que les sulfures d'arsenic. Les zones profondes, souvent plus réductrices, favorisent la formation de sulfures d'arsenic, des composés beaucoup plus stables à long terme que les formes simplement adsorbées. En revanche, les biofiltres de laboratoire

et pilotes sont conçus de manière plus homogène et plus compacte, ce qui favorise un écoulement uniforme et limite la formation de zones réductrices profondes. En conséquence, les biofiltres de terrain favorisent la formation des sulfures d'arsenic (FeAsS, AsS) dans les couches profondes tandis que des oxyhydroxydes métalliques se forment dans les couches superficielles. Les biofiltres de laboratoire, quant à eux, favorisent l'adsorption d'arsenic sur les oxyhydroxydes de fer (goethite, ferrihydrite) en surface. Ces phases adsorbées sont plus susceptibles à se remobiliser en cas de modifications des conditions chimiques (pH et/ou de potentiel redox). Contrairement aux phases adsorbées, les sulfures d'arsenic peuvent offrir une rétention plus efficace à long terme en conditions réductrices, bien que leur stabilité soit fortement dépendante du potentiel redox et de l'absence d'oxygène et d'activité bactérienne (ex. thiobacillus) qui pourraient accélérer l'oxydation. Les résultats soulignent l'importance de tests à grande échelle avant la mise en œuvre sur des sites miniers afin de mieux évaluer la stabilité des phases minérales formées et la durabilité des mécanismes de rétention. Par ailleurs, l'optimisation des biofiltres, notamment par un ajustement de la composition des mélanges réactifs et les conditions d'écoulement, pourrait renforcer l'immobilisation des métaux et de réduire la production de résidus lixiviables, améliorant ainsi la performance globale du traitement passif. En termes de stabilité à long terme, la présence d'oxyhydroxydes métalliques et de sulfures dans les biofiltres joue un rôle déterminant dans la rétention de l'arsenic. Cependant, ces phases présentent des conditions de stabilité distinctes en fonction du potentiel redox et du pH. Les oxyhydroxydes de fer, comme la goethite et la ferrihydrite, favorisent l'adsorption de l'arsenic sous forme As(V) en milieu oxydant et à pH neutre à légèrement acide. Cependant, ces phases peuvent devenir instables. Par ailleurs, l'augmentation de l'activité microbienne anaérobie, stimulée par la consommation d'oxygène et l'apport de matière organique, peut entraîner la formation de zones anoxiques dans les biofiltres. Dans ces zones, des micro-organismes réducteurs favorisent la transformation des oxyhydroxydes de fer entraînant leur dissolution réductrice et libérant ainsi l'arsenic. En revanche, les sulfures d'arsenic, tels que la FeAsS (arsénopyrite) et AsS (réalgar), formés en milieu anoxique, sont extrêmement stables tant que les conditions réductrices sont maintenues. Toutefois, une oxydation accidentelle, causée par un changement des conditions environnementales, pourrait entraîner la transformation de ces phases en oxyhydroxydes et à la libération des formes dissoutes d'arsenic, principalement sous forme As(V), augmentant ainsi le risque de contamination. Pour maximiser la stabilisation de l'arsenic dans les résidus issus du traitement passif, une approche combinant stabilisation et

solidification semble prometteuse. Cette stratégie permettrait de maintenir simultanément les phases oxydées et réduites dans un état physico-chimique stable, limitant ainsi les risques de relargage en cas de fluctuations du potentiel redox ou du pH, et assurant ainsi une rétention durable de l'arsenic dans des contextes miniers caractérisés par une variabilité géochimique complexe qui peut entraîner des phénomènes de dissolution, désorption ou transformation minérale.

CHAPITRE 8 CONCLUSION ET RECOMMANDATIONS

Les biofiltres passifs traitant le DNC-As génèrent des résidus de post-traitement modérément riches en As, Fe et d'autres contaminants. Les propriétés de ces résidus sont fortement influencées par plusieurs facteurs, notamment la qualité du DNC-As, les concentrations en As et en Fe, le type de mélange de remplissage et l'échelle du système de traitement. Ainsi, l'évaluation de la stabilité de ces résidus et les risques de lixiviation de l'As à court, moyen et long termes nécessite une approche spécifique à chaque cas. Cette évaluation doit combiner des caractérisations physico-chimique, minéralogique et environnementale pour fournir une compréhension complète de leur comportement sous différentes conditions.

La présente étude visait l'évaluation et la quantification de la contribution relative des mécanismes d'enlèvement et de la stabilité de l'As du DNC-As dans les biofiltres passifs à différentes échelles (laboratoire, pilote et terrain) en climat froid. Le biofiltre de Wood-Cadillac est un système de traitement à grande échelle, rempli des copeaux de bouleau jaune, et traitant efficacement un DNC-As depuis 1999. Le biofiltre de laboratoire et les deux biofiltres pilotes de terrain fonctionnait avec un mélange de remplissage à base de tourbe et de boue de traitement actif du drainage minier. Ces systèmes traitent respectivement un DNC-As synthétique (As allant jusqu'à 2,5 mg/L) et DNC-As réel (As< 1 mg/L). Pour répondre aux objectifs énoncés, les résidus de post-traitement issus des différents biofiltres ont subi une caractérisation physicochimique, minéralogique et environnemental (incluant des essais de lixiviation statique).

Les conclusions principales des résultats obtenus dans le cadre de ce projet sont les suivantes :

- Les résidus de Wood-Cadillac contenaient des concentrations significatives en contaminants (Al, As, Fe, S) avec des teneurs plus élevées dans les couches supérieures pour tous les éléments sauf le soufre qui était plus concentré en profondeur
- L'As est principalement retenu par sorption sur les oxyhydroxydes métalliques présents dans les couches supérieures du biofiltre et via précipitation sous forme de sulfures d'arsenic et sulfures métalliques au fonds du biofiltre de Wood-Cadillac
- D'après les résultats des tests TCLP et SPLP, les résidus de post-traitement de Wood-Cadillac ont été classés comme non dangereux au regard des réglementations de l'USEPA.

Cependant, 66% des lixiviats TCLP et 20% des résultats SPLP sont lixiviables pour l'As selon la directive D019

- Le test de FLT_m a suggéré que tous les résidus de Wood-Cadillac sont lixiviables pour l'As ce qui indique que les résidus ne devraient pas être séchés et broyés
- Dans l'ensemble, l'étude suggère que les résidus de post-traitement de Wood-Cadillac doivent être gérés avec précaution après leur excavation en évitant leurs séchage
- Les résidus de post-traitement du biofiltre de laboratoire présentaient des concentrations élevées en As qui ont été principalement sorbés aux oxyhydroxydes métalliques
- Les oxyhydroxydes métalliques (Fe et Al) sont les phases majeures dans les résidus de post-traitement des biofiltres pilotes de terrain
- La rétention de l'As dans les biofiltres pilotes de terrain est due principalement à la sorption aux oxyhydroxydes de Fe
- Les résidus des biofiltres pilote de terrain sont non dangereux avec aucun risque à la suite du contact avec des pluies acides selon les essais TCLP et SPLP et les normes USEPA

L'évaluation des effets d'échelle met en évidence que les différences de stabilité et de rétention de l'As dans les biofiltres sont influencées par la configuration du système (laboratoire, pilote ou terrain) et par la nature des phases minérales formées :

- Dans les biofiltres de laboratoire, l'As est principalement retenu par adsorption sur des oxyhydroxydes de fer, une forme efficace à court terme mais plus vulnérable à la remobilisation à long terme en cas de fluctuation du pH ou du potentiel redox.
- Dans les biofiltres de terrain, notamment Wood-Cadillac, l'As est précipité sous forme de sulfures dans les zones profondes, garantissant une meilleure stabilité en milieu réducteur.
- La nature des phases porteuses de l'As est influencée par l'échelle du biofiltre et la stabilité des résidus à long terme dépend également de la variabilité des conditions opérationnelles et de la composition du mélange réactif. Les biofiltres de terrain présentent une stabilisation plus durable en raison de leur capacité à maintenir des gradients redox plus marqués, tandis que les biofiltres de laboratoire, de conception plus homogène, présentent une répartition plus uniforme des phases, avec des performances de rétention parfois moins robustes.

Pour les travaux futurs de l'étude actuelle, il est recommandé de :

- Réaliser des essais de lixiviation dynamiques (cellules humides et colonnes) pour mieux évaluer le comportement environnemental des différents résidus de post-traitement
- Effectuer des cycles gel/dégel sur les résidus pour mieux comprendre l'effet de la variation saisonnière des températures sur la lixiviation des contaminants
- Réaliser des essais de stabilisation/solidification sur les résidus pour suggérer des voies de gestion potentielles à la fin de vie du biofiltre Wood-Cadillac
- Réaliser une analyse du cycle de vie des résidus post-traitement du site Wood-Cadillac
- Réaliser une étude technicoéconomique sur les coûts d'installation d'un biofiltre de terrain à la mine Éléonore.

RÉFÉRENCES

Aubertin, M., Pabst, T., Bussière, B., James, M., Mbonimpa, M., Benzaazoua, M., Maqsoud, A., 2015. Revue des meilleures pratiques de restauration des sites d'entreposage de rejets miniers générateurs de DMA. Symposium 2015 sur l'environnement et les mines, Rouyn-Noranda, Québec, Juin 14-17.

Bussière, B., Guittonny, M., 2021. Introduction. Dans: B. Bussiere & M. Guittonny (éds.), Hard Rock Mine Reclamation: From Prediction to Management of Acid Mine Drainage, CRC Press, 409p.

Calugaru, I.L., Neculita, C.M., Genty, T., Zagury, G.J., 2019. Removal efficiency of As(V) and Sb(III) in contaminated neutral mine drainage by Fe-loaded biochar. ESPR, 26(9), 9322-9332. https://doi.org/https://doi.org/10.1007/s11356-019-04381-1

Dabrowska, M., Debiec-Andrzejewska, K., Andrunik, M., Bajda, T., Drewniak, L., 2021. The biotransformation of arsenic by spent mushroom compost _ An effective bioremediation agent. Ecotoxicol. Environ. Saf., 213, 112054. https://doi.org/https://doi.org/10.1016/j.ecoenv.2021.112054

Genty, T., Neculita, C.M., Bussière, B., Zagury, G.J., 2012. Environmental behaviour of sulphate-reducing passive bioreactor mixture. In: Proc. of the 9th International Conference on Acid Rock Drainage, Ottawa, Canada, May 20–26.

Germain, D., Gagnon, A., 2013. Site minier Wood Cadillac: Évaluation de la performance du biofiltre et de la qualité des eaux du ruisseau Pandora. Direction de la restauration des sites minier – Ministère des Ressources Naturelles, CI121.0, 40 p.

Jong, T., Parry, D.L., 2005. Evaluation of the stability of arsenic immobilized by microbial sulfate reduction using TCLP extractions and long-term leaching techniques. Chemosphere, 60(2), 254–265. https://doi.org/10.1016/j. chemosphere.2004.12.046

Jouini, M., Neculita, C.M., Genty, T., Benzaazoua, M., 2020. Environmental behaviour of metal-rich residues from the passive treatment of acid mine drainage. Sci. Total Environ., 712, 136541. https://doi.org/10.1016/j.scitotenv.2020.136541

Jouini, M., Benzaazoua, M., Neculita, C.M., 2021. Stabilization/solidification of acid mine drainage treatment sludge. Dans: D.C. Tsang & L. Wang (éds.), Low Carbon Stabilization and Solidification of Hazardous Wastes (p 175-200), Elsevier.

Lee, G., Cui, M., Yoon, Y., Khim, J., Jang, M., 2018. Passive treatment of arsenic and heavy metals contaminated circumneutral mine drainage using granular polyurethane impregnated by coal mine drainage sludge. J. Clean. Prod., 186, 282-292. https://doi.org/https://doi.org/10.1016/j.jclepro.2018.03.156

Libero, C., 2007. Étude écotoxicologique au site minier Wood Cadillac avant et après bio-traitement passif. Mémoire de maîtrise, Université de Montréal, QC, Canada, 161 p.

Macías, F., Caraballo, M.A., Nieto, J.M., 2012. Environmental assessment and management of metal-rich wastes generated in acid mine drainage passive remediation systems. J. Hazard. Mater., 229–230, 107–114. https://doi.org/10.1016/j.jhazmat.2012.05.080

McCann, J.I., Nairn, R.W., 2022. Characterization of residual solids from mine water passive treatment oxidation ponds at the tar creek superfund site, Oklahoma, USA: Potential for reuse or disposal. Cleaner Waste Syst., 3, 100031. https://doi.org/ 10.1016/j.clwas.2022.100031

Mehdaoui, H.Y., Guesmi, Y., Jouini, M., Neculita, C.M., Pabst, T., Benzaazoua, M., 2023. Passive treatment residues of mine drainage: Mineralogical and environmental assessment, and management avenues. Miner. Eng., 204, 108362. https://doi.org/https://doi.org/10.1016/j.mineng.2023.108362

Ministère de Justice, 2025. Règlement sur les effluents des mines de métaux et des mines de diamants (DORS/2002-222) Consulté le 30 03 2025, https://laws-lois.justice.gc.ca/fra/reglements/dors-2002-222/

Ministère de l'Environnement, de la Lutte contre les Changements Climatiques, de la Faune et des Parcs (MELCCFP), 2025. Directive 019 sur l'industrie minière. Québec's Government, QC, Canada, 978-2-555-00464-1, 96 p.

Neculita, C.M., Zagury, G.J., Bussière, B., 2021. Passive treatment of acid mine drainage at the reclamation stage. Dans: B. Bussiere & M. Guittonny (éds), Hard Rock Mine Reclamation: From Prediction to Management of Acid Mine Drainage (p 271-296), CRC Press.

Nordstrom, D.K., Blowes, D.W., Ptacek, C.J., 2015. Hydrogeochemistry and microbiology of mine drainage: An update. Appl. Geochem., 57, 3-16. https://doi.org/10.1007/s12665-018-7700-3

Pantuzzo, F.L., Ciminelli, V.S.T., 2010. Arsenic association and stability in long-term disposed arsenic residues. Water Res., 44(19), 5631-5640. 10.1016/j.watres.2010.07.011

Turcotte, S., Trépanier, S., Bussière, B., 2021. Restauration des sites miniers abandonnés au Québec : Un état de la situation et revue des solutions appliquées. Symposium 2021 sur l'Environnement et les Mines, Rouyn-Noranda, Québec, Juin 14-16.

ANNEXE A MATÉRIEL SUPPLÉMENTAIRE PUBLIÉ AVEC L'ARTICLE 3

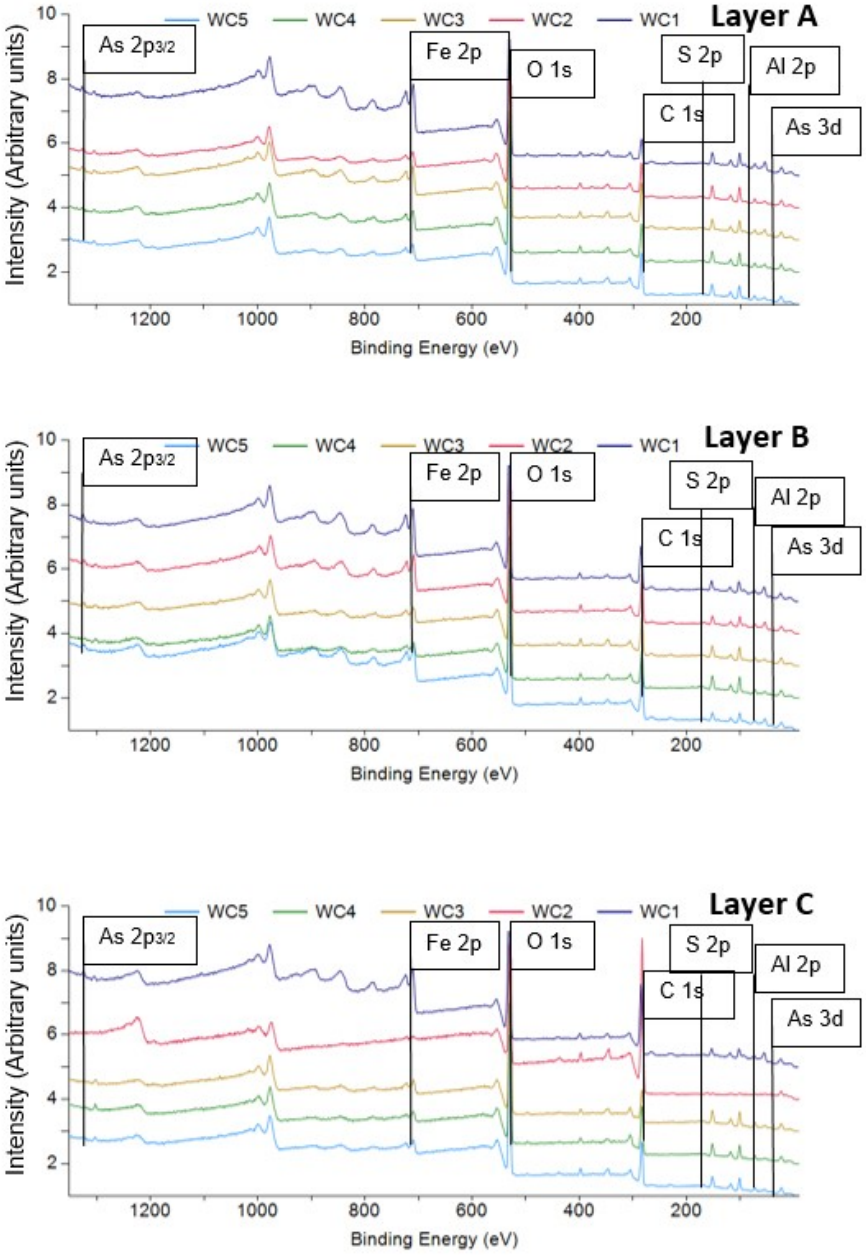

Figure A1. XPS survey scans. Peaks of special interest are labeled. Al2p and Al2s (74 and 120 eV), Si2p and Si2s (103 and 153 eV), Ca2p and Ca2s (348 and 439 eV), N1s (400 eV), Fe KLL Auger electron peaks between 780-938 eV, O KLL from 977-1013 eV, CKLL at 1

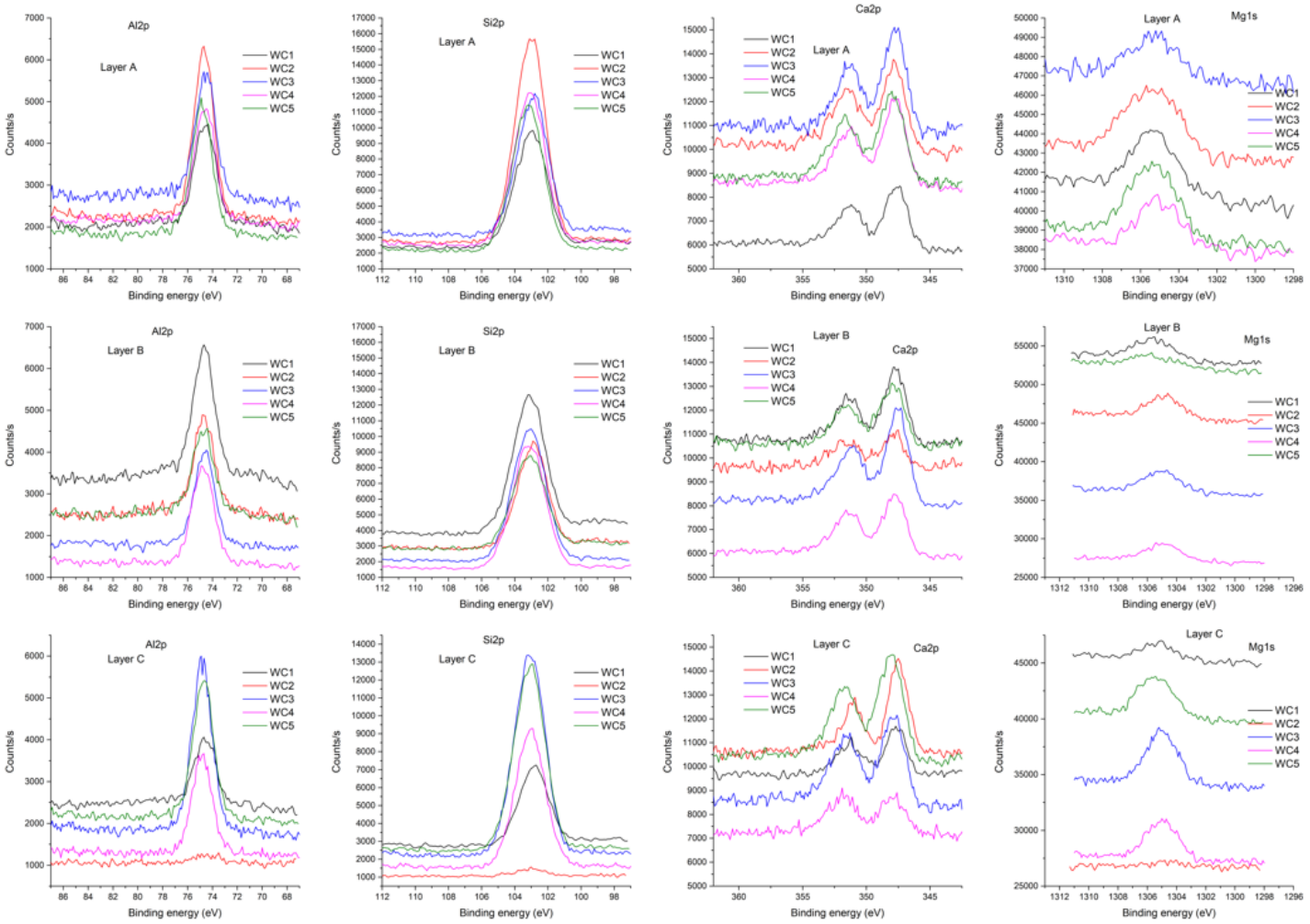

Figure A2. XPS high resolution spectra for Al2p, Si2p, Ca2p, and Mg1s for layer A, layer B and layer C, respectively

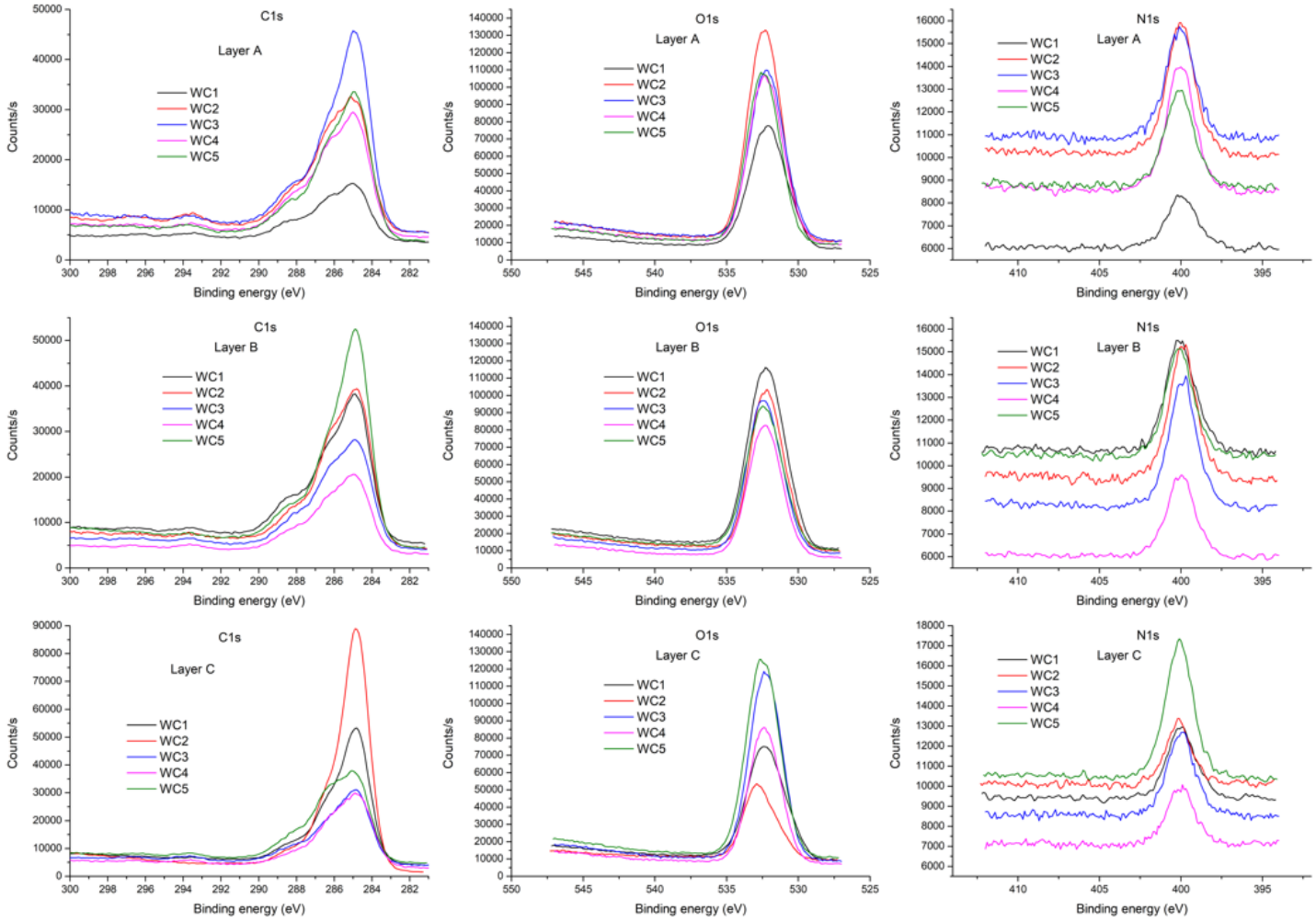

Figure A3. XPS high resolution spectra for C1s, O1s, and N1s.

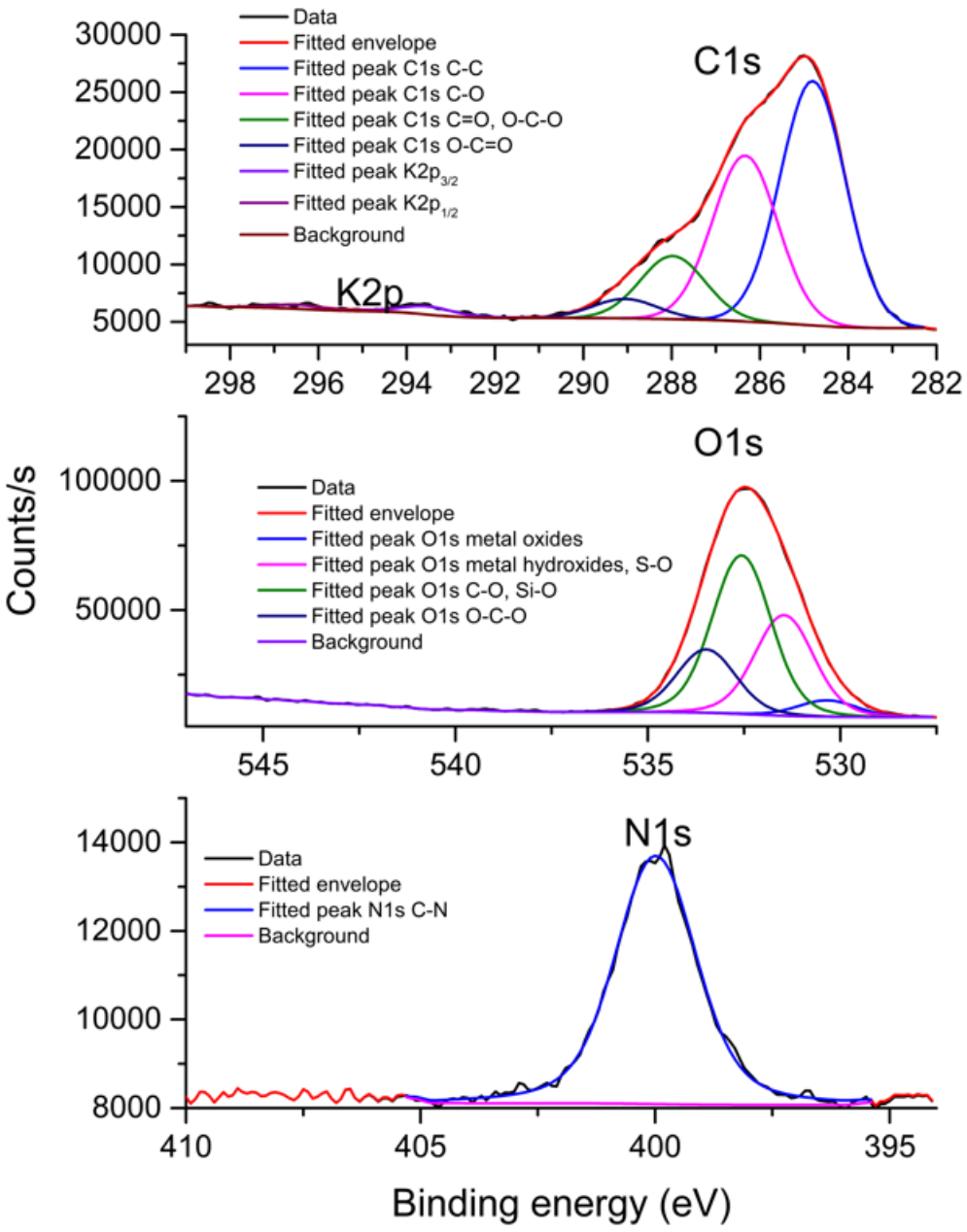

Figure A4. Peak fitting of C1s, O1s, and N1s for sample WC3 layer B

Table A1. Chemical characterization of post-treatment residues

Layers	**g/kg**	**Al**	**As**	**Ca**	**Fe**	**K**	**Mg**	**S**	**Zn**
n[a]		**36**	**36**	**36**	**36**	**36**	**36**	**36**	**36**
A	Average	20.5±5	2.3±0.9	10.6±1.8	38.3±11	1.7±0.4	6.6±2	3.6±2	0.2±0.03
	Min. (spot)	12.6 (WC3)	1.1 (WC4)	8.3 (WC1)	23.1 (WC3)	1.2 (WC3)	4.3 (WC5)	1.7 (WC5)	0.2 (WC1)
	Max. (spot)	29.3 (WC4)	3.7 (WC1)	13.7 (WC3)	57.8 (WC1)	2.5 (WC4)	9.1 (WC4)	6.6 (WC3)	0.3 (WC4)
B	Average	19.5±7	2.3±0.8	10.1±1	41.1±9	1.8±0.4	6.9±2	3.5±1	0.2±0.03
	Min. (spot)	15.1 (WC5)	1.2 (WC4)	8.4 (WC1)	30.3 (WC3)	1.5 (WC3)	5.2 (WC5)	2.1 (WC1)	0.2 (WC2)
	Max. (spot)	28.1 (WC4)	3.5 (WC1)	11.3 (WC3)	53.7 (WC1)	2.4 (WC4)	8.9 (WC4)	4.4 (WC2)	0.3 (WC4)
C	Average	8.7±4	1.4±0.7	10.4±3	18.0±7	0.7±0.3	3.1±1	6.5±3	0.1±0.05
	Min. (spot)	6.0 (WC1)	1.2 (WC2)	6.8 (WC5)	14.7 (WC1)	0.6 (WC1)	2.2 (WC5)	1.1 (WC5)	0.1 (WC2)
	Max. (spot)	11.6 (WC3)	1.7 (WC5)	11.6 (WC4)	2.5 (WC3)	1.1 (WC3)	4.3 (WC3)	11.4 (WC4)	0.2 (WC4)

Table A2. Relative atomic percentage of elements identified in XPS survey scans

	WC1.A	**WC1.B**	**WC1.C**	**WC2.A**	**WC2.B**	**WC2.C**	**WC3.A**	**WC3.B**	**WC3.C**	**WC4.A**	**WC4.B**	**WC4.C**	**WC5.A**	**WC5.B**	**WC5.C**
Al	6.7	6.2	5.5	5.6	4.1	0.5	5.5	4.1	6.7	4.7	5.8	4.4	5.0	3.5	4.0
Si	10.3	7.1	7.7	11.5	6.3	0.6	7.7	9.8	11.3	10.0	11.0	9.2	9.7	5.9	9.0
S	0.1	<D.L	<D.L	0.1	0.8	0.4	<D.L	<D.L	0.1	1.4	0.5	<D.L	0.8	0.4	1.3
C	22.1	33.5	35.5	27.9	39.1	72.0	35.5	32.1	27.9	31.3	29.3	37.7	32.9	44.6	35.1
Ca	1.0	0.5	1.2	0.9	0.4	1.2	1.2	1.2	0.9	0.9	1.0	0.8	0.9	0.6	1.1
K	0.7	2.8	<D.L	<D.L	<D.L	<D.L	<D.L	<D.L	<D.L	<D.L	<D.L	<D.L	<D.L	0.5	<D.L
N	2.5	43.3	2.9	3.0	2.9	2.2	2.8	3.6	2.6	3.5	2.8	2.4	2.6	2.7	2.9
O	49.4	0.1	42.8	46.8	40.5	22.7	42.8	45.4	47.0	44.4	45.5	42.6	44.5	37.9	43.4
Mn	0.2	<D.L	<D.L	<D.L	<D.L	<D.L	<D.L	0.3	<D.L	0.1	0.1	<D.L	0.2	<D.L	<D.L
Fe	5.4	4.8	3.0	2.6	5.9	0.4	3.0	1.6	2.4	2.9	2.5	1.7	2.3	3.1	1.9
Mg	0.5	0.5	0.6	0.6	0.5	<D.L	0.6	0.7	0.8	0.3	0.8	0.8	0.5	0.2	0.6
As	0.4	0.6	0.5	0.5	0.4	<D.L	0.5	0.2	0.1	0.3	0.3	0.2	0.1	0.4	0.2

*Potassium and sulfur could not be quantified from survey scans for some samples because the peak is too small but was visible in high resolution scans; D.L = Detection limit.

Table A3. Identification of chemical state or chemical groups and quantification from high resolution scans

Element and orbital	Peak BE (eV)	Identification	Relative atomic percentage							
			WC1.A	WC1.B	WC1.C	WC2.A	WC2.B	WC2.C	WC3.A	WC3.B
As3d5/2	40.7	FeAsS or AsS	0.08	0.05	0.05	0.06	0.03	N.D	0.06	0.03
	43.0	As(III)	0.07	0.12	0.15	0.11	0.14	N.D	0.11	0.07
	44.5	As(V)	0.23	0.25	0.19	0.09	0.17	N.D	0.22	0.17
Al2p	74.6	Al oxide/hydroxide	4.9	3.9	2.5	4.9	3.5	0.5	3.9	3.8
Si2p	103.0	Silicate	10.4	7.1	4.1	10.6	5.8	0.5	7.5	9.4
S2p3/2	162.5	Metal sulfide	0.06	0.05	0.12	0.04	0.19	N.D	0.04	0.04
	163.5	C-S	N.D	0.07	0.12	0.08	0.22	0.33	0.11	0.11
	167.5	Sulfite	0.05	0.06	0.09	0.07	0.09	0.01	0.09	0.08
	169.0	sulfate	0.09	0.07	0.11	0.06	0.54	0.03	0.15	0.14
C1s	284.8	C-C	10.6	18.8	32.6	15.0	21.4	56.0	24.0	17.2
	286.2	C-O	7.1	10.2	13.2	10.6	13.9	16.1	11.1	11.7
	287.6	O-C-O, C=O	2.4	3.9	3.0	4.2	4.1	3.1	4.2	4.4
	288.7	O-C=O	2.4	1.8	2.5	1.0	1.3	1.8	1.2	1.4
K2p3/2	293.6	K in mineral or salt possible	0.3	0.2	0.1	0.4	0.2	N.D	0.1	0.2
Ca2p3/2	347.6	Ca in mineral or salt possible	0.9	0.6	0.4	0.8	0.4	0.8	0.9	1.0
N1s	398.1	Cyanide	0.3	0.3	0.4	N.D	N.D	N.D	N.D	N.D
	400.0	C-N, O=C-N	1.8	2.2	1.9	2.9	3.3	1.9	2.6	3.6
	402.2	C-N+ or N-O	0.2	N.D	N.D	N.D	N.D	N.D	N.D	N.D
O1s	530.4	Metal oxides	7.0	5.8	4.8	2.8	5.1	1.6	3.7	2.1
	531.6	Metal hydroxides, S-O, C=O	18.4	15.4	11.1	15.2	14.0	4.0	13.7	12.9
	532.7	C-O, Si-O	18.3	15.8	13.1	20.2	15.3	8.4	16.0	20.4
	533.8	O-C-O, O*-C=O	5.5	5.2	3.5	7.7	4.3	4.4	5.6	8.1
Fe2p3/2	709.0	Fe(II)	0.9	0.6	0.7	0.1	0.2	0.1	0.3	0.1
	710.8-716.5	Fe(III) in oxides/hydroxides	7.2	7.0	4.9	2.6	5.6	0.5	4.0	2.4
Mg1s	1303.7	Mg in other mineral possible	N.D	N.D	N.D	N.D	N.D	N.D	N.D	N.D
	1305.2	Mg in mineral possible	0.9	0.5	0.2	0.7	0.5	0.1	0.4	0.6

N.D = not detected

Table A3. Identification of chemical state or chemical groups and quantification from high resolution scans (suite)

Element and orbital	**Peak BE (eV)**	**Identification**	**Relative atomic percentage**						
			WC3.C	**WC4.A**	**WC4.B**	**WC4.C**	**WC5.A**	**WC5.B**	**WC5.C**
As3d5/2	40.7	FeAsS or AsS	0.02	0.03	0.02	0.01	0.03	0.05	0.03
	43.0	As(III)	0.04	0.06	0.03	0.06	0.06	0.09	0.09
	44.5	As(V)	0.03	0.12	0.08	---	0.03	0.22	0.09
Al2p	74.6	Al oxide/hydroxide	5.6	4.1	4.9	4.1	4.2	3.2	4.0
Si2p	103.0	Silicate	10.6	9.8	11.2	9.1	8.9	5.4	8.4
S2p3/2	162.5	Metal sulfide	0.02	0.05	0.04	0.06	0.11	0.10	0.11
	163.5	C-S	0.1	0.09	0.06	0.17	0.10	0.18	0.10
	167.5	Sulfite	0.08	0.10	0.04	0.09	0.14	0.18	0.13
	169.0	sulfate	0.08	0.28	0.15	0.11	0.19	0.23	0.39
C1s	284.8	C-C	17.8	16.1	15.7	22.2	20.1	28.8	17.7
	286.2	C-O	9.3	10.9	9.7	13.5	11.4	12.1	13.6
	287.6	O-C-O, C=O	3.6	4.5	3.5	3.8	4.1	3.6	4.7
	288.7	O-C=O	1.1	1.6	2.2	1.1	0.9	2.1	1.6
K2p3/2	293.6	K in mineral or salt possible	0.3	0.2	0.3	0.3	0.2	0.1	0.2
Ca2p3/2	347.6	Ca in mineral or salt possible	0.9	0.8	0.8	0.6	0.9	0.6	0.9
N1s	398.1	Cyanide	N.D	N.D	N.D	N.D	0.14	0.2	N.D
	400.0	C-N, O=C-N	2.5	3.3	2.8	2.2	2.2	2.3	3.2
	402.2	C-N+ or N-O	N.D	N.D	N.D	N.D	0.1	N.D	N.D
O1s	530.4	Metal oxides	0.8	3.5	3.2	4.7	5.5	3.2	2.7
	531.6	Metal hydroxides, S-O, C=O	14.5	16.9	18.3	14.2	16.2	11.5	15.6
	532.7	C-O, Si-O	21.1	19.6	18.8	16.6	16.4	15.0	19.0
	533.8	O-C-O, O*-C=O	8.5	4.1	5.2	5.0	4.7	5.6	4.7
Fe2p3/2	709.0	Fe(II)	0.03	0.2	0.2	0.1	0.1	0.4	0.1
	710.8-716.5	Fe(III) in oxides/hydroxides	2.06	3.1	2.2	1.6	2.5	4.5	2.1
Mg1s	1303.7	Mg in other mineral possible	N.D	N.D	N.D	N.D	N.D	0.1	0.2
	1305.2	Mg in mineral possible	0.8	0.5	0.6	0.7	0.8	0.2	0.5

N.D = not detected

Table A4. Physicochemical parameters of the eluates after TCLP and SPLP tests

Total extractable TCLP							
	pH	**Metals (mg/L)**					**SO_4^{2-} (mg/L)**
		Al	**As**	**Fe**	**Mg**	**Mn**	
n[a]	36	36	36	36	36	36	36
A	5.0±0.03	0.39±0.05	0.3±0.1	0.3±0.04	4.0±0.3	4.3±2	2.0±1.0
B	5.0±0.02	0.41±0.05	0.35±0.1	0.4±0.05	3.9±0.3	5.1±2	5.0±0.2
C	4.9±0.02	0.35±0.04	0.42±0.1	0.2±0.05	3.5±0.2	1.6±0.1	8.6±5.0
Total extractable SPLP							
	pH	**Metals (mg/L)**					
		Al	**As**	**Fe**	**Mg**	**Mn**	
n[a]	36	36	36	36	36	36	
A	6.1±0.09	0.07±0.01	0.16±0.05	0.16±0.05	0.98±0.2	0.06±0.01	
B	6.1±0.09	0.07±0.01	0.15±0.03	0.17±0.06	1.1±0.2	0.08±0.02	
C	5.8±0.02	0.07±0.01	0.14±0.03	0.16±0.03	1.1±0.3	0.11±0.01	

[a]Number of analyzed samples

Table A5. Physicochemical parameters of the eluates after TCLP test

	pH	**Metals (mg/L)**					**SO^4_{2-} (mg/L)**
		Al	**As**	**Fe**	**Mg**	**S**	
na	36	36	36	36	36	36	36
WC1.1.A	5.0	0.41	0.30	0.31	4.27	5.99	<1
WC1.1.B	5.0	0.40	0.22	0.28	4.58	6.87	<1
WC1.1.C	4.9	0.31	0.16	0.14	3.43	0.94	10
WC1.2.A	5.0	0.37	0.12	0.26	4.78	9.58	<1
WC1.2.B	5.0	0.45	0.86	0.39	4.31	10.21	<1
WC1.2.C	4.9	0.32	0.43	0.16	3.17	1.94	6
WC2.1.A	4.9	0.38	0.22	0.22	3.94	3.00	1
WC2.1.B	4.9	0.45	0.26	0.38	3.82	3.97	<1
WC2.1.C	4.9	0.33	0.37	0.16	3.57	1.77	3
WC2.2.A	4.9	0.44	0.3	0.36	3.27	2.52	<1
WC2.2.B	5.0	0.50	0.99	0.47	3.62	3.50	<1
WC2.2.C	5.0	0.34	0.21	0.19	3.54	1.59	5
WC3.1.A	5.0	0.37	0.19	0.3	4.11	1.06	5
WC3.1.B	4.9	0.38	0.2	0.38	3.63	2.70	5
WC3.1.C	4.9	0.42	0.77	0.41	3.47	1.29	33
WC3.2.A	4.9	0.23	0.44	0.11	3.23	0.28	12
WC3.2.B	4.9	0.27	0.29	0.13	4.00	0.26	17
WC3.2.C	4.9	0.23	0.27	<0.108	2.91	0.24	18
WC4.1.A	4.9	0.41	0.19	0.3	4.08	4.59	<1
WC4.1.B	5.0	0.42	0.12	0.3	4.54	4.85	<1
WC4.1.C	5.0	0.47	1.06	0.33	4.32	1.91	3
WC4.2.A	5.0	0.45	0.06	0.23	4.06	0.77	1
WC4.2.B	5.0	0.46	0.06	0.24	3.82	0.84	<1
WC4.2.C	5.0	0.39	0.26	0.23	3.62	0.66	2

Table A5. Physicochemical parameters of the eluates after TCLP test (suite)

	pH	**Metals (mg/L)**					**SO^4_2- (mg/L)**
		Al	**As**	**Fe**	**Mg**	**Mn**	
na	36	36	36	36	36	36	36
WC5.1.A	5.0	0.50	1.03	0.40	3.75	2.39	1.00
WC5.1.B	4.9	0.39	0.12	0.27	3.87	1.95	<1
WC5.1.C	4.9	0.35	0.44	0.20	3.90	0.75	12
WC5.1.A dupli	5.0	0.37	0.95	0.33	3.69	3.73	<1
WC5.1.B dupli	5.0	0.37	0.71	0.27	3.66	4.15	<1
WC5.1.C dupli	4.9	0.35	0.31	0.20	3.91	1.95	3.00
WC5.1.A trip	4.9	0.49	0.67	0.44	4.3	4.63	<1
WC5.1.B trip	4.9	0.51	0.82	0.45	4.29	5.4	<1
WC5.1.C trip	4.9	0.31	0.25	0.22	3.74	1.49	4.00
WC5.2.A	4.9	0.46	0.10	0.43	3.53	4.12	<1
WC5.2.B	4.9	0.43	0.12	0.4	4.01	4.86	<1
WC5.2.C	4.8	0.33	0.16	0.25	3.74	1.37	4.00
Average	4.9	0.39	0.39	0.28	3.84	3.05	7.63
minimum	4.8	0.23	0.06	0.1	2.91	0.24	<1
maximum	5.0	0.51	1.06	0.47	4.78	10.21	33
Standard deviation	0.16	0.07	0.3	0.09	0.4	2.4	7.8
Coefficient of variation (%)	0.8	0.04	0.1	0.03	0.01	0.07	0.59

[a]Number of analyzed samples.

Table A6. Physicochemical parameters of the eluates after SPLP test

	pH	**Metals (mg/L)**				
		Al	**As**	**Fe**	**Mg**	**Mn**
na	36	36	36	36	36	36
WC1.1.A	6.2	0.07	0.07	<0.1	0.8	<0.004
WC1.1.B	6.0	0.06	0.06	<0.1	1.15	<0.004
WC1.1.C	5.2	0.03	0.07	<0.1	1.31	0.1
WC1.2.A	6.0	0.08	0.09	0.15	1.19	0.05
WC1.2.B	5.9	0.08	0.12	0.16	1.1	0.12
WC1.2.C	5.2	0.06	0.15	<0.1	0.9	0.17
WC2.1.A	6.2	0.08	0.12	0.16	0.88	<0.004
WC2.1.B	6.0	0.09	0.15	0.16	0.89	<0.004
WC2.1.C	6.1	0.07	0.22	<0.1	0.85	0.08
WC2.2.A	5.9	0.08	0.13	0.11	0.67	<0.004
WC2.2.B	6.1	0.07	0.15	0.11	0.76	<0.004
WC2.2.C	5.8	0.08	0.17	<0.1	0.71	<0.004
WC3.1.A	6.3	0.08	0.17	<0.1	0.72	<0.004
WC3.1.B	6.2	0.06	0.14	<0.1	1.01	<0.004
WC3.1.C	6.1	0.07	0.15	<0.1	0.95	<0.004
WC3.2.A	6.2	0.06	0.32	<0.1	1.44	0.06
WC3.2.B	6.1	0.07	0.28	<0.1	1.65	0.06
WC3.2.C	5.9	0.07	0.12	<0.1	1.92	0.12
WC4.1.A	6.2	0.06	0.08	0.15	1.12	<0.004
WC4.1.B	6.1	0.06	0.06	<0.1	1.04	<0.004
WC4.1.C	5.9	0.07	0.09	<0.1	1	<0.004
WC4.2.A	6.0	0.14	0.06	0.24	0.84	0.01
WC4.2.B	6.1	0.09	0.06	0.13	0.85	<0.004
WC4.2.C	5.0	0.03	<0.02	<0.1	2.34	0.07

[a]Number of analyzed samples.

Table A6. Physicochemical parameters of the eluates after SPLP test (suite)

	pH	**Metals (mg/L)**				
		Al	**As**	**Fe**	**Mg**	**Mn**
na	36	36	36	36	36	36
WC5.1.A	6.2	0.12	0.10	0.21	1.14	0.01
WC5.1.B	6.1	0.07	0.11	0.14	1.27	0.01
WC5.1.C	5.9	0.026	0.10	0.31	1.05	0.07
WC5.1.A dup	6.2	0.09	0.11	0.29	1.14	0.07
WC5.1.B dup	6.0	0008	0.10	0.46	1.06	0.09
WC5.1.C dup	5.4	0.05	0.13	<0.1	0.92	0.16
WC5.1.A trip	6.0	0.09	0.11	0.28	1.20	0.02
WC5.1.B trip	5.8	0.07	0.10	0.15	1.00	0.15
WC5.1.C trip	5.3	0.05	0.12	0.16	1.05	0.10
WC5.2.A	6.0	0.09	0.10	0.19	1.02	0.01
WC5.2.B	6.0	0.10	0.09	0.24	0.82	<0.004
WC5.2.C	5.2	0.04	0.09	<0.1	1.10	0.07
Average	5.9	0.08	0.12	0.20	1.07	0.08
minimum	5.2	0.03	0.02	0.10	0.67	0.004
maximum	6.3	0.26	0.32	0.46	1.92	0.17
Standard deviation	0.3	0.03	0.05	0.08	0.33	0.06
Coefficient of variation (%)	0.02	$3 .10^{-5}$	$7 .10^{-5}$	$2 .10^{-4}$	$4 .10^{-3}$	$6 .10^{-5}$

[a]Number of analyzed samples.

Table A7. Physicochemical parameters of the eluates after FLTm test

	pH	**Metals (mg/L)**						
		Al	**As**	**Ca**	**Fe**	**Mg**	**Mn**	**S**
na	36	36	36	36	36	36	36	36
WC1.1.A	7.1	0.4	0.9	17.8	0.6	3.6	1.9	4.7
WC1.1.B	5.9	0.4	1.3	20.3	0.6	3.9	2.4	5.7
WC1.1.C	5.2	0.8	2.9	27.2	0.9	5.0	1.5	19.1
WC1.2.A	6.3	0.4	1.2	17.9	0.6	3.5	2.7	4.1
WC1.2.B	6.4	0.3	1.6	18.4	0.6	3.7	1.4	5.5
WC1.2.C	5.3	0.7	2.4	21.6	0.7	3.9	1.3	18.0
WC2.1.A	5.9	0.4	1.4	25.2	0.5	4.0	1.2	14.3
WC2.1.B	5.9	0.3	1.8	26.8	0.6	4.0	2.0	13.3
WC2.1.C	5.6	0.5	3.3	24.9	0.6	4.0	2.0	9.5
WC2.1.A dup	6.0	0.4	1.4	23.1	0.5	3.9	1.2	13.6
WC2.1.B dup	6.2	0.3	1.4	11.4	0.5	1.6	0.9	4.7
WC2.1.C dup	5.9	0.2	1.7	11.6	0.3	1.8	0.9	3.8
WC2.1.A trip	6.0	0.4	1.4	22.8	0.5	3.8	2.0	13.1
WC2.1.B trip	6.0	0.4	1.7	21.6	0.6	3.4	1.7	11.2
WC2.1.C trip	5.7	0.2	3.2	23.3	0.6	3.8	1.9	8.8
WC2.2.A	7	0.4	2.9	20.5	0.5	3.3	1.0	8.3
WC2.2.B	6.0	0.4	2.5	13.1	0.5	2	0.8	3.9
WC2.2.C	6.0	0.2	0.8	6.9	0.2	1.0	0.3	3.5
WC3.1.A	5.8	0.6	3.7	30.5	0.6	4.5	0.6	11.5
WC3.1.B	6.0	0.4	1.9	29.7	0.6	4.3	1.3	8.4
WC3.1.C	5.6	0.5	3.2	32.3	0.6	4.6	0.8	13.7
WC3.2.A	5.4	0.5	3.3	60.3	0.4	6.9	0.5	46.3
WC3.2.B	5.5	0.5	3.1	55.2	0.3	6.5	0.4	40.3
WC3.2.C	5.3	0.4	1.5	26.4	0.3	3.2	0.2	22.5

[a]Number of analyzed samples.

Table A7. Physicochemical parameters of the eluates after FLTm test (suite)

	pH	**Metals (mg/L)**						
		Al	**As**	**Ca**	**Fe**	**Mg**	**Mn**	**S**
na	36	36	36	36	36	36	36	36
WC4.1.A	6.2	0.4	0.9	23.7	0.5	3.8	0.7	13.5
WC4.1.B	6.2	0.4	0.9	22.8	0.5	3.6	0.7	12.8
WC4.1.C	5.7	0.3	0.8	12.0	0.4	1.7	0.2	8.4
WC4.2.A	6.1	0.4	1.1	25.7	0.4	4.0	0.2	12.2
WC4.2.B	6.1	0.4	1.2	24.3	0.4	3.8	0.3	11.2
WC4.2.C	4.8	1.1	2.9	67.6	3.0	8.2	1.1	43.6
WC5.1.A	6.2	0.3	1.4	24.5	0.5	4.1	1.5	5.0
WC5.1.B	6.2	0.3	1.5	27.2	0.6	4.6	1.8	5.1
WC5.1.C	5.4	0.6	3.6	32.3	0.5	5.4	1.2	16.1
WC5.2.A	6.4	0.3	0.9	19.1	0.5	3.1	1.2	11.7
WC5.2.B	6.3	0.4	1.2	20.8	0.6	3.4	1.5	12.9
WC5.2.C	5.5	0.5	1.6	27.8	0.5	4.7	0.7	21.7
Average	5.9	0.45	1.9	25.5	0.6	3.9	1.2	13.4
minimum	4.8	0.2	0.8	6.9	0.3	1.0	0.2	3.5
maximum	7.1	1.1	3.7	67.6	3	8.2	2.7	46.3
Standard deviation	0.45	0.16	0.89	12.2	0.4	104	0.68	10.3
Coefficient of variation (%)	0.02	$7 .10^{-4}$	0.01	3.1	$2 .10^{-3}$	0.05	$8 .10^{-3}$	1.38

[a]Number of analyzed samples.

ANNEXE B MATÉRIEL SUPPLÉMENTAIRE PUBLIÉ AVEC L'ARTICLE 4

Figure B1. Field experimental work: a) Site location (adapted from https://www.google.ca/maps), b) On-site sampling of As-CND, c) Preparation of the reactive mixture, d) Sampling of post-treatment residues of field-pilot biofilters

Figure B2. Laboratory experimental work: Sampling of post-treatment residues

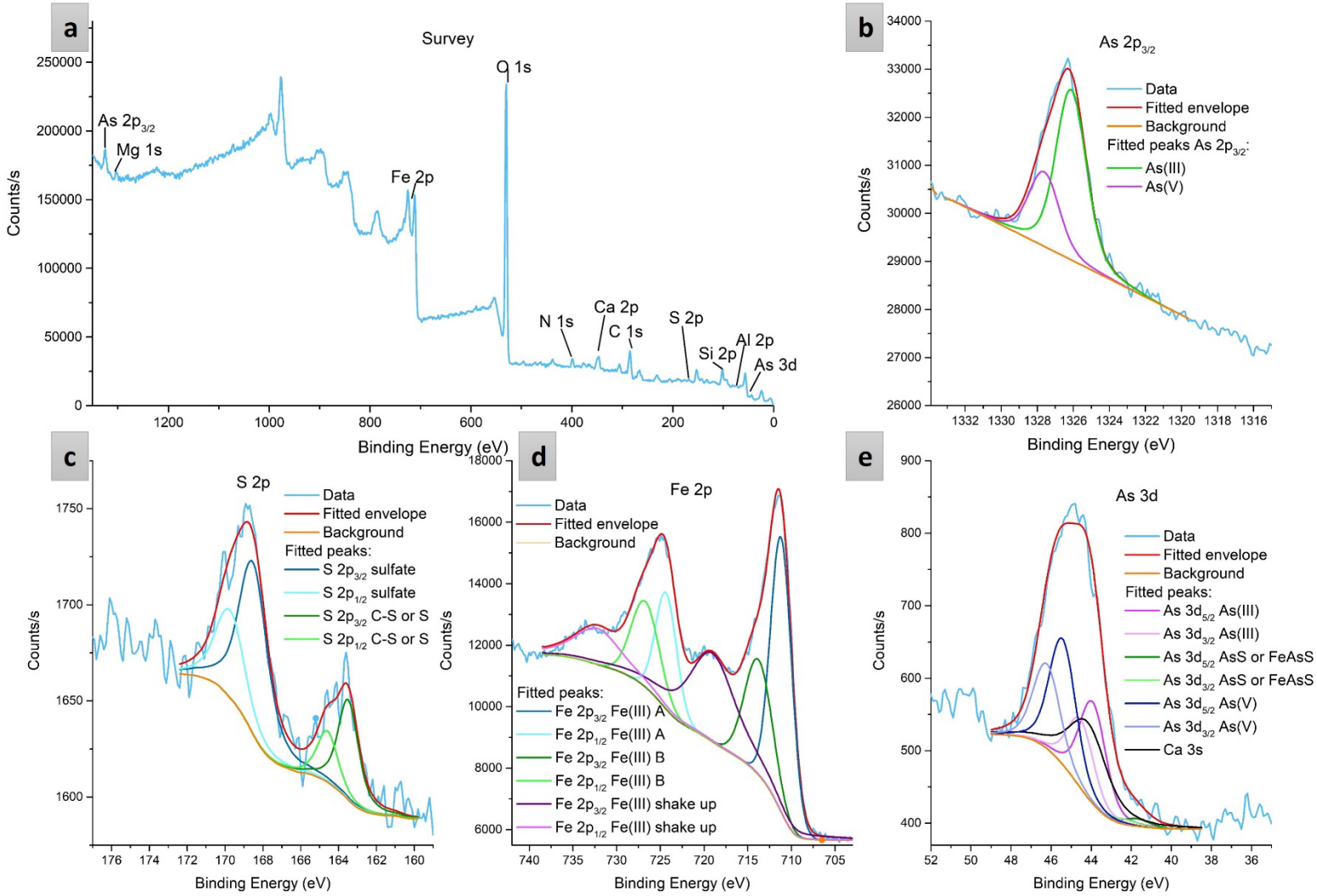

Figure B3. XPS of MD-S: (a) Survey scan, (b) high-resolution As2p3/2, (c) S2p, (d) Fe2p, and (e) As3d

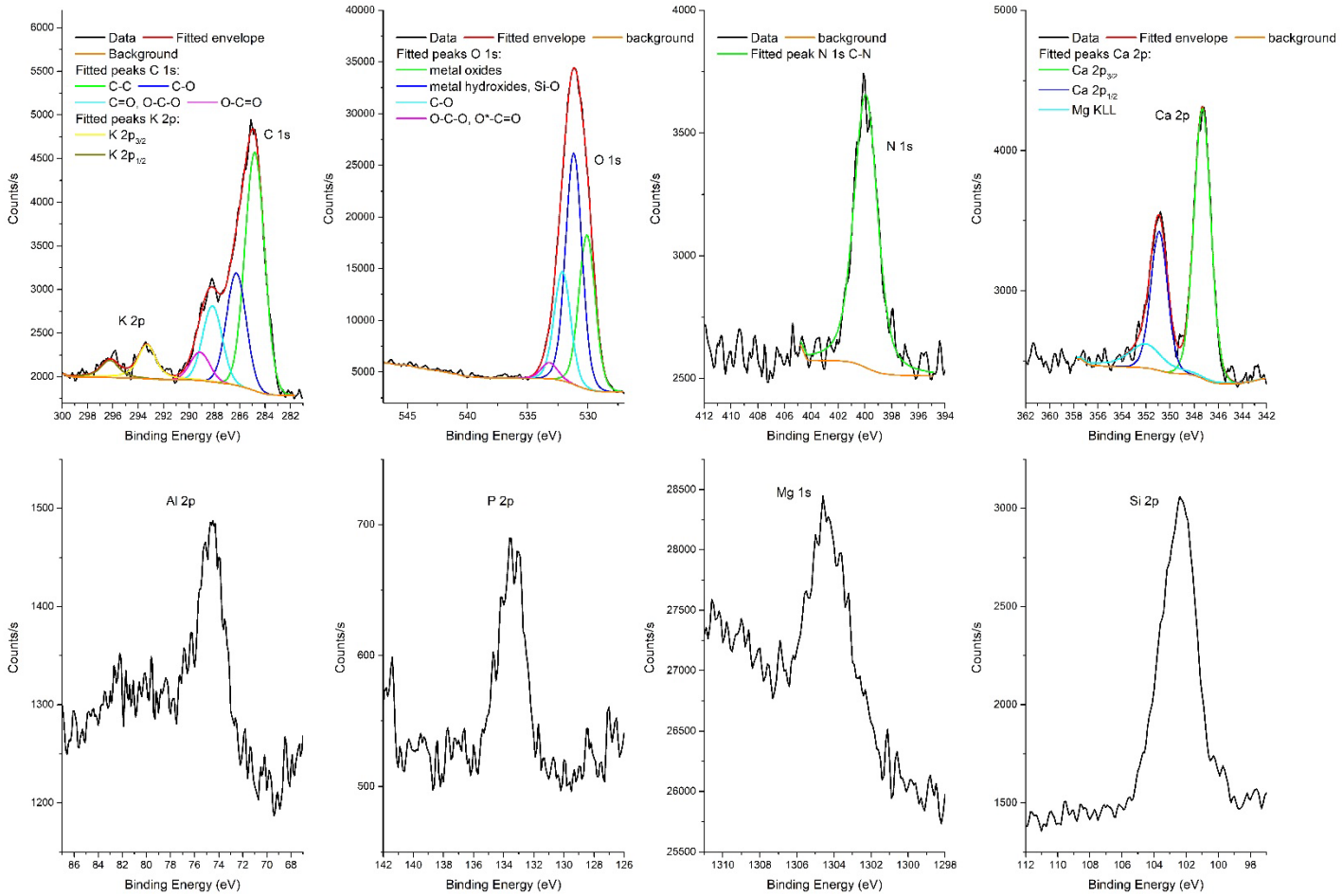

Figure B4. Peak fitting of C1s, O1s, N1s, Ca2p, Al2p, P2p, Mg1s and Si2p for AMD-S

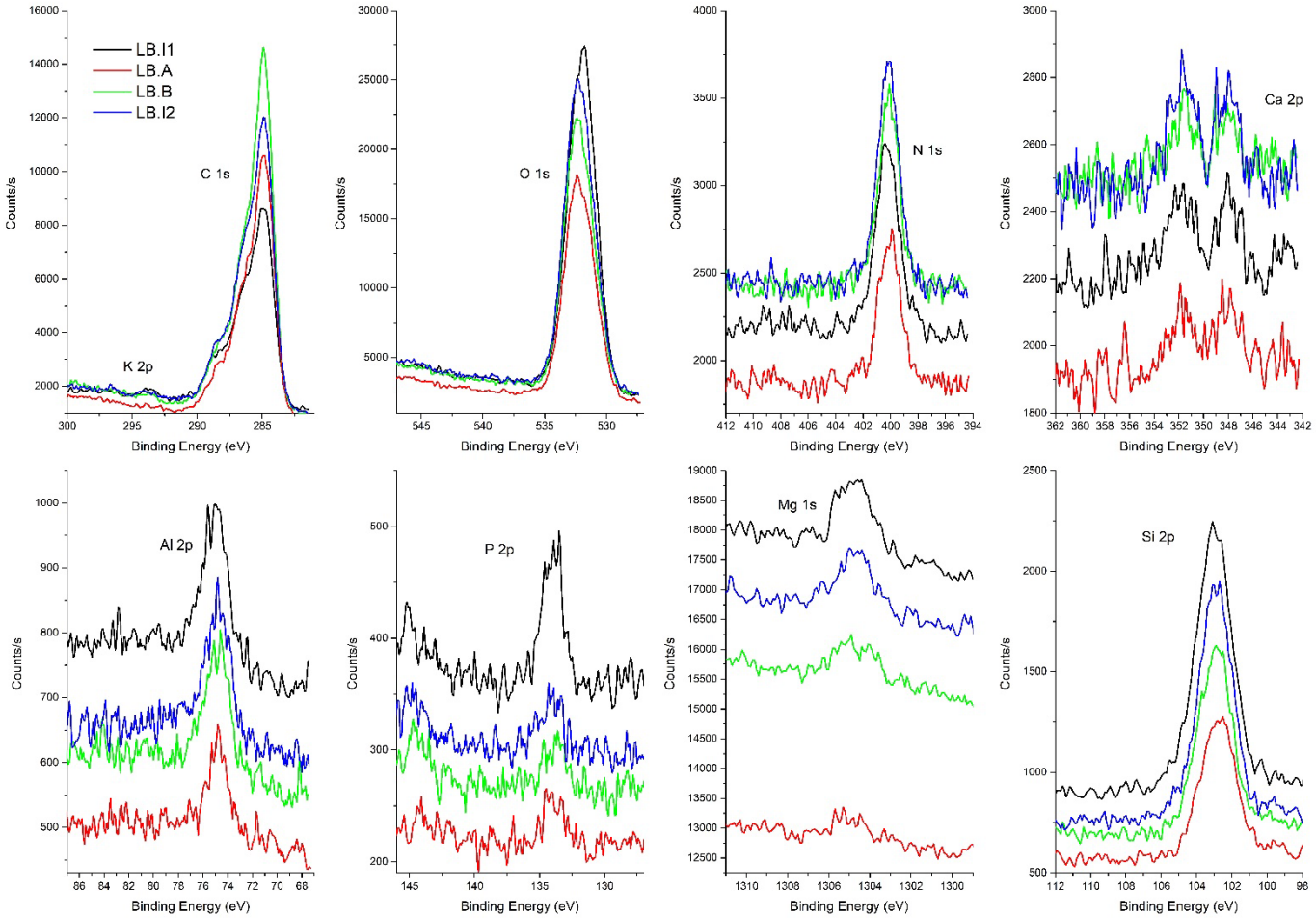

Figure B5. XPS high resolution spectra for C1s, O1s, N1s, Ca2p, Al2p, P2p, Mg1s and Si2p for layers I-1, A, B and I-2 of laboratory biofilter, respectively

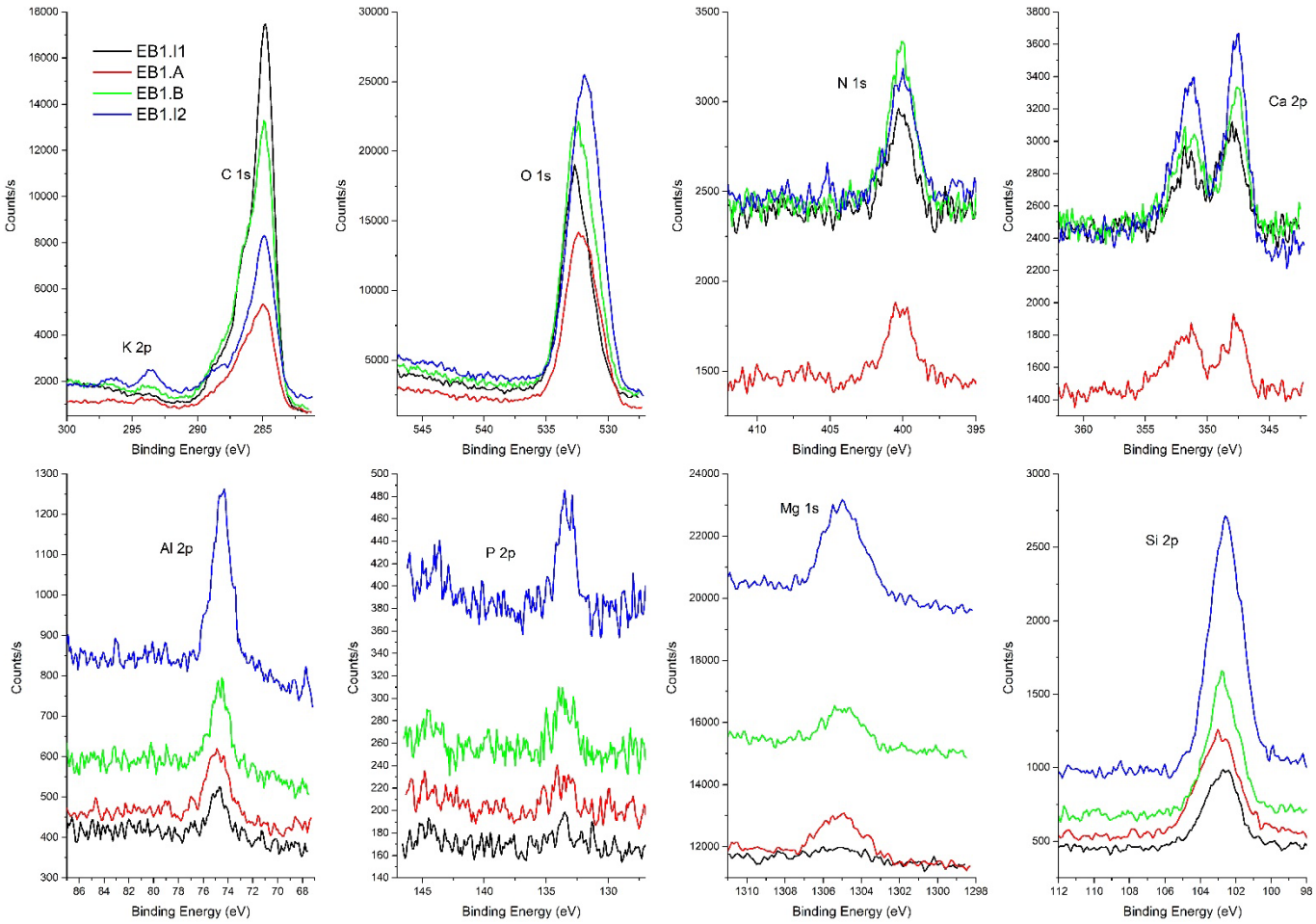

Figure B6. XPS high resolution spectra for C1s, O1s, N1s, Ca2p, Al2p, P2p, Mg1s and Si2p for layers I-1, A, B and I-2 of field-pilot 1 biofilter, respectively

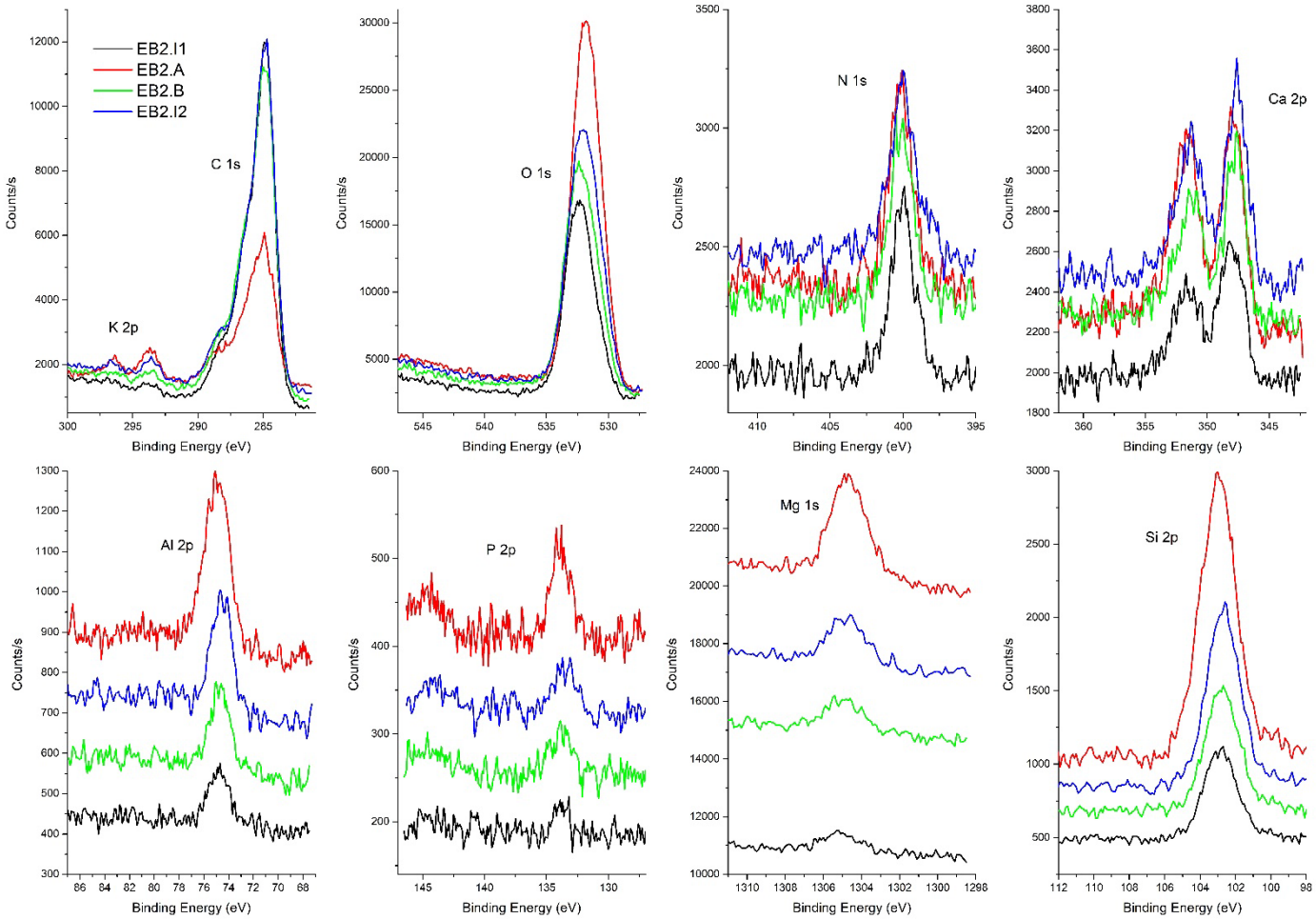

Figure B7. XPS high resolution spectra for C1s, O1s, N1s, Ca2p, Al2p, P2p, Mg1s and Si2p for layers I-1, A, B and I-2 of field-pilot 2 biofilter, respectively

Table B1. As-CND qualities for pilot biofilters

	Inlet	**Treated**	
		Pilot 1	**Pilot 2**
pH	7.6±0.2	6.9±0.5	6.9±0.5
Eh (mV)	207.1±36.7	222.6±29.7	220.6±29.0
Al (mg/L)	0.02±0.0	0.03±0.03	0.03±0.03
As (mg/L)	0.8±0.1	0.03±0.02	0.05±0.03
Ca (mg/L)	489.6±43.2	418.4±68.8	420.3±66.8
Fe (mg/L)	0.01±0.01	0.2±0.2	0.2±0.2
K (mg/L)	265.9±2.1	238.9±54.9	236.2±52.6
Mg (mg/L)	37.9±3.3	34.8±3.5	35.3±5.7
Na (mg/L)	873.5±38.2	808.6±190.6	792.3±179.1
P (mg/L)	<0.9	<0.9	<0.9
SO42- (mg/L)	2695.3±198.3	2387.5±512.1	2369.7±417.0

Table B2. Peat and MD-sludge characteristics

Physicochemical parameters								
	Paste pH	**TC (%)**	**OC (%)**	**IC (%)**	**TS (%)**	**Ssulfate (%)**	**Ssulfur (%)**	**TN (%)**
Peat	4.2±0.1	46.4±0.1	43.6±0.3	2.7	0.2±0.0	0.0±0.0	0.2	0.8±0.0
MD-S	8.0±0.2	5.2±0.0	4.1±0.0	1.1	0.9±0.0	0.23±0.0	0.7	0.9±0.0
Metals (g/kg)								
	Al	As	Ca	Fe	K	Mg	P	S
Peat	0.8±0.0	0.0±0.0	2.2±0.0	2.1±0.0	0.3±0.0	0.9±0.0	0.3±0.0	0.9±0.0
MD-S	15.3±0.0	10.7±0.1	30.6±0.1	172.9±0.2	6.8±0.0	11.2±0.0	8.3±0.0	9.4±0.1
Environmental characterization								
	Final pH		Al (mg/L)		As (mg/L)		Fe (mg/L)	
	TCLP	SPLP	TCLP	SPLP	TCLP	SPLP	TCLP	SPLP
Peat	4.7±0.0	3.8±0.0	0.03±0.0	<0.027	0.03±0.0	0.03±0.0	0.3±0.0	<0.108
MD-S	5.8±0.4	7.0±0.1	1.3±0.0	<0.027	19.1±2.7	0.6±0.1	668.5±12.9	<0.108

Table B3. Chemical characterization of post-treatment residues of laboratory biofilter

g/kg	**Al**	**As**	**Ca**	**Fe**	**Mg**	**Na**	**P**	**S**
na	5	5	5	5	5	5	5	5
I-1	5.13	1.97	6.51	60.44	3.15	0.27	2.46	1.99
A	6.09	2.29	6.80	66.85	6.66	0.43	2.65	2.20
B	5.49	2.70	7.80	58.81	3.34	0.42	2.22	2.34
B-duplicate	5.57	2.77	7.93	59.88	3.38	0.45	2.26	2.39
I-2	4.96	3.58	6.82	58.45	3.05	0.28	2.17	1.70
Average	5.45	2.66	7.17	60.89	3.92	0.37	2.35	2.12
minimum	4.96	1.97	6.51	58.45	3.05	0.27	2.17	1.70
maximum	6.09	3.58	7.93	66.85	6.66	0.45	2.65	2.39
Standard deviation	0.39	0.54	0.58	3.07	1.38	0.08	0.18	0.25
Coefficient of variation (%)	7.19	20.39	8.06	5.04	35.17	21.14	7.59	11.93

[a]Number of analyzed samples

Table B4. Chemical characterization of post-treatment residues of field pilot biofilter 1

g/kg	**Al**	**As**	**Ca**	**Fe**	**Mg**	**Na**	**P**	**S**
na	10	10	10	10	10	10	10	10
I-1_1	7.00	1.28	11.57	45.16	5.94	4.28	1.49	5.41
I-1_2	7.69	1.02	11.22	40.55	6.44	5.02	1.39	6.10
A_1	6.19	2.53	19.76	72.01	5.04	5.60	2.60	6.32
A_2	6.84	2.45	15.64	72.36	5.35	4.57	2.82	5.62
B_1	5.77	1.94	20.00	55.00	4.97	6.85	2.23	7.41
B_1-duplicate	5.65	1.92	19.99	54.65	4.89	6.87	2.23	7.39
B_2	7.34	2.54	17.28	72.90	5.99	5.15	2.89	6.49
B_2-duplicate	6.98	2.48	16.69	70.74	5.79	4.96	2.81	6.32
I-2_1	8.10	3.74	21.79	88.61	6.63	5.02	3.73	6.10
I-2_2	7.68	3.30	20.79	84.03	6.38	5.25	3.50	6.81
Average	6.92	2.32	17.47	65.60	5.74	5.34	2.57	6.44
minimum	5.65	1.02	11.22	40.55	4.89	4.57	1.39	5.41
maximum	8.10	3.74	21.79	88.61	6.63	6.87	3.73	7.41
Standard deviation	0.79	0.79	3.54	15.21	0.61	0.83	0.72	0.62
Coefficient of variation (%)	11.39	33.91	20.28	23.18	10.67	15.60	28.13	9.66

[a]Number of analyzed samples

Table B5. Chemical characterization of post-treatment residues of field pilot biofilter 2

g/kg	**Al**	**As**	**Ca**	**Fe**	**Mg**	**Na**	**P**	**S**
na	10	10	10	10	10	10	10	10
I-1_1	7.96	1.34	12.11	47.76	6.65	3.54	1.79	5.26
I-1_2	7.05	1.16	12.49	41.76	5.96	4.70	1.55	6.27
A_1	5.98	2.05	17.88	59.41	4.97	5.50	2.29	6.29
A_1_ duplicate	6.02	2.06	17.97	60.43	5.15	5.52	2.33	6.31
A_2	5.44	1.60	18.50	49.14	4.51	5.48	1.91	6.17
A_2_ duplicate	5.48	1.56	18.54	49.34	4.49	5.45	1.90	6.15
B_1	6.61	2.34	19.91	64.73	5.15	5.19	2.57	6.12
B_2	6.63	2.05	17.91	58.57	5.45	5.39	2.25	6.49
I-2_1	6.06	3.42	24.68	78.65	5.13	6.37	3.21	7.48
I-2_2	7.02	3.25	22.56	83.71	5.79	6.70	3.31	8.28
Average	6.43	2.08	18.26	59.35	5.30	5.38	2.31	6.48
minimum	5.44	1.16	12.11	41.76	4.49	3.54	1.55	5.26
maximum	7.96	3.42	24.68	83.71	6.65	6.70	3.31	8.28
Standard deviation	0.74	0.72	3.66	12.82	0.64	0.82	0.55	0.79
Coefficient of variation (%)	11.58	34.38	20.05	21.61	12.07	15.15	23.93	12.12

[a]Number of analyzed samples

Table B6. Relative atomic percentage of elements identified in XPS survey scans

	BG	**LB.I-1**	**LB.A**	**LB.B**	**LB.I-2**	**EB1.I-1**	**EB1.A**	**EB1.B**	**EB1.I-2**	**EB2.I-1**	**EB2.A**	**EB2.B**	**EB2.I-2**
Al	<D.L	3.2	1.6	2.1	1.8	0.6	2.4	1.8	2.6	0.4	3.5	<D.L	2.3
As	0.5	<D.L	0.3	0.3	0.5	<D.L	0.1	0.2	0.7	<D.L	0.5	<D.L	0.5
C	17.0	35.7	51.0	51.5	45.6	62.7	35.8	50.3	28.4	55.4	20.3	48.6	41.8
Ca	1.8	0.5	0.6	0.5	0.5	0.8	0.9	0.9	1.3	1.2	0.9	1.0	1.2
Cl	<D.L	<D.L	<D.L	<D.L	<D.L	<D.L	0.3	<D.L	0.3	<D.L	<D.L	<D.L	<D.L
F	<D.L	<D.L	<D.L	<D.L	<D.L	<D.L	0.7	<D.L	<D.L	<D.L	0.8	<D.L	<D.L
Fe	7.7	4.2	3.4	3.5	3.9	1.1	6.4	2.9	4.1	2.1<D.L	6.3	3.1	4.7
K	<D.L	<D.L	<D.L	<D.L	<D.L	<D.L	<D.L	<D.L	1.1	<D.L	0.3	<D.L	<D.L
Mg	1.0	0.7	<D.L	0.3	0.7	0.5	1.4	0.7	1.3	0.3	1.6	0.6	1.1
N	3.1	2.6	2.7	2.5	2.4	1.5	1.4	1.7	1.5	2.0	2.7	2.2	2.8
Na	0.6	0.4	<D.L	<D.L	<D.L	<D.L	1.2	<D.L	1.4	0.7	1.2	1.1	0.9
O	59.6	45.8	35.6	35.7	39.0	29.7	42.6	37.0	49.2	34.0	52.3	38.9	40.7
P	1.0	1.0	0.9	<D.L	0.5	0.3	0.7	0.9	<D.L	0.4	1.1	0.3	0.0
S	0.6	0.3	0.4	0.4	0.4	0.5	0.4	0.3	0.8	0.8	1.7	0.3	0.0
Si	7.2	5.6	3.4	3.3	4.8	2.4	5.5	3.2	7.3	2.8	7.0	3.9	3.9

*Potassium and sulfur could not be quantified from survey scans for some samples because the peak is too small but was visible in high resolution scans.; D.L = Detection limit

Table B7. Identification of chemical state or chemical groups and quantification from high resolution scans

Element and orbital	Peak BE (eV)	Identification	Relative atomic percentage						
			BG	LB.I-1	LB.A	LB.B	LB.I-2	EB1.I-1	EB1.A
As3d5/2	41.5-42.0	As(0) and/or As-metal	0.04	0.03	0.02	0.02	0.02	0.03	0.02
	43.5-44.0	As(III)	0.44	0.04	0.02	0.05	0.01	N.D	0.04
	45.0-45.5	As(V)	0.42	0.32	0.18	0.18	0.25	0.1	0.13
Al2p	74.6	Al oxide/hydroxide	1.50	1.68	1.03	1.26	1.25	0.78	1.99
Si2p	103.0	Silicate	7.50	5.66	3.78	3.62	4.51	2.31	5.75
P2p	133.6	Phosphate	1.26	1.11	0.46	0.36	0.49	0.17	0.67
S2p3/2	162.7	Metal sulfide	N.D	N.D	N.D	N.D	N.D	0.04	N.D
	163.5	C-S and/or S	0.11	0.07	0.06	0.09	0.09	0.04	0.02
	166.2	Sulfite	N.D	N.D	N.D	N.D	N.D	0.05	0.05
	168.7	sulfate	0.26	0.22	0.23	0.18	0.18	0.37	0.21
C1s	284.8	C-C	8.58	20.3	31.89	33.86	27.16	42.38	20.82
	286.3	C-O, C-O-C	4.05	10.42	14.38	14.13	13.31	14.96	11.64
	288.1	O-C-O, C=O	2.73	3.45	5.23	5.06	3.93	4.11	4.56
	288.7	O-C=O*-C=O	1.02	3.47	1.33	1.94	3.90	2.63	1.97
K2p3/2	293.6	K in mineral or salt possible	0.46	0.32	0.12	0.12	0.19	0.18	0.47
Ca2p3/2	347.6	Ca in mineral or salt possible	1.45	0.21	0.21	0.16	0.23	0.70	0.56
N1s	399.9	C-N, O=C-N	2.75	2.75	2.29	2.20	2.63	1.63	2.34
O1s	530.1	Metal oxides	16.10	6.64	3.77	3.87	4.30	2.10	6.75
	531.2	Si-O, Metal-OH, S-O, P-O	24.15	19.29	11.52	10.05	10.83	7.29	14.53
	532.1	C-O, C=O	11.41	14.28	14.39	13.25	15.45	13.68	15.85
	533.2	O-C-O, O*-C=O	1.68	2.84	4.68	5.75	6.78	4.59	4.36
Fe2p3/2	709.0-715.5	Fe(II) + Fe(II) shake-up	N.D	N.D	0.49	0.1	0.21	0.19	0.25
	711.2-719.0	Fe(III) in oxides/hydroxides	12.88	6.06	3.42	3.3	3.66	1.19	5.39
Mg1s	1303.7	Mg in other mineral possible	0.39	0.23	0.07	0.21	0.08	0.32	0.59
	1305.2	Mg in mineral possible	0.81	062	0.35	0.23	0.54	0.18	1.01

N.D = not detected

Table B7. Identification of chemical state or chemical groups and quantification from high resolution scans (suite)

Element and orbital	Peak BE (eV)	Identification	Relative atomic percentage					
			EB1.B	EB1.I-2	EB2.I-1	EB2.A	EB2.B	EB2.I-2
As3d5/2	41.5-42.0	As(0) and/or As-metal	0.03	0.05	0.03	0.02	0.03	0.02
	43.5-44.0	As(III)	0.04	0.06	N.D	0.03	0.04	0.05
	45.0-45.5	As(V)	0.12	0.21	0.13	0.24	0.16	0.16
Al2p	74.6	Al oxide/hydroxide	1.08	2.26	0.93	2.78	1.21	1.64
Si2p	103.0	Silicate	3.37	7.22	3.14	8.50	3.83	4.99
P2p	133.6	Phosphate	0.39	0.61	0.33	0.91	0.69	0.64
S2p3/2	162.7	Metal sulfide	0.03	0.04	N.D	N.D	N.D	0.04
	163.5	C-S and/or S	0.05	0.05	0.04	0.05	0.04	0.07
	166.2	Sulfite	0.06	0.07	0.05	0.06	0.04	N.D
	168.7	sulfate	0.28	0.55	0.57	0.41	0.30	0.31
C1s	284.8	C-C	30.49	20.62	35.39	11.93	31.36	29.38
	286.3	C-O, C-O-C	15.41	7.05	14.79	6.14	13.21	11.19
	288.1	O-C-O, C=O	5.04	2.60	4.56	2.35	4.15	4.13
	288.7	O-C=O*-C=O	2.15	1.38	1.81	2.10	1.81	0.83
K2p3/2	293.6	K in mineral or salt possible	0.28	0.81	0.27	0.96	0.40	0.39
Ca2p3/2	347.6	Ca in mineral or salt possible	0.61	1.23	0.84	1.01	0.85	0.90
N1s	399.9	C-N, O=C-N	2.02	1.84	2.24	2.01	1.95	1.97
O1s	530.1	Metal oxides	4.76	7.61	4.23	7.06	4.46	5.95
	531.2	Si-O, Metal-OH, S-O, P-O	10.28	16.79	8.47	17.36	10.78	13.17
	532.1	C-O, C=O	15.02	15.69	12.17	19.48	13.98	14.19
	533.2	O-C-O, O*-C=O	4.53	4.64	7.14	6.00	6.15	4.01
Fe2p3/2	709.0-715.5	Fe(II) + Fe(II) shake-up	0.17	0.48	0.14	N.D	N.D	0.15
	711.2-719.0	Fe(III) in oxides/hydroxides	2.93	6.16	2.15	8.42	3.62	4.67
Mg1s	1303.7	Mg in other mineral possible	0.13	0.66	0.18	0.36	0.37	0.22
	1305.2	Mg in mineral possible	0.74	1.32	0.40	1.82	0.57	0.94

N.D = not detected

Table B8. Physicochemical parameters of the eluates after TCLP on residues of laboratory biofilter

		Elements (mg/L)				
	pH	**As**	**Ca**	**Fe**	**Mg**	**Ni**
na	5	5	5	5	5	5
I-1	4.92	0.41	15.90	0.71	0.55	0.07
A	4.91	0.18	18.20	0.84	0.65	0.11
A _ duplicate	4.93	0.18	14.70	0.79	0.65	0.11
B	4.93	0.26	12.80	1.86	0.60	0.08
I-2_1	4.93	0.33	12.00	1.59	0.59	0.07
Average	4.92	0.27	14.72	1.16	0.60	0.09
minimum	4.91	0.18	12.00	0.71	0.55	0.07
maximum	4.93	0.41	18.20	1.86	0.65	0.11

[a]Number of analyzed samples

Table B9. Physicochemical parameters of the eluates after SPLP on residues of laboratory biofilter

		Elements (mg/L)				
	pH	**As**	**Ca**	**Fe**	**Mg**	**Na**
na	5	5	5	5	5	5
I-1	5.82	0.27	1.54	0.07	0.09	0.30
A	5.89	0.02	2.30	0.15	0.17	0.39
A _ duplicate	5.82	0.06	2.52	0.77	0.19	0.33
B	5.70	0.03	1.42	0.12	0.12	0.35
I-2_1	5.60	0.01	2.42	0.04	0.16	0.34
Average	5.76	0.08	2.04	0.23	0.15	0.34
minimum	5.60	0.01	1.42	0.04	0.09	0.30
maximum	5.89	0.27	2.52	0.77	0.19	0.39

[a]Number of analyzed samples

Table B10. Physicochemical parameters of the eluates after FLT on residues of laboratory biofilter

		Elements (mg/L)				
	pH	**As**	**Ca**	**Fe**	**Mg**	**Na**
na	5	5	5	5	5	5
I-1	6.43	0.27	0.47	0.13	0.05	0.47
A	5.96	0.15	0.90	0.23	0.12	0.67
A _ duplicate	5.94	0.29	0.98	0.21	0.10	0.62
B	5.84	0.34	1.09	0.21	0.11	0.69
I-2_1	5.64	0.31	1.15	0.23	0.11	0.55
Average	5.96	0.28	0.92	0.20	0.09	0.60
minimum	5.64	0.15	0.47	0.13	0.05	0.47
maximum	6.43	0.34	1.15	0.23	0.12	0.69

[a]Number of analyzed samples

Table B11. Physicochemical parameters of the eluates after TCLP on residues of field pilot biofilter 1

		Elements (mg/L)					
	pH	**As**	**Ca**	**Fe**	**Mg**	**Ni**	**SO_4^{2-}**
na	8	8	8	8	8	8	8
I-1_1	4.89	0.09	72.30	0.84	4.34	0.33	44.71
I-1_2	4.93	0.07	38.20	1.79	2.33	0.10	44.78
A_1	4.90	0.16	52.30	0.58	3.34	0.37	53.92
A_2	4.85	0.05	40.90	0.27	3.12	0.05	70.22
B_1	4.90	0.04	58.40	0.50	2.93	0.07	50.43
B_2	4.89	0.06	57.40	0.55	3.84	0.10	60.24
I-2_1	4.92	0.09	75.65	0.67	4.25	0.22	58.64
I-2_2	4.89	0.11	62.30	0.78	3.87	0.30	47.00
Average	4.90	0.08	57.18	0.75	3.50	0.19	53.74
minimum	4.85	0.05	38.20	0.27	2.33	0.05	44.71
maximum	4.93	0.16	75.65	1.79	4.34	0.37	70.22

[a]Number of analyzed samples

Table B12. Physicochemical parameters of the eluates after SPLP on residues of field pilot biofilter 1

		Elements (mg/L)				
	pH	**As**	**Ca**	**Fe**	**Mg**	**Na**
na	8	8	8	8	8	8
I-1_1	7.50	0.02	9.59	0.17	0.79	18.59
I-1_2	7.54	0.01	6.91	0.04	0.63	14.23
A_1	7.54	0.02	10.63	0.22	0.88	24.68
A_2	7.30	0.02	10.18	0.12	0.84	22.14
B_1	7.65	0.03	11.97	0.19	0.96	23.43
B_2	7.54	0.02	12.47	0.09	0.98	23.50
I-2_1	7.99	0.05	18.74	0.06	1.31	26.24
I-2_2	7.67	0.03	16.67	0.07	1.14	20.78
Average	7.59	0.02	12.14	0.12	0.94	21.70
minimum	7.30	0.01	6.91	0.04	0.63	14.23
maximum	7.99	0.05	18.74	0.22	1.31	26.24

[a]Number of analyzed samples

Table B13. Physicochemical parameters of the eluates after FLT on residues of field pilot biofilter 1

		Elements (mg/L)				
	pH	**As**	**Ca**	**Fe**	**Mg**	**Na**
na	8	8	8	8	8	8
I-1_1	8.36	0.08	4.00	0.07	0.37	8.89
I-1_2	8.12	0.27	2.45	1.09	0.24	24.90
A_1	7.72	0.06	10.66	0.08	0.89	24.70
A_2	7.97	0.10	6.64	0.16	0.57	32.78
B_1	7.86	0.04	5.17	0.05	0.49	11.51
B_2	7.81	0.10	9.87	0.15	0.81	31.55
I-2_1	8.56	0.25	11.40	0.09	0.70	17.48
I-2_2	8.18	0.17	18.30	0.10	1.29	34.32
Average	8.07	0.14	8.56	0.22	0.67	23.26
minimum	7.72	0.04	2.45	0.05	0.24	8.89
maximum	8.56	0.27	18.30	1.09	1.29	34.32

[a]Number of analyzed samples

Table B14. Physicochemical parameters of the eluates after TCLP on residues of field pilot biofilter 2

		Elements (mg/L)					
	pH	**As**	**Ca**	**Fe**	**Mg**	**Ni**	**SO_4^{2-}**
na	8	8	8	8	8	8	8
I-1_1	4.89	0.05	45.10	0.53	2.77	0.04	45.35
I-1_2	4.94	0.07	37.70	0.80	2.60	0.03	48.16
A_1	4.90	0.05	63.25	0.28	3.89	0.03	61.20
A_2	4.96	0.08	54.90	0.34	4.05	0.03	69.06
B_1	4.97	0.06	66.70	0.45	3.91	0.07	50.10
B_2	4.95	0.07	34.60	0.97	2.31	0.09	40.30
I-2_1	5.00	0.08	112.00	0.45	5.43	0.49	67.18
I-2_2	4.96	0.07	57.45	0.85	3.29	0.17	54.20
Average	4.95	0.05	58.96	0.58	3.53	0.12	54.44
minimum	4.89	0.08	37.70	0.28	2.31	0.03	40.30
maximum	5.00	0.07	112.00	0.97	5.43	0.49	69.06

[a]Number of analyzed samples

Table B15. Physicochemical parameters of the eluates after SPLP on residues of field pilot biofilter 2

		Elements (mg/L)				
	pH	**As**	**Ca**	**Fe**	**Mg**	**Na**
na	8	8	8	8	8	8
I-1_1	7.44	0.01	9.92	0.09	0.84	20.22
I-1_2	7.57	0.03	9.62	0.20	0.78	17.25
A_1	7.28	0.02	11.89	0.14	1.00	29.37
A_2	7.5	0.05	11.80	0.33	0.86	18.83
B_1	7.37	0.03	10.27	0.20	0.79	18.73
B_2	7.55	0.03	10.32	0.20	0.86	20.39
I-2_1	7.66	0.04	16.10	0.07	1.00	19.63
I-2_2	7.52	0.02	12.27	0.07	0.75	20.68
Average	7.50	0.03	11.52	0.16	0.87	20.64
minimum	7.28	0.01	9.62	0.07		17.25
maximum	7.66	0.05	16.10	0.33		29.37

[a]Number of analyzed samples

Table B16. Physicochemical parameters of the eluates after FLT on residues of field pilot biofilter 2

		Elements (mg/L)				
	pH	**As**	**Ca**	**Fe**	**Mg**	**Na**
na	8	8	8	8	8	8
I-1_1	7.67	0.09	4.53	0.16	0.43	22.75
I-1_2	7.68	0.08	2.45	0.10	0.29	9.07
A_1	7.34	0.06	12.42	0.12	1.08	35.69
A_2	7.27	0.04	18.31	0.04	1.46	34.74
B_1	7.90	0.10	7.53	0.08	0.66	18.29
B_2	7.73	0.10	11.45	0.08	0.98	26.05
I-2_1	8.40	0.22	4.41	0.12	0.35	8.50
I-2_2	7.89	0.18	5.51	0.15	0.45	13.91
Average	7.74	0.11	8.33	0.11	0.71	21.12
minimum	7.27	0.04	2.45	0.04	0.29	8.50
maximum	8.40	0.22	18.31	0.16	1.46	35.69

[a]Number of analyzed samples